



EDUCACIÓN

SECRETARÍA DE EDUCACIÓN PÚBLICA



TECNOLÓGICO
NACIONAL DE MÉXICO

Tecnológico Nacional de México

Centro Nacional de Investigación
y Desarrollo Tecnológico

Tesis de Doctorado

Diseño de sensores virtuales basados en
observadores para la estimación de variables y la
detección de fallas en sistemas biológicos

presentada por

MC. Dulce Alejandra Serrano Cruz

como requisito para la obtención del grado de
Doctora en Ciencias en Ingeniería Electrónica

Director de tesis

Dr. Carlos Manuel Astorga Zaragoza

Codirector de tesis

Dr. Gerardo Vicente Guerrero Ramírez

Cuernavaca, Morelos, México. Diciembre de 2024.

 <small>Centro Nacional de Investigación y Desarrollo Tecnológico</small>	ACEPTACIÓN DE IMPRESIÓN DEL DOCUMENTO DE TESIS DOCTORAL	Código: CENIDET-AC-006-D20
	Referencia a la Norma ISO 9001:2008 7.1, 7.2.1, 7.5.1, 7.6, 8.1, 8.2.4	Revisión: 0
		Página 1 de 1

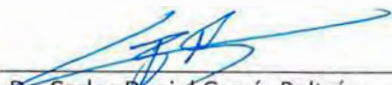
Cuernavaca, Mor., a 03 de octubre de 2024

Dr. Carlos Manuel Astorga Zaragoza
 Subdirector Académico
 Presente

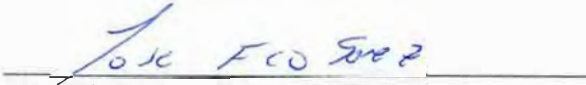
At'n: Dr. Víctor Manuel Alvarado Martínez
 Presidente del Claustro Doctoral
 del Departamento de Ingeniería Electrónica

Los abajo firmantes, miembros del Comité Tutorial de la estudiante **Dulce Alejandra Serrano Cruz** manifiestan que después de haber revisado el documento de tesis titulado **“DISEÑO DE SENSORES VIRTUALES BASADOS EN OBSERVADOR PARA LA ESTIMACIÓN DE VARIABLES Y LA DETECCIÓN DE FALLAS EN SISTEMAS BIOLÓGICOS”**, realizado bajo la dirección del **Dr. Carlos Manuel Astorga Zaragoza** y la codirección del **Dr. Gerardo Vicente Guerrero Ramírez**, el trabajo se **ACEPTA** para proceder a su impresión.

ATENTAMENTE



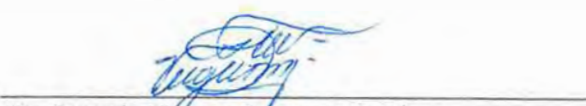
 Dr. Carlos Daniel García Beltrán
 TecNM/CENIDET



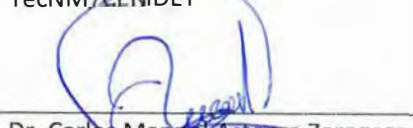
 Dr. José Francisco Gómez Aguilar
 TecNM/CENIDET



 Dr. Juan Reyes Reyes
 TecNM/CENIDET



 Dr. Gerardo Vicente Guerrero Ramírez
 TecNM/CENIDET



 Dr. Carlos Manuel Astorga Zaragoza
 TecNM/CENIDET

c.c.p: M.T.I Maria Elena Gómez Torres/ Jefa del Departamento de Servicios Escolares.
 c.c.p: Dr. Jarniel García Morales / Jefe del Departamento de Ingeniería Electrónica.
 c.c.p: Expediente.

Cuernavaca, Mor.,
No. De Oficio:
Asunto:

07/octubre/2024
SAC/330/2024
Autorización de
impresión de tesis

**DULCE ALEJANDRA SERRANO CRUZ
CANDIDATA AL GRADO DE DOCTORA EN CIENCIAS
EN INGENIERÍA ELECTRÓNICA
P R E S E N T E**

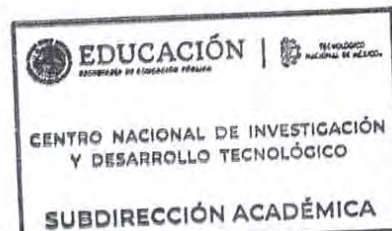
Por este conducto, tengo el agrado de comunicarle que el Comité Tutorial asignado a su trabajo de tesis titulado “DISEÑO DE SENSORES VIRTUALES BASADOS EN OBSERVADOR PARA LA ESTIMACIÓN DE VARIABLES Y LA DETECCIÓN DE FALLAS EN SISTEMAS BIOLÓGICOS”, ha informado a esta Subdirección Académica, que están de acuerdo con el trabajo presentado. Por lo anterior, se le autoriza a que proceda con la impresión definitiva de su trabajo de tesis.

Esperando que el logro del mismo sea acorde con sus aspiraciones profesionales, reciba un cordial saludo.

ATENTAMENTE
Excelencia en Educación Tecnológica



CARLOS MANUEL ASTORGA ZARAGOZA
SUBDIRECTOR ACADÉMICO



C. c. p. Departamento de Ingeniería Electrónica
Departamento de Servicios Escolares

CMAZ/lmz



Agradecimientos

Quiero expresar mi gratitud a quienes han sido fundamentales en este recorrido.

A mis asesores en México, Dr. Carlos Manuel Astorga Zaragoza y el Dr. Gerardo Vicente Guerrero Ramírez, quienes me guiaron, apoyaron y siempre me brindaron su amistad. ¡Infinitas gracias!

A mis asesores en Francia, Dr. Mohamed Darouach y en especial a la Dra. Latifa BOUTAT-BADDAS sin su excelente asesoramiento y apoyo durante toda la tesis, este proyecto nunca hubiera sido posible. También le agradezco sus valiosos comentarios y sugerencias tanto durante el trabajo como durante la fase final de redacción.

A mis hermanos Sara, Elisa, Monse y Angel, por ser mis primeros compañeros de vida, por el apoyo incondicional y por compartir cada momento, bueno o difícil, a lo largo de este proceso. Su amor y respaldo me han dado la fortaleza para seguir adelante cuando más lo necesitaba.

A mi padre Reynaldo Serrano, quien me ha enseñado el valor del esfuerzo y la determinación. Gracias por tus consejos y por ser un pilar de estabilidad en mi vida. Todo lo que he logrado lleva también tu huella y tus enseñanzas.

A mis amigos, quienes han sido mi refugio y mi fuente de alegría en los momentos de agotamiento.

Y Alex, gracias por tu cariño y constante apoyo. Tu confianza en mí ha sido una luz en los momentos de duda.

Al Consejo Nacional de Ciencias y Tecnología (CONACYT) por el apoyo económico brindado para poder realizar y culminar mis estudios de doctorado.

Finalmente, agradezco profundamente al Centro Nacional de Investigación y Desarrollo Tecnológico (CENIDET) por darme la oportunidad de estudiar y prepararme, así como de tener un ambiente muy agradable de trabajo y una atención excelente en todo momento.

Quiero dedicar esta tesis a la memoria de mi madre, cuya influencia ha sido una constante fuente de inspiración y fuerza en mi vida. A pesar de que ya no está físicamente conmigo, siento cada día su presencia en mi corazón y en cada logro que he alcanzado. Mamá, tu dedicación, tu esfuerzo y tus enseñanzas siempre me guiaron y me recordaron la importancia del conocimiento y la perseverancia. Sin ti, este logro no hubiera sido posible, y es a ti a quien dedico cada página de este trabajo. Gracias por enseñarme a soñar y a trabajar duro por esos sueños. Esta tesis es para ti, con todo mi amor y mi eterno agradecimiento.

Résumé du travail:

Cette thèse propose une nouvelle méthodologie pour le diagnostic et la détection des anomalies du système cardiovasculaire (CVS) dans des conditions où l'état est linéairement non observable.

Le premier apport majeur consiste en l'extension de la forme normale d'observabilité quadratique, initialement développée pour les systèmes non linéaires SISO, aux systèmes MIMO. Cette extension est appliquée aussi bien aux cas où la partie linéaire est observable qu'à ceux où elle présente une variété non observable. La forme normale met en évidence la surface des singularités d'observabilité. L'identification de ces singularités permet de rétablir l'observabilité des systèmes non linéaires à l'aide de termes résonants (en états ou en entrées), garantissant ainsi un bon fonctionnement de l'observateur malgré les zones inobservables.

Le deuxième apport porte sur la synthèse d'un observateur à mode glissant, basé sur cette forme normale d'observabilité équivalente. Cet observateur reconstruit le comportement dynamique du système en intégrant des termes résonants quadratiques spécifiques, compensant ainsi la perte d'observabilité tout en tenant compte de la surface de singularité d'observabilité. Cette approche repose sur l'utilisation d'un filtre qui adapte la correction de l'observateur à proximité de la surface de singularité, garantissant une estimation robuste.

Le troisième apport concerne l'application de cette méthodologie au diagnostic et à la détection des anomalies cardiovasculaires, telles que la régurgitation et la sténose. En transformant le modèle du CVS en une forme normale quadratique d'observabilité, les singularités d'observabilité du système sont mises en évidence, permettant ainsi de concevoir un observateur à mode glissant capable de détecter et d'isoler ces défauts en exploitant les termes résonants du système. La méthodologie proposée a été validée par des simulations numériques, démontrant que l'observateur à mode glissant est capable de détecter et d'isoler les anomalies du système cardiovasculaire, même lorsque certaines parties deviennent temporairement inobservables.

Les résultats montrent que le modèle reproduit fidèlement les paramètres hémodynamiques et permet d'estimer des variables critiques telles que les pressions ventriculaire et auriculaire. En cas d'anomalies comme la régurgitation mitrale ou aortique, l'observateur peut reconstruire le comportement dynamique du système en utilisant des termes non linéaires spécifiques, compensant ainsi la perte d'observabilité. Cela assure un diagnostic fiable et précis, même dans des conditions pathologiques complexes.

Mots-clés: Forme d'observabilité Brunovsky, systèmes non linéaires multi-entrées multi-sorties, système cardiovasculaire; maladies cardiaques; boucles pression-volume; forme normale; observateur en mode glissant; détection et isolation des défauts; états inobservables.

Abstract

This thesis proposes a new methodology for diagnosing and detecting anomalies in the cardiovascular system (CVS) under conditions where the state is linearly unobservable.

The first major contribution consists of extending the quadratic observability normal form, initially developed for nonlinear SISO systems, to MIMO systems. This extension is applied to both cases where the linear part is observable and where it presents an unobservable manifold. The normal form highlights the surface of observability singularities. Identifying these singularities allows the restoration of observability in nonlinear systems using resonant terms (in states or inputs), thereby ensuring the proper functioning of the observer despite unobservable regions.

The second contribution involves the synthesis of a sliding mode observer based on this equivalent observability normal form. This observer reconstructs the system's dynamic behavior by integrating specific quadratic resonant terms, thus compensating for the loss of observability while accounting for the observability singularity surface. This approach relies on the use of a filter that adjusts the observer's correction near the singularity surface, ensuring robust estimation.

The third contribution concerns the application of this methodology to the diagnosis and detection of cardiovascular anomalies, such as regurgitation and stenosis. By transforming the CVS model into a quadratic observability normal form, the system's observability singularities are revealed, allowing for the design of a sliding mode observer capable of detecting and isolating these faults by exploiting the system's resonant terms. The proposed methodology has been validated through numerical simulations, demonstrating that the sliding mode observer can detect and isolate cardiovascular system anomalies, even when certain parts become temporarily unobservable. The results show that the model accurately reproduces hemodynamic parameters and enables the estimation of critical variables such as ventricular and atrial pressures. In the case of anomalies like mitral or aortic regurgitation, the observer can reconstruct the system's dynamic behavior by using specific nonlinear terms, thereby compensating for the loss of observability. This ensures a reliable and precise diagnosis, even in complex pathological conditions.

Keywords: Brunovsky observability form, multi-input multi-output nonlinear systems, cardiovascular system; heart diseases; pressure-volume loops; normal form; sliding mode observer; fault detection and isolation; unobservable states.

Contents

Résumé du travail:

General introduction	xviii
-----------------------------	--------------

1	Introduction	xviii
2	Problem formulation	xix
3	Objectives of the thesis	xix
3.1	General objective	xix
3.2	Specific objectives	xx
4	Main contributions	xx
5	Outline of the thesis	xxi

Chapter 1

Definitions and issues related to observability and the Poincaré normal form

1.1	Introduction	1
1.2	Basic properties of observability and nonlinear systems	2
1.2.1	Linear systems	2
1.2.2	Nonlinear systems.	3
1.2.2.1	Observability and range conditions	3
1.3	Design of observers	5
1.3.1	State estimation principle	5
1.3.2	Luenberger observer	5
1.3.3	Kalman filter	5
1.3.4	Extended Kalman filter	6
1.3.5	High-gain observer	7
1.3.6	Sliding mode observers	9
1.3.6.1	Nonlinear sliding mode observer	10
1.3.6.2	Sliding mode observer in the triangular input form	11
1.3.6.3	High-order sliding mode observers	12
1.3.7	Characteristics of sing function approximation forms	14

1.4	Higher-order linearization and normal form	16
1.4.1	The resonances	16
1.4.2	Poincaré Normal Forms computation	18
1.5	Quadratic observability normal form for nonlinear SISO system	21
1.5.1	Quadratic equivalence modulo an output injection	22
1.5.2	Linearly observable case for nonlinear SISO system	23
1.5.2.1	Practical example for linearly observable case	27
1.5.3	One dimensional linearly unobservable case	28
1.5.3.1	Example: Lorentz system	30
1.6	Conclusion	33

Chapter 2

Quadratic observability normal form for MIMO systems

2.1	Introduction	34
2.2	Quadratic observability normal form for nonlinear multi-output systems	35
2.2.1	Linearly observable case	36
2.2.1.1	Quadratic observability normal form	37
2.2.1.2	Illustrative example: Linearly observable case	41
2.2.2	Linearly unobservable case	42
2.2.2.1	Quadratic observability normal form	43
2.2.2.2	Illustrative example: Linearly unobservable case	47
2.3	Quadratic observability normal form for nonlinear multi-input multi-output systems	48
2.3.1	Linearly observable case	50
2.3.2	Linearly unobservable case	54
2.4	Sliding mode observer design	60
2.4.1	Application to Generalized Lorenz System	62
2.4.1.1	Generalized Lorenz System description	62
2.4.1.2	Quadratic observability normal form calculation	63
2.4.1.3	sliding mode observer of Generalized Lorenz	64
2.4.1.4	Simulation results	65
2.5	Conclusion	65

Chapter 3

Aplicacion to cardiovascular system
--

3.1	Introduction	67
3.2	Presentation of cardiovascular system	68
3.2.1	State of the art of cardiovascular system models	68
3.2.2	Anatomy and physiology of the cardiac cycle	69
3.2.3	Valve pathologies	71

3.3	Description of the cardiovascular system model	71
3.3.1	Equivalent electric model	71
3.3.2	Elastance	72
3.3.3	Cardiovascular system modeling phases	74
3.3.4	Mathematical model of the cardiovascular system	80
3.4	Quadratic normal form of the cardiovascular system	80
3.4.1	Validation of the quadratic normal form of the CVS model	81
3.5	Observability analysis and observer design of the cardiovascular system	83
3.5.1	Observability analysis of the cardiovascular system	83
3.5.2	Sliding mode observers design for CVS	84
3.6	Conclusion	87

Chapter 4

Diagnostic and detection anomaly of CVS
--

4.1	Introduction	88
4.2	Diagnostic and fault detection methodology	89
4.2.1	Classification of fault detection and diagnosis methods	90
4.3	Expansion of the cardiovascular model for detection of anomalies	92
4.3.1	Residual generator for cardiovascular anomalies detection	93
4.4	Simulation Results	95
4.4.1	Scenario 1: Mitral Regurgitation	98
4.4.2	Scenario 2: Aortic Regurgitation	102
4.4.3	Scenario 3: Simultaneous mitral and aortic regurgitation	105
4.5	Conclusions	107

General conclusions and perspectives

Bibliography

List of Figures

1.1	Discrete-time Kalman filter algorithm.	7
1.2	Classification and Types of Sliding Mode Observers.	10
1.3	Sign function approximations.	15
1.4	Plot the dynamics of Lorenz system	32
1.5	Trajectories in the phase plane.	33
3.1	Blood flow of the human heart.	68
3.2	Cardiac cycle of circulatory system.	70
3.3	Cardiovascular circuit model.	72
3.4	Plot the elastance function for a healthy heart during a single cardiac cycle.	74
3.5	Interpretation of the cardiac cycle using a hybrid system	74
3.6	Electrical representation of the Filling phase ($q_1 = F$)	75
3.7	Electrical representation of the ejection phases ($q_2 = E$)	77
3.8	Electrical representation of the isovolumic phase ($q_3 = I$)	79
3.9	Hemodynamic waveforms of the CVS mode: Original states $x_i(t)$ and QNF states $\xi_i(t)$ of CVS	83
3.10	Hemodynamic of left ventricular volume (LVV) and preload volume (PLV) in original and QNF system	83
4.1	Stages of model-based fault detection and diagnosis	89
4.2	Stages of model-based fault detection and diagnosis	91
4.3	Kalman Filtering	92
4.4	Cardiovascular system with fault in the mitral valve.	93
4.5	Bank of observers for all actuator faults estimation.	94
4.6	States of u_3 , E_{SM} , u_4 and E_{SA}	95
4.7	Hemodynamic waveforms of the original states $x_i(t)$ and observer states $\hat{x}_i(t)$ for a normal heart	97
4.8	Hemodynamic of the left ventricular volume (LVV) and preload volume (PLV) in original and SMO of CVS.	97
4.9	Error between the original states $x_i(t)$ and observer states $\hat{x}_i(t)$ error	98
4.10	States of input with fault f_m	98
4.11	Original states $x_i(t)$ and observer states $\hat{x}_i(t)$ of CVS for an unhealthy heart ($i = 1, 2$)	99
4.12	Hemodynamic waveforms of the original states $x_i(t)$ and observer states $\hat{x}_i(t)$ of CVS for an unhealthy heart ($i = 3, 4, 5$)	100
4.13	Left ventricular volume (LVV) in original and SMO of CVS	100
4.14	Preload volume (PLV) in original and SMO of CVS	101
4.15	Estimation error of the original states $x_i(t)$ and observer states $\hat{x}_i(t)$ of CVS	101
4.16	Input with fault $f_{a\phi}$	102
4.17	Original states $x_i(t)$ and observer states $\hat{x}_i(t)$ of CVS for an unhealthy heart ($i = 1, 2$)	102
4.18	Original states $x_i(t)$ and observer states $\hat{x}_i(t)$ of CVS for an unhealthy heart ($i = 3, 4, 5$)	103

4.19	Hemodynamic for left ventricular volume (LVV) in original and SMO of CVS	103
4.20	Simulated hemodynamic waveforms for preload volume (PLV) in original and SMO of CVS .	104
4.21	Estimation error of the original states $x_i(t)$ and observer states $\hat{x}_i(t)$ of CVS	104
4.22	States of input with fault in f_m and f_{ao}	105
4.23	Original states $x_i(t)$ and observer states $\hat{x}_i(t)$ of CVS for an unhealthy heart ($i = 1, 2, 3, 4$) . .	106
4.24	Original states $x_5(t)$ and observer states $\hat{x}_5(t)$ of CVS for an unhealthy heart	107
4.25	Hemodynamic for a Left ventricular volume (LVV) in original and SMO of CVS	107
4.26	Hemodynamic for a reload volume (PLV) in original and SMO of CVS	108
4.27	Estimation error of the original states $x_i(t)$ and observer states $\hat{x}_i(t)$ of CVS	108

List of Tables

3.1	State variables of the cardiovascular system and their physiological significance of the circuit model shown in Figure 3.3.	72
3.2	Parameter values of the CVS circuit model shown in Figure 3.3.	73
4.1	Types of faults in systems.	89
4.2	Signature for the residual generation.	95

Notation and acronyms

Sets and norms

Symbol	Description
\mathbb{R}	Set of all real numbers.
\mathbb{R}^n	Set of n -dimensional real matrices.
$\mathbb{R}^{n \times m}$	Set of $n \times m$ dimensional real matrices.
$f^{[2]}$	Polynomials of degree 2.
$g^{[1]}$	Polynomials of degree 1.
$\Phi^{[r]}$	Homogeneous polynomials of degree r .

Acronyms

Symbol	Description	Units
MIMO	Multiple-Input Multiple-Output	
SISO	Single-Input Single-Output	
MOI	Modulo an Output Injection	
QEMOI	Quadratically Equivalent Modulo an Output Injection	
CVD	Cardiovascular disease	
WHO	World Health Organization	
CVS	Cardiovascular system	
LVP	Left ventricular pressure	mmHg
LV	Left ventricle	mmHg
LVV	Left ventricular volume	mmHg
EDV	End-diastolic volume	
ESV	End-systolic volume	
SMO	Sliding mode observer	
FDI	Fault detection and isolation	
PV	Pressure–volume	mmHg
PVA	Pressure–volume area	mmHg
LA	Left atria	
H_R	Heart rate	
LAP	Left atrial pressure	
AoP	Ascending aorta pressure	mmHg
F	Total flow	mL/s

General introduction

1 Introduction

In the field of nonlinear control systems, understanding the observability properties of multi-input multi-output (MIMO) systems is crucial for accurate state estimation, effective control, and reliable fault detection. Observability defines whether the internal states of a system can be deduced from its outputs over time, forming a foundational concept in the design of observers that ensure robust system performance across diverse operational conditions. However, traditional approaches to observability in nonlinear systems often encounter limitations with complex dynamics and higher-order terms, underscoring the need for more generalized approaches.

This thesis introduces a novel approach for analyzing observability in nonlinear MIMO systems by developing a higher-order observability normal form, specifically based on the second-order Poincaré normal form. The proposed method extends the classical theory of observability by incorporating higher-order terms, thereby providing a more comprehensive understanding of the observability properties of nonlinear systems. Unlike existing approaches, this method offers a new solution to homological equations, allowing for a broader application to both linearly observable and linearly unobservable systems. The study focuses on the quadratic observability normal form, outlining its characteristics in different scenarios and providing a deeper analysis of system dynamics that were previously inaccessible through traditional means.

A key contribution of this research is the application of the quadratic observability normal form to the modeling and analysis of a nonlinear cardiovascular system. The cardiovascular system is a complex, nonlinear system that is not fully observable using standard linear techniques. By transforming the cardiovascular model into a quadratic observability normal form, the research demonstrates how this representation facilitates the design of a sliding mode observer (SMO) capable of estimating unobservable state variables. This transformation is critical for detecting faults such as mitral and aortic valve dysfunctions, which are significant risk factors for cardiovascular diseases. The observer is designed to overcome the limitations of conventional methods, allowing for accurate state reconstruction even in the presence of observability singularities.

The practical significance of this approach is highlighted through numerical simulations, which show that the sliding mode observer can effectively detect and isolate cardiovascular anomalies. The results indicate that the proposed observer is capable of reconstructing system dynamics under various fault conditions, offering a less invasive, cost-effective, and efficient alternative for monitoring cardiovascular health. This research not only advances the theoretical understanding of observability in nonlinear systems but also provides a valuable tool for clinical decision support in cardiology.

The thesis is organized as follows: Section 2 introduces the quadratic equivalence of two systems modulo an output injection, leading to the formulation of homological equations. Sections 3 and 4 explore the general cases of linearly observable and linearly unobservable systems, respectively, presenting the necessary conditions for transforming a given system into its quadratic observability normal form. Section 5 applies

these findings to the design of a sliding mode observer for a nonlinear cardiovascular model, providing both theoretical insights and practical examples. Finally, the effectiveness of the proposed methods is validated through numerical simulations and compared with existing clinical data.

By combining advanced mathematical techniques with practical observer design, this thesis aims to bridge the gap between theoretical control methods and their application to real-world biomedical systems. The results demonstrate the potential for wider applications in fields where precise state estimation and fault detection are crucial, setting the stage for future research in nonlinear system observability and control.

2 Problem formulation

The problematic to be addressed the challenge of analyzing and controlling nonlinear multi-input multi-output (MIMO) systems, with a specific focus on observability in complex systems. Traditional methods often struggle with nonlinearities and the complexity of multi-input and multi-output configurations. This thesis introduces a novel method for higher-order observability normal form, leveraging the second-order Poincaré normal form to resolve homological equations. The research aims to advance the theoretical framework of observability by outlining the characteristics of quadratic observability normal forms, both in linearly observable and unobservable scenarios.

The core problem revolves around the development and application of this novel method to the cardiovascular system (CVS), which presents both normal and pathological conditions within systemic circulation. The challenge is to accurately simulate the CVS through a quadratic normal form representation and to implement a Sliding Mode Observer (SMO) for effective state estimation and anomaly detection. This includes identifying valvular heart diseases that are critical risk factors for cardiovascular health.

This research provides a significant advancement in nonlinear observability theory, offering a novel approach to resolving complex systems through quadratic observability normal forms. The application to cardiovascular system modeling aims to enhance diagnostic capabilities and improve the detection of critical conditions, potentially leading to better management of cardiovascular diseases.

3 Objectives of the thesis

3.1 General objective

The main objective of this research is to develop analysis and design of observer-based virtual sensors through of the transformation to the quadratic observability normal form of Multiple-Input Multiple-Output (MIMO) systems. Application to the monitoring of cardiovascular system dynamics.

Unlike of the quadratic observability normal for of Single-Input Single-Output (SISO) systems, for or Multiple-Input Multiple-Output (MIMO) systems, there is no straightforward, universally accepted "observability normal form". The reasons include the increased dimensionality and the more complex interdependencies between inputs and outputs in MIMO systems. The observability normal forms simplify the analysis and design by transforming the system into a specific canonical form that makes it easier to analyze observability properties. However, for MIMO systems, the situation is more complex due to the presence of multiple inputs and outputs. The following research objectives will be achieved:

3.2 Specific objectives

- To select the model of the cardiovascular system.
- To study the operation and dynamics of the model of the cardiovascular system to design a appropriate observer.
- Transformation of MIMO nonlinear systems to the observable quadratic normal form, with application to the cardiovascular system model.
- To perform observability using observable normal form of nonlinear systems.
- Structural observability analysis by using the system dynamics.

4 Main contributions

The main contribution of this thesis is develop and implement a methodology for transforming nonlinear Multiple-Input Multiple-Output (MIMO) systems into a quadratic observability normal form, thereby advancing the analysis and design of observer-based virtual sensors for monitoring complex systems such as cardiovascular dynamics. This involves extending existing methods for Single-Input Single-Output (SISO) systems has been done in ([10]) to MIMO systems, addressing the increased complexity and interdependence's, and demonstrating the utility of this approach through theoretical developments and numerical examples. The scientific contributions of this thesis are listed as follows:

- **Development of a novel methodology:** A significant contribution is the extension of the quadratic observability normal form methodology to nonlinear multi-input multi-output (MIMO) systems, which has not been addressed in existing literature. This builds on and refines existing approaches, particularly those outlined in previous works such as ([10]).
- **Extension of existing methods:** Expansion of methods originally designed for SISO systems to accommodate the concept of observability normal form of MIMO systems, providing a more comprehensive framework for simplify the analysis and design by transforming the system into a specific canonical form that makes it easier to analyze observability properties and design observer-based virtual sensors.
- **Resolution of homological equations:** The thesis develops a novel approach to solving homological equations in the second-order Poincaré normal form of observability. This approach enhances the resolution of these equations, contributing new insights into the quadratic observability normal form for nonlinear systems.
- **Characterization of quadratic observability:** Detailed analysis of the quadratic observability normal form in both linearly observable and linearly unobservable scenarios, enhancing the theoretical foundation for observability analysis.
- **Illustrative numerical examples:** The thesis includes practical applications and numerical examples demonstrating how the proposed methodology can be applied to real-world systems, such as cardiovascular dynamics, thereby validating the approach and showcasing its practical utility.
- **Development of a new model of the cardiovascular system:** The research presents a new mathematical representation of the cardiovascular system that leverages novel transformations to place the system into a quadratic observability normal form, demonstrating how the proposed methodology can be applied. This contribution makes it easier to analyze observability properties and design of observers for cardiovascular system.

- **Observer based virtual sensor design:** By transforming the cardiovascular system model into the quadratic observability normal form, the research facilitates the design of observer-based virtual sensors. These sensors are crucial for monitoring cardiovascular dynamics and investigating the impact of various pathologies. These contributions not only advance the theoretical understanding of observability in complex MIMO systems but also provide practical tools and methodologies for monitoring and analyzing cardiovascular system dynamics.

5 Outline of the thesis

This thesis consists of four principal chapters. The following paragraphs gives more details about the content of each part :

Chapter 1 introduces key concepts of observability in nonlinear systems and the role of the Poincaré normal form in their analysis. It covers the Poincaré linearization technique, which approximates nonlinear systems with simpler linear models using polynomial methods. Additionally, it discusses higher-order stability forms and the quadratic observability normal form for SISO systems. Real-world examples, such as the Lorentz system, are provided to illustrate the importance of these theoretical concepts in system analysis and control.

Chapter 2 focuses on applying the quadratic observability normal form to nonlinear multi-output systems. It begins by studying this form, distinguishing between linearly observable and unobservable cases, and then extends these concepts to MIMO systems, exploring both observable and unobservable situations. It also introduces the design of sliding mode observers for these systems. Illustrative examples demonstrate the practical utility of the quadratic observability normal form for system analysis and observer design in real-world MIMO scenarios.

Chapter 3 is dedicated to applies the concepts of quadratic observability normal form to the cardiovascular system (CVS). It begins with an introduction to the anatomy and physiology of the cardiac cycle, including common valve pathologies. The chapter then presents a model of the cardiovascular system, detailing its equivalent electric model, elastance, and the underlying mathematical framework. In addition, the quadratic normal form of the CVS is discussed, alongside validation techniques for this model. An observability analysis is conducted, assessing the observability of the cardiovascular system and leading to the design of sliding mode observers specifically tailored for the CVS. The chapter concludes by emphasizing the significance of these methods in improving the understanding and monitoring of cardiovascular dynamics.

Chapter 4 provides the methodologies for diagnosing and detecting anomalies within the cardiovascular system. It begins with an introduction to the principles of diagnostic techniques and fault detection methodologies, including a classification of various methods used in the field. The chapter then expands on the cardiovascular model to enhance anomaly detection, introducing a residual generator specifically designed for detecting cardiovascular anomalies. Simulation results are presented to demonstrate the effectiveness of the proposed methods, with scenarios including mitral regurgitation, aortic regurgitation, and simultaneous occurrences of both conditions. These simulations illustrate the application of the diagnostic methodologies in identifying and understanding cardiovascular anomalies.

Chapter 1

Definitions and issues related to observability and the Poincaré normal form

Contents

1.1	Introduction	1
1.2	Basic properties of observability and nonlinear systems	2
1.2.1	Linear systems	2
1.2.2	Nonlinear systems.	3
1.3	Design of observers	5
1.3.1	State estimation principle	5
1.3.2	Luenberger observer	5
1.3.3	Kalman filter	5
1.3.4	Extended Kalman filter	6
1.3.5	High-gain observer	7
1.3.6	Sliding mode observers	9
1.3.7	Characteristics of sing function approximation forms	14
1.4	Higher-order linearization and normal form	16
1.4.1	The resonances	16
1.4.2	Poincaré Normal Forms computation	18
1.5	Quadratic observability normal form for nonlinear SISO system	21
1.5.1	Quadratic equivalence modulo an output injection	22
1.5.2	Linearly observable case for nonlinear SISO system	23
1.5.3	One dimensional linearly unobservable case	28
1.6	Conclusion	33

1.1 Introduction

This chapter presents the fundamental concepts of observability and observer design for nonlinear systems, with a particular focus on the sliding mode observer. It also examines the Poincaré linearization technique, which relies on polynomial methods to simplify the analysis of nonlinear systems by approximating them

with linear or higher-order models. Additionally, it introduces the quadratic normal form of observability for SISO systems, providing a detailed view of observability near singularities. These theoretical principles are illustrated through practical examples, notably the Lorenz system, highlighting the relevance of these approaches for the analysis and control of complex dynamic systems.

1.2 Basic properties of observability and nonlinear systems

In control theory, observability characterizes the property of being able to recover (statically or dynamically) by a combination of measurements and their derivatives all the quantities of a system. Checking the observability of a system is crucial for determining whether the internal state of a system can be inferred from its outputs over time, given certain inputs. The rank test of the observability matrix is one of the most common methods for this purpose. Here's a step-by-step explanation of how to apply the rank test in linear and nonlinear systems.

1.2.1 Linear systems

We recall here the classic results of observability and synthesis of observers for linear systems such as can be found in [42, 104].

$$\begin{aligned}\dot{x}(t) &= Ax(t) + Bu(t) \\ y(t) &= Cx(t) + Du(t)\end{aligned}\tag{1.1}$$

where $x \in \mathbb{R}^n$ is the state vector, $u \in \mathbb{R}^m$ is input, $y \in \mathbb{R}^p$ represents the measured output vector. Matrices A , B and C are real and of appropriate dimensions.

The observability property of such a system corresponds to the fact that the state $x(t)$ can be determined on any interval $[t_0, t_1]$ from the knowledge of $u(t)$ and $y(t)$ and can be formalized as follows

Definition 1.2.1 [42, 104] *The system (1.1) is observable if, given an instant t_0 , there exists a finite instant t_1 such that knowledge of $y(t_0, t_1)$ and $u(t_0, t_1)$ uniquely determines the state $x(t_0) = x_0$, whatever the system input. The observability matrix \mathcal{O} is constructed using the system matrices A and C . For an n -dimensional state vector, the observability matrix is given by:*

$$\mathcal{O} = \begin{bmatrix} C \\ CA \\ CA^2 \\ \vdots \\ CA^{n-1} \end{bmatrix}.$$

To determine if the system is observable, compute the rank of the observability matrix \mathcal{O} .

Definition 1.2.2 *The system (1.1) is observable if and only if:*

$$\text{rank}(\mathcal{O}) = n.$$

We then say that the pair (C, A) is observable. If the rank is less than n , the system is not fully observable.

1.2.2 Nonlinear systems.

In the context of nonlinear systems, the problem of observability of nonlinear systems is complicated, since observability in this case depends on the applied input. The observability of nonlinear systems is defined in terms of indistinguishability. A synthesis on the question is given in [30]. In the following, the different definitions of observability will be given considering the nonlinear system described by the following equations:

$$\Sigma \begin{cases} \dot{x}(t) &= f(x(t)) \\ y(t) &= h(x(t)) = [h^1(x(t)), h^2(x(t)), \dots, h^p(x(t))]^T \end{cases} \quad (1.2)$$

with $x \in \mathbb{R}^n$ is the state vector, $u \in \mathbb{R}^m$ is input, $y \in \mathbb{R}^p$ represents the measured output vector. Matrices A , B and C are real and of appropriate dimensions.

1.2.2.1 Observability and range conditions

Definition 1.2.3 (*Distinguishability [30, 29, 66, 100]*): Two initial states $x(t_0) = x_1$ and $x(t_0) = x_2$ such that $x_1 \neq x_2$ are said to be distinguishable for the system (1.2), if $\forall t \geq t_0$, $y_1(t) \neq y_2(t)$, we have the corresponding outputs $y_1(t)$ and $y_2(t)$ verify $y_1(t) \neq y_2(t)$.

Definition 1.2.4 (*Indistinguishability [30, 29, 66, 100]*): Two initial states $x(t_0) = x_1$ and $x(t_0) = x_2$ are said to be indistinguishable for the system (1.2) if $\forall t \in [t_0, t_1]$, the corresponding outputs $y_1(t)$ and $y_2(t)$ are the same for both states over any finite time interval, for every possible input $u(t)$ of the system.

It is now possible to define the observability of a system at a point, and by extension, to define an observable system.

Definition 1.2.5 (*Observability [30, 29, 66, 100]*): The system (1.2) is observable at x_0 if x_0 is distinguishable from all $x \in \mathbb{R}^n$. The system (1.2) is observable if $\forall x_0 \in \mathbb{R}^n$, x_0 is distinguishable

Definition 1.2.6 (*Local observability [30, 29, 66, 100]*): The state x_0 is locally observable if there exists an open neighborhood V of x_0 such that for any open neighborhood U of x_0 contained in V , $I_U(x_0) = \{x_0\}$; and the system (1.2) is said to be locally observable if for any $x \in U$ of \mathbb{R}^n , $I_U(x) \cap V(x) = x$.

In the context of nonlinear systems, local observability is important concept for understanding how well the state of a system can be inferred from observations, particularly when the states are close to each other. The local observability ensures that the trajectories of the system do not need to deviate much from the initial conditions to distinguish two points. This notion of observability becomes locally weak when we are only interested in the discernibility of initial states close to each other. A system is locally observable at a point x_0 if the observability space at x_0 spans the entire space of possible output changes. Specifically:

Definition 1.2.7 The observability space ($d\mathcal{O}(x_0)$)(i.e. evaluated at x_0) characterizes the local observability at x_0 of the system (1.2). The system (1.2) is said to satisfy the condition of observability rank at x_0 if

$$\dim d\mathcal{O}(x_0) = \dim \mathcal{X} = n \quad (1.3)$$

The system (1.2) satisfies the observability rank condition if, for all $x \in \mathbb{R}^n$

$$\dim d\mathcal{O}(x) = \dim \mathcal{X} = n \quad (1.4)$$

- Rank condition

Let the observability space \mathcal{O} be generated on \mathbb{R}^n by all the one-forms associated with h and the derivatives of h . Therefore, according to (1.2), we have:

$$y^{(1)}(t) = \frac{dh(x(t))}{dt} = \frac{\partial h(x(t))}{\partial x} \cdot \frac{dx(t)}{dt} = \frac{\partial h(x(t))}{\partial x} \cdot f(x(t)) = L_f^1 h(x(t)) \quad (1.5)$$

with $L_f^1 h(x(t))$ is the Lie derivative of the function h with respect to the function f at the first order. Indeed, we define the successive Lie derivatives of the function h with respect to the function f as:

$$L_f^k h(x(t)) = L_f[L_f^{k-1} h(x(t))]; \text{ with } L_f^0 h(x(t)) = h(x(t)) = y(t) \quad (1.6)$$

In the same way, we can write :

$$\begin{aligned} y^{(2)}(t) &= \frac{d^2 h(x(t))}{dt^2} = \frac{d}{dt} \left[\frac{dh(x(t))}{dt} \right] = \frac{d}{dt} \left[L_f^1 h(x(t)) \right] \\ &= \frac{\partial [L_f^1 h(x(t))]}{\partial x} \cdot \frac{dx(t)}{dt} = \frac{\partial [L_f^1 h(x(t))]}{\partial x} \cdot f(x(t)) = L_f \left[L_f^1 h(x(t)) \right] \\ &= L_f^2 h(x(t)) \end{aligned}$$

From which we can deduce that property (1.2) is also verified at order 2 and subsequently, it is easy to verify it up to order n :

$$y^{(n)}(t) = L_f^n h(x(t)) \quad \forall n \in \mathbb{N}$$

We call the rank of observability, denoted $rank(\mathcal{O})$, we can then verify

$$rang \begin{pmatrix} y \\ dy^{(1)} \\ dy^{(2)} \\ \vdots \\ dy^{(n-1)} \end{pmatrix} = rang \begin{pmatrix} h \\ L_f h(x) \\ L_f^2 h(x) \\ \vdots \\ L_f^{(n-1)} h(x) \end{pmatrix}$$

Note that the definitions of observability given above are all for free systems (i.e. independent of the system's input), but in practice, all systems are controlled and admit possible inputs. In this context, the concept of observability is defined in terms of inputs which, as for the state of free systems, is based on the principle of indistinguishability.

Definition 1.2.8 (Universal input [30, 29, 66, 100]): Given the system (1.2), the input $u(t)$ is said to be a universal input on the time interval $[0, t]$ if it distinguishes any pair of different initial points $\{x_0, \tilde{x}_0\}$ can be discerned by the outputs on the interval $[0, t]$, that is, if there exists $\tau \in [0, t]$ such that $h(\chi_u(t, x_0)) \neq h(\chi_u(t, \tilde{x}_0))$.

In other words, the universality of an input means the possibility, for this given input, of discerning all pairs of initial states.

Definition 1.2.9 Singular inputs: A non-universal input will be called a singular input.

When there is no singular input among the set of admissible inputs R_m , then any pair of initial states are distinguishable. This property is called observability for any input.

Definition 1.2.10 (Observability for any input [100]): A system for which all admissible inputs valued in \mathbb{R}^m are universal is said to be observable for any input (and we will subsequently say uniformly observable).

1.3 Design of observers

The application of state observers, also known as software sensors, in system control is a trend that continues to grow. Initially, the purpose of the observation was to estimate quantities that were difficult to measure, such as temperature fluctuations in chemical reactions, pressure variations in fluid dynamics, or rotor fluxes in an asynchronous machine, to enhance control performance. However, state observers are now employed for a variety of purposes such as senseless control, fault tolerant control, parameter identification and estimation.

This section focuses on the presentation of overview of the state estimation principle and the synthesis of observers for of linear and nonlinear systems.

1.3.1 State estimation principle

Definition 1.3.1 *State estimation involves the process of estimating the internal state of a system based on available measurements and a mathematical model. It is crucial for enabling effective control when direct measurement of all states is not feasible.*

Definition 1.3.2 *A state observer is a mathematical algorithm that is used to estimate (reconstruct) the state x of a dynamic system, from the available measurements (outputs y) and inputs u , based on a representative model of the system.*

1.3.2 Luenberger observer

Theorem 1.3.1 [69] *If a linear invariant system is observable, then there exists an observer of the form:*

$$\dot{\hat{x}} = A\hat{x} + Bu + K(y - C\hat{x}) = (A - KC)\hat{x} + Bu + Ky \quad (1.7)$$

In this case, the eigenvalues of the matrix $A - KC$ can be arbitrarily placed in the left half-plane, by choosing the matrix K of dimension $n \times p$

The dynamics of the observation error $\tilde{x} = x - \hat{x}$ is:

$$\dot{\tilde{x}} = (A - KC)\tilde{x} \quad (1.8)$$

The same matrix $A - KC$ appears in the dynamics of the observed state and in that of the error. Therefore, if the observer is stable, the error \tilde{x} tends to 0 asymptotically ($\lim_{t \rightarrow +\infty} \tilde{x} = 0$). In a Luenberger type observer, the choice of the matrix K is said by pole placement (of the observer, therefore of the eigenvalues of the matrix $A - KC$). The matrix K is constant in this case.

1.3.3 Kalman filter

The Kalman filter is a linear quadratic estimator that estimates unknown variables of a system from (possibly noisy) measurements. It is named after one of its first developers Rudolph E. Kalman [43, 44].

The Kalman filter finds its applications in a wide variety of technological fields. We will restrict our presentation to its application as a state observer in a deterministic context. In this case, the Kalman filter is an optimal observer, in the sense that its synthesis constitutes a dual version of the search for a state feedback by quadratic linear control.

For linear systems, the observation structure by Kalman filtering is the same as that of a Luenberger type observer:

$$\dot{\hat{x}} = A\hat{x}(t) + Bu(t) + K(t)[y(t) - C\hat{x}(t)] \quad (1.9)$$

The originality of the filter is in the calculation of the gain matrix $K(t)$, which is not (necessarily) constant, which makes the Kalman filter better suited to time-varying systems. The formula for the observer gain is:

$$K(t) = P(t)C^T R^{-1} \quad (1.10)$$

where $P(t)$, the observation error covariance matrix, is the solution to the Riccati differential equation

$$\dot{P}(t) = AP(t) + P(t)A^T + Q - P(t)C^T R^{-1} CP(t); P(0) = P_0 \quad (1.11)$$

The matrices Q , R and P_0 are positive definite symmetric matrices. In the context of state reconstruction, they are considered as weighting matrices that are used to adjust the observer dynamics, if we increase all the coefficients of Q , the reconstruction dynamics becomes faster, and if, conversely, we increase all the coefficients of R , the filtering of measurement noise becomes more important, and the observation dynamics slows down. There are no systematic methods to calculate these two matrices, their adjustment requires expertise on Kalman filtering and on the observed system.

The matrix P_0 plays a role on the observer dynamics at the start of the algorithm; large values of its coefficients mean that a large initial error is expected, which generates faster observation dynamics at start-up, and vice versa.

1.3.4 Extended Kalman filter

For nonlinear systems, there is an extended (local) version of the Kalman filter, based on the linearization of the system. Let us the observation error:

$$\dot{\tilde{x}} = F(x, u) - f(\hat{x}, u)K(\cdot)[h(x) - h\hat{x}] \quad (1.12)$$

The Taylor series expansion of this equation around $\tilde{x} = 0$, by evaluating the Jacobian around \hat{x} , gives

$$\dot{\tilde{x}} = [A(t) - K(t)C(t)]\tilde{x} + \delta(\tilde{x}, x, u) \quad (1.13)$$

where

$$A(t) = \frac{\partial f}{\partial x}(\hat{x}(t), u(t)); C(t) = \frac{\partial h}{\partial x}(\hat{x}(t)) \quad (1.14)$$

and

$$\delta = f(x, u) - f(\hat{x}, u) - A(t)\tilde{x} - K(t)[h(x) - h(\hat{x}) - C(t)\tilde{x}] \quad (1.15)$$

The extended Kalman filter is widely used in industry for nonlinear systems.

On the other hand, the discrete-time Kalman filter algorithm consists of two main steps: Prediction and Correction. Here's the algorithm for the discrete version [48]:

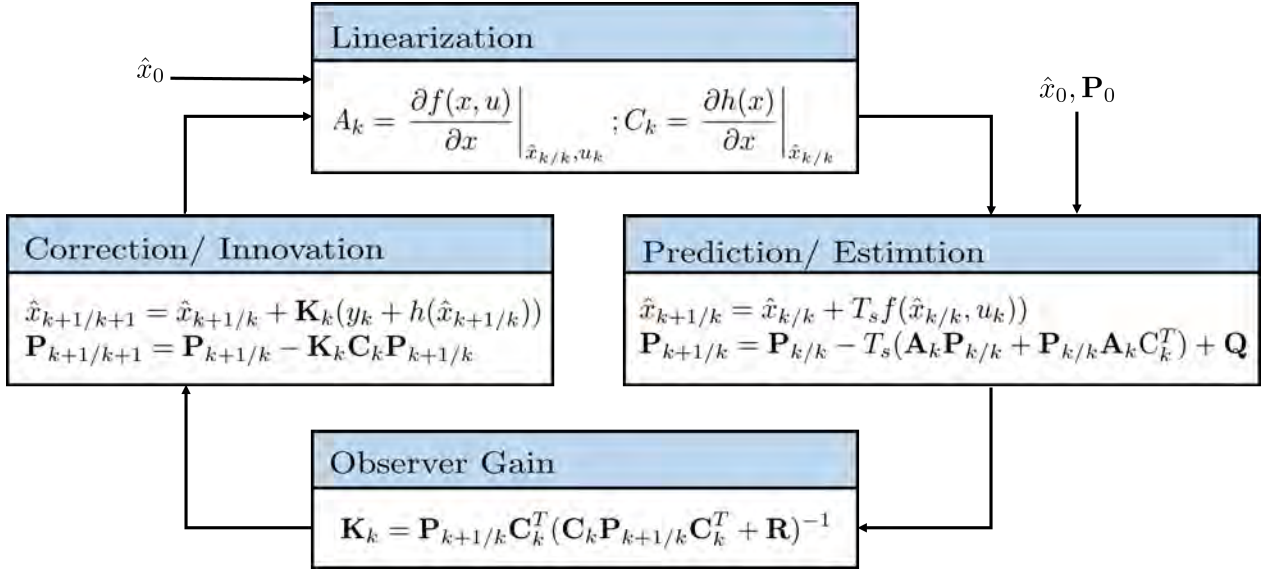


Figure 1.1: Discrete-time Kalman filter algorithm.

1.3.5 High-gain observer

A high-gain observer is a type of state observer designed to provide robust state estimation for dynamic systems, especially in the presence of disturbances and measurement noise. It achieves high accuracy in state estimation by employing large observer gains. One of the most comprehensive and satisfactory contributions to the theory of nonlinear observers has been provided by [28]. It belongs to the family of high-gain observers. The authors demonstrate that, with an appropriate change of coordinates, the states of the nonlinear system can be tracked not only locally but also globally in an asymptotic manner. The tuning or calibration of this type of observer is done by adjusting a single parameter, called the observer gain, determined by solving a Lyapunov equation.

High-gain observers essentially require the existence of a globally defined change of coordinates that satisfies the Lipschitz condition. If the system is uniformly observable for any input, then a global and convergent observer can be constructed for a nonlinear system with inputs, also referred to as a non-autonomous system.

This section presents the methodology and the necessary conditions to develop a high-gain observer, whose objective is to estimate the states of a control-affine nonlinear system. To formulate the high-gain observer, we start from the general form of control-affine nonlinear systems:

$$\begin{aligned} \dot{x}(t) &= f(x(t)) + \sum_{i=1}^m u_i(t) g_i(x(t)) \\ y(t) &= h(x(t)) \end{aligned} \quad (1.16)$$

where $x(t) \in \mathbb{R}^n$, $u_i(t) \in \mathbb{R}^m$, $i = 1, \dots, m$ where m it is the number of inputs $y(t) \in \mathbb{R}^p$, $f(x(t)) \in \mathbb{R}^n$, and $g_i(x(t)) \in \mathbb{R}^n$ these last two are vector fields.

The design of the observer is based on the following hypothesis

- The nonlinear system is uniformly observable.

- The observability matrix is of rank n at a point x_0 , i.e., it is invertible.

- The matrix $\phi(x) = \begin{bmatrix} h(x(t)) \\ L_f h(x(t)) \\ \vdots \\ L_f^{n-1} h(x(t)) \end{bmatrix}$ is a diffeomorphism.

Given the previous characteristics, it is possible to perform a change of coordinates or a transformation of the original system where:

$$z(t) = \phi(x(t)) = [h(x(t)) \quad L_f h(x(t)) \quad \dots \quad L_f^{n-1} h(x(t))]^T \quad (1.17)$$

The notation $L_f(\cdot)$ represents the Lie derivative of a real function evaluated at $f(x(t))$. By definition, the Lie derivative is:

$$L_f h(x(t)) = \frac{\partial h(x(t))}{\partial x} f(x(t)) = \sum_{i=1}^n \frac{\partial h(x(t))}{\partial x} f_i(x(t)) \quad (1.18)$$

Such a coordinate transformation $\phi(x(t))$ defines a diffeomorphism that transforms the nonlinear system into a triangular form as

$$\begin{aligned} \dot{z}(t) &= Az(t) + \psi(z(t)) + \sum_{i=1}^m \phi_i(z(t))u_i(t) \\ y(t) &= Cz(t) \end{aligned} \quad (1.19)$$

where

$$z_1 = h(x(t)), z_2 = L_f h(x(t)), z_3 = \dots, z_n = L_f^{n-1} h(x(t)) \quad (1.20)$$

$$\begin{aligned} A &= \begin{bmatrix} 0 & 1 & 0 & 0 \\ \vdots & \dots & 0 & 0 \\ 0 & \ddots & 0 & 1 \\ 0 & \dots & 0 & 0 \end{bmatrix} & \psi(z(t)) &= \begin{bmatrix} 0 \\ \vdots \\ 0 \\ L_f^n h(x(t)) \end{bmatrix} \\ C &= [1 \quad 0 \quad \dots \quad 0] \end{aligned} \quad (1.21)$$

The elements of $\phi_i(z(t))$ are:

$$\begin{aligned} \phi(z(t)) &= \phi_1(z_1(t)) \\ \phi(z(t)) &= \phi_2(z_1(t), z_2(t)) \\ &\vdots \\ \phi_n(z(t)) &= \phi_n(z_1(t), \dots, z_{n-1}(t)) \end{aligned} \quad (1.22)$$

This transformation allows us to return to the original coordinates, $x(t) = \phi^{-1}(z(t))$. The observer proposed by [28] for the estimation of the transformed states has the following form:

$$\dot{\hat{z}}(t) = A\hat{z}(t) + \psi(\hat{z}(t)) + \sum_{i=1}^m \phi_i(\hat{z}(t))u_i(t)S_\theta^{-1}C^T(C\hat{z}(t) - y(t)) \quad (1.23)$$

where the symbol $\hat{\cdot}$ signifies the estimated value. As can be seen, the observer is just a copy of the transformed system, plus a correction term that depends on the measured output of the system. The matrix S_θ is the solution to the Lyapunov equation:

$$\theta S_\theta + A^T S_\theta + S_\theta A = C^T C \quad (1.24)$$

where the parameter $\theta > 0$ is called the observer gain. This parameter determines the convergence rate of the estimation and is set by the designer. The form of the gain matrix S_θ for a second-order system is presented below:

$$S_\theta = \begin{bmatrix} \frac{1}{\theta} & -\frac{1}{\theta^2} \\ -\frac{1}{\theta^2} & \frac{2}{\theta^3} \end{bmatrix} \quad (1.25)$$

In general, the coefficients of S_θ are of the form:

$$S_{i,j} = \frac{S_{i,j}}{\theta^{i+j-1}}, 1 \leq i, j \leq n \quad (1.26)$$

In the original coordinates, the system from Eq. (1.23) is rewritten as follows:

$$\begin{aligned} \dot{\hat{x}}(t) &= f(\hat{x}(t)) + g(\hat{x}(t))u(t) + \left[\frac{\partial \phi(\hat{x}(t))}{\partial \hat{x}} \right]^{-1} S_\theta^{-1} C^T [y(t) - \hat{y}(t)] \\ \hat{y} &= C \hat{x}(t) \end{aligned} \quad (1.27)$$

The structure of the observer consists of a copy of the mathematical model of the system, plus a correction term where $\frac{\partial \phi(x(t))}{\partial x}$ is the Jacobian matrix of $\phi(x(t))$, and $\phi(\hat{x}(t)) = \phi(x(t))|_{x(t)=\hat{x}(t)}$. To verify that the system is observable, the matrix $\frac{\partial \phi(x(t))}{\partial x}$ must be of full rank.

1.3.6 Sliding mode observers

The main purpose of this section is to briefly introduce the types of the sliding mode observer and to demonstrate the main properties of this observers. Among the different types of observers, sliding mode observers (SMO) stand out for their robustness in the presence of system uncertainties and external perturbations. Sliding mode observers are based on the principle of sliding mode control, which consists of applying a high-frequency switched control signal to drive the system states towards a predefined sliding surface. After the system reaches this surface, the dynamics is governed by a reduced-order system, less sensitive to uncertainties and disturbances. This property makes SMO particularly suitable for systems with nonlinear dynamics or time-varying parameters [102].

The design and classification of sliding mode observers can be organized based on various criteria, such as the system model (linear or nonlinear), the type of sliding surface, or the observer structure. Some common classifications include:

The following information is applicable to both linear [25] and nonlinear systems [76], as the methods discussed can be adapted to the characteristics and dynamics of either system type. High-order sliding mode observers, discrete sliding mode observers, and adaptive sliding mode observers are versatile techniques that enhance performance in a wide range of applications, regardless of the linearity or nonlinearity of the system.

- **High-Order Sliding Mode Observers (HOSMOs)**

Traditional sliding mode observers can suffer from chattering, a phenomenon caused by high-frequency oscillations near the sliding surface. High-order sliding mode observers address this issue by incorporating higher-order terms into the observer design, leading to smoother estimates and reduced chattering.

- **Discrete Sliding Mode Observers (DSMOs)**

These observers are designed for discrete-time systems, which are particularly relevant in digital control applications. The observer operates based on sampled data, making it ideal for systems where continuous measurements are not available.

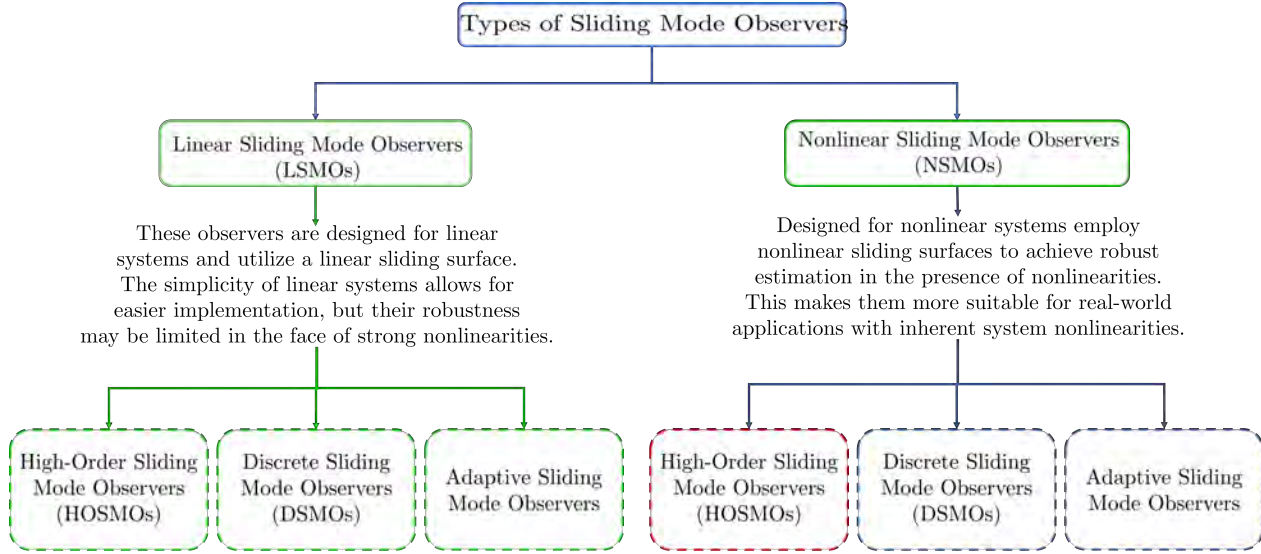


Figure 1.2: Classification and Types of Sliding Mode Observers.

- **Adaptive Sliding Mode Observers**

These observers adjust their parameters in real time to handle uncertainties or changes in system dynamics. This adaptability improves performance in systems with time-varying or uncertain parameters.

In the following section, the structure for nonlinear systems is presented, excluding linear ones, since the analysis and techniques discussed in this thesis are specifically designed to address the unique characteristics of nonlinear systems, which are the primary focus of this work.

1.3.6.1 Nonlinear sliding mode observer

Walcott and Zak made separate early contributions to this topic, as did Slotine et al. We assume the sliding mode observer to have the form [95, 97].

$$\begin{aligned}
 \hat{\dot{x}}_1 &= -\alpha_1 e_1 + \hat{x}_2 - k_1 \text{sign}(e_1) \\
 \hat{\dot{x}}_2 &= -\alpha_2 e_2 + \hat{x}_3 - k_2 \text{sign}(e_1) \\
 &\vdots \\
 \hat{\dot{x}}_n &= -\alpha_n e_1 + \hat{f} - k_n \text{sign}(e_1)
 \end{aligned} \tag{1.28}$$

where $e_1 = \hat{x} - x_1$, \hat{f} is an estimate of $f(x, t)$ and the constant variable α_i are chosen as for a classical Luenberger observer to ensure asymptotic error of a corresponding linearised system, where $k_i = 0$. The resulting error dynamics can be written:

$$\begin{aligned}
 \dot{e}_1 &= -\alpha_1 e_1 + e_2 - k_1 \text{sign}(e_1) \\
 \dot{e}_2 &= -\alpha_2 e_1 + e_3 - k_2 \text{sign}(e_1) \\
 &\vdots \\
 \dot{e}_n &= -\alpha_n e_1 + \Delta f - k_n \text{sign}(e_1)
 \end{aligned} \tag{1.29}$$

where $\Delta f = \hat{f} - f$ is assumed bounded and

$$k_n \geq |\Delta f| \tag{1.30}$$

The sliding condition is defined by $(d/dt)(e_1)^2 < 0$ is satisfied in the region

$$\begin{aligned} e_1 + \alpha_1 e_1 & \text{ if } e_1 > 0 \\ e_2 \geq -k_1 + \alpha_1 e_1 & \text{ if } e_1 < 0 \end{aligned} \quad (1.31)$$

form $\dot{e}_1 = -\alpha_1 e_1 + e_2 - k_1 \text{sign}(e_1)$, when a sliding mode is attained on $e_1 = 0$ with

$$e_2 - k_1 \text{sign}(e_1) = 0 \quad (1.32)$$

and consequently

$$\begin{aligned} \dot{e}_1 &= e_3 - \frac{k_2}{k_1} e_2 \\ &\vdots \\ \dot{e}_n &= \Delta f - \frac{k_n}{k_1} e_2 \end{aligned} \quad (1.33)$$

The next significant advancement in the development of sliding mode observers for non-linear systems is found in the article by Drakunov and Utkin [20], where the concept of equivalent injection was introduced for observer design. Following this, Boukhobza et al. [9] applied the output injection approach proposed by Krener and Isidori [49] to design a sliding mode observer. This same team also developed a sliding mode observer for non-linear systems in triangular input form in Barbot et al.[6]. These systems were initially explored in the foundational work by [20] and are noteworthy because they enable the development of an observer for nonlinear systems in triangular input form.

1.3.6.2 Sliding mode observer in the triangular input form

Considering the system presented in [6], the authors in [20, 9] and [6] establish the following result

$$\begin{aligned} \dot{\hat{\xi}}_1 &= \hat{\xi}_2 + \bar{g}_1(\xi_1, u) + \lambda_1 \text{sign}(\xi_1 - \hat{\xi}_1) \\ \dot{\hat{\xi}}_2 &= \hat{\xi}_3 + \bar{g}_2(\xi_1, \xi_2, u) + \lambda_2 \text{sign}(\tilde{\xi}_2 - \hat{\xi}_2) \\ &\vdots \\ \dot{\hat{\xi}}_{n-1} &= \hat{\xi}_n + \bar{g}_{n-1}(\xi_1, \tilde{\xi}_2, \dots, \tilde{\xi}_{n-1}, u) + \lambda_{n-1} \text{sign}(\tilde{\xi}_{n-1} - \hat{\xi}_{n-1}) \\ \dot{\hat{\xi}}_n &= \bar{f}_n(\xi_1, \tilde{\xi}_2, \dots, \tilde{\xi}_n) + \bar{g}_n(\xi_1, \dots, \tilde{\xi}_n, u) + \lambda_n \text{sign}(\tilde{\xi}_n - \hat{\xi}_n) \end{aligned} \quad (1.34)$$

where

$$\tilde{\xi}_i = \hat{\xi}_i + \lambda_{i-1} \text{sign}(\xi_{i-1} - \hat{\xi}_{i-1}) \quad (1.35)$$

for $i = 2, \dots, n_1$, the function $\text{sign}(\cdot)$ is determined using filtered versions of the argument. The manifolds are approached sequentially, and $e_i = \tilde{\xi}_i - \hat{\xi}_i$ converges to zero if $e_j = \tilde{\xi}_j - \hat{\xi}_j$ with $j < i$ has already converged to zero. This sequential consideration of a series of first-order dynamics is evident when forming the error dynamics for $e_i = \xi - \hat{\xi}_i$:

$$\begin{aligned} \dot{e}_1 &= e_2 - \lambda_1 \text{sign}(\xi_1 - \hat{\xi}_1) \\ \dot{e}_2 &= e_3 + \bar{g}_2(\xi_1, \xi_2, u) - \bar{g}_2(\xi_1, \tilde{\xi}_2, u) - \lambda_2 \text{sign}(\tilde{\xi}_2 - \hat{\xi}_2) \\ &\vdots \\ \dot{e}_{n-1} &= \hat{\xi}_n - \bar{g}_{n-1}(\xi_1, \tilde{\xi}_2, \dots, \tilde{\xi}_{n-1}, u) - \lambda_{n-1} \text{sign}(\tilde{\xi}_{n-1} - \hat{\xi}_{n-1}) \\ \dot{e}_n &= \bar{f}_n(\xi_1, \dots, \xi_n) - \bar{f}_n(\xi_1, \tilde{\xi}_2, \dots, \tilde{\xi}_n) + \bar{g}_n(\xi_1, \xi_2, \dots, \xi_{n-1}, u) - \bar{g}_n(\xi_1, \dots, \tilde{\xi}_n, u) - \\ &\quad \lambda_n \text{sign}(\tilde{\xi}_n - \hat{\xi}_n) \end{aligned}$$

It can be shown that for sufficiently large λ_1 , the system reaches a sliding mode at $e_1 = 0$ within a finite time, which implies that

$$e_2 = \lambda_1 \text{sign}(\xi_1 - \hat{\xi}_1)$$

together with 1.35 results in $\tilde{\xi}_2 = x_2$. The dynamics of the observation error are then expressed as follows:

$$\begin{aligned} \dot{e}_1 &= 0 \\ \dot{e}_2 &= e_3 - \lambda_2 \text{sign}(\tilde{\xi}_2 - \hat{\xi}_2) \\ &\vdots \\ \dot{e}_{n-1} &= \hat{\xi}_n - \bar{g}_{n-1}(\xi_1, \xi_2, \dots, \tilde{\xi}_{n-1}, u) - \lambda_{n-1} \text{sign}(\tilde{\xi}_{n-1} - \hat{\xi}_{n-1}) \\ \dot{e}_n &= \bar{f}_n(\xi_1, \dots, \xi_n) - \tilde{f}_n(\xi_1, \xi_2, \dots, \tilde{\xi}_n) + \bar{g}_n(\xi_1, \xi_2, \dots, \xi_{n-1}, u) \\ &\quad - \tilde{g}_n(\xi_1, \dots, \tilde{\xi}_n, u) - \lambda_n \text{sign}(\tilde{\xi}_n - \hat{\xi}_n) \end{aligned} \tag{1.36}$$

Continuing in the same manner, it can be demonstrated that for sufficiently large λ_2 , a sliding mode is achieved at $e_2 = 0$ within a finite time, leading to the conclusion that

$$e_3 = \lambda_2 \text{sign}(\tilde{x}_2 - \hat{x}_2)$$

which results in $\tilde{x}_3 = x_3$. Continuing with the same methodology throughout the dynamics yields:

$$\begin{aligned} e_1 &= 0 \\ e_2 &= 0 \\ &\vdots \\ e_{n-1} &= 0 \\ e_n &= -\lambda_n \text{sign}(\tilde{\xi}_n - \hat{\xi}_n) \end{aligned}$$

It follows naturally that a sliding mode is ultimately achieved at $e_n = 0$ within a finite time.

1.3.6.3 High-order sliding mode observers

High-order sliding mode observers are advanced observers designed to mitigate the chattering phenomenon commonly encountered in traditional sliding mode observers. By incorporating higher-order dynamics into the observer design, they provide smoother state estimates and improved robustness against uncertainties and disturbances.

Let's visualize the structure of a high gain observer presented in [67]. Consider a system as

$$\begin{aligned} \dot{x}_2 &= -ax_2 - bx_1 + ku(t) \\ y &= x_1 \end{aligned} \tag{1.37}$$

Let the high gain observer be defined as

$$\begin{aligned} \hat{x}_1 &= \hat{x}_2 + \frac{\alpha_1}{\epsilon} (y - \hat{x}_1) \\ \dot{\hat{x}}_2 &= -ax_2 - bx_1 + ku + \frac{\alpha_2}{\epsilon^2} (y - \hat{x}_1) \end{aligned} \tag{1.38}$$

where α_1 and α_2 are positive values, and $\epsilon \ll 1$.

By choosing the parameters:

$$h_1 = \frac{\alpha_1}{\epsilon}, \quad h_2 = \frac{\alpha_2}{\epsilon^2}$$

the observer equations become:

$$\begin{aligned} \dot{\hat{x}}_1 &= \hat{x}_2 + h_1(y - \hat{x}_1) \\ \dot{\hat{x}}_2 &= -ax_2 - bx_1 + ku(t) + h_2(y - \hat{x}_1) \end{aligned} \tag{1.39}$$

where $\tilde{x} = x - \hat{x}$ represents the estimation error.

From equations (1.37) and (1.38), we obtain:

$$\begin{aligned}\dot{\tilde{x}}_1 &= -h_1\tilde{x}_1 + \tilde{x}_2 \\ \dot{\tilde{x}}_2 &= h_2\tilde{x}_1 - a\tilde{x}_2\end{aligned}\tag{1.40}$$

and:

$$y = x_1$$

i.e.,

$$\dot{\tilde{x}} = A\tilde{x},$$

where the matrixs are defined as:

$$A = \begin{bmatrix} -h_1 & 1 \\ -h_2 & -a \end{bmatrix}, \quad \tilde{x} = \begin{bmatrix} \tilde{x}_1 \\ \tilde{x}_2 \end{bmatrix}.$$

If the matrix A is Hurwitz, the error dynamics $\tilde{x}(t)$ will decay exponentially. This behavior can be expressed as:

$$\|\tilde{x}(t)\| \leq \varphi_0 \|\tilde{x}(t_0)\| e^{-\sigma_0(t-t_0)}\tag{1.41}$$

where φ_0 and σ_0 are positive constants. Equation (1.41) shows that the precision of the convergence for $\|\tilde{x}(t)\|$ depends on σ_0 , which is related to the smallest eigenvalue of the matrix A . When ϵ is reduced, the values of h_1 and h_2 increase, leading to a smaller minimum eigenvalue of A . As the minimum eigenvalue grows, the value of σ_0 becomes larger, resulting in faster convergence of $\|\tilde{x}(t)\|$. Consequently, the performance of the high-gain observer improves the precision of the error decay significantly.

Super Twisting Sliding Mode Observer

A well-known second-order sliding mode algorithm that offer finite reaching time and is applicable for sliding mode-based observation is the super-twisting algorithm. The STSMO reduces chattering by utilizing a super-twisting algorithm. This observer achieves finite-time convergence of the estimation error while providing smoother estimates [64, 91]. The proposed super-twisting observer has the form [91].

$$\begin{aligned}\dot{\hat{x}}_1 &= \hat{x}_2 + z_1 \\ \dot{\hat{x}}_2 &= f(t, x_1, \hat{x}_2 + z_2)\end{aligned}\tag{1.42}$$

where x_1 and \hat{x}_2 are the state estimates while the correction variables z_1 and z_2 are output error injections of the form

$$\begin{aligned}z_1 &= \lambda |x_1 - \hat{x}_1|^{1/2} \text{sign}(x_1 - \hat{x}_1) \\ z_2 &= \alpha \text{sign}(x_1 - \hat{x}_1)\end{aligned}\tag{1.43}$$

Considering that $\tilde{x}_1 = x_1 - \hat{x}_1$ and $\tilde{x}_2 = x_2 - \hat{x}_2$ we obtain the equations for the errors.

$$\begin{aligned}\dot{\tilde{x}}_1 &= \tilde{x}_2 - \lambda |\tilde{x}_1|^{1/2} \text{sign}(\tilde{x}_1) \\ \dot{\tilde{x}}_2 &= F(t, x_1, x_2, \hat{x}_2) - \alpha \text{sign}(\tilde{x}_1)\end{aligned}\tag{1.44}$$

where

$$F(t, x_1, x_2, \hat{x}_2) = f(t, x_1, x_2, u) - f(t, x_1, \hat{x}_2, u) + \xi(t, x_1, x_2, y)\tag{1.45}$$

Assuming the system states are bounded, the existence of a constant f^+ is guaranteed, such that the inequality

$$|F(t, x_1, x_2, \hat{x}_2)| < f^+\tag{1.46}$$

holds for any possible t, x_1, x_2 and $|\hat{x}_2| \leq 2 \sup |x_2|$.

Super Twisting Observer with Multiple Sliding Surfaces

By adding numerous sliding surfaces, this method expands on the super twisting method and achieves resilience against many disturbance kinds. For a system that is explained by:

$$\dot{x}(t) = Ax(t) + Bu(t) + d(t) \quad (1.47)$$

The observer can be defined with multiple sliding surfaces:

$$\dot{\hat{x}}(t) = A\hat{x}(t) + Bu(t) + L_1 \operatorname{sgn}(s_1(t)) + L_2 \operatorname{sgn}(s_2(t)) \quad (1.48)$$

where $s_1(t) = y(t) - C_1\hat{x}(t)$ $s_2(t) = y(t) - C_2\hat{x}(t)$ are different sliding surfaces, and L_1 and L_2 are gain matrices for each surface. This approach allows for enhanced robustness and adaptability to varying conditions.

1.3.7 Characteristics of sing function approximation forms

The conventional sliding mode observer uses a sign (sgn) function to define its sliding mode surface [67, 98]. This binary switching characteristic of the sgn function contributes to the robustness of the SMO by forcing the system into the sliding surface, but it can also induce chattering in the output signal. As shown in Figure 1.3, the sgn function, it is defined as follows:

$$\operatorname{sgn}(x) \begin{cases} 1 & \text{if } x \geq 0 \\ -1 & \text{if } x < 0 \end{cases} \quad (1.49)$$

The equivalent value of the real speed signal must be recovered from the discontinuous signal with chattering using a low-pass filter. The simplest filter to utilize is the first-order transfer function.

The sign function (1.49) can be approximated into a continuous form. There are two alternative approaches: saturation and sigmoid functions.

- ① The saturation function can be described as follows

$$\operatorname{sat}(x) \begin{cases} \frac{x}{\varepsilon}, & \text{where } |x| \leq \varepsilon \\ \operatorname{sgn}(x), & \text{where } |x| > \varepsilon \end{cases} \quad (1.50)$$

- ② There are many different types of sigmoid functions. Some of them are listed below

$$\operatorname{sigm}_1(x) = \frac{2}{1 + e^{-x/\varepsilon}} - 1 \quad (1.51a)$$

$$\operatorname{sigm}_2(x) = \tanh(x/\varepsilon) \quad (1.51b)$$

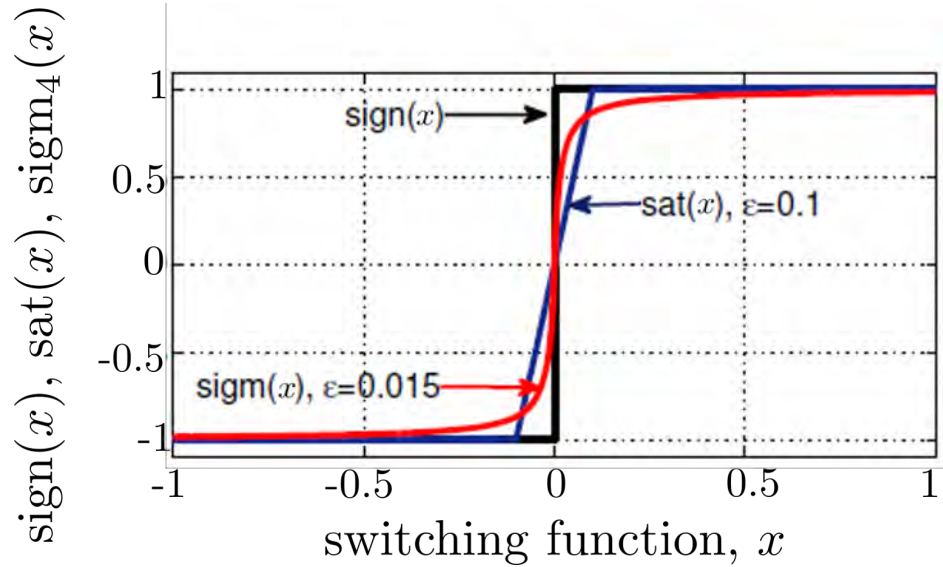
$$\operatorname{sigm}_3(x) = \frac{2}{\pi} \arctan(x/\varepsilon) \quad (1.51c)$$

$$\operatorname{sigm}_4(x) = \frac{x}{\varepsilon + |x|} \quad (1.51d)$$

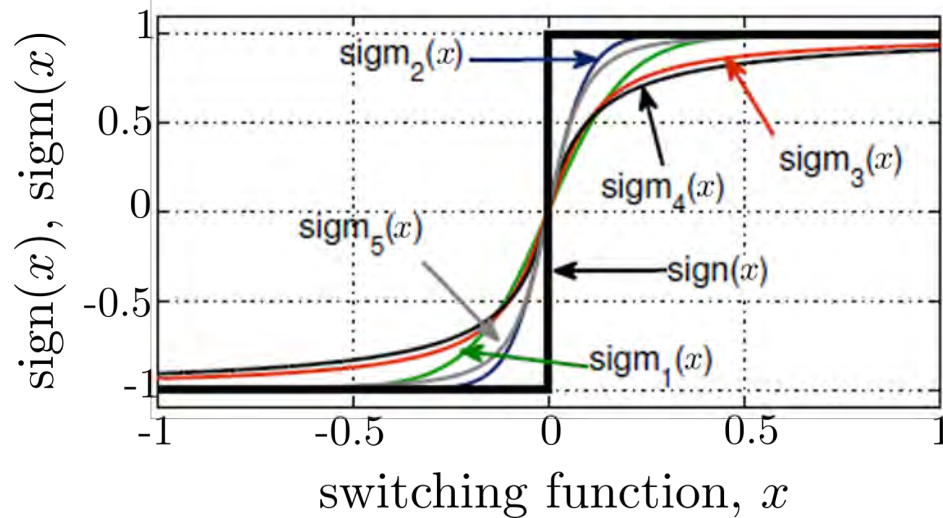
$$\operatorname{sigm}_5(x) = \frac{x/\varepsilon}{\sqrt{1 + (x/\varepsilon)^2}} \quad (1.51e)$$

$$(1.51f)$$

The results are standardized to fall between ± 1 . Changing the ε value affects the slope of the $\text{sat}(x)$ and $\text{sigm}(x)$ functions. Figure 1.3a (from [98]) shows the comparison of the sign, saturation and sigmoid functions. At the same time, Figure 1.3b shows the set of sigmoid functions. Despite the significant divergence between the functions for certain values of ε for each function, the functions become very similar for this reason if sigm_4 is chosen it seems to be an optimal solution because the computations are the simplest.



(a) Comparison of sign, saturation and one of sigmoid functions.



(b) Set of sigmoid functions for the same.

Figure 1.3: Sign function approximations.

1.4 Higher-order linearization and normal form

The basic idea behind this technique stems from the results of H. Poincaré’s research into the normalization of differential equations. The concept of normal form has its origin in the work of Henri Poincaré, who provided the first formal normalization theorem for a differential equation. The goal is to study the local behavior of solutions near equilibrium points of differential equations by simplifying the system. The best case scenario is to linearize the system, but this is not always possible due to the presence of resonant terms, which create obstacles to linearization.

In addition to its simplicity of design and application, H. Poincaré’s linearization technique provides a general proof of the efficacy or otherwise of linear designs, applied to systems that contain a general non-linearity. This has motivated a large number of researchers in various fields to adopt this approach. In this section, we set out H. Poincaré’s main results in this field.

In the following, we review the technique ([36], [103],[4], [3],[2]). Consider a nonlinear system:

$$\dot{x} = F(x), \tag{1.52}$$

where $x \in \mathbb{R}^n$ and $F(x)$ is a smooth vector field with an equilibrium point at the origin, $f(0) = 0$. The aim of the Poincaré-Dulac normal form theory is to transform this system into a simpler, more structured form via a series of coordinate transformations, which helps in analyzing the dynamics in a neighborhood of the equilibrium.

The normal form computation relies on decomposing the vector field $F(x)$ into its linear and nonlinear parts:

$$\dot{x} = Ax + f(x), \tag{1.53}$$

where $x \in \mathbb{R}^n$, A is the Jacobian matrix of $F(x)$ evaluated at the origin, and $f(x)$ contains the higher-order nonlinear terms.

1.4.1 The resonances

Definition 1.4.1 ([36], [103],[4], [3],[2])

Let us consider a matrix $A \in \mathbb{R}^{n \times n}$ with eigenvalues λ_i , (for $1 \leq i \leq n$), the n -tuple $\lambda(\lambda_1, \dots, \lambda_n)$ is resonant if among the eigenvalues there exists a relation of the form:

$$(k, \lambda) = \sum_{i=1}^n k_i \lambda_i = \lambda_j \tag{1.54}$$

where $k = \{k_1, \dots, k_n\}$, $k_i \geq 0$ with $\sum_{i=1}^n k_i \geq 2$ such a relation is called a resonance.

The number $r = \sum_{i=1}^n k_i$ is called the order of the resonance.

We say that A is resonant (resp. λ_j is resonant), and number $r = \sum_{i=1}^n k_i$ is called the order of the resonance. Otherwise, A is said to be non-resonant (resp. λ_j is non-resonant).

Example 1.4.1 The relation $\lambda_1 = 2\lambda_2$ is a resonance of order 2.

The relation $2\lambda_1 = 3\lambda_2$ is not a resonance.

The relation $\lambda_1 + \lambda_2 = 0$, or equivalently $\lambda_1 = 2\lambda_1 + \lambda_2$, is a resonance of order 3.

Theorem 1 (Poincaré's Theorem) ([3],[4]) If the eigenvalues of the matrix A are non-resonant, then the non-linear system (1.52) can be reduced to the following linear system:

$$\dot{z} = Az$$

by a formal change of variable $x = z + \dots$. (The dots denote series starting with terms of degree two or higher.)

Remark 1.4.1 ([3], [4]) If the n -tuple $\lambda = (\lambda_1, \dots, \lambda_n)$ is resonant, we will say that

$$x_1^{k_1} \dots x_n^{k_n} e_i$$

is resonant if $\lambda_i = (k, \lambda)$, $\sum_{i=1}^n k_i \geq 2$ with e_i a vector in the eigenbasis of A and x_i are the coordinates with respect to the basis e_i .

For example, for the resonance $\lambda_1 = 2\lambda_2$, the unique resonant monomial is $x_2^2 e_1$. For the resonance $\lambda_1 + \lambda_2 = 0$, all monomials $(x_1 x_2)^k x_s e_s$ are resonant.

Example 1.4.2 The eigenvalues $\lambda_1 = 3, \lambda_2 = 2$. Let us see if there exist non-negative integers k_1, k_2 such that $\lambda_1 = k_1 \lambda_1 + k_2 \lambda_2$ where $k_1 + k_2 = r \Rightarrow k_2 = r - k_1$, then

$$\begin{aligned} 3 &= 3k_1 + 2(r - k_1) \\ 3 &= k_1 + 2r \\ k_1 &= 3 - 2r \end{aligned} \tag{1.55}$$

as $r \geq 2$, then there are no integers such that $\lambda_1 = k_1 \lambda_1 + k_2 \lambda_2$. Similarly, let's see if there exist non-negative integers k_1, k_2 such that $\lambda_2 = k_1 \lambda_1 + k_2 \lambda_2$ and $k_1 + k_2 = r \Rightarrow k_2 = r - k_1$ then

$$\begin{aligned} 2 &= 3k_1 + 2(r - k_1) \\ 2 &= k_1 + 2r \\ k_1 &= 2 - 2r \end{aligned} \tag{1.56}$$

as $r \geq 2$, then there are no integers such that $\lambda_1 = k_1 \lambda_1 + k_2 \lambda_2$. Therefore the eigenvalues are non-resonant.

Example 1.4.3 The eigenvalues $\lambda_1 = 3, \lambda_2 = 1$. Let us see if there exist non-negative integers k_1, k_2 such that

$$\lambda_1 = k_1 \lambda_1 + k_2 \lambda_2 \quad \text{where} \quad k_1 + k_2 = r \Rightarrow k_2 = r - k_1$$

then

$$\begin{aligned} 3 &= 3k_1 + (r - k_1) \\ 3 &= 2k_1 + r \\ 2k_1 &= 3 - r \end{aligned} \tag{1.57}$$

as $r \geq 2$, let us note that the only solution that satisfies the above equation is for $r = 3, k = (0, 3)$ and $i = 1$. Similarly, let's see if there exist non-negative integers k_1, k_2 such that:

$$\lambda_2 = k_1 \lambda_1 + k_2 \lambda_2 \quad \text{where} \quad k_1 + k_2 = r \Rightarrow k_2 = r - k_1$$

then

$$\begin{aligned} 1 &= 3k_1 + (r - k_1) \\ 1 &= 2k_1 + r \\ 2k_1 &= 1 - r \end{aligned} \tag{1.58}$$

as $r \geq 2$, then there is no solution. Therefore, there is only the resonant term (1.57).

1.4.2 Poincaré Normal Forms computation

The Poincaré transformation is briefly described here: we're looking for a change of variable that preserves the linear part (i.e. a change of variable tangent to the identity), which conjugates the initial field to a "simpler" field. We proceed degree by degree.

Consider the differential equation (1.53), $f(x)$ contains the higher-order nonlinear terms can be decomposed as:

$$\dot{x} = Ax + f^{[r]}(x) + O^{[r+1]}(x) \quad (1.59)$$

where

$$f^{[r]}(x) = f_2(x) + f_3(x) + \dots + O^{[r+1]}(x). \quad (1.60)$$

To systematically simplify this system, we look for a transformation that preserves the linear part and reduces the higher-order terms. This process is carried out degree by degree in the expansion.

Our goal is to remove all nonlinear terms in the first phase. This methodology is iterative: terms of degree 2 are eliminated first, followed by those of degree 3, and so forth. Every elimination will be carried out using a matching transformation, which we'll presume to be known beforehand. We assume that in the vicinity of (x_e) , the field takes the following form:

$$x = z + \Phi^{[r]}(z), \forall r \geq 2 \quad (1.61)$$

We briefly describe here the Poincaré transformation: we are looking for a change of variables that preserves the linear part (thus a change of variables tangent to the identity) which conjugates the original vector field to a "simpler" one. This is done degree by degree.

If we make the change of variables

$$x = z + \Phi^{[2]}(z), \text{ we obtain:}$$

$$\dot{x} = (Id + D\Phi^{[2]}(z))\dot{z} = Az + A\Phi^{[2]}(z) + f_2(z) + \dots + O^{[r+1]}(x),$$

for $m \geq 2$, each term

$$f_m(z + \Phi^{[2]}(z)) = f_m(z) + Df_m(z)D\Phi^{[2]}(z) + \dots$$

is at least of degree 3 in z , except for the contribution $f_2(z)$ of degree 2. Therefore, the previous equation is rewritten, for the second-order term:

$$(Id + D\Phi^{[2]}(z))\dot{z} = Az + A\Phi^{[2]}(z) + \dots + f_2(z) + \dots + O^{[r+1]}(x).$$

For sufficiently small z , the matrix $Id + D\Phi^{[2]}(z)$ is invertible, and its inverse is:

$$(Id + D\Phi^{[2]}(z))^{-1} = Id - D\Phi^{[2]}(z) + O^{[2]}(x),$$

which finally gives:

$$\begin{aligned} \dot{z} &= (Id - D\Phi^{[2]}(z) + O^{[2]}(z))(Az + A\Phi^{[2]}(z) + f_2(z) + \dots + O^{[2]}(z)), \\ &= Az + A\Phi^{[2]}(z) + f_2(z) - D\Phi^{[2]}(z)Az + \text{higher - degree terms...} \end{aligned}$$

We then obtain the following equation for the second degree:

$$\tilde{f}_2(z) = f_2(z) - [\Phi^{[2]}(z)Az - A\Phi^{[2]}(z)],$$

where \tilde{f}_2 is the "simplified" form of the field; the best possible simplification would obviously be $\tilde{f}_2 = 0$.

It can be generalized and shown in the same way that for a change of variable $x = z + \Phi^{[k]}(z)$, the equation obtained is:

$$\tilde{f}_k(z) = f_k(z) - [D\Phi^{[k]}(z)Az - A\Phi^{[k]}(z)].$$

Note that if f_k is fixed, the f_m for $m < k$ are not modified: a supplementary term of fixed degree is stabilized at each step, successively applying the changes of variables $x = z + \Phi^{[2]}(z)$, then $x = z + \Phi^{[3]}(z)$, and so on.

The eigenvalues of the matrix A play a crucial role in determining the nature of the coordinate transformations.

Theorem 1.4.1 (Poincaré-Dulac Theorem [3],[4]) *If the eigenvalues of the matrix A are resonant, then the nonlinear system (1.59) can be reduced to the following system:*

$$\dot{z} = Az + \tilde{f} \tag{1.62}$$

by a formal change of variable $x = z + \Phi^{[r]}(z)$ (the r of degree two or higher), where all monomials in the series \tilde{f} are resonant.

Example 1.4.4 Case without resonances

Consider a dynamical system around the origin $(0, 0)$ in \mathbb{R}^2 given by:

$$\begin{cases} \dot{x}_1 &= \lambda_1 x_1 + x_1^2 \\ \dot{x}_2 &= \lambda_2 x_2 + x_1 x_2 \end{cases}$$

where $x = (x_1, x_2)^T$, A is a linear matrix, and $f(x) = (x_1^2, x_1 x_2)^T$ represents the nonlinear terms.

Suppose the matrix A has distinct eigenvalues, for example:

$$A = \begin{pmatrix} \lambda_1 & 0 \\ 0 & \lambda_2 \end{pmatrix}$$

with $\lambda_1 = 1$ and $\lambda_2 = 1$. This implies that the eigenvalues do not satisfy any resonance relations (e.g., $k_1 \lambda_1 + k_2 \lambda_2 = \lambda_k$ for integers k_1, k_2 , and k).

The normal form is constructed by eliminating non-resonant terms in $f(x)$ using nonlinear transformations of the Poincaré.

We assume the following transformation:

$$\begin{cases} x_1 &= z_1 + \phi_1(z_1, z_2) \\ x_2 &= z_2 + \phi_2(z_1, z_2) \end{cases}$$

where

$$\begin{cases} \phi_1(z) &= a_1 z_1^2 + a_2 z_2^2 + a_{12} z_1 z_2 \\ \phi_2(z) &= b_1 z_1^2 + b_2 z_2^2 + b_{12} z_1 z_2 \end{cases}$$

Consequently

$$\begin{cases} \dot{z}_1 &= \dot{x}_1 + D\phi_1(z_1, z_2)\dot{z} \\ \dot{z}_2 &= \dot{x}_2 + D\phi_2(z_1, z_2)\dot{z} \end{cases} \tag{1.63}$$

by replacing \dot{x}_1 , \dot{x}_2 , x_1 and x_2 in (1.64), we find

$$\begin{cases} \dot{z}_1 &= z_1 + (1 - a_1)z_1^2 - a_2z_2^2 - a_{12}z_1z_2 \\ \dot{z}_2 &= 2z_2 - b_1z_1^2 - b_2z_2^2 + (1 - b_{12})z_1z_2 \end{cases}$$

And by choosing $\phi_1(z) = z_1^2$ and $\phi_2(z) = z_1z_2$, we obtain a new system "the normal form" where the non-resonant terms disappear.

$$\begin{cases} \dot{z}_1 &= \lambda_1 z_1 \\ \dot{z}_2 &= \lambda_2 z_2. \end{cases}$$

Example 1.4.5 Case with resonances In the resonant case, the eigenvalues of A do satisfy a relation of the form given above. This resonance condition implies that some nonlinear terms cannot be eliminated through coordinate transformations. These terms must be retained in the normal form, and they play an important role in the system's long-term dynamics.

Consider a dynamical system around the origin $(0, 0)$ in \mathbb{R}^2 given by:

$$\begin{cases} \dot{x}_1 &= \lambda_1 x_1 + x_1^2 \\ \dot{x}_2 &= \lambda_2 x_2 + x_1^2 + x_1 x_2 \end{cases}$$

where $x = (x_1, x_2)^T$, A is a linear matrix, and $f(x) = (x_1^2, x_1^2 + x_1 x_2 x_2)^T$ represents the nonlinear terms.

Suppose the matrix A has distinct eigenvalues, for example:

$$A = \begin{pmatrix} \lambda_1 & 0 \\ 0 & \lambda_2 \end{pmatrix}$$

with $\lambda_1 = 1$ and $\lambda_2 = 2$. This implies that the eigenvalues satisfy the resonance relations (e.g., $0^* \lambda_1 + \lambda_2 = \lambda_2$ and $\lambda_2 = 2\lambda_2$, and k).

The normal form is constructed by eliminating non-resonant terms in $f(x)$ using nonlinear transformations of the Poincaré.

We assume the following transformation:

$$\begin{cases} x_1 &= z_1 + \phi_1(z_1, z_2) \\ x_2 &= z_2 + \phi_2(z_1, z_2) \end{cases}$$

where

$$\begin{cases} \phi_1(z) &= a_1 z_1^2 + a_2 z_2^2 + a_{12} z_1 z_2 \\ \phi_2(z) &= b_1 z_1^2 + b_2 z_2^2 + b_{12} z_1 z_2 \end{cases}$$

Consequently

$$\begin{cases} \dot{z}_1 &= \dot{x}_1 + D\phi_1(z_1, z_2)\dot{z} \\ \dot{z}_2 &= \dot{x}_2 + D\phi_2(z_1, z_2)\dot{z} \end{cases} \quad (1.64)$$

by replacing \dot{x}_1 , \dot{x}_2 , x_1 and x_2 in (1.64), we find

$$\begin{cases} \dot{z}_1 &= z_1 + (1 - a_1)z_1^2 - 3a_2z_2^2 - 2a_{12}z_1z_2 \\ \dot{z}_2 &= 2z_2 + Rz_1^2 - 2b_2z_2^2 + (1 - b_{12})z_1z_2 \end{cases}$$

And by choosing $\phi_1(z) = z_1^2$ and $\phi_2(z) = z_1z_2$, we obtain a new system "the normal form" where the non-resonant terms disappear.

$$\begin{cases} \dot{z}_1 &= \lambda_1 z_1 \\ \dot{z}_2 &= \lambda_2 z_2 + z_1^2. \end{cases}$$

Remark 1.4.2 In this example, the only possible resonance is $\lambda_2 = 2\lambda_1$, which implies that the only potentially resonant term is z_1^2 in the direction z_2 . However, if $R = 0$ this resonance term is **genetically zero**. This means that, even if the resonance theoretically exists between the eigenvalues, the corresponding term in the nonlinearity is zero in the normal form of the system, as it cannot appear naturally from the original equations.

The normal form theory helps in understanding the stability of the equilibrium by focusing on the essential dynamics and ignoring the higher-order nonlinearities that do not affect the qualitative behavior.

1.5 Quadratic observability normal form for nonlinear SISO system

In this section, we recall a result from [10] this work focuses on the analysis of the singularities in the observability and detectability of nonlinear dynamic systems, specifically in the context of chaotic electronic circuits. The research addresses the importance of these properties in the design and implementation of synchronization systems, which are fundamental in applications such as cryptography, communication, and signal processing. The results show that the singularities in observability and detectability can significantly influence the success of synchronization in chaotic circuits. Specific conditions are established under which effective synchronization can be achieved, and critical parameters that affect the stability of the system are identified. For this reason, our work is based on the findings of this research.

In Boutat [10] a quadratic observability normal form for nonlinear SISO system is presented. The following system is considered :

$$\begin{cases} \dot{\xi} &= f(\xi) + g(\xi)u \\ y &= h(\xi) \end{cases} \quad (1.65)$$

where $\xi \in \mathbb{R}^n$ is the state, $y \in \mathbb{R}^p$ is outputs, $f(\xi) \in \mathbb{R}^n$ are the vector fields such that $f(\xi) : U \subset \mathbb{R}^n \rightarrow \mathbb{R}^n$ are assumed to be real analytic, such that $f(0) = 0$.

Setting: $A = \frac{\partial f}{\partial \xi}(0)$ and $B = g(0)$ have been developed in Taylor series around the equilibrium points $\xi_e = 0$, with

$$\text{rank}(O(A, h)) = \text{rank} \left(\begin{bmatrix} h(\xi) & L_f h(\xi) & L_f^2 h(\xi) & \dots & L_f^{n-1} h(\xi) \end{bmatrix} \right)^T = n - r$$

the system can be rewritten in the following form:

$$\begin{cases} \dot{\xi} &= A\xi + Bu + f^{[2]}(\xi) + g^{[1]}(\xi)u + O^{[3]}(\xi, u) \\ y &= C\xi \end{cases} \quad (1.66)$$

In (1.66), A is the Jacobian matrix of f of dimension $n \times n$ en $x_e = 0$, $f^{[2]}(x, u)$ is a vector field in \mathbb{R}^n whose components are homogeneous polynomials of degree n on (x, u) :

$$f^{[2]}(\xi) = \begin{bmatrix} f_1^{[2]}(\xi) \\ f_2^{[2]}(\xi) \\ \vdots \\ f_n^{[2]}(\xi) \end{bmatrix}^T \quad \text{and} \quad g^{[1]}(\xi) = \begin{bmatrix} g_1^{[1]}(\xi) \\ g_2^{[1]}(\xi) \\ \vdots \\ g_n^{[1]}(\xi) \end{bmatrix}^T$$

such as $\forall i, 1 \leq i \leq n$, $f_i^{[2]}(\xi)$ and $g_i^{[1]}(\xi)$ are respectively homogeneous polynomials of degree 2 and 1 in ξ .

Definition 1.5.1

- i) We call $f^{[2]}(\xi)$ the quadratic part of system (1.66).
- ii) A quadratic transformation is defined by the following change of coordinates:

$$z = x + \Phi^{[2]}(x)$$

1.5.1 Quadratic equivalence modulo an output injection

The concept of quadratic equivalence modulo output injection serves as a powerful method to reduce the inherent complexity of nonlinear dynamical systems. By providing a clearer normal form, this approach significantly aids the analysis of fundamental properties such as observability and detectability. In particular, this form of equivalence makes it possible to identify and investigate observability singularities - those critical points where traditional observational methods fail to accurately determine the system state.

In nonlinear dynamical systems, these challenges are often related to phenomena such as state separation, where the evolution of the system state makes it difficult to distinguish individual state components. In addition, the presence of non-universal inputs - inputs that do not have a uniform influence across all operating conditions - can lead to unpredictable system responses, further complicating the task of monitoring and reconstructing system behaviour. Quadratic equivalence modulo output injection provides a methodical approach to addressing these issues, enabling a reduction in system complexity that allows analysts to isolate specific vulnerabilities.

In addition, this equivalence plays an important role in providing a clearer distinction between observable and unobservable state components. Further examination of the applications and implications of quadratic equivalence, as explored in ([10], [41], [53], [71], [56], [40], [39], [34], [27], [60], [72], [57], [54], [85], [58], [55], [59]), shows how this approach can enhance our understanding of system dynamics under various conditions. These results demonstrate the utility of the method in improving both the robustness and reliability of observability assessments, and offer a refined perspective on how system states can be effectively reconstructed even when the state is not linearly observable.

Definition 1.5.2 *The following system is considered ([10]):*

$$\begin{cases} \dot{z} &= Az + Bu + f^{[2]}(z) + g^{[1]}(z)u + O^{[3]}(z, u) \\ y &= Cz \end{cases} \quad (1.67)$$

and

$$\begin{cases} \dot{x} &= Ax + Bu + \bar{f}^{[2]}(x) + \bar{g}^{[1]}(x)u + \beta^{[2]}(y) + \gamma^{[1]}(y)u + O^{[3]}(x, u) \\ y &= Cx \end{cases} \quad (1.68)$$

- i) We call $f^{[2]}(\xi)$ the quadratic part of system (1.66). We say that the system (1.67) having the quadratic part $f^{[2]}(z) + g^{[1]}(z)u$ is quadratically transformable modulo an output injection to the system(1.68) having the quadratic part $\bar{f}^{[2]}(x) + \bar{g}^{[1]}(x)u$ if there exists an output injection:

$$\beta^{[2]}(y) + \gamma^{[1]}(y)u$$

- ii) We say that there exists a diffeomorphism of the form:

$$x = z - \Phi^{[2]}(z)$$

which transforms the quadratic part $f^{[2]}(z) + g^{[1]}(z)u$ in the quadratic part $\bar{f}^{[2]}(x) + \bar{g}^{[1]}(x)u + [\beta^{[2]}(y) + \gamma^{[1]}(y)u]$ where $\Phi^{[2]}(z) = [\Phi_1^{[2]}(z), \dots, \Phi_n^{[2]}(z)]^T$, $\beta^{[2]}(y) = [\beta_1^{[2]}(y), \dots, \beta_n^{[2]}(y)]^T$ and $\gamma^{[1]}(y) = [\gamma_1^{[1]}(y), \dots, \gamma_n^{[1]}(y)]^T$,

for $i \in [1, n]$, $\Phi_i^{[2]}(z)$ and $\beta_i^{[2]}(y)$ are respectively homogeneous polynomials of degree 2 en z and y , and the $\gamma_i^{[1]}(y)$ are homogeneous polynomials of degree 1 in y .

Proposition 1.5.1 *System (1.67) is quadratically equivalent modulo an output injection to system (1.68), if and only if the two following homological equations are verified:*

$$\begin{cases} i) & \bar{f}^{[2]}(z) - f^{[2]}(z) + \beta^{[2]}(z_1) = A\Phi^{[2]}(z) - \frac{\partial \Phi^{[2]}}{\partial z} Az \\ ii) & \bar{g}^{[1]}(z) - g^{[1]}(z) + \gamma^{[1]}(z_1) = -\frac{\partial \Phi^{[2]}}{\partial z} B \end{cases} \quad (1.69)$$

Proof 1.5.1 [10] *Consider these two systems (1.67) and (1.68), let us $x = z - \Phi^{[2]}(z)$ then $\dot{x} = \dot{z} - \frac{\partial \Phi^{[2]}}{\partial z} \dot{z}$, which gives:*

$$\begin{aligned} \dot{x} &= Az + Bu + f^{[2]}(z) + g^{[1]}(z)u + O^3(z, u) \\ &\quad - \frac{\partial \Phi^{[2]}}{\partial z} (Az + Bu + f^{[2]}(z) + g^{[1]}(z)u + O^3(z, u)) \end{aligned}$$

and by comparing the quadratic part with

$$\begin{aligned} \dot{x} &= A(z - \Phi^{[2]}(z)) + Bu + \bar{f}^{[2]}(z - \Phi^{[2]}(z)) + \bar{g}^{[1]}(z - \Phi^{[2]}(z))u \\ &\quad + \beta^{[2]}(z_1) + \gamma^{[1]}(z_1)u + O^3(z - \Phi^{[2]}(z), u) \end{aligned}$$

we have:

$$\begin{aligned} Az - A\Phi^{[2]}(z) + \bar{f}^{[2]}(z) + \bar{g}^{[1]}(z)u + \beta^{[2]}(z_1) + \gamma^{[1]}(z_1)u \\ = \\ Az + f^{[2]}(z) + g^{[1]}(z)u - \frac{\partial \Phi^{[2]}}{\partial z} (Az + Bu) \end{aligned}$$

which implies:

$$\begin{aligned} i) & \begin{cases} \bar{f}^{[2]}(z) - f^{[2]}(z) + \beta^{[2]}(z_1) = A\Phi^{[2]}(z) - \frac{\partial \Phi^{[2]}}{\partial z} Az \\ \bar{f}^{[2]}(z) + \beta^{[2]}(z_1) = A\Phi^{[2]}(z) - \frac{\partial \Phi^{[2]}}{\partial z} Az + f^{[2]}(z) \end{cases} \\ ii) & \begin{cases} \bar{g}^{[1]}(z) - g^{[1]}(z) + \gamma^{[1]}(z_1) = -\frac{\partial \Phi^{[2]}}{\partial z} B \\ \bar{g}^{[1]}(z) + \gamma^{[1]}(z_1) = g^{[1]}(z) - \frac{\partial \Phi^{[2]}}{\partial z} B \end{cases} \end{aligned}$$

1.5.2 Linearly observable case for nonlinear SISO system

Applying the normal form method to linearly observable systems allows the reduction of the system's complexity to its strict minimum, while respecting its topological properties. The first step consists in classically normalizing the linear part of the system (1.66).

In Boutat-Baddas ([10]) a well known result on the linear observable normal form is presented.

Lemma 1.5.1 [12] *Assume that the pair (A, C) of the system (1.66) is observable, (i.e. the linear observability matrix $\text{rank}(O(A, h)) = \text{rank}([\ h(\xi) \quad L_f h(\xi) \quad L_f^2 h(\xi) \quad \dots \quad L_f^{n-1} h(\xi) \])^T$ is full range n).*

Under this lemma, then there exist a linear change of coordinates $z = T\xi$ and a Taylor expansion which transforms the linear part of the system (1.66) in the following form:

$$\begin{cases} \dot{z} &= A_{obs}z + B_{obs}u + f^{[2]}(z) + g^{[1]}(z)u + O^{[3]}(z, u) \\ y &= C_{obs}x \end{cases} \quad (1.70)$$

where:

$$A_{obs} = \begin{pmatrix} a_1 & 1 & 0 & \cdots & \cdots & 0 \\ a_2 & 0 & 1 & 0 & \ddots & \vdots \\ \vdots & 0 & 0 & \ddots & \ddots & \ddots \\ \vdots & \vdots & \cdots & \ddots & \ddots & 0 \\ a_{n-1} & 0 & \vdots & \vdots & 0 & 1 \\ a_n & 0 & \cdots & \cdots & \cdots & 0 \end{pmatrix}, \quad B_{obs} = \begin{bmatrix} b_1 \\ b_2 \\ \vdots \\ \vdots \\ \vdots \\ b_n \end{bmatrix} \quad \text{and} \quad C_{obs} = \begin{bmatrix} 1 \\ 0 \\ \vdots \\ 0 \end{bmatrix}$$

Remark 1.5.1 *The system (1.70) is said to have its linear part in the observable Brunovsky form [14] Moreover, the output is always taken equal to the first state component. Consequently, the diffeomorphism $(x = z - \Phi^{[2]}(z))$ is such that $\Phi_1^{[2]}(z) = 0$*

Proposition 1.5.2 *Under lemma 1.5.1 the system (1.67), is quadratic equivalence modulo an output injection to system (1.68), if and only if the following two homological equations are verified:*

$$\begin{cases} i) & \bar{f}^{[2]}(z) - f^{[2]}(z) + \beta^{[2]}(z_1) = A_{obs}\Phi^{[2]}(z) - \frac{\partial\Phi^{[2]}}{\partial z}A_{obs}z \\ ii) & \bar{g}^{[1]}(z) - g^{[1]}(z) + \gamma^{[1]}(z_1) = -\frac{\partial\Phi^{[2]}}{\partial z}B_{obs} \end{cases} \quad (1.71)$$

where

$$\frac{\partial\Phi^{[2]}}{\partial z}A_{obs}z := \left(\frac{\partial\Phi^{[2]}}{\partial\xi}A_{obs}z + \cdots + \frac{\partial\Phi^{[2]}}{\partial\xi}A_{obs}z \right)^T$$

and $\frac{\partial\Phi^{[2]}}{\partial z}$ is the Jacobian of $\Phi^{[2]}$ for all $1 \leq i \leq n$.

In solving the homological equations (1.71), the resonant terms are those that cannot be cancelled by the right-hand side of the equations (1.71) and that appear in the left-hand side.

We can give two canonical forms, one favoring nonlinearity in the input by solving the homological equation

$$\bar{g}^{[1]}(z) - g^{[1]}(z) + \gamma^{[1]}(z_1) = -\frac{\partial\Phi^{[2]}}{\partial z}B$$

and the other favors non-linearity as it stands, solving the equation homological

$$\bar{f}^{[2]}(z) - f^{[2]}(z) + \beta^{[2]}(z_1) = A\Phi^{[2]}(z) - \frac{\partial\Phi^{[2]}}{\partial z}Az .$$

This is the last solution that we have chosen. Indeed, it allows us to treat indifferently systems with command and without command.

Now, we can give the normal form associated to the QEMOI relation

Theorem 1.5.1 [12] *There exists a quadratic diffeomorphism which transforms the quadratic part of system (1.70) into the quadratic equivalence modulo an output injection:*

$$\left\{ \begin{array}{l} \dot{x}_1 = a_1 x_1 + x_2 + b_1 u + \beta_1^{[2]}(y) + \gamma_1^{[1]}(y)u + \sum_{i=2}^n k_{1i} x_i u + O^{[3]}(x, u) \\ \dot{x}_2 = a_2 x_1 + x_3 + b_2 u + \beta_2^{[2]}(y) + \gamma_2^{[1]}(y)u + \sum_{i=2}^n k_{2i} x_i u + O^{[3]}(x, u) \\ \vdots = \vdots \\ \dot{x}_{n-1} = a_{n-1} x_1 + x_n + b_{n-1} u + \beta_{n-1}^{[2]}(y) + \gamma_{n-1}^{[1]}(y)u + \sum_{i=2}^n k_{(n-1)i} x_i u + O^{[3]}(x, u) \\ \dot{x}_n = a_n x_1 + b_n u + \beta_n^{[2]}(y) + \gamma_n^{[1]}(y)u + \sum_{i=2}^n h_{ij} x_i x_j + \sum_{i=2}^n k_{ni} x_i u + O^{[3]}(x, u) \end{array} \right. \quad (1.72)$$

Proof 1.5.2 As $\bar{f}^{[2]}(z) = 0$ and $\bar{g}^{[1]}(z) = 0$, then the homological equations became [12]:

$$\begin{array}{l} i) A_{obs} \Phi^{[2]}(z) - \frac{\partial \Phi^{[2]}}{\partial z} A_{obs} z = -f^{[2]}(z) + \beta^{[2]}(z_1) \\ ii) -\frac{\partial \Phi^{[2]}}{\partial z} B_{obs} = -g^{[1]}(z) + \gamma^{[1]}(z_1) \end{array}$$

with the condition $\Phi_1^{[2]}(z) = 0$ (i.e. $y = z_1 = x_1$) and thanks to the structure of A_{obs} , we have **for the first homological equation:**

$$\begin{array}{l} \Phi_2^{[2]}(z) = -f_1^{[2]}(z) + \beta_1^{[2]}(z_1) \\ \Phi_3^{[2]}(z) = \sum_{i=1}^{n-1} \frac{\partial \Phi_2^{[2]}}{\partial z_i} (a_i z_1 + z_{i+1}) + \frac{\partial \Phi_2^{[2]}}{\partial z_n} a_n z_1 - f_2^{[2]}(z) + \beta_2^{[2]}(z_1) \\ \Phi_4^{[2]}(z) = \sum_{i=1}^{n-1} \frac{\partial \Phi_3^{[2]}}{\partial z_i} (a_i z_1 + z_{i+1}) + \frac{\partial \Phi_3^{[2]}}{\partial z_n} a_n z_1 - f_3^{[2]}(z) + \beta_3^{[2]}(z_1) \\ \vdots = \vdots \\ \Phi_n^{[2]}(z) = \sum_{i=1}^{n-1} \frac{\partial \Phi_{n-1}^{[2]}}{\partial z_i} (a_i z_1 + z_{i+1}) + \frac{\partial \Phi_{n-1}^{[2]}}{\partial z_n} a_n z_1 - f_{n-1}^{[2]}(z) + \beta_{n-1}^{[2]}(z_1) \end{array}$$

and for the last row

$$0 = \sum_{i=1}^{n-1} \frac{\partial \Phi_n^{[2]}}{\partial z_i} (a_i z_1 + z_{i+1}) + \frac{\partial \Phi_n^{[2]}}{\partial z_n} a_n z_1 - f_n^{[2]}(z) + \beta_n^{[2]}(z_1) .$$

The $(n-1)$ first equations give the value of $\Phi^{[2]}(z)$, which cancel all the quadratic terms in the $(n-1)$ first lines of $f^{[2]}(z)$. Moreover, as $\beta^{[2]}(z_1)$ is a free homogeneous vector field it is also possible to cancel some terms of $f_n^{[2]}(z)$. More precisely, setting $\beta_i^{[2]}(z_1) = \beta_i z_1^2$, we have for **the first equation:**

$$\Phi_2^{[2]}(z) = -f_1^{[2]}(z) + \beta_1 z_1^2$$

and for the second equation we obtain:

$$\Phi_3^{[2]}(z) = \sum_{i=1}^{n-1} \frac{\partial (-f_1^{[2]}(z) + \beta_1 z_1^2)}{\partial z_i} (a_i z_1 + z_{i+1}) - \frac{\partial f_1^{[2]}(z)}{\partial z_n} a_n z_1 - f_2^{[2]}(z) + \beta_2 z_1^2 .$$

Thus, we rewrite the term $\Phi_3^{[2]}(z)$ as follows:

$$\Phi_3^{[2]}(z) = 2\beta_1 z_1 z_2 + \beta_2 z_1^2 + \bar{\Phi}_3^{[2]}(z, \beta_1 z_1^2)$$

with

$$\bar{\Phi}_3^{[2]}(z, \beta_1 z_1^2) = 2\beta_1 a_1 z_1^2 - f_2^{[2]}(z) - \sum_{i=1}^{n-1} \frac{\partial f_1^{[2]}(z)}{\partial z_i} (a_i z_1 + z_{i+1}) - \frac{\partial f_3^{[2]}(z)}{\partial z_n} a_n z_1.$$

Therefore, **the third equation** becomes:

$$\Phi_4^{[2]}(z) = \sum_{i=1}^{n-1} \frac{\partial (2\beta_1 z_1 z_2 + \beta_2 z_1^2 + \bar{\Phi}_3^{[2]}(z, \beta_1 z_1^2))}{\partial z_i} (a_i z_1 + z_{i+1}) + \frac{\partial \bar{\Phi}_3^{[2]}(z, \beta_1 z_1^2)}{\partial z_n} a_n z_1 - f_3^{[2]}(z) + \beta_3 z_1^2.$$

which we can rewrite as follows:

$$\Phi_4^{[2]}(z) = 2\beta_1 z_1 z_3 + 2\beta_2 z_1 z_2 + \beta_3 z_1^2 + \bar{\Phi}_4^{[2]}(z, \beta_1 z_1^2, \beta_1 z_1 z_2, \beta_2 z_1^2)$$

and we are considered outside the function $\bar{\Phi}_4^{[2]}$ where, only terms of the form $\beta_i z_1 z_j$, with $j + i \geq 4$, thus we have:

$$\begin{aligned} \bar{\Phi}_4^{[2]}(z, \beta_1 z_1^2, \beta_1 z_1 z_2, \beta_2 z_1^2) &= 2(\beta_2 a_1 + \beta_1 a_2) z_1^2 + 2\beta_1 z_2^2 + 2\beta_1 a_1 z_1 z_2 \\ &+ \sum_{i=1}^{n-1} \frac{\partial \bar{\Phi}_3^{[2]}(z, \beta_1 z_1^2)}{\partial z_i} (a_i z_1 + z_{i+1}) \\ &+ \frac{\partial \bar{\Phi}_3^{[2]}(z, \beta_1 z_1^2)}{\partial z_n} a_n z_1 - f_3^{[2]}(z). \end{aligned}$$

Recursively, we obtain:

$$\begin{aligned} \Phi_n^{[2]}(z) &= 2\beta_1 z_1 z_{n-1} + 2\beta_2 z_1 z_{n-2} + 2\beta_3 z_1 z_{n-3} + \dots + 2\beta_{n-2} z_1 z_2 + \beta_{n-1} z_1^2 \\ &+ \bar{\Phi}_n^{[2]} \left(z, \beta_1 \sum_{j \geq i=1}^{n-2} z_i z_j, \beta_2 \sum_{j \geq i=1}^{n-3} z_i z_j, \dots, \beta_{n-1} z_1^2 \right) \\ \Phi_n^{[2]}(z) &= 2z_1 \sum_{i=2}^{n-1} \beta_{n-i} z_i + \beta_{n-1} z_1^2 \\ &+ \bar{\Phi}_n^{[2]} \left(z, \beta_1 \sum_{j \geq i=1}^{n-2} z_i z_j, \beta_2 \sum_{j \geq i=1}^{n-3} z_i z_j, \dots, \beta_{n-1} z_1^2 \right) \end{aligned}$$

and finally the last equation is:

$$0 = \sum_{i=1}^{n-1} (a_i z_1 + z_{i+1}) \frac{\partial \left(2z_1 \sum_{j=2}^{n-1} \beta_{n-j} z_j + \beta_{n-1} z_1^2 + \bar{\Phi}_n^{[2]}(\dots) \right)}{\partial z_i} + \frac{\partial \bar{\Phi}_n^{[2]}(\dots)}{\partial z_n} a_n z_1 - f_n^{[2]} + \beta_n z_1^2$$

which gives:

$$\begin{aligned} -2z_1 \sum_{i=2}^{n-1} \beta_{n-i} z_i - \beta_n z_1^2 &= \sum_{i=1}^{n-1} \frac{\partial \bar{\Phi}_n^{[2]}(\dots)}{\partial z_i} (a_i z_1 + z_{i+1}) + \frac{\partial \bar{\Phi}_n^{[2]}(\dots)}{\partial z_n} a_n z_1 - f_n^{[2]} \\ &+ 2 \sum_{i=1}^{n-1} \beta_{n-i} z_i (a_1 z_1 + z_2) + 2\beta_{n-1} z_1 (a_1 z_1 + z_2) \end{aligned}$$

Consequently, the free vector field $\beta^{[2]}(z_1)$ can only cancel the quadratic term $z_1 z_i$ for all $i \in \{1, \dots, n\}$ in the last equation.

For the second homological equation, we have only $\gamma^{[1]}(z_1)$ as a free vector field. Thus in $\gamma^{[1]}(z_1) = -\frac{\partial \bar{\Phi}^{[2]}}{\partial z} B + g^{[1]}(z)$, the vector field $\gamma^{[1]}(z_1)$ is only able to cancel terms in z_1 .

Remark 1.5.2 In reference to the work of Poincaré, we call the terms $h_{ij}x_i x_j$ (for all $n \geq i \geq j \geq 2$) and $k_{li}x_i u$ (for all $n \geq l \geq 1$ and $n \geq i \geq 2$) the resonant terms.

Corollary 1.5.1 Under the lemma 1.5.1, if the system (1.67) is quadratically equivalent to the system (1.68) where the h_{ij} and k_{li} are zero for all $n \geq i \geq j \geq 2$ and $n \geq l \geq 1$, then the system (1.67) is quadratically linearizable modulo an output injection.

1.5.2.1 Practical example for linearly observable case

Example 1.5.1 [12] Let us consider the following linearly observable system

$$\begin{cases} \dot{z}_1 &= a_1 z_1 + z_2 + k_1 z_2^2 + l_1 z_3^2 \\ \dot{z}_2 &= a_2 z_1 + z_3 + k_2 z_2^2 + l_2 z_3^2 \\ \dot{z}_3 &= a_3 z_1 + k_3 z_2^2 + l_3 z_3^2 \\ y &= z_1 \end{cases} \quad (1.73)$$

Suppose there exists a diffeomorphism $x = z - \Phi^{[2]}(z)$, which transforms the system (1.73) into

$$\begin{cases} \dot{x}_1 &= a_1 x_1 + x_2 + \Phi_2^{[2]}(x) + k_1 x_2^2 + l_1 x_3^2 - \frac{\partial \Phi_1^{[2]}(x)}{\partial x} A x + O^{[3]}(x) \\ \dot{x}_2 &= a_2 x_1 + x_3 + \Phi_3^{[2]}(x) + k_2 x_2^2 + l_2 x_3^2 - \frac{\partial \Phi_2^{[2]}(x)}{\partial x} A x + O^{[3]}(x) \\ \dot{x}_3 &= a_3 x_1 + k_3 x_2^2 + l_3 x_3^2 - \frac{\partial \Phi_3^{[2]}(x)}{\partial x} A x + O^{[3]}(x) \\ y &= x_1 \end{cases}$$

with

$$A = \begin{bmatrix} a_1 & 1 & 0 \\ a_2 & 0 & 1 \\ a_3 & 0 & 0 \end{bmatrix} \text{ and } \begin{bmatrix} f_1^{[2]}(z) &= & k_1 z_2^2 + l_1 z_3^2 \\ f_2^{[2]}(z) &= & k_2 z_2^2 + l_2 z_3^2 \\ f_3^{[2]}(z) &= & k_3 z_2^2 + l_3 z_3^2 \end{bmatrix}$$

By using the homological equations we have:

$$\begin{cases} \Phi_1^{[2]}(z) &= & 0 \\ \Phi_2^{[2]}(z) &= & -k_1 z_2^2 - l_1 z_3^2 + \beta_1 z_1^2 \\ \Phi_3^{[2]}(z) &= & (2\beta_1 a_1 + \beta_2) z_1^2 + (2\beta_1 - 2k_1 a_2) z_1 z_2 \\ & & -2k_1 z_2 z_3 - 2l_1 a_3 z_1 z_3 - k_2 z_2^2 - l_2 z_3^2 \end{cases}$$

then by choosing

$$\begin{cases} \beta_1 &= & l_1 a_1 a_3 + 2k_1 a_2 + l_2 a_3, \\ \beta_2 &= & -3\beta_1 a_1 + k_1 a_1 a_2 + k_2 a_2 + k_1 a_3 \end{cases}$$

the normal form of system (1.73) is:

$$\begin{cases} \dot{x}_1 &= & a_1 x_1 + x_2 + \beta_1 x_1^2 + O^{[3]}(x) \\ \dot{x}_2 &= & a_2 x_1 + x_3 + \beta_2 x_1^2 + O^{[3]}(x) \\ \dot{x}_3 &= & a_3 x_1 + (k_3 - 2\beta_1 + 2k_1 a_2) x_2^2 + (l_3 + 2k_1) x_3^2 \\ & & + (2l_1 a_3 + 2k_2) x_2 x_3 + O^{[3]}(x) \end{cases}$$

so the resonant terms that cannot be cancelled are: $(k_3 - 2\beta_1 + 2k_1 a_2) x_2^2$, $(l_3 + 2k_1) x_3^2$ and $(2l_1 a_3 + 2k_2) x_2 x_3$.

1.5.3 One dimensional linearly unobservable case

Assumption 1.5.1 *Let us consider the system (1.65) and assume that the pair (A, C) has one unobservable real mode (i.e. the linear observability matrix $O(A, C) = [C, CA, \dots, CA^{n-1}]^T$ is of range $n - 1$).*

Under this assumption, there exists a linear change of coordinates $z = T\xi$ and a Taylor expansion which transform the system (1.65) in the following form:

$$\begin{cases} \dot{\tilde{z}} &= A_{obs}\tilde{z} + B_{obs}u + \tilde{f}^{[2]}(z) + \tilde{g}^{[1]}(z)u + O^{[3]}(z, u) \\ \dot{z}_n &= \alpha_n z_n + \sum_{i=1}^{n-1} \alpha_i z_i + b_n u + f_n^{[2]}(z) + g_n^{[1]}(z)u + O^{[3]}(z, u) \\ y &= C_{obs}\tilde{z} \end{cases} \quad (1.74)$$

where:

$$A_{obs} = \begin{pmatrix} a_1 & 1 & 0 & \cdot & \cdot & 0 \\ a_2 & 0 & 1 & 0 & \cdot & \cdot \\ \cdot & 0 & \cdot & \cdot & 0 & \cdot \\ \cdot & 0 & \cdot & 0 & \cdot & 0 \\ a_{n-2} & 0 & \cdot & \cdot & 0 & 1 \\ a_{n-1} & 0 & \cdot & \cdot & \cdot & 0 \end{pmatrix}, \quad B_{obs} = \begin{bmatrix} b_1 \\ b_2 \\ \cdot \\ b_{n-2} \\ b_{n-1} \end{bmatrix} \quad \text{and } C_{obs} = [1, 0, \dots, 0].$$

z_n is the linearly unobservable state, $\tilde{z} = [z_1, z_2, \dots, z_{n-1}]^T$ is the linearly observable state vector, $z = [\tilde{z}^T, z_n]^T$ is the global state vector, $\tilde{f}^{[2]}(z) = [f_1^{[2]}(z), f_2^{[2]}(z), \dots, f_{n-1}^{[2]}(z)]^T$ and $\tilde{g}^{[1]}(z) = [g_1^{[1]}(z), g_2^{[1]}(z), \dots, g_{n-1}^{[1]}(z)]^T$ with $\tilde{f}_i^{[2]}(z)$ and $\tilde{g}_i^{[1]}(z)$ are respectively homogeneous polynomials of degree 2 and 1 in $z \forall i, 1 \leq i \leq n$. The linear part of the system (1.74) has a non-observable ‘‘real’’ mode of value α_n .

After having decomposed the system (1.66) into a linearly observable part \tilde{z} and a linearly unobservable part z_n , we define the quadratic equivalence modulo an output injection.

Definition 1.5.3 *Let us consider the two systems*

$$\begin{cases} \dot{\tilde{z}} &= A_{obs}\tilde{z} + B_{obs}u + \tilde{f}^{[2]}(z) + \tilde{g}^{[1]}(z)u + O^{[3]}(z, u) \\ \dot{z}_n &= \alpha_n z_n + \sum_{i=1}^{n-1} \alpha_i z_i + b_n u + f_n^{[2]}(z) + g_n^{[1]}(z)u + O^{[3]}(z, u) \\ y &= C_{obs}\tilde{z} \end{cases} \quad (1.75)$$

is said to be quadratically equivalent to the modulo an output injection (QEMOI) to the system

$$\begin{cases} \dot{\tilde{x}} &= A_{obs}\tilde{x} + B_{obs}u + \bar{f}^{[2]}(x) + \bar{g}^{[1]}(x)u + \bar{\beta}^{[2]}(y) \\ &\quad + \bar{\gamma}^{[1]}(y)u + O^{[3]}(x, u) \\ \dot{x}_n &= \alpha_n x_n + \sum_{i=1}^{n-1} \alpha_i x_i + b_n u + f_n^{[2]}(x) + g_n^{[1]}(x)u + \beta_n^{[2]}(y) \\ &\quad + \gamma_n^{[1]}(y)u + O^{[3]}(x, u) \\ y &= C_{obs}\tilde{x} \end{cases} \quad (1.76)$$

if there exists a modulo an output injection

$$\bar{\beta}^{[2]}(y) + \bar{\gamma}^{[1]}(y)u \quad \text{and} \quad \beta_n^{[2]}(y) + \gamma_n^{[1]}(y)u$$

and a diffeomorphism of the form:

$$\tilde{x} = \tilde{z} - \tilde{\Phi}^{[2]}(z) \quad \text{and} \quad x_n = z_n - \Phi_n^{[2]}(z) \quad (1.77)$$

which transforms the one to the quadratic part of (1.75) of the other one to the quadratic part of (1.76). With x_n the linearly unobservable state, $\tilde{x} = [x_1, x_2, \dots, x_{n-1}]^T$ is the linearly observable state vector, $x = [\tilde{x}^T, x_n]^T$ is the global state vector and $\tilde{\Phi}^{[2]}(z) = [\Phi_1^{[2]}(z), \dots, \Phi_{n-1}^{[2]}(z)]^T$, $\tilde{\beta}^{[2]}(y) = [\beta_1^{[2]}(y), \dots, \beta_{n-1}^{[2]}(y)]^T$ are homogeneous polynomials in z , respectively, in y , of degree two, and $\tilde{\gamma}^{[1]}(y) = [\gamma_1^{[1]}(y), \dots, \gamma_{n-1}^{[1]}(y)]^T$ is homogeneous of degree one in y .

In the same way as in the linearly observable case, we will give in the following proposition the necessary and sufficient conditions for the existence of a diffeomorphism (1.77) and this modulo the output injection.

Proposition 1.5.3 *System (1.75) is quadratically equivalent to system (1.76), modulo an. output injection if and only if, the two sets of following homological equations are verified*

$$\begin{aligned}
 i) \quad & \begin{cases} \bar{f}^{[2]}(z) - \tilde{f}^{[2]}(z) + \tilde{\beta}^{[2]}(z_1) &= A_{obs} \tilde{\Phi}^{[2]}(z) - \frac{\partial \tilde{\Phi}^{[2]}}{\partial z_n} (\alpha_n z_n + \sum_{i=1}^{n-1} \alpha_i z_i) - \frac{\partial \tilde{\Phi}^{[2]}}{\partial \tilde{z}} A_{obs} \tilde{z} \\ \bar{g}^{[1]}(z) - \tilde{g}^{[1]}(z) + \tilde{\gamma}^{[1]}(z_1) &= -\frac{\partial \tilde{\Phi}^{[2]}}{\partial \tilde{z}} B_{obs} - \frac{\partial \tilde{\Phi}^{[2]}}{\partial z_n} b_n \end{cases} \\
 ii) \quad & \begin{cases} \bar{f}_n^{[2]}(z) - f_n^{[2]}(z) + \beta_n^{[2]}(z_1) &= \sum_{i=1}^{n-1} \alpha_i \Phi_i^{[2]}(z) + \alpha_n \Phi_n^{[2]}(z) - \frac{\partial \Phi_n^{[2]}}{\partial \tilde{z}} A_{obs} \tilde{z} \\ &- \frac{\partial \Phi_n^{[2]}}{\partial z_n} (\alpha_n z_n + \sum_{i=1}^{n-1} \alpha_i z_i) \\ \bar{g}_n^{[1]}(z) - g_n^{[1]}(z) + \gamma_n^{[1]}(z_1) &= -\frac{\partial \Phi_n^{[2]}}{\partial z_n} b_n - \frac{\partial \Phi_n^{[2]}}{\partial \tilde{z}} B_{obs} \end{cases}
 \end{aligned}$$

Now as the linearly observable part is already in the normal form (i.e. Brunovsky) we give:

Theorem 1.5.2 [12, 11] *The normal form with respect to the quadratic equivalence modulo an output injection of the system(1.75) is:*

$$\begin{aligned}
 \dot{x}_1 &= a_1 x_1 + b_1 u + \beta_1^{[2]}(y) + \gamma_1^{[1]}(y) u + \sum_{i=2}^n k_{1i} x_i u + O^{[3]}(x, u) \\
 \dot{x}_2 &= a_2 x_1 + b_2 u + \beta_2^{[2]}(y) + \gamma_2^{[1]}(y) u + \sum_{i=2}^n k_{2i} x_i u + O^{[3]}(x, u) \\
 \vdots &= \vdots \\
 \dot{x}_{n-2} &= a_{n-2} x_1 + b_{n-2} u + \beta_{n-2}^{[2]}(y) + \gamma_{n-2}^{[1]}(y) u + \sum_{i=2}^n k_{(n-2)i} x_i u + O^{[3]}(x, u) \\
 \dot{x}_{n-1} &= a_{n-1} x_1 + b_{n-1} u + \beta_{n-1}^{[2]}(y) + \gamma_{n-1}^{[1]}(y) u + \sum_{j \geq i=2}^n h_{ij} x_i x_j + h_{1n} x_1 x_n \\
 &\quad + \sum_{i=2}^n k_{(n-1)i} x_i u + O^{[3]}(x, u) \\
 \dot{x}_n &= \alpha_n x_n + \sum_{i=1}^{n-1} \alpha_i x_i + b_n u + \beta_n^{[2]}(y) + \gamma_n^{[1]}(y) u + \sum_{i=2}^n k_{(n-1)i} x_i u \\
 &\quad + f_n^{[2]}(x) + \alpha_n \Phi_n^{[2]}(x) + \sum_{i=1}^{n-1} \alpha_i \Phi_i^{[2]}(x) - \frac{\partial \Phi_n^{[2]}}{\partial \tilde{x}} A_{obs} \tilde{x} \\
 &\quad - \frac{\partial \Phi_n^{[2]}}{\partial x_n} (\alpha_n x_n + \sum_{i=1}^{n-1} \alpha_i x_i) + O^{[3]}(x, u)
 \end{aligned} \tag{1.78}$$

the coefficients $h_{i,j}$ and $k_{i,i}$, for $2 \leq i \leq j \leq n$ are called quadratic normal numbers.

Proof 1.5.3 For the linearly observable part, the proof is identical to that of theorem 1.5.1. For the linearly unobservable part, to cancel all quadratic terms in the last \dot{x}_n dynamic, $\Phi_n^{[2]}(x)$ for this, we must check the following equation:

$$-f_n^{[2]}(x) + \beta_n^{[2]}(x_1) = \alpha_n \Phi_n^{[2]}(x) + \sum_{i=1}^{n-1} \alpha_i \Phi_i^{[2]}(x) - \frac{\partial \Phi_n^{[2]}}{\partial \tilde{x}} A_{obs} \tilde{x} - \frac{\partial \Phi_n^{[2]}}{\partial x_n} (\alpha_n x_n + \sum_{i=1}^{n-1} \alpha_i x_i)$$

which generally does not admit a solution for all α_n and α_i . Nevertheless, the conditions are less restrictive than the usual ones thanks to the output injection $\beta_n^{[2]}(x_1)$.

The remaining resonant terms:

Corollary 1.5.2

- 1) Thanks to the terms $k_{(n-1)n} x_n u$ in the normal form (1.78), it is possible with a well-chosen input u (universal input [11]), to reconstruct the local quadratic observability of x_n .
- 2) Thanks to the terms $h_{in} x_i x_n$ ($i \in [1, n-1]$) in the normal form (1.78), it is also possible to locally recover the quadratic observability of x_n .
- 3) In normal form (1.78), if the k_{ij} are all zero $\forall 1 \leq i \leq n-1$, isolating the terms in the unobservable direction x_n , the locally unobservable manifold is:

$$S_n = \left\{ x, \text{ such as } \sum_{i=1}^{n-1} h_{in} x_i + 2h_{nn} x_n + k_{(n-1)n} u = 0 \right\}$$

- 4) The resonant terms on the last under dynamics \dot{x}_n , do not contribute anything for the local quadratic observability.

Remark 1.5.3 In the case where all $k_{(n-1)n}$ and h_{in} are zero, α_n guarantees us or not the detectability of the state x_n :

- a) if $\alpha_n < 0$, then the state x_n is detectable,
- b) if $\alpha_n > 0$, x_n is unstable and consequently undetectable,
- c) if $\alpha_n = 0$, we can use the center manifold theory in order to analyze the stability or in stability of x_n and consequently its detectability or undetectability [11].

1.5.3.1 Example: Lorentz system

In this section, by means of an example we will to illustrate the presented results in section 2.2.2, let us consider the following Lorentz system presented in reference [51]:

$$\begin{cases} \dot{\xi}_1 &= -10\xi_1 + 10\xi_2 \\ \dot{\xi}_2 &= 28\xi_1 - \xi_2 - \xi_1\xi_3 \\ \dot{\xi}_3 &= \alpha\xi_3 + \xi_1\xi_2 \end{cases} \quad (1.79)$$

Now, consider the following change of coordinates:

$$\begin{cases} z_1 &= \xi_1 \\ z_2 &= \xi_1 + 10\xi_2 \implies \xi_2 = -\frac{1}{10}z_1 + \frac{1}{10}z_2 \\ z_u &= \xi_3 \end{cases}$$

which transforms the system into the Brunovsky normal form:

$$\begin{cases} \dot{z}_1 &= -11z_1 + z_2 \\ \dot{z}_2 &= 270z_1 - 10z_1z_u \\ \dot{z}_u &= -\frac{8}{3}z_u - \frac{1}{10}(z_1)^2 + \frac{1}{10}z_1z_2 \end{cases} \quad (1.80)$$

Now, consider the change of coordinates $x_o = z_o - \varphi_o(z)$ and $x_u = z_u - \varphi_u(z)$, such that:

$$\begin{aligned} x_o &= \begin{bmatrix} x_1 \\ x_2 \end{bmatrix} = \begin{bmatrix} z_1 - \varphi_1(z) \\ z_2 - \varphi_2(z) \end{bmatrix} \\ x_u &= x_u = z_u - \varphi_u(z) \end{aligned}$$

and by using the homological equations we have:

$$\begin{aligned} \varphi_1(z) &= 0 \\ \varphi_2(z) &= 0. \end{aligned}$$

Note: For x_u the Sylvester equation gives a solution $\varphi_u(x) = 0$. Thus, the quadratic term cannot be cancelled.

$$\begin{aligned} \dot{x}_u &= -\frac{8}{3}x_u + \frac{8}{3}\varphi_u(x_1) - \frac{\partial\varphi_u(x_1)}{\partial x}Ax + \frac{1}{10}x_1x_2 - \frac{1}{10}(x_1)^2 \\ &= -\frac{8}{3}x_u + \frac{1}{10}x_1x_2 - \frac{1}{10}(x_1)^2 \end{aligned}$$

and we obtain the following observability quadratic normal form of the Lorentz system:

$$\begin{cases} \dot{x}_1 &= -11x_1 + x_2 \\ \dot{x}_2 &= 270x_1 - 10x_1x_u \\ \dot{x}_u &= -\frac{8}{3}x_u + \frac{1}{10}x_1x_2 - \frac{1}{10}(x_1)^2 \end{cases} \quad (1.81)$$

Now, for this example to design the sliding mode observer we take as output the state x_1 .

Moreover, the first two states are linearly observable and the third state is unobservable. The eigenvalues of the considered system are $\{-22.8277, 11.8277, -2.6667\}$, then we can see that the unobservable mode is -2.6667 so the system is linearly detectable. Then the observer for system (2.35) is given by:

$$\begin{cases} \dot{\hat{x}}_1 &= -11x_1 + \hat{x}_2 + \delta_1 \text{sign}(x_1 - \hat{x}_1) \\ \dot{\hat{x}}_2 &= 270x_1 - 10x_1\hat{x}_u + E_1\delta_2 \text{sign}(\hat{x}_2 - \hat{x}_2) \\ \dot{\hat{x}}_u &= -\frac{8}{3}\hat{x}_u + \frac{1}{10}x_1\hat{x}_2 - \frac{1}{10}(x_1)^2 + E_2\delta_3 \text{sign}(\hat{x}_3 - \hat{x}_3) \end{cases} \quad (1.82)$$

In system (2.36) the auxiliary components \tilde{z}_i are determined algebraically:

$$\begin{aligned} \tilde{x}_2 &= \hat{x}_2 + E_1\delta_1 \text{sign}(x_1 - \hat{x}_1) \\ \tilde{x}_u &= \hat{x}_u + \frac{E_2E_S\delta_2}{10x_1+E_S-1} \text{sign}(\tilde{x}_2 - \hat{x}_2) \end{aligned}$$

with the following conditions:

$$\begin{aligned} &\text{if } x_1 = \hat{x}_1 \text{ then } E_1 = 1, \text{ otherwise } E_1 = 0, \\ &\text{if } \tilde{x}_2 = \hat{x}_2 \text{ and } x_1 = \hat{x}_1 \text{ then } E_2 = 1 \text{ otherwise } E_2 = 0, \\ &\text{if } x_1 = 0 \text{ then } E_s = 0 \text{ otherwise } E_s = 1. \end{aligned}$$

Remark 1.5.4 We can see that when $x_1 = 0$, \tilde{x}_u tends to infinity, meaning that observability singularity occurs. Thus, to avoid the explosion of x_u we introduce a filter E_S as follows: If $x_1 = 0$, then $E_S = 0$ otherwise $E_S = 1$. In this case \tilde{x}_u becomes:

$$\tilde{x}_u = \hat{x}_u + \frac{E_2 E_S}{\delta} 10x_1 + E_S - 1 \text{sign}(\tilde{x}_2 - \hat{x}_2).$$

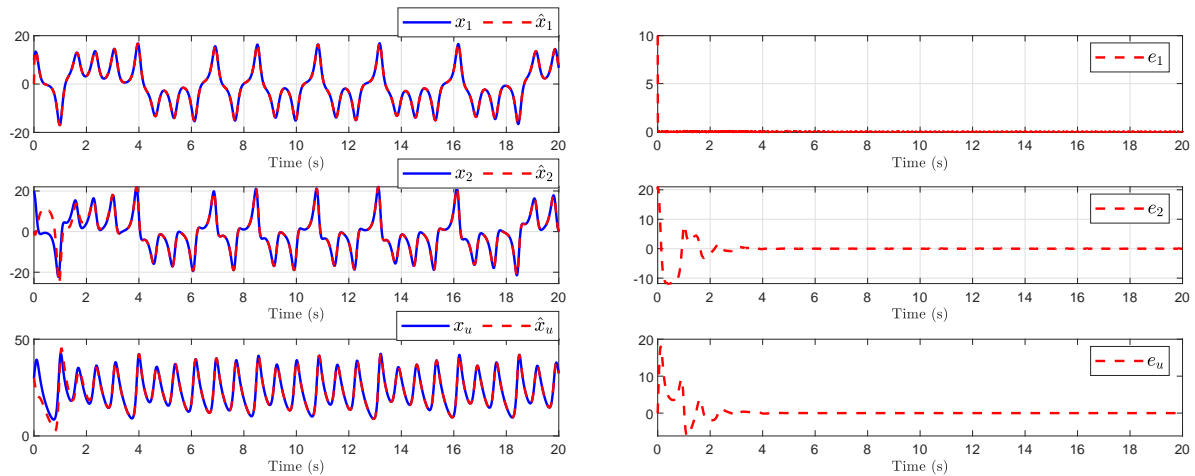
In order to not lose the observability for a long time at singularity surface, we must set correctly E_S by taking $E_S = 0$ during a short period of time. Before providing the simulation results, note that:

$$\begin{cases} \hat{x}_1 &= \hat{\xi}_1 \\ \hat{x}_2 &= \hat{\xi}_1 + 10\hat{\xi}_2 \implies \hat{\xi}_2 = -\frac{1}{10}\hat{x}_1 + \frac{1}{10}\hat{x}_2 \\ \hat{x}_u &= \hat{\xi}_3 \end{cases}$$

However, we can see that $x_1 = 0$, so the observability is not lost.

Simulation results

Figures 1.4a show the obtained simulation results for the Lorenz system. Figure 1.4 illustrates the dynamics of the observer and the Lorenz system for 20s, for this simulations, we have considered the following initial conditions $x_1 = 10$, $x_2 = 20$, $x_u = 30$ and $\hat{x}_1 = 0$, $\hat{x}_2 = 0$, $\hat{x}_u = 30$. Figure 1.4b illustrates the estimation error, it can then be noticed that the observer's state x_1^1 converges in 1.6sec and for the other states the convergence is obtained in 6sec.



(a) Dynamics of Lorenz system and the observer

(b) Estimation errors of the Lorenz observer

Figure 1.4: Plot the dynamics of Lorenz system

Figure 1.5 illustrates the trajectories in the phase plane of the observer and the Lorenz system.

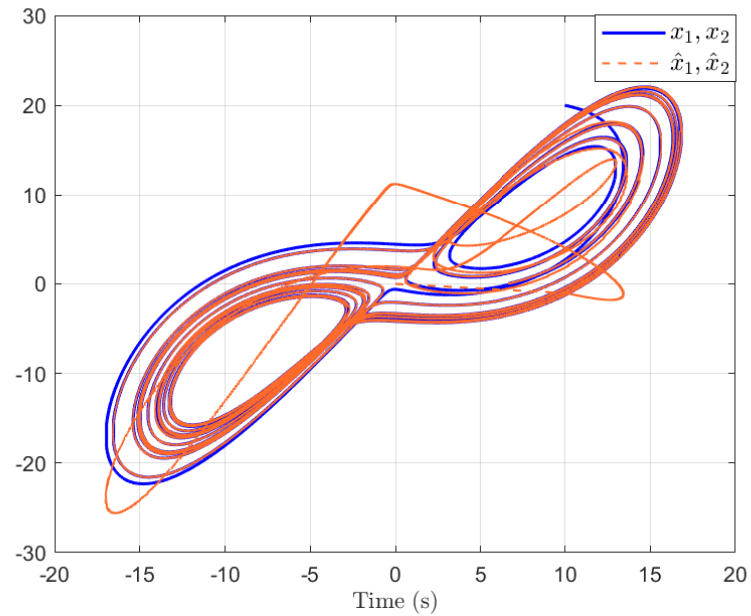


Figure 1.5: Trajectories in the phase plane.

1.6 Conclusion

In conclusion, this chapter has provided a comprehensive exploration of observability in nonlinear systems. We explored the essential characteristics of both linear and nonlinear systems, highlighting key concepts such as observability requirements and various observer strategies, including sliding mode observers and Kalman filters.

To address the limitations of traditional observability concepts, we introduced the quadratic observability normal form for single-input single-output (SISO) systems. This form enhances the classical linear observability framework by incorporating higher-order terms, allowing for a more refined characterization of a system's observability properties. It facilitates the transformation of nonlinear systems into equivalent representations where state variables and their interactions are expressed up to the second order. This approach not only enhances our understanding of the system's dynamics but also aids in designing effective observers for state estimation and fault detection.

Chapter 2

Quadratic observability normal form for MIMO systems

Contents

2.1	Introduction	34
2.2	Quadratic observability normal form for nonlinear multi-output systems	35
2.2.1	Linearly observable case	36
2.2.2	Linearly unobservable case	42
2.3	Quadratic observability normal form for nonlinear multi-input multi-output systems	48
2.3.1	Linearly observable case	50
2.3.2	Linearly unobservable case	54
2.4	Sliding mode observer design	60
2.4.1	Application to Generalized Lorenz System	62
2.5	Conclusion	65

2.1 Introduction

In this chapter, we introduce our first major contribution to the field of observability analysis for dynamical systems. Our work focuses on extending existing results on the quadratic normal form ([10]), which was initially developed for single-input, single-output (SISO) linear systems, to for nonlinear multi-input multi-output systems. This general framework enhances our understanding of observability in complex contexts, particularly for multi-variable systems where dynamic interactions are richer and more varied.

We begin with a detailed description of the computational technique for deriving the quadratic normal form of observability, distinguishing between linearly observable and linearly unobservable systems. This distinction is fundamental, as it influences how information about the system's state can be extracted from observations. For linearly observable systems, observability can be analyzed directly through the system's linear structure, whereas for unobservable systems, additional methods are required to capture the nonlinearities affecting observability.

Finally, to demonstrate the feasibility and effectiveness of our approach, we provide numerical examples in which we develop this transformation step by step.

2.2 Quadratic observability normal form for nonlinear multi-output systems

This section focuses on the concept of quadratic equivalence in the context of nonlinear systems. First, we establish the definition of this quadratic equivalence. Throughout the section, we examine a Multi-Output nonlinear system governed by the following equations:

$$\begin{cases} \dot{\xi} &= F(\xi) \\ y &= h(\xi) \end{cases} \quad (2.1)$$

where $\xi \in \mathbb{R}^n$ is the state vector of the system, $y \in \mathbb{R}^p$ is the output vector and $F(\xi) \in \mathbb{R}^n$ is the vector field such that $F(\xi) : U \subset \mathbb{R}^n \rightarrow \mathbb{R}^n$ is assumed to be real analytic and the output vector $y \in \mathbb{R}^p$ represents the measurable outputs of the system. Without loss of generality, we assume that $F(0) = 0$. Moreover, by setting: $A = \frac{\partial F}{\partial \xi}(0)$ and performing a Taylor series development around the equilibrium point $\xi_e = 0$ of system (2.1). We write the system (2.1) as follows:

$$\begin{cases} \dot{\xi} &= A\xi + f(\xi) + O^3(\xi) \\ y &= C\xi \end{cases} \quad (2.2)$$

where $f(\xi)$ is a homogeneous polynomial of degree 2 in ξ and $O^3(\xi)$ is terms of higher order > 2 .

Let's start by define the notion of quadratic equivalence under coordinates change and output injection. Note that, in this section the term "output injection" refers to the injection of all available variables, output and known input. First let us define the so-called quadratic equivalence.

Definition 2.2.1 *The system (2.2) is said to be quadratically equivalent to the following system:*

$$\begin{cases} \dot{\zeta} &= A\zeta + \bar{f}(\zeta) + \beta(y) + O^3(\zeta) \\ y &= Cx \end{cases} \quad (2.3)$$

Modulo an Output Injection (MOI) $\beta(y)$ if there exists a diffeomorphism of the form:

$$\zeta = \xi - \varphi(\xi) \quad (2.4)$$

which transforms the quadratic part $f(\xi)$ of system (2.2) into the quadratic part $\bar{f}(\zeta)$ of system (2.3) modulo the output injection $\beta(y)$. Where $\varphi(\xi)$ is quadratic homogeneous polynomial term in ξ and $\beta(y)$ is quadratic homogeneous polynomial term in y .

Remark 2.2.1 *We note that output injection refers to the injection of all output variables. The equivalence modulo an output injection is justified by the fact that the output injection cancels out in the observation error dynamics (see [49], [50], [70]).*

The problem we will address here is: what is the quadratic observability normal form associated with the system (2.2) respecting the quadratic equivalence modulo an output injection $\beta(y)$?

In what follows, we will give the so-called quadratic observability normal form associated to system (2.2) modulo the output injection $\beta(y)$ by examining two cases:

1. The linearly observable systems.
2. The linearly unobservable systems.

2.2.1 Linearly observable case

Before delving into the assumptions that will guide our analysis, it's essential to highlight the significance of the observable case within the framework of quadratic observability. Observability is a critical concept in control theory, as it determines the ability to infer the internal state of a system from its outputs. In the context of nonlinear systems, establishing the observable case is vital for ensuring that we can achieve quadratic equivalence. This equivalence is crucial for developing effective control strategies, as it allows us to accurately characterize the system's dynamics and design appropriate observers, thereby enhancing our ability to control complex systems effectively.

In this section we will make this assumption:

Assumption 2.2.1 *We assume that the pair (A, C) of system (2.2) is observable thus that*

$$\text{rank} \begin{pmatrix} C \\ CA \\ \vdots \\ CA^{n-1} \end{pmatrix} = n.$$

Under this assumption and Brunovsky's work [14], we can assume the linear part of system (2.2) in the observable Brunovsky form. We can provide the following lemma.

Lemma 2.2.1 [14] *Under the assumption 2.2.1, there exists a linear change of coordinates $z = T\xi$ which transforms system (2.2) into the following form:*

$$\begin{cases} \dot{z}^1 = A_o^1 z^1 + f^1(z) + O^3(z) \\ \dot{z}^2 = A_o^2 z^2 + f^2(z) + O^3(z) \\ \vdots = \vdots \\ \dot{z}^p = A_o^p z^p + f^p(z) + O^3(z) \\ y = C_o z \end{cases} \quad (2.5)$$

where $z^q \in \mathbb{R}^{r_q}$ is the state vector observed by the output $y_q = z_1^q$ for $1 \leq q \leq p$, with $\sum_{q=1}^p r_q = n$. We put:

$$z = [z^1 \quad z^2 \quad \dots \quad z^p]^T \in \mathbb{R}^n,$$

$$z^q = [z_1^q \quad z_2^q \quad \dots \quad z_{r_q}^q]^T \in \mathbb{R}^{r_q},$$

$$A_o = \begin{bmatrix} A_o^1 & [0]_{r_1 r_2} & \dots & [0]_{r_1 r_p} \\ [0]_{r_2 r_1} & A_o^2 & \vdots & \vdots \\ \vdots & \dots & \ddots & \vdots \\ [0]_{r_2 r_p} & \dots & 0 & A_o^p \end{bmatrix} \in \mathbb{R}^{n \times n}, \text{ where } A_o^q = \begin{bmatrix} a_1^q & 1 & 0 & \dots & 0 \\ a_2^q & 0 & 1 & 0 & \vdots \\ \vdots & \vdots & \ddots & \ddots & 0 \\ a_{r_q-1}^q & 0 & \ddots & 0 & 1 \\ a_{r_q}^q & 0 & \dots & 0 & 0 \end{bmatrix} \in \mathbb{R}^{r_q \times r_q},$$

$$C_o = \begin{bmatrix} C_o^1 & [0]_{1 r_2} & \dots & [0]_{1 r_p} \\ [0]_{1 r_1} & C_o^2 & \vdots & \vdots \\ \vdots & \dots & \ddots & \vdots \\ [0]_{1 r_1} & \dots & \dots & C_o^p \end{bmatrix} \in \mathbb{R}^{p \times n}, \text{ with } C_o^q = [1 \quad 0 \quad \dots \quad 0] \in \mathbb{R}^{1 \times r_q},$$

$$\begin{aligned} f(z) &= [f^1(z) \quad f^2(z) \quad \dots \quad f^p(z)]^T \in \mathbb{R}^n \text{ with} \\ f^q(z) &= [f_1^q(z) \quad f_2^q(z) \quad \dots \quad f_{r_q}^q(z)]^T \in \mathbb{R}^{r_q} \end{aligned}$$

and where $f_i^q(z)$ is a homogeneous polynomial of degree 2 in z .

Remark 2.2.2 If the pair (A, C) is observable then

$$\text{rank} \begin{pmatrix} C_o^q \\ C_o^q A_o^q \\ \vdots \\ C_o^q A_o^{q(r_q-1)} \end{pmatrix} = r_q \text{ for } 1 \leq q \leq p \text{ with } \sum_{q=1}^p r_q = n.$$

2.2.1.1 Quadratic observability normal form

Now, we will determine the necessary and sufficient conditions to quadratic equivalence modulo an output injection associated to system (2.3).

Proposition 2.2.1 System (2.5) is Quadratically Equivalent Modulo an Output Injection (QEMOI) to system

$$\begin{cases} \dot{x}^1 &= A_o^1 x^1 + \bar{f}^1(x) + \beta^1(y) + O^3(x) \\ \dot{x}^2 &= A_o^2 x^2 + \bar{f}^2(x) + \beta^2(y) + O^3(x) \\ &\vdots \\ \dot{x}^p &= A_o^p x^p + \bar{f}^p(x) + \beta^p(y) + O^3(x) \\ y &= C_o x \end{cases} \quad (2.6)$$

if and only if there exist a diffeomorphism $(x^q = z^q - \varphi^q(z))$ and an output injection $\beta^q(y)$ that satisfy the following homological equation:

$$\bar{f}^q(x) + \beta^q(y) = A_o^q \varphi^q(x) + f^q(x) - \frac{\partial \varphi^q(x)}{\partial x} A_o x.$$

where $\varphi^q(z) \in \mathbb{R}^{r_q}$ and $\beta(y) \in \mathbb{R}^{r_q}$ are quadratic homogeneous polynomial terms in z and y .

Proof 2.2.1 Let $x^q = z^q - \varphi^q(z)$. Then $\dot{x}^q = \dot{z}^q - \frac{\partial \varphi^q(z)}{\partial z} \dot{z}$

Substituting the expression for z from System (2.5) into the equation above, we get:

$$\dot{x}^q = A_o^q z^q + f^q(z) + O^3(z) - \frac{\partial \varphi^q(z)}{\partial z} (A_o z + f(z) + O^3(z))$$

By substituting x^q with $z^q - \varphi^q(z)$ in System (2.6), we have:

$$\dot{x}^q = A_o^q (z^q - \varphi^q(z)) + \bar{f}^q(z - \varphi(z)) + O^3(z - \varphi(z)) + \beta^q(y)$$

For system (2.5) to be quadratically equivalent to system (2.6), their quadratic parts must be equal:

$$A_o^q z^q - A_o^q \varphi^q(z) + \bar{f}^q(z) + \beta^q(y) = A_o^q z^q + f^q(z) - \frac{\partial \varphi^q(z)}{\partial z} A_o z$$

This equality leads to the following homological equation:

$$\bar{f}^q(z) + \beta^q(y) = A_o^q \varphi^q(z) + f^q(z) - \frac{\partial \varphi^q(z)}{\partial z} A_o z.$$

Now, the problem we will address here is: what is the quadratic observability normal form associated to system (2.5) with respect to the quadratic equivalence modulo an output injection

$$\beta(y) = [\beta^1(y) \quad \beta^2(y) \quad \dots \quad \beta^p(y)]^T \in \mathbb{R}^n \text{ with}$$

$$\beta^q(y) = [\beta_1^q(y) \quad \beta_2^q(y) \quad \dots \quad \beta_{r_q}^q(y)]^T \in \mathbb{R}^{r_q} \text{ for } 1 \leq q \leq p \text{ with } \sum_{q=1}^p r_q = n?$$

In what follows, we will present an explicit procedure to compute the diffeomorphism and the output injection, enabling us to derive the quadratic observability normal form for nonlinear Multi-Output systems. To achieve this, for $1 \leq q \leq p$, let us consider the diffeomorphism $x^q = z^q - \varphi^q(z)$ which ensures that the outputs remain unchanged. Where $\varphi^q(z) = [\varphi_1^q(z) \quad \varphi_2^q(z) \quad \dots \quad \varphi_{r_q}^q(z)]^T \in \mathbb{R}^{r_q} \in \mathbb{R}^{r_q}$ and $\beta^q(y) \in \mathbb{R}^{r_q}$ are quadratic homogeneous polynomial terms respectively in z and y .

In this work, we don't allow any quadratic transformation on the output, which leads us to make this assumption.

Assumption 2.2.2 *To ensure that the outputs remain unchanged, the diffeomorphism ($x^q = z^q - \varphi^q(z)$) is choosing such such that $\varphi_1^q(z) = 0$ for $1 \leq q \leq p$.*

Based on this foundation, we can establish the following theorem.

Theorem 2.2.1 *Under assumption 2.2.2, if the pair (A_0, C_0) is observable there exist a diffeomorphism $x = z - \varphi(z)$ and an output injection witch transform (2.5) in the following quadratic observability normal form:*

$$\left\{ \begin{array}{l} \dot{x}_1^q = a_1^q x_1^q + x_2^1 + \beta_1^q(y) \\ \dot{x}_2^q = a_2^q x_1^q + x_3^1 + \beta_2^q(y) \\ \vdots = \vdots \\ \dot{x}_{r_q-1}^q = a_{r_q-1}^q x_1^q + x_{r_q}^q + \beta_{r_q-1}^q(y) \\ \dot{x}_{r_q}^q = a_{r_q}^q x_1^q + \bar{f}_{r_q}^q(x) + \beta_{r_q}^q(y) \end{array} \right. \quad (2.7)$$

for $1 \leq q \leq p$ with $\sum_{i=q}^p r_q = n$ where:

$$\bar{f}_{r_q}^q(x) = f_{r_q}^q(x) - \frac{\partial \varphi_{r_q}^q(x)}{\partial x} A_0 x.$$

and where the components of the quadratic part of the diffeomorphism are derived by induction from the following equations:

$$\begin{aligned} \varphi_1^q(x) &= 0 \\ \varphi_i^q(x) &= \frac{\partial \varphi_{i-1}^q(x)}{\partial x} A_0 x - f_{i-1}^q(x) + \beta_{i-1}^q(y) \text{ for all } 2 \leq i \leq r_q. \end{aligned} \quad (2.8)$$

Proof 2.2.2 *For the initial dynamics, we have:*

$$\dot{z}_1^q = a_1^q z_1^q + z_2^q + f_1^q(z) + O^3(z)$$

with the transformation:

$$x_1^q = z_1^q - \varphi_1^q(z)$$

we obtain:

$$\begin{aligned} \dot{x}_1^q &= \dot{z}_1^q - \frac{\partial \varphi_1^q}{\partial z} \dot{z} \\ \dot{x}_1^q &= a_1^q z_1^q + z_2^q + f_1^q(z) + O^3(z) - \frac{\partial \varphi_1^q(z)}{\partial z} (A_0 z + f(z) + O^3(z)) \end{aligned}$$

By substituting $z_i^q = x_i^q + \varphi_i^q(x)$ in the previous expression and retaining terms of orders 1 and 2, we arrive at:

$$\dot{x}_1^q = a_1^q x_1^q + a_1^q \varphi_1^q(x) + x_2^q + \varphi_2^q(x) + f_1^q(x) - \frac{\partial \varphi_1^q(x)}{\partial x} A_0 x$$

by assumption the output $y = z_1^q$ is unchanged ($\varphi_1^q(x) = 0$), therefore we have:

$$\dot{x}_1^q = a_1^q x_1^q + x_2^q + \varphi_2^q(x) + f_1^q(x) - \frac{\partial \varphi_1^q(x)}{\partial x} A_0 x + O^3(x)$$

Now, let's compare this with the desired form stated in Theorem 2.2.1:

$$a_1^q x_1^q + x_2^q + \varphi_2^q(x) + f_1^q(x) - \frac{\partial \varphi_1^q(x)}{\partial x} A_0 x = a_1^q x_1^q + x_2^q + \bar{f}_1^q(x) + \beta_1^q(y)$$

After simplification, we obtain:

$$\bar{f}_1^q(x) = \varphi_2^q(x) - \frac{\partial \varphi_1^q(x)}{\partial x} A_0 x + f_1^q(x) - \beta_1^q(y)$$

to have $\bar{f}_1^q(x) = 0$ we choose:

$$\varphi_2^q(x) = \frac{\partial \varphi_1^q(x)}{\partial x} A_0 x - f_1^q(x) + \beta_1^q(y)$$

Similarly, for each index $i = r_q - 1$, we obtain:

$$\bar{f}_i^q(x) = \varphi_{i+1}^q(x) - \frac{\partial \varphi_i^q(x)}{\partial x} A_0 x + f_i^q(x) - \beta_i^q(y)$$

to have $\bar{f}_i^q(x) = 0$ we choose:

$$\varphi_{i+1}^q(x) = \frac{\partial \varphi_i^q(x)}{\partial x} A_0 x - f_i^q(x) + \beta_i^q(y) \quad (2.9)$$

The first $(r_q - 1)$ equations provide the value of $\varphi^q(z)$, which cancels all the quadratic terms in the first $(r_q - 1)$ lines of $f^q(z)$. For the last equation, we have $x_{r_q}^q = z_{r_q}^q - \varphi_{r_q}^q(z)$, then:

$$\begin{aligned} \dot{x}_{r_q}^q &= \dot{z}_{r_q}^q - \frac{\partial \varphi_{r_q}^q}{\partial z} \dot{z} \\ \dot{x}_{r_q}^q &= a_{r_q}^q z_1^q + f_{r_q}^q(z) + O^3(z) - \frac{\partial \varphi_{r_q}^q(z)}{\partial z} (A_0 z + f(z)) + O^3(z) \end{aligned}$$

By substituting $z_{r_q}^q = x_{r_q}^q + \varphi_{r_q}^q(x)$ in the previous expression and retaining only terms of order 1 and 2, we obtain:

$$\dot{x}_{r_q}^q = a_{r_q}^q x_1^q + a_1^q \varphi_1^q(x) + f_{r_q}^q(x) - \frac{\partial \varphi_{r_q}^q(x)}{\partial x} A_0 x$$

Comparing with the desired form stated in Theorem 2.2.1:

$$a_{r_q}^q x_1^q + f_{r_q}^q(x) - \frac{\partial \varphi_{r_q}^q(x)}{\partial x} A_0 x = a_{r_q}^q x_1^q + \bar{f}_{r_q}^q(x) + \beta_{r_q}^q(y)$$

After simplification, we obtain:

$$\bar{f}_{r_q}^q(x) = -\frac{\partial \varphi_{r_q}^q(x)}{\partial x} A_0 x + f_{r_q}^q(x) - \beta_{r_q}^q(y)$$

For $\bar{f}_{r_q}^q(x) = 0$ we must have:

$$0 = \frac{\partial \varphi_{r_q}^q(x)}{\partial x} A_0 x - f_{r_q}^q(x) + \beta_{r_q}^q(y)$$

Given that $\varphi_1^q(x) = 0$ for all $1 \leq q \leq p$, we derive the quadratic components of quadratic transformation $x_i^q = z_i^q - \varphi_i^q(z)$ from the equation (2.9). Inductively, we obtain:

$$\varphi_i^q(x) = \frac{\partial \varphi_{i-1}^q(x)}{\partial x} A_0 x - f_{i-1}^q(x) + \beta_{i-1}^q(y) \text{ for all } 2 \leq i \leq r_q$$

Thus, through this quadratic transformation, the dynamical system (2.5) is placed into the desired form (2.7).

Remark 2.2.3 We recall that resonant terms, as defined by Poincaré, refer to $\bar{f}_{r_q}^q(x)$ for $1 \leq q \leq p$.

Remark 2.2.4 For nonlinear single-input single-output systems ($p = 1$ et $r_1 = n$), we have (see [10]):

$$\bar{f}_{r_q}^q(x) = \bar{f}_n(x) = \sum_{j \geq i=2}^n h_{ij} x_i x_j$$

Remark 2.2.5 Putting together all these equations (2.8), we obtain the following homological equation:

$$A_0^q \varphi^q(x) - \frac{\partial \varphi^q(x)}{\partial x} A_0 x = -f^q(x) + \beta^q(y) \text{ for all } 1 \leq q \leq p$$

In other terms,

$$A_0 \varphi(x) - \frac{\partial \varphi}{\partial z} A_0 x = -f(x) + \beta(y)$$

which is equivalent to

$$[A_0 x, \varphi(x)] = -f(x) + \beta(y)$$

where $[\cdot, \cdot]$ stands for the Lie bracket.

In conclusion, Theorem 2.2.1 establishes the quadratic observability normal form, which is a pivotal development in the analysis of nonlinear multi-output systems. This form not only provides a systematic approach for transforming system dynamics but also underscores the essential conditions for achieving quadratic equivalence under output injection. The implications of this normal form are profound: it enhances our understanding of system observability, facilitates the design of effective observers, and aids in the implementation of robust control strategies. By characterizing the system's dynamics in this way, we empower engineers and researchers to tackle the complexities of nonlinear systems with greater confidence, ultimately improving performance in various applications across control engineering and related fields.

The following numerical example illustrates the obtained results in Theorem 2.2.1.

2.2.1.2 Illustrative example: Linearly observable case

In this section, by means of an example we will demonstrate how to use the quadratic normal form and the efficiency of the proposed approach. Consider the following linearly observable system:

$$\left\{ \begin{array}{l} \dot{\xi}_1 = 7\xi_1 + \xi_2 + 3\xi_1\xi_2 + 2\xi_1\xi_3 - 4\xi_1\xi_5 + 6(\xi_2)^2 + 5\xi_2\xi_3 + 4\xi_2\xi_5 - 5\xi_3\xi_3 \\ \quad + 9\xi_3\xi_5 + 4\xi_4\xi_2 - 2\xi_4\xi_3 + 2\xi_4\xi_5 + 4\xi_5\xi_5 \\ \dot{\xi}_2 = 9\xi_1 + \xi_3 - 6\xi_1\xi_2 + 2\xi_1\xi_3 + 7\xi_1\xi_5 - 3\xi_2\xi_2 + 5\xi_2\xi_3 + 3\xi_2\xi_5 - 6\xi_3\xi_3 \\ \quad + 7\xi_3\xi_5 + 5\xi_4\xi_2 + 2\xi_4\xi_3 + 2\xi_4\xi_5 - 4\xi_5\xi_5 \\ \dot{\xi}_3 = -5\xi_1 + 3\xi_1\xi_2 - 2\xi_1\xi_3 + 5\xi_1\xi_5 + 3\xi_2\xi_2 - 7\xi_2\xi_3 - 2\xi_2\xi_5 + 2\xi_3\xi_3 + 9\xi_3\xi_5 \\ \quad - 6\xi_4\xi_2 + 5\xi_4\xi_3 + 2\xi_4\xi_5 + 2\xi_5\xi_5 \\ \dot{\xi}_4 = 2\xi_4 + \xi_5 - 9\xi_1\xi_2 + 7\xi_1\xi_3 - 4\xi_1\xi_5 + 5\xi_2\xi_2 + 9\xi_2\xi_3 - 8\xi_2\xi_5 + 7\xi_3\xi_3 \\ \quad + 6\xi_3\xi_5 + 5\xi_4\xi_2 - 2\xi_4\xi_3 + 2\xi_4\xi_5 + 3\xi_5\xi_5 \\ \dot{\xi}_5 = 3\xi_4 + 9\xi_1\xi_2 + 4\xi_1\xi_3 + 4\xi_1\xi_5 + 4\xi_2\xi_2 + 3\xi_2\xi_3 - 2\xi_2\xi_5 + 6\xi_3\xi_3 + 3\xi_3\xi_5 \\ \quad - 8\xi_4\xi_2 + 8\xi_4\xi_3 + 2\xi_4\xi_5 - 4\xi_5\xi_5 \end{array} \right. \quad (2.10)$$

Let us assume two outputs $y_1 = \xi_1$ and $y_2 = \xi_2$. Let us set $\begin{bmatrix} \xi_1 = z_1^1 \\ \xi_2 = z_2^1 \\ \xi_3 = z_3^1 \\ \xi_4 = z_1^2 \\ \xi_5 = z_2^2 \end{bmatrix}$.

Now, let $x_{r_1} = z_{r_1} - \varphi_{r_1}(z)$ and $x_{r_2} = z_{r_2} - \varphi_{r_2}(z)$, such that:

$$\begin{aligned} x_{r_1} &= \begin{bmatrix} x_1^1 \\ x_2^1 \\ x_3^1 \end{bmatrix} = \begin{bmatrix} z_1^1 - \varphi_1^1(z) \\ z_2^1 - \varphi_2^1(z) \\ z_3^1 - \varphi_3^1(z) \end{bmatrix} \\ x_{r_2} &= \begin{bmatrix} x_1^2 \\ x_2^2 \end{bmatrix} = \begin{bmatrix} z_1^2 - \varphi_1^2(z) \\ z_2^2 - \varphi_2^2(z) \end{bmatrix} \end{aligned}$$

By employing the homological equations, we derive:

$$\begin{aligned} \varphi_1^1(z) &= 0 \\ \varphi_2^1(z) &= -3z_1^1z_2^1 - 2z_1^1z_3^1 + 4z_1^1z_2^2 - 6z_2^1z_2^1 - 5z_2^1z_3^1 - 4z_2^1z_2^2 + 5z_3^1z_3^1 - 9z_3^1z_2^2 - 4z_2^1z_2^2 \\ &\quad + 2z_2^1z_3^1 - 2z_1^2z_2^2 - 4z_2^2z_2^2 + \beta_{11}^{11}(z_1^1)^2 + \beta_{12}^{11}z_1^1z_1^2 + \beta_{22}^{11}(z_1^2)^2 \\ \varphi_3^1(z) &= (2\beta_{11}^{11} - 98)z_1^1z_2^1 - 114z_1^1z_3^1 + (30 + \beta_{12}^{11})z_1^1z_2^2 + (9\beta_{12}^{11} - 34)z_1^1z_1^2 - 19z_2^1z_3^1 \\ &\quad + (\beta_{12}^{11} - 25)z_2^1z_1^2 - 9z_3^1z_2^2 - 29z_3^1z_1^2 + (2\beta_{22}^{11} - 30)z_2^1z_2^2 - 3z_2^1z_2^2 + (14\beta_{11}^{11} - 17)(z_1^1)^2 \\ &\quad + (z_3^1)^2 + 2(z_2^2)^2 - (6 - 4\beta_{22}^{11})(z_1^2)^2 + \beta_{11}^{12}(z_1^1)^2 + \beta_{12}^{12}z_1^1z_1^2 + \beta_{22}^{12}(z_1^2)^2 \\ \varphi_1^2(z) &= 0 \\ \varphi_2^2(z) &= -f_1^2(z) + \beta_{11}^{21}(z_1^1)^2 + \beta_{12}^{21}z_1^1z_1^2 + \beta_{22}^{21}(z_1^2)^2. \end{aligned}$$

Finally, by setting:

$$\begin{aligned} &\left\{ \begin{array}{l} \beta_{11}^{11} = \frac{1075}{2} \\ \beta_{12}^{11} = 115 \\ \beta_{22}^{11} = 5 \end{array} \right\}, \left\{ \begin{array}{l} \beta_{11}^{12} = -\frac{21947}{2} \\ \beta_{12}^{12} = -2029 \\ \beta_{22}^{12} = 1 \end{array} \right\}, \left\{ \begin{array}{l} \beta_{11}^{13} = -39154 \\ \beta_{12}^{13} = -3804 \\ \beta_{22}^{13} = -5700 \end{array} \right\} \\ &\text{and} \\ &\left\{ \begin{array}{l} \beta_{11}^{21} = -13.5 \\ \beta_{12}^{21} = -22 \\ \beta_{22}^{21} = 12 \end{array} \right\}, \left\{ \begin{array}{l} \beta_{11}^{22} = -73.0 \\ \beta_{12}^{22} = -241 \\ \beta_{22}^{22} = 42 \end{array} \right\} \end{aligned}$$

We derive the following normal form for system (2.10):

$$\begin{cases} \dot{x}_1^1 = 7x_1^1 + x_2^1 + \beta_{11}^{11}(x_1^1)^2 + \beta_{12}^{11}x_1^1x_2^1 + \beta_{22}^{11}(x_2^1)^2 \\ \dot{x}_2^1 = 9x_1^1 + x_3^1 + \beta_{11}^{12}(x_1^1)^2 + \beta_{12}^{12}x_1^1x_2^1 + \beta_{22}^{12}(x_2^1)^2 \\ \dot{x}_3^1 = -5x_1^1 - 974(x_2^1)^2 + 107x_2^1x_3^1 - 237x_2^1x_2^2 + 21(x_3^1)^2 + 41x_3^1x_2^2 + 22(x_2^2)^2 \\ \quad + 29x_2^1x_1^2 + \beta_{11}^{13}(x_1^1)^2 + \beta_{12}^{13}x_1^1x_2^1 + \beta_{22}^{13}(x_2^1)^2 \\ \dot{x}_1^2 = 2x_1^2 + x_2^2 + \beta_{11}^{21}(x_1^1)^2 + \beta_{12}^{21}x_1^1x_2^1 + \beta_{22}^{21}(x_2^1)^2 \\ \dot{x}_2^2 = 3x_1^2 - 5(x_2^1)^2 - 1x_2^1x_2^2 - 2(x_2^2)^2 + 55x_1^1x_3^1 + 20x_2^1x_3^1 + 27x_3^1x_1^2 - 7x_3^1x_2^2 \\ \quad + 15(x_3^1)^2 - 109x_1^1x_2^2 + \beta_{11}^{22}(x_1^1)^2 + \beta_{12}^{22}x_1^1x_2^1 + \beta_{22}^{22}(x_2^1)^2 \end{cases} \quad (2.11)$$

with $y_1 = x_1^1$ and $y_2 = x_1^2$.

Hence, the resonant terms that cannot be canceled are: $-974(x_2^1)^2$, $107x_2^1x_3^1$, $-237x_2^1x_2^2$, $21(x_3^1)^2$, $41x_3^1x_2^2$, $22(x_2^2)^2$, $29x_2^1x_1^2$ and $-1x_2^1x_2^2$, $-5(x_2^1)^2$, $2(x_2^2)^2$, $55x_1^1x_3^1$, $20x_2^1x_3^1$, $27x_3^1x_1^2$, $7x_3^1x_2^2$, $15(x_3^1)^2$, $-109x_1^1x_2^2$.

2.2.2 Linearly unobservable case

In this section, we outline a method to construct the quadratic observability normal form for nonlinear multi-output systems (2.2) in cases where the linear part is not observable. (i.e. the pair (A, C) is not observable).

Assumption 2.2.3 Assume that the linear part of system (2.2) has n_o observable modes ξ_o and n_u unobservable modes ξ_u . In other words

$$\text{rank} \begin{pmatrix} C_o^q \\ C_o^q A_o^q \\ \vdots \\ C_o^q A_o^{q(r_q-1)} \end{pmatrix} = r_q - 1 \text{ for } 1 \leq q \leq p \text{ with } \sum_{q=1}^p r_q = n_o < n.$$

Lemma 2.2.2 Under assumption 2.2.3, there exists a linear change of coordinates $z = T\xi$ which transforms system (2.2) into the following form:

$$\begin{cases} \dot{z}_o = A_o z_o + f_o(z) \\ \dot{z}_u = A_u z_u + \bar{A} z_o + f_u(z) \\ y = C_o z \end{cases} \quad (2.12)$$

where for $1 \leq q \leq p$ with $\sum_{q=1}^p r_q = n_o$:

$$\begin{aligned} z &= \begin{bmatrix} z_o & z_u \end{bmatrix}^T \in \mathbb{R}^n, \text{ with} \\ z_o &= \begin{bmatrix} z^1 & z^2 & \dots & z^p \end{bmatrix}^T \in \mathbb{R}^{n_o}, \\ z^q &= \begin{bmatrix} z_1^q & z_2^q & \dots & z_{r_q}^q \end{bmatrix}^T \in \mathbb{R}^{r_q} \\ z_u &= \begin{bmatrix} z_u^1 & z_u^2 & \dots & z_u^p \end{bmatrix}^T \in \mathbb{R}^{n_u} \text{ and} \\ f_u(z) &= \begin{bmatrix} f_u^1(z) & f_u^2(z) & \dots & f_u^p(z) \end{bmatrix}^T \in \mathbb{R}^{n_u}, \\ f(z) &= \begin{bmatrix} f^1(z) & f^2(z) & \dots & f^p(z) \end{bmatrix}^T \in \mathbb{R}^n \text{ with} \\ f^q(z) &= \begin{bmatrix} f_1^q(z) & f_2^q(z) & \dots & f_{r_q}^q(z) \end{bmatrix}^T \in \mathbb{R}^{r_q} \end{aligned}$$

where $f_i^q(z)$ are homogeneous polynomials of degree 2 in z , for $1 \leq q \leq p$ and $1 \leq i \leq r_q$ with $\sum_{q=1}^p r_q = n_o$ and $f_u^i(z)$ are homogeneous polynomials of degree 2 in z , for $1 \leq i \leq n_u$. In this case, we put

$$A = \begin{bmatrix} A_o & \\ \bar{A} & A_u \end{bmatrix} \in \mathbb{R}^{n \times n}, \quad \text{where}$$

$$A_o = \begin{bmatrix} A_o^1 & [0]_{r_1 r_2} & \cdots & [0]_{r_1 r_p} \\ [0]_{r_2 r_1} & A_o^2 & \vdots & \vdots \\ \vdots & \cdots & \ddots & \vdots \\ [0]_{r_2 r_p} & \cdots & 0 & A_o^p \end{bmatrix} \in \mathbb{R}^{n_o \times n_o},$$

$$A_u = \begin{bmatrix} \alpha^1 & 0 & \cdots & 0 \\ 0 & \alpha^2 & \cdots & 0 \\ \vdots & \vdots & \cdots & \vdots \\ 0 & 0 & \cdots & \alpha^p \end{bmatrix} \in \mathbb{R}^{n_u \times n_u} \text{ and}$$

$$\bar{A} = \begin{bmatrix} [\lambda_{11}^1 \cdots \lambda_{1r_1}^1] & [\lambda_{21}^1 \cdots \lambda_{2r_2}^1] & \cdots & [\lambda_{p1}^1 \cdots \lambda_{pr_p}^1] \\ [\lambda_{11}^2 \cdots \lambda_{1r_1}^2] & [\lambda_{21}^2 \cdots \lambda_{2r_2}^2] & \cdots & [\lambda_{p1}^2 \cdots \lambda_{pr_p}^2] \\ \vdots & \vdots & \cdots & \vdots \\ [\lambda_{11}^{r_p} \cdots \lambda_{1r_1}^{r_p}] & [\lambda_{21}^{r_p} \cdots \lambda_{2r_2}^{r_p}] & \cdots & [\lambda_{p1}^{r_p} \cdots \lambda_{pr_p}^{r_p}] \end{bmatrix} \in \mathbb{R}^{n_u \times n_o}.$$

Thus, system (2.12) has $n_u = n - n_o$ unobservable states. After decomposing system (2.12) into a linearly observable part z_o and a linearly unobservable part z_u , we define the quadratic equivalence modulo an output injection.

2.2.2.1 Quadratic observability normal form

Definition 2.2.2 System (2.12) is quadratically equivalent modulo the output injections $\beta_o(y)$ and $\beta_u(y)$ to:

$$\begin{cases} \dot{x}_o &= A_o x_o + \bar{f}_o(x) \\ \dot{x}_u &= A_u x_u + \bar{A} x_o + \bar{f}_u(x) \\ y &= Cx, \end{cases} \quad (2.13)$$

if there exists a diffeomorphism of the form:

$$\begin{aligned} x_o &= z_o - \varphi_o(z) \\ x_u &= z_u - \varphi_u(z) \end{aligned}$$

which transforms the quadratic part of (2.12) into the quadratic part of (2.13), where:

$$\begin{aligned} \varphi_o(z) &= [\varphi_o^1(z) \quad \varphi_o^2(z) \quad \cdots \quad \varphi_o^q(z)]^T \in \mathbb{R}^{r_q}, \\ \varphi_o^q(z) &= [\varphi_1^q(z) \quad \varphi_2^q(z) \quad \cdots \quad \varphi_{r_q}^q(z)]^T \in \mathbb{R}^{r_q}, \\ \varphi_u(z) &= [\varphi_u^1(z) \quad \varphi_u^2(z) \quad \cdots \quad \varphi_u^{n_u}(z)]^T \in \mathbb{R}^{n_u}, \end{aligned}$$

$$\beta_o(y) = [\beta^1(y) \quad \beta^2(y) \quad \cdots \quad \beta^q(y)]^T \in \mathbb{R}^{n_o},$$

and

$$\beta_u(y) = [\beta_u^1(y) \quad \beta_u^2(y) \quad \cdots \quad \beta_u^{n_u}(y)]^T \in \mathbb{R}^{n_u}.$$

Now, we determine the set of homological equations necessary for constructing the quadratic normal form associated with system (2.12), as outlined in the subsequent result.

Proposition 2.2.2 *System (2.12) is quadratically equivalent to system (2.13), modulo an output injection if and only if, the two sets of following homological equations are satisfied:*

(i) *For the linearly observable part, for $1 \leq q \leq p$ with $\sum_{q=1}^p r_q = n_o$, we have:*

$$\begin{aligned} \bar{f}^q(x) - f^q(x) + \beta^q(y) \\ = \\ A_o^q \varphi_o^q(x) - \frac{\partial \varphi_o^q(x)}{\partial x_o} A_o x_o - \frac{\partial \varphi_o^q(x)}{\partial x_u} (\bar{A} x_o + A_u x_u). \end{aligned}$$

(ii) *For the linearly unobservable part, for $1 \leq q \leq n_u \leq p$, with $n_u + n_o = n$, we have:*

$$\bar{f}_u^q(x) - f_u^q(x) + \beta_u^q(y) = \alpha^q \varphi_u^q(x) + \bar{A} \varphi_o^q(x) - \frac{\partial \varphi_u^q(x)}{\partial x} Ax.$$

Proof 2.2.3 *The proof is exactly the one given in Proposition 2.2.1.*

In what follows, we will present an explicit procedure to compute the diffeomorphism and the output injection, enabling us to derive the quadratic observability normal form for system (2.12).

Theorem 2.2.2 *The normal form with respect to the quadratic equivalence modulo an output injection of the system (2.12) for $1 \leq q \leq p$ with $\sum_{i=q}^p r_i = n_o$ is given by:*

$$\left\{ \begin{array}{l} \dot{x}_1^q = a_1^q x_1^q + x_2^q + \beta_1^q(y) \\ \dot{x}_2^q = a_2^q x_1^q + x_3^q + \beta_2^q(y) \\ \vdots = \vdots \\ \dot{x}_{r_q-1}^q = a_{r_q-1}^q x_1^q + x_{r_q}^q + \beta_{r_q-1}^q(y) \\ \dot{x}_{r_q}^q = a_{r_q}^q x_1^q + \bar{f}_{r_q}^q(x) + \beta_{r_q}^q(y) \\ \dot{x}_u^q = \alpha^q x_u^q + \sum_{i=1}^p \sum_{j=1}^{r_i} \lambda_{ij}^q x_i^j + \bar{f}_u^q(x) + \beta_u^q(y) \end{array} \right. \quad (2.14)$$

where

$$\bar{f}_{r_q}^q(x) = f_{r_q}^q(x) - \frac{\partial \varphi_{r_q}^q(x)}{\partial x_o} A_o x_o - \frac{\partial \varphi_{r_q}^q(x)}{\partial x_u} (A_u + \bar{A}) x_u$$

and

$$\bar{f}_u^q(x) = f_u^q(x) - \sum_{i=1}^p \sum_{j=1}^{r_i} \lambda_{ij}^q \varphi_j^q(x) + \alpha^q \varphi_u^q(x) - \frac{\partial \varphi_u^q(x)}{\partial x} Ax.$$

Proof 2.2.4 *For the linearly observable part, the proof is exactly the one given in Theorem 2.2.1. Now, let us proceed with the proof of the linearly unobservable part. We have:*

$$\bar{f}_u^q(x) - f_u^q(x) + \beta_u^q(y) = \alpha^q \varphi_u^q(x) + \bar{A} \varphi_o^q(x) - \frac{\partial \varphi_u^q(x)}{\partial x} Ax \quad (2.15)$$

Then:

$$\bar{f}_u^q(x) - f_u^q(x) + \beta_u^q(y) = \alpha^q \varphi_u^q(x) + \sum_{i=1}^p \sum_{j=1}^{r_i} \lambda_{ij}^q \varphi_j^q(x) - \frac{\partial \varphi_u^q(x)}{\partial x} (Ax)$$

For $\bar{f}_u^q(x) = 0$, to cancel all quadratic terms in x on the linearly unobservable sub-dynamics \dot{x}_u^q , $\varphi_u^q(x)$ must satisfy the following equation:

$$-f_u^q(x) + \beta_u^q(y) = \alpha^q \varphi_u^q(x) + \sum_{i=1}^p \sum_{j=1}^{r_i} \lambda_{ij}^q \varphi_j^q(x) - \frac{\partial \varphi_u^q(x)}{\partial x} (Ax)$$

which generally does not have any solutions.

Now we will provide the condition for the existence of the quadratic part $\varphi_u^q(x)$ of the diffeomorphism that cancels all quadratic terms in sub-dynamic \dot{x}_u^q . To achieve this, we will express the homological equations using matrices.

As $\varphi_i^q(x)$, $f_u^q(x)$, and $\beta_u(y)$ are quadratic homogeneous polynomial terms in x , they can be rewritten in the following matrix form:

$$\varphi_i^q(x) = x^T \Phi_i^q x, \quad f_u^q(x) = x^T F_u^q x, \quad \bar{f}_u^q(x) = x^T \bar{F}_u^q x$$

and

$$\beta_u^q(y) = y^T \Pi_u^q y = C_o^{qT} \Pi_u^q C_o^q$$

where Φ_i^q , F_u^q , \bar{F}_u^q and Π_u^q are symmetric matrices.

Based on this foundation, we can establish the following theorem.

Theorem 2.2.3 ([65], [18]) *In quadratic observability normal form (2.28) for system (2.12), the elimination of all quadratic terms $f_u^q(x)$ in the sub-dynamic unobservable mode is achievable, if and only if the Sylvester equation*

$$\hat{A} \Phi_u^q - \Phi_u^q \hat{B} = \hat{C} \quad (2.16)$$

has a unique solution $\Phi_u^q \in \mathbb{R}^{p \times n}$ for any $\hat{C} \in \mathbb{R}^{p \times n}$, which implies that \hat{A} and \hat{B} have no common eigenvalues. where:

$$\begin{aligned} \hat{A} &= [\alpha^q I_n - A^T] \in \mathbb{R}^{n \times n}, \quad \hat{B} = -A \in \mathbb{R}^{n \times n} \text{ and} \\ \hat{C} &= -F_u^q + C_o^T \Pi_u^q C_o + \sum_{i=1}^p \sum_{j=1}^{r_i} \lambda_{ij}^q \Phi_i^j \in \mathbb{R}^{p \times n} \end{aligned}$$

Proof 2.2.5 As $\varphi_i^q(x)$, $f_u^q(x)$, and $\beta_u^q(y)$ are quadratic homogeneous polynomial terms in x , they can be rewritten in the following matrix form:

$$\varphi_i^q(x) = x^T \Phi_i^q x, \quad f_u^q(x) = x^T F_u^q x$$

and

$$\beta_u^q(y) = y^T \Pi_u^q y = x^T C_o^{qT} \Pi_u^q C_o^q x$$

where Φ_i^q , F_u^q and Π_u^q are symmetric matrices. Therefore we have:

$$\begin{aligned} \frac{\partial \varphi_u^q(x)}{\partial x} (Ax) &= \frac{\partial (x^T \Phi_u^q x)}{\partial x} (Ax) = (Ax)^T \Phi_u^q x + x^T \Phi_u^q (Ax) \\ &= x^T (A^T \Phi_u^q + \Phi_u^q A) x. \end{aligned}$$

For $\bar{f}_u^q(x) = 0$, the equation (2.15) became:

$$-f_u^q(x) + \beta_u^q(y) = \alpha^q \varphi_u^q(x) + \sum_{i=1}^p \sum_{j=1}^{r_i} \lambda_{ij}^q \varphi_j^q(x) - \frac{\partial \varphi_u^q(x)}{\partial x} (Ax)$$

which is equivalent in a matrix form to:

$$\begin{aligned} -x^T F_u^q x + x^T C_o^T \Pi_u^q C_o x + \sum_{i=1}^p \sum_{j=1}^{r_i} \lambda_{ij}^q x^T \Phi_i^j x \\ = \\ \alpha^q x^T \Phi_u^q x - x^T (A^T \Phi_u^q + \Phi_u^q A) x \end{aligned}$$

Then:

$$-F_u^q + C_o^T \Pi_u^q C_o + \sum_{i=1}^p \sum_{j=1}^{r_i} \lambda_{ij}^q \Phi_i^j = [\alpha^q I_n - A^T] \Phi_u^q - \Phi_u^q A.$$

Now let:

$$\begin{aligned} \hat{A} &= [\alpha^q I_n - A^T] \in \mathbb{R}^{n \times n}, \quad \hat{B} = -A \in \mathbb{R}^{n \times n} \text{ and} \\ \hat{C} &= -F_u^q + C_o^T \Pi_u^q C_o + \sum_{i=1}^p \sum_{j=1}^{r_i} \lambda_{ij}^q \Phi_i^j \in \mathbb{R}^{p \times n} \end{aligned}$$

So, to eliminate the terms of $\bar{f}^q(x)$, the problem reduces to finding the $\Phi_u^q \in \mathbb{R}^{p \times n}$ symmetric matrix solution to the following Sylvester equation:

$$\hat{A} \Phi_u^q - \Phi_u^q \hat{B} = \hat{C}.$$

Based on the work of Dincic, Z.y. Li and H.Zhou (see [18] and [65]) Φ_u^q exists if and only \hat{A} and \hat{B} have no common eigenvalues.

Remark 2.2.6 The Sylvester equation (2.16) constitutes a linear system with $p \times n$ unknowns and the same number of equations.

Corollary 2.2.1 1) if $\bar{f}_{r_q}^q(x) = \bar{f}_{r_q}^q(x_u^q, x_o) = x_u^q \tilde{f}_{r_q}^q(x_o)$, we can recover quadratically the observability of x_u^q , otherwise we have to pass to the equivalence of order 3, otherwise of order 4 and so on until we can recover the observability from the higher resonant terms.

2) In normal form (2.14), by isolating the terms in the unobservable direction x_u^q , the locally observability singularity surface is:

$$S_u^q = \left\{ x, \text{ such that } \frac{d}{dx_u^q} \left(\bar{f}_{r_q}^q(x) \right) = \tilde{f}_{r_q}^q(x_o) = 0 \right\}.$$

3) If $\tilde{f}_{r_q}^q(x_o) = 0$ we can have the following cases:

- a) if $\alpha^q < 0$, x_u^q is detectable,
- b) if $\alpha^q > 0$, x_u^q is locally unstable.
- c) if $\alpha^q = 0$, we use the center manifold theory to analyze the stability and the detectability of x_u^q (see [16, 31]).

4) The resonant terms on the last sub-dynamic \dot{x}_u^q contribute nothing to the local quadratic observability.

Remark 2.2.7 For nonlinear single-output systems ($p = 1$ et $r_1 = n - 1$), we have (see [10]):

$$\bar{f}_{r_q}^q(x) = \bar{f}_{n-1}(x) = \sum_{j \geq i=2}^n h_{ij} x_i x_j + h_{1n} x_1 x_n$$

and

$$\bar{f}_u^q(x) = \bar{f}_u(x) = -\sum_{i=1}^{n-1} \lambda_i \varphi_i(x) + \alpha \varphi_u(x) - \frac{\partial \varphi_u(x)}{\partial x} A_o x.$$

The following numerical example illustrates the obtained results in Section 2.2.2.

2.2.2.2 Illustrative example: Linearly unobservable case

In this section, by means of an example we will demonstrate how to use the quadratic normal form and the efficiency of the proposed approach.

Consider the following linearly unobservable system:

$$\left\{ \begin{array}{l} \dot{\xi}_1 = 7z_1 + \xi_2 + 3\xi_1\xi_2 + 2\xi_1\xi_3 - 4\xi_1\xi_5 + 6\xi_2\xi_2 + 5\xi_2\xi_3 + 4\xi_2\xi_5 - 5\xi_3^2 \\ \quad + 9\xi_3\xi_5 + 4\xi_4\xi_2 - 2\xi_4\xi_3 + 2\xi_4\xi_5 + 4\xi_5^2 \\ \dot{\xi}_2 = 9\xi_1 - 6\xi_1\xi_2 + 2\xi_1\xi_3 + 7\xi_1\xi_5 - 3\xi_2^2 + 5\xi_2\xi_3 + 3\xi_2\xi_5 - 6\xi_3^2 + 7\xi_3\xi_5 \\ \quad + 5\xi_4\xi_2 + 2\xi_4\xi_3 + 2\xi_4\xi_5 - 4\xi_5^2 \\ \dot{\xi}_3 = -5\xi_1 + 3\xi_2 + 2\xi_3 + 4\xi_4 + 3\xi_1\xi_2 - 2\xi_1\xi_3 + 5\xi_1\xi_5 + 3\xi_2^2 - 7\xi_2\xi_3 \\ \quad - 2\xi_2\xi_5 + 2\xi_3^2 + 9\xi_3\xi_5 - 6\xi_4\xi_2 + 5\xi_4\xi_3 + 2\xi_4\xi_5 + 2\xi_5^2 \\ \dot{\xi}_4 = 2\xi_4 - 9\xi_1\xi_2 + 7\xi_1\xi_3 - 4\xi_1\xi_5 + 5\xi_2^2 + 9\xi_2\xi_3 - 8\xi_2\xi_5 + 7\xi_3^2 + 6\xi_3\xi_5 \\ \quad + 5\xi_4\xi_2 - 2\xi_4\xi_3 + 2\xi_4\xi_5 + 3\xi_5^2 \\ \dot{\xi}_5 = 3\xi_4 + 2\xi_1 + 4\xi_2 + 5\xi_5 + 9\xi_1\xi_2 + 4\xi_1\xi_3 + 4\xi_1\xi_5 + 4\xi_2^2 + 3\xi_2\xi_3 - 2\xi_2\xi_5 \\ \quad + 6\xi_3^2 + 3\xi_3\xi_5 - 8\xi_4\xi_2 + 8\xi_4\xi_3 + 2\xi_4\xi_5 - 4\xi_5^2 \end{array} \right. \quad (2.17)$$

endowed with two outputs $y_1 = \xi_1$ and $y_2 = \xi_4$ as the outputs and $\begin{bmatrix} \xi_1 = z_1^1 \\ \xi_2 = z_2^1 \\ \xi_3 = z_3^1 \\ \xi_4 = z_1^2 \\ \xi_5 = z_2^2 \end{bmatrix}$.

Let $x_o = z_o - \varphi_o(z)$ and $x_u = z_u - \varphi_u(z)$, such that:

$$\begin{aligned} x_o &= \begin{bmatrix} x_1^1 \\ x_2^1 \\ x_1^2 \end{bmatrix} = \begin{bmatrix} z_1^1 - \varphi_1^1(z) \\ z_2^1 - \varphi_2^1(z) \\ z_1^2 - \varphi_1^2(z) \end{bmatrix} \\ x_u &= \begin{bmatrix} x_u^1 \\ x_u^2 \end{bmatrix} = \begin{bmatrix} z_u^1 - \varphi_u^1(z) \\ z_u^2 - \varphi_u^2(z) \end{bmatrix} \end{aligned}$$

and by using the homological equations we have:

$$\begin{aligned} \varphi_1^1(z) &= 0 \\ \varphi_2^1(z) &= -3z_1^1z_2^1 - 2z_1^1z_3^1 + 4z_1^1z_2^2 - 6(z_2^1)^2 - 5z_2^1z_3^1 - 4z_2^1z_2^2 \\ &\quad + 5(z_3^1)^2 - 9z_3^1z_2^2 - 4z_2^1z_1^2 + 2z_1^2z_3^1 - 2z_1^2z_2^2 - 4(z_2^2)^2 \\ &\quad + \beta_{11}^{11}(z_1^1)^2 + \beta_{12}^{11}z_1^1z_1^2 + \beta_{22}^{11}(z_1^2)^2 \\ \varphi_1^2(z) &= 0. \end{aligned}$$

Then, by setting:

$$\left\{ \begin{array}{l} \beta_{11}^{11} = 48 \\ \beta_{12}^{11} = 47 \\ \beta_{22}^{11} = 0 \\ \beta_{11}^{21} = 0 \\ \beta_{12}^{21} = 0 \\ \beta_{22}^{21} = 0 \end{array} \right\}, \left\{ \begin{array}{l} \beta_{11}^{12} = 663 \\ \beta_{12}^{12} = 377 \\ \beta_{22}^{12} = 2 \\ \beta_{11}^{22} = 192 \\ \beta_{12}^{22} = 188 \\ \beta_{22}^{22} = 0 \end{array} \right\}, \left\{ \begin{array}{l} \beta_{11}^{13} = -144 \\ \beta_{12}^{13} = -141 \\ \beta_{22}^{13} = 0 \end{array} \right\} \text{ and}$$

we obtain the following matrices solution to the Sylvester equation

$$\Phi_u^1 = \begin{bmatrix} 49.90 & -49.28 & -29.30 & -95.95 & -1.17 \\ -49.28 & 46.71 & 27.47 & 81.22 & 1.52 \\ -29.30 & 27.47 & 8.50 & -11.55 & -1.80 \\ -95.95 & 81.22 & -11.55 & 40.83 & 1.79 \\ -1.17 & 1.52 & -1.80 & 1.79 & -1.25 \end{bmatrix}$$

and

$$\Phi_u^2 = \begin{bmatrix} -186 & 100 & 27 & 78 & 37 \\ 100 & -35 & -25 & -140 & -31 \\ 27 & -25 & -26 & -137 & -8 \\ 78 & -140 & -137 & -957 & 23 \\ 37 & -31 & -8 & 23 & -5 \end{bmatrix}$$

these matrices cancel all quadratic terms in \dot{z}_u^1 and \dot{z}_u^2 and the system becomes:

$$\begin{cases} \dot{x}_1^1 &= 7x_1^1 + x_2^1 + \beta_{11}^{11}(x_1^1)^2 + \beta_{12}^{11}x_1^1x_2^1 + \beta_{22}^{11}(x_2^1)^2 \\ \dot{x}_2^1 &= 9x_1^1 + x_3^1 + 97x_1^1x_3^1 - 66x_1^1x_2^1 + 31(x_2^1)^2 + 23x_2^1x_3^1 + 78x_2^1x_2^1 + 19x_3^1x_1^2 \\ &\quad - 26(x_3^1)^2 + 70x_3^1x_2^2 + 76x_1^2x_2^2 + 36(x_2^2)^2 + \beta_{11}^{12}(x_1^1)^2 + \beta_{12}^{12}x_1^1x_2^1 + \beta_{22}^{12}(x_2^1)^2 \\ \dot{x}_u^1 &= -5x_1^1 + 3x_2^1 + 2x_3^1 + 4x_1^2 + \beta_{11}^{13}(x_1^1)^2 + \beta_{12}^{13}x_1^1x_2^1 + \beta_{22}^{13}(x_2^1)^2 \\ \dot{x}_1^2 &= 2x_1^2 + x_2^2 - 9x_1^1x_2^1 + 7x_1^1x_3^1 - 4x_1^1x_2^2 + 5x_2^1x_2^1 + 9x_2^1x_3^1 - 8x_2^1x_2^2 + 7x_3^1x_1^3 \\ &\quad + 6x_3^1x_2^2 + 5x_1^2x_2^1 - 2x_1^2x_3^1 + 2x_1^2x_2^2 + 3x_2^2x_2^2 + \beta_{11}^{21}(x_1^1)^2 + \beta_{12}^{21}x_1^1x_2^1 + \beta_{22}^{21}(x_2^1)^2 \\ \dot{x}_u^2 &= 2x_1^2 + 4x_2^2 + 3x_1^2 + 5x_2^2 + \beta_{11}^{22}(x_1^1)^2 + \beta_{12}^{22}x_1^1x_2^1 + \beta_{22}^{22}(x_2^1)^2 \end{cases} \quad (2.18)$$

2.3 Quadratic observability normal form for nonlinear multi-input multi-output systems

The method of normal form turns out to be a powerful device in the study of dynamical systems and this as well as stability analysis than controllability analysis. Nevertheless, at our knowledge normal forms are not yet used for observability analysis. In this work, we only present the method and we point out the interest of Poincaré's normal form for the observability analysis and observer design.

Throughout the section, we consider a nonlinear Multi Input Multi Output system described by the following equations:

$$\begin{cases} \dot{\xi} &= F(\xi) + G(\xi)u \\ y &= h(\xi) \end{cases} \quad (2.19)$$

where $\xi \in \mathbb{R}^n$ is the state vector, $y \in \mathbb{R}^p$ and $u \in \mathbb{R}^m$ are the inputs and outputs vectors and $F(\xi), G(\xi) \in \mathbb{R}^n$ are the vector fields such that $F(\xi), G(\xi) : U \subset \mathbb{R}^n \rightarrow \mathbb{R}^n$ are assumed to be real analytic, such that $F(0) = 0$. By setting: $A = \frac{\partial F}{\partial \xi}(0)$ and $B = G(0)$ and by Taylor series development around the equilibrium points $(\xi_e, u_e) = 0$, the system can be rewritten as:

$$\begin{cases} \dot{\xi} &= A\xi + Bu + f(\xi) + g(\xi)u \\ y &= C\xi \end{cases} \quad (2.20)$$

where $f(\xi)$ and $g(\xi)$ are homogeneous polynomials of degree 2 and 1 in ξ .

Definition 2.3.1 System (2.20) is said to be quadratically equivalent to the following system modulo an output injection $M(y, u)$:

$$\begin{cases} \dot{x} = Ax + Bu + \bar{f}(x) + \bar{g}(x)u + M(y, u) \\ y = Cx \end{cases} \quad (2.21)$$

where $M(y, u) = \beta(y) + \gamma(y)u$ is Modulo an Output Injection (MOI) if there exists a diffeomorphism of the form:

$$x = \xi - \Phi(\xi) \quad (2.22)$$

which transforms the quadratic part of (2.20) into the quadratic part of (2.21) modulo the output injection $M(y, u)$. Where $\Phi(\xi) \in \mathbb{R}^n$ and $\beta\left(y, \frac{dy}{dt}, \dots, \frac{d^{r_i}y}{dt^{r_i}}\right) \in \mathbb{R}^n$ are a quadratic homogeneous polynomial term in ξ , and $\gamma(y) \in \mathbb{R}^n$ is a linear homogeneous polynomial in ξ .

Remark 2.3.1 We note that output injection means injection of all output variables. The equivalence MOI is justified by the fact that the output injection (see [49], [50], [70]) will be canceled in the observation error dynamics, in fact let us consider the linearly observable system:

$$\dot{x} = Ax + Bu + \beta(y) + \gamma(y)u$$

with $y = Cx$ and let us take the following Luenberger observer (see [70]) :

$$\dot{\hat{x}} = A\hat{x} + Bu + \beta(y) + \gamma(y)u + K(y - \hat{y})$$

then the estimation error $e = x - \hat{x}$ it is easy to show that the dynamic of the observation error is given by:

$$\dot{e} = (A - KC)e.$$

Now, we will give a necessary and sufficient conditions to quadratic equivalence modulo an output injection.

Proposition 2.3.1 System (2.20) is Quadratically Equivalent Modulo an Output Injection (QEMOI) to system (2.21), if and only if there exist a diffeomorphism $(\Phi(z))$ and $\beta(y), \gamma(y)$ which satisfy the two following homological equations:

$$(i) \quad A\Phi(z) - \frac{\partial\Phi(z)}{\partial z}Az = \bar{f}(z) - f(z) + \beta(y),$$

$$(ii) \quad -\frac{\partial\Phi(z)}{\partial z}B = \bar{g}(z) - g(z) + \gamma(y).$$

Where $\Phi(\xi) \in \mathbb{R}^n$ and $\beta(y) \in \mathbb{R}^n$ are quadratic homogeneous polynomial terms in ξ and y .

This condition ensures that the transformations appropriately handle the nonlinearities in the system, aligning the quadratic observability normal forms through the chosen diffeomorphism and output injection terms.

Proof 2.3.1 (Proof of Proposition 2.3.1) Let $x = \xi - \Phi(\xi)$, then

$$\begin{aligned} \dot{x} &= \dot{\xi} - \frac{\partial\Phi(\xi)}{\partial\xi}\dot{\xi}, \\ \dot{x} &= A\xi + Bu + f(\xi) + g(\xi)u - \frac{\partial\Phi(\xi)}{\partial\xi}(A\xi + Bu + f(\xi) + g(\xi)u) \end{aligned} \quad (2.23)$$

and by replacing x by $\xi - \Phi(\xi)$ in system (2.21), we obtain the following equality:

$$\dot{x} = A(\xi - \Phi(\xi)) + Bu + \bar{f}(\xi - \Phi(\xi)) + \bar{g}(\xi - \Phi(\xi))u + \beta(y) + \gamma(y)u.$$

Then system (2.20) is quadratically equivalent to (2.21) if and only if their quadratic parts are equal, that is:

$$\begin{aligned} A\xi + Bu - A\Phi(\xi) + \bar{f}(\xi) + \bar{g}(\xi)u + \beta(y) + \gamma(y)u \\ = \\ A\xi + Bu + f(\xi) + g(\xi)u - \frac{\partial\Phi^{[2]}}{\partial\xi}(A\xi + Bu) \end{aligned}$$

which leads to the following homological equation:

1.

$$\bar{f}(\xi) + \beta(y) = A\Phi(\xi) + f(\xi) - \frac{\partial\Phi(\xi)}{\partial\xi}A\xi$$

2.

$$\bar{g}(\xi) + \gamma(y) = g(\xi) - \frac{\partial\Phi(\xi)}{\partial\xi}B$$

These equations establish the necessary conditions for quadratic equivalence modulo an output injection.

Now, before presenting so called quadratic equivalence modulo an output injection, in the following subsections we will consider two cases:

1. The linearly observable systems: Here, the system meets conditions that ensure observability in the linear approximation, leading to specific behaviors and guarantees for the observer design.
2. The linearly unobservable systems: In this case, we analyze how the absence of observability in the linear approximation affects the overall system dynamics and the potential for quadratic equivalence.

2.3.1 Linearly observable case

Throughout the this subsection, we assume that the pair (A, C) in system (2.20) is observable such that

$$\text{rank} \begin{pmatrix} C \\ CA \\ \vdots \\ CA^{n-1} \end{pmatrix} = n.$$

Under this assumption and Brunovsky's work [14], we can give the following lemma.

Lemma 2.3.1 [14] *Assume that the pair (A, C) of system (2.20) is observable. Then, there exists a linear change of coordinates $z = T\xi$ which transform system (2.19) into the following form:*

$$\begin{cases} \dot{z}^1 = A_o^1 z^1 + B_o^1 u + f^{1[2]}(z) + g^1(z)u \\ \dot{z}^2 = A_o^2 z^2 + B_o^2 u + f^{2[2]}(z) + g^2(z)u \\ \vdots = \vdots \\ \dot{z}^p = A_o^p z^p + B_o^p u + f^{p[2]}(z) + g^p(z)u \\ y = C_o z \end{cases} \quad (2.24)$$

such that z^q is the state vector observed by the output $y_q = z_1^q$, where, for $1 \leq q \leq p$, $z^q \in \mathbb{R}^{r_q}$ with $\sum_{q=1}^p r_q = n$, we put

$$z = [z^1 \quad z^2 \quad \dots \quad z^p]^T \in \mathbb{R}^n,$$

$$z^q = [z_1^q \quad z_2^q \quad \dots \quad z_{r_q}^q]^T \in \mathbb{R}^{r_q},$$

$$A_o = \begin{bmatrix} A_o^1 & [0]_{r_1 r_2} & \dots & [0]_{r_1 r_p} \\ [0]_{r_2 r_1} & A_o^2 & \vdots & \vdots \\ \vdots & \dots & \ddots & \vdots \\ [0]_{r_2 r_{r_p}} & \dots & 0 & A_o^p \end{bmatrix} \in \mathbb{R}^{n \times n} \text{ where, } A_o^q = \begin{bmatrix} a_1^q & 1 & 0 & \dots & 0 \\ a_2^q & 0 & 1 & 0 & \vdots \\ \vdots & \vdots & \ddots & \ddots & 0 \\ a_{r_q-1}^q & 0 & \dots & 0 & 1 \\ a_{r_q}^q & 0 & \dots & 0 & 0 \end{bmatrix} \in \mathbb{R}^{r_q \times r_q},$$

$$B_o = \begin{bmatrix} B_o^1 \\ B_o^2 \\ \vdots \\ B_o^p \end{bmatrix} \in \mathbb{R}^{n \times m} \text{ where, } B_o^q = \begin{bmatrix} b_1^{q1} & b_2^{q1} & \dots & b_m^{q1} \\ b_1^{q2} & b_2^{q2} & \dots & b_m^{q2} \\ \vdots & \vdots & \dots & \vdots \\ b_1^{qr_q} & b_2^{qr_q} & \dots & b_m^{qr_q} \end{bmatrix} \in \mathbb{R}^{r_q \times m},$$

$$C_o = \begin{bmatrix} C_o^1 & [0]_{1 r_2} & \dots & [0]_{1 r_p} \\ [0]_{1 r_1} & C_o^2 & \vdots & \vdots \\ \vdots & \dots & \ddots & \vdots \\ [0]_{1 r_1} & \dots & \dots & C_o^p \end{bmatrix} \in \mathbb{R}^{p \times n}, \text{ with } C_o^q = [1 \quad 0 \quad \dots \quad 0] \in \mathbb{R}^{1 \times r_q},$$

$$f(z) = [f^1(z) \quad f^2(z) \quad \dots \quad f^p(z)]^T \in \mathbb{R}^n, \text{ where}$$

$$f^q(z) = [f_1^q(z) \quad f_2^q(z) \quad \dots \quad f_{r_q}^q(z)]^T \in \mathbb{R}^{r_q},$$

$$g(z) = [g^1(z) \quad g^2(z) \quad \dots \quad g^p(z)]^T \in \mathbb{R}^n, \text{ where}$$

$$g^q(z) = [g_1^q(z) \quad g_2^q(z) \quad \dots \quad g_{r_q}^q(z)]^T \in \mathbb{R}^{r_q},$$

and where $f_i^q(z)$ and $g_i^q(z)$ are respectively homogeneous polynomials of degree 2 and 1 in z , for $1 \leq q \leq p$ with $\sum_{q=1}^p r_q = n$.

Remark 2.3.2 If the pair (A, C) is observable then $\text{rank} \begin{pmatrix} C_o^q \\ C_o^q A_o^q \\ \vdots \\ C_o^q A_o^{q(r_q-1)} \end{pmatrix} = r_q$ for

$1 \leq q \leq p$ with $\sum_{q=1}^p r_q = n$; is obviously the $y_q = C_o^q z^q = z_1^q$ for $1 \leq q \leq p$ are linearly independent components, thus the dynamical system fulfills the observability rank condition; i. e. $\text{rank}(A, C) = n$.

Now, the problem that we will answer here is: what is the quadratic observability normal form associated to system (2.20) with respect to the quadratic equivalence modulo an output injection $M(y, u) = \beta(y) + \gamma(y)u$?

In what follows, we will present an explicit procedure to compute the diffeomorphism and output injection in order two which will allow us to give the quadratic observability normal form for nonlinear MIMO systems. For this, let us consider the diffeomorphism $(x^q = z^q - \Phi^q(z))$ such that $\Phi_1^q(z) = 0$ and for $1 \leq q \leq p$ with $\sum_{q=1}^p r_q = n$ and

$$\begin{aligned}\Phi^q(z) &= \left[\Phi_1^q(z) \quad \Phi_2^q(z) \quad \dots \quad \Phi_{r_q}^q(z) \right]^T \in \mathbb{R}^{r_q} \\ &= \left[z^T \Phi_1^q z \quad z^T \Phi_2^q z \quad \dots \quad z^T \Phi_{r_q}^q z \right]^T \in \mathbb{R}^{r_q}\end{aligned}$$

Remark 2.3.3 We will not allow a quadratic transformation on the output, consequently, the diffeomorphism $(x^q = z^q - \Phi^q(z))$ is such that $\Phi_1^q(z) = 0$ for $1 \leq q \leq p$ with $\sum_{q=1}^p r_q = n$.

On this basis we can establish the following theorem.

Theorem 2.3.1 The quadratic observability normal form associated to system (2.24) modulo an output injection for $1 \leq q \leq p$ with $\sum_{i=q}^p r_q = n$ is given by the following equations

$$\left\{ \begin{array}{l} \dot{x}_1^q = a_1^q x_1^q + x_2^1 + \sum_{j=1}^m b_j^{q1} u_j + \Delta g_1^q + M_1^q \\ \dot{x}_2^q = a_2^q x_1^q + x_3^1 + \sum_{j=1}^m b_j^{q2} u_j + \Delta g_2^q + M_2^q \\ \vdots = \vdots \\ \dot{x}_{r_q-1}^q = a_{r_q-1}^1 x_1^q + x_{r_q}^q + \sum_{j=1}^m b_j^{q(r_q-1)} u_j + \Delta g_{r_q-1}^q + M_{r_q-1}^q \\ \dot{x}_{r_q}^q = a_{r_q}^q x_1^q + \sum_{j=1}^m b_j^{q(r_q-1)} u_j + \Delta f_{r_q}^q + \Delta g_{r_q}^q + M_{r_q}^q \end{array} \right.$$

where

$$\begin{aligned}\Delta f_{r_q}^q &= f_{r_q}^q - \sum_{i=1}^p \sum_{j=1}^{r_i-1} \frac{\partial \Phi_{r_q}^q}{\partial z_j^i} (a_j^i z_1^i + z_{j+1}^i) - \sum_{i=1}^p \frac{\partial \Phi_{r_q}^q}{\partial z_{r_i}^i} a_{r_i}^i z_1^i + \sum_{j \geq i=1}^p \beta_{ij}^{qr_q} z_1^i z_1^j \\ \Delta g_s^q &= \sum_{l=1}^m \sum_{i=1}^p \sum_{j=2}^{r_i} k_{jl}^{is} x_j^i u_l && \text{for } 1 \leq s \leq p \\ M_s^q &= \beta_s^q(y) + \gamma_s^q(y) u && \text{for } 1 \leq s \leq p\end{aligned}$$

with

$$\beta_s^q(y) = \sum_{j \geq i=1}^p \beta_{ij}^{qs} x_1^i x_1^j \quad \text{and} \quad \gamma_s^q(y) u = \sum_{l=1}^m \sum_{i=1}^p \gamma_{il}^{qs} x_1^i u_l.$$

Proof 2.3.2 (Proof of Theorem 2.3.1) As $\bar{f}^q(z) = 0$, $\bar{g}^q(z) = 0$ and $x^q = z^q - \Phi^q(z)$, then the system

(2.24) became:

$$\left\{ \begin{array}{l} \dot{x}_1^q = z_1^q - \frac{\partial \Phi_1^q}{\partial z} A_o z = a_1^q x_1^q + x_2^1 + f_1^q(x) + \Phi_2^1(x) + \sum_{j=1}^m b_j^{q1} u_j + \Delta g_1^q + M_1^q \\ \dot{x}_2^q = z_2^q - \frac{\partial \Phi_2^q}{\partial z} A_o z = a_2^q x_1^q + x_3^1 + f_2^q(x) + \Phi_3^q(x) - \frac{\partial \Phi_2^q}{\partial z} A_o z + \sum_{j=1}^m b_j^{q2} u_j + \Delta g_2^q + M_2^q \\ \vdots = \vdots \\ \dot{x}_{r_q-1}^q = z_{r_q-1}^q - \frac{\partial \Phi_{r_q-1}^q}{\partial z} A_o z = a_{r_q-1}^1 x_1^q + x_{r_q}^q + f_{r_q-1}^q(x) + \Phi_{r_q}^q(x) - \frac{\partial \Phi_{r_q-1}^q}{\partial z} A_o z \\ \quad + \sum_{j=1}^m b_j^{q(r_q-1)} u_j + \Delta g_{r_q-1}^q + M_{r_q-1}^q \\ \dot{x}_{r_q}^q = z_{r_q}^q - \frac{\partial \Phi_{r_q}^q}{\partial z} A_o z = a_{r_q}^q x_1^q + f_{r_q}^q - \frac{\partial \Phi_{r_q}^q}{\partial z} A_o z + \sum_{j=1}^m b_j^{q(r_q-1)} u_j + \Delta g_{r_q}^q + M_{r_q}^q \end{array} \right.$$

For the first homological equation we obtain

$$A_o^q \Phi^q(z) - \frac{\partial \Phi^q(z)}{\partial z} A_o z = -f^q(z) + \beta^q(y),$$

with the condition $\Phi_1^q(z) = 0$ (i.e. $y_q = z_1^q = x_1^q$) and by considering the Bronowsky structure of matrix A_o^q and A_o , we can obtain the homological equation in a more explicit form: for $1 \leq q \leq p$,

$$\left\{ \begin{array}{l} \Phi_2^q(z) = -f_1^q(z) + \sum_{j \geq i=1}^p \beta_{ij}^{q1} z_1^i z_1^j \\ \Phi_3^q(z) = \frac{\partial \Phi_2^q(z)}{\partial z} A_o z - f_2^q(z) + \sum_{j \geq i=1}^p \beta_{ij}^{q2} z_1^i z_1^j \\ \vdots = \vdots \\ \Phi_{r_q}^q(z) = \frac{\partial \Phi_{r_q-1}^q(z)}{\partial z} A_o z - f_{r_q-1}^q(z) + \sum_{j \geq i=1}^p \beta_{ij}^{q(r_q-1)} z_1^i z_1^j \\ 0 = \frac{\partial \Phi_{r_q}^q(z)}{\partial z} A_o z - f_{r_q}^q(z) + \sum_{j \geq i=1}^p \beta_{ij}^{qr_q} z_1^i z_1^j \end{array} \right. \quad (2.25)$$

The $(r_q - 1)$ first equations in systems (2.25) give the value of $\Phi^q(z)$, which cancel all the quadratic terms in the $(r_q - 1)$ first rows of $f^q(z)$. Moreover, by using the fact that $\beta^q(y)$ is a free homogeneous vector field it is also possible to cancel some terms of $f_{r_q}^q(z)$ and we obtain

$$\Delta f_{r_q}^q = f_{r_q}^q - \frac{\partial \Phi_{r_q}^q}{\partial z} A_o z.$$

For the second homological equation we have

$$-\frac{\partial \Phi^q(z)}{\partial z} B_o = -g^q(z) + \gamma^q(y).$$

we have only $\gamma^q(y)$ is a free vector field. Thus in $\gamma^q(y)u = -\frac{\partial \Phi^q(z)}{\partial z} B_o^q + g^q(z)$, the vector field $\gamma^q(y)$ is only able to cancels terms in z_1^i for $1 \leq i \leq p$.

Remark 2.3.4 We recall that resonant terms according to Poincaré's works are defined by $\Delta f_{r_q}^q$ and Δg_s^q for $1 \leq q \leq p$.

Remark 2.3.5 For nonlinear single-input single-output systems ($p = m = 1$), we have (see [10]).

$$\begin{aligned} \Delta f_{r_q}^q &= \Delta f_n^1 = \sum_{j \geq i=2}^n h_{ij} x_i^1 x_j^1 \quad \text{and} \\ \Delta g_i^q &= \Delta g_i^{q1} = \sum_{j=2}^n k_{ij} x_j^1 u \quad \text{for } 1 \leq i \leq n. \end{aligned}$$

2.3.2 Linearly unobservable case

In this subsection, we provide a method for constructing the quadratic observability normal form for nonlinear multi-input multi-output systems (2.20) where the linear part is not observable. (i.e. the pair (A, C) is not observable).

Now, assume that the linear part of system (2.20) has n_o observable modes ξ_o and n_u unobservable modes ξ_u . The following lemma gives the decomposition of these systems into observable and unobservable parts.

Lemma 2.3.2 Let us consider system (2.20) and assume that the pair (A, C) is unobservable such that

$\text{rank} \begin{pmatrix} C^q \\ C^q A^q \\ \vdots \\ C^q A^{q(r_q-1)} \end{pmatrix} = n_o < n$. Then after a linear change of coordinate $z = T\xi$ which transform system (2.20) into the following form:

$$\begin{cases} \dot{z}_o = A_o z_o + B_o u + f_o(z) + g(z)u \\ \dot{z}_u = A_u z_u + \bar{A} z_o + B_u u + f_u(z) + g_u(z)u, \\ y = C_o z, \end{cases} \quad (2.26)$$

where for $1 \leq q \leq p$ with $\sum_{q=1}^p r_q = n_o$:

$$z = [z_o \quad z_u]^T \in \mathbb{R}^n, \quad \text{with} \quad z_o = [z^1 \quad z^2 \quad \dots \quad z^p]^T \in \mathbb{R}^{n_o},$$

$$z^q = [z_1^q \quad z_2^q \quad \dots \quad z_{r_q}^q]^T \in \mathbb{R}^{r_q} \quad z_u = [z_u^1 \quad z_u^2 \quad \dots \quad z_u^p]^T \in \mathbb{R}^{n_u}$$

and

$$\begin{aligned} f(z) &= [f^1(z) \quad f^2(z) \quad \dots \quad f^p(z)]^T \in \mathbb{R}^n \\ \text{with} \\ f^q(z) &= [f_1^q(z) \quad f_2^q(z) \quad \dots \quad f_{r_q}^q(z)]^T \in \mathbb{R}^{r_q}, \\ f_u(z) &= [f_u^1(z) \quad f_u^2(z) \quad \dots \quad f_u^p(z)]^T \in \mathbb{R}^{n_u} \end{aligned}$$

where $f_j^q(z)$ are homogeneous polynomials of degree 2 in z , for $1 \leq q \leq p$ with $\sum_{q=1}^p r_q = n_o$ and $f_u^i(z)$ are homogeneous polynomials of degree 2 in z , for $1 \leq i \leq n_u$.

In this case, we put $A = \begin{bmatrix} A_o & \\ \bar{A} & A_u \end{bmatrix} \in \mathbb{R}^{n \times n}$, where :

$$A_o = \begin{bmatrix} A_o^1 & [0]_{r_1 r_2} & \cdots & [0]_{r_1 r_p} \\ [0]_{r_2 r_1} & A_o^2 & \vdots & \vdots \\ \vdots & \cdots & \ddots & \vdots \\ [0]_{r_2 r_{r_p}} & \cdots & 0 & A_o^p \end{bmatrix} \in \mathbb{R}^{n_o \times n_o}, \quad A_u = \begin{bmatrix} \alpha^1 & 0 & \cdots & 0 \\ 0 & \alpha^2 & \cdots & 0 \\ \vdots & \vdots & \cdots & \vdots \\ 0 & 0 & \cdots & \alpha^p \end{bmatrix} \in \mathbb{R}^{n_u \times n_u}$$

and

$$\bar{A} = \begin{bmatrix} [\lambda_{11}^1 \cdots \lambda_{1r_1}^1] & [\lambda_{21}^1 \cdots \lambda_{2r_2}^1] & \cdots & [\lambda_{p1}^1 \cdots \lambda_{pr_p}^1] \\ [\lambda_{11}^2 \cdots \lambda_{1r_1}^2] & [\lambda_{21}^2 \cdots \lambda_{2r_2}^2] & \cdots & [\lambda_{p1}^2 \cdots \lambda_{pr_p}^2] \\ \vdots & \vdots & \cdots & \vdots \\ [\lambda_{11}^{r_p} \cdots \lambda_{1r_1}^{r_p}] & [\lambda_{21}^{r_p} \cdots \lambda_{2r_2}^{r_p}] & \cdots & [\lambda_{p1}^{r_p} \cdots \lambda_{pr_p}^{r_p}] \end{bmatrix} \in \mathbb{R}^{n_u \times n_o},$$

$$B_o \text{ is a } n_o \times m \text{ matrix} \quad B_u = \begin{bmatrix} b_1^{u1} & b_2^{u1} & \cdots & b_m^{u1} \\ b_1^{u2} & b_2^{u2} & \cdots & b_m^{u2} \\ \vdots & \vdots & \cdots & \vdots \\ b_1^{un_u} & b_2^{un_u} & \cdots & b_m^{un_u} \end{bmatrix} \in \mathbb{R}^{n_u \times m},$$

$$f_u(z) = [f_u^1(z) \quad f_u^2(z) \quad \cdots \quad f_u^p(z)]^T \in \mathbb{R}^{n_u},$$

$$g_u(z) = [g_u^1(z) \quad g_u^2(z) \quad \cdots \quad g_u^p(z)]^T \in \mathbb{R}^{n_u},$$

$$f(z) \in \mathbb{R}^{n_o}, \quad f^q(z) \in \mathbb{R}^{r_q}, \quad g(z) \in \mathbb{R}^{n_o}, \quad \text{and } g^q(z) \in \mathbb{R}^{r_q},$$

with $f_j^q(z)$ and $g_j^q(z)$ are respectively homogeneous polynomials of degree 2 and 1 in z , for $1 \leq q \leq p$ with $\sum_{q=1}^p r_q = n_o$ and $f_u^i(z)$ and $g_u^i(z)$ are respectively homogeneous polynomials of degree 2 and 1 in z , for $1 \leq i \leq n_u$. Now we can make the following assumption.

Assumption 2.3.1 We assume that the pair (C_o^q, A_o^q) is observable for $1 \leq q \leq p$ with $\sum_{q=1}^p r_q = n_o$.

Under Assumption 2.3.1, system (2.26) has $n_u = n - n_o$ unobservable states. After decomposing system (2.26) into a linearly observable part z_o and a linearly unobservable part z_u , we define the quadratic equivalence modulo an output injection.

Definition 2.3.2 System (2.26) is quadratically equivalent modulo the output injection $\beta_o(y) + \gamma_o(y)u$ and $\beta_u(y) + \gamma_u(y)u$ to:

$$\begin{cases} \dot{x}_o &= A_o x_o + B_o u + \bar{f}(x) + \bar{g}(x)u \\ \dot{x}_u &= A_u x_u + \bar{A} x_o + B_u u + \bar{f}_u(x) + \bar{g}_u(x)u \\ y &= Cx \end{cases} \quad (2.27)$$

if there exists a diffeomorphism of the form:

$$\begin{aligned} x_o &= z_o - \Phi_o(z) \\ x_u &= z_u - \Phi_u(z) \end{aligned}$$

which transforms the quadratic part of (2.26) into the quadratic part of (2.27), where:

$$\begin{aligned} \Phi_o(z) &= [\Phi_o^1(z) \quad \Phi_o^2(z) \quad \cdots \quad \Phi_o^p(z)]^T \in \mathbb{R}^{r_q}, \\ \Phi_o^q(z) &= [\Phi_1^q(z) \quad \Phi_2^q(z) \quad \cdots \quad \Phi_{r_q}^q(z)]^T \in \mathbb{R}^{r_q}, \\ \Phi_u(z) &= [\Phi_u^1(z) \quad \Phi_u^2(z) \quad \cdots \quad \Phi_u^{n_u}(z)]^T \in \mathbb{R}^{n_u}, \\ \beta_o(y) &= [\beta^1(y) \quad \beta^2(y) \quad \cdots \quad \beta^p(y)]^T \in \mathbb{R}^{n_o}, \\ \beta_u(y) &= [\beta_u^1(y) \quad \beta_u^2(y) \quad \cdots \quad \beta_u^{n_u}(y)]^T \in \mathbb{R}^{n_u}, \end{aligned}$$

and

$$\begin{aligned}\gamma_o(y)u &= [\gamma^1(y)u \quad \gamma^2(y)u \quad \dots \quad \gamma^p(y)u]^T \in \mathbb{R}^{n_u}, \\ \gamma_u(y)u &= [\gamma_u^1(y)u \quad \gamma_u^2(y)u \quad \dots \quad \gamma_u^p(y)u]^T \in \mathbb{R}^{n_u}.\end{aligned}$$

Now we determine the set of homological equations which will allow us to construct the quadratic normal form associated to system (2.26).

Proposition 2.3.2 *System (2.26) is quadratically equivalent to system (2.27), modulo an output injection if and only if, the two sets of following homological equations are satisfied*

(i) *For the linearly observable part, for $1 \leq q \leq p$ with $\sum_{q=1}^p r_q = n_o$, we have*

$$\begin{cases} \bar{f}^q(x) - f^q(x) + \beta^q(y) &= A_o^q \Phi_o^q(x) - \frac{\partial \Phi_o^q(x)}{\partial x_o} A_o x_o - \frac{\partial \Phi_o^q(x)}{\partial x_u} (\bar{A}x_o + A_u x_u) \\ \bar{g}^q(x) - g^q(x) + \gamma^q(y) &= -\frac{\partial \Phi_o^q}{\partial x_o} B_o - \frac{\partial \Phi_o^q}{\partial x_u} B_u \end{cases}$$

(ii) *For the linearly unobservable part, for $1 \leq q \leq n_u \leq p$, with $n_u + n_o = n$, we have*

$$\begin{cases} \bar{f}_u^q(x) - f_u^q(x) + \beta_u^q(y) &= \alpha^q \Phi_u^q(x) + \bar{A} \Phi_o^q(x) - \frac{\partial \Phi_u^q(x)}{\partial x} Ax \\ \bar{g}_u^q(x) - g_u^q(x) + \gamma_u^q(y)u &= -\frac{\partial \Phi_u^q(z)}{\partial x_o} B_o - \frac{\partial \Phi_u^q(x)}{\partial x_u} B_u \end{cases}$$

Theorem 2.3.2 *The normal form with respect to the quadratic equivalence modulo an output injection of the system (2.26) for $1 \leq q \leq p$ with $\sum_{i=q}^p r_i = n_o$ is given by*

$$\begin{cases} \dot{x}_1^q &= a_1^q x_1^q + x_2^1 + \sum_{j=1}^m b_j^{q1} u_j + \Delta g_1^q + M_1^q \\ \dot{x}_2^q &= a_2^q x_1^q + x_3^1 + \sum_{j=1}^m b_j^{q2} u_j + \Delta g_2^q + M_2^q \\ &\vdots \\ \dot{x}_{r_q-1}^q &= a_{r_q-1}^1 x_1^q + x_{r_q}^q + \sum_{j=1}^m b_j^{q(r_q-1)} u_j + \Delta g_{r_q-1}^q + M_{r_q-1}^q \\ \dot{x}_{r_q}^q &= a_{r_q}^q x_1^q + \sum_{j=1}^m b_j^{qr_q} u_j + \Delta f_{r_q}^q + \Delta g_{r_q}^q + M_{r_q}^q \\ \dot{x}_u^q &= \alpha^q x_u^q + \sum_{i=1}^p \sum_{j=1}^{r_i} \lambda_{ij}^q x_i^j + \sum_{j=1}^m b_j^q u_j + \Delta f_u^q + \Delta g_u^q(x)u + M_u^q \end{cases} \quad (2.28)$$

where

$$\begin{aligned}
 \Delta f_{r_q}^q &= f_{r_q}^q(x) - \frac{\partial \Phi_{r_q}^q(x)}{\partial x_o} A_o x_o - \frac{\partial \Phi_{r_q}^q(x)}{\partial x_u} (A_u + \bar{A}) x_u + \sum_{j \geq i=1}^p \beta_{ij}^{qr_q} x_1^i x_1^j \\
 \Delta f_u^q &= f_u^q(x) + \alpha^q \Phi_u^q(x) - \sum_{i=1}^p \sum_{j=1}^{r_i} \lambda_{ij}^q \Phi_j^q(x) - \frac{\partial \Phi_u^q(x)}{\partial x} Ax \\
 \Delta g_i^q &= \sum_{l=1}^m \sum_{s=1}^p \sum_{j=2}^{r_s} k_{jl}^{si} x_j^s u_1 + \sum_{l=1}^m \sum_{i=2}^{n_u} k_l^i x_u^i u_l \\
 \Delta g_u^q &= \sum_{l=1}^m \sum_{i=1}^p \sum_{j=2}^{r_i} k_{jl}^{iq} x_j^i u_l + \sum_{l=1}^m \sum_{i=2}^{n_u} k_l^i x_u^i u_l
 \end{aligned}$$

Proof 2.3.3 (Proof of Theorem 2.3.2) For the linearly observable part, the proof is exactly the one given in theorem 1. For the linearly unobservable part, we have for $1 \leq q \leq n_u \leq p$:

$$\begin{cases}
 \bar{f}_u^q(z) - f_u^q(z) + \beta_u^q(y) &= \alpha^q \Phi_u^q(x) + \sum_{i=1}^p \sum_{j=1}^{r_i} \lambda_{ij}^q \Phi_j^q(x) - \frac{\partial \Phi_u^q(z)}{\partial z} Ax, \\
 \bar{g}_u^q(x) - g_u^q(x) + \gamma_u^q(y)u &= -\frac{\partial \Phi_u^q(x)}{\partial x_o} B_o - \frac{\partial \Phi_u^q(x)}{\partial x_u} B_u.
 \end{cases}$$

Since $\bar{f}_u^q(x) = \bar{g}_u^q(x) = 0$, then, to cancel all quadratic terms in x on the linearly unobservable sub-dynamics \dot{x}_u^q , $\Phi_u^{q[2]}(x)$ must satisfy the following equation:

$$-f_u^q(x) + \beta_u^q(y) = \alpha^q \Phi_u^q(x) + \sum_{i=1}^p \sum_{j=1}^{r_i} \lambda_{ij}^q \Phi_j^q(x) - \frac{\partial \Phi_u^q(x)}{\partial x} (Ax)$$

which in general has no solutions.

Now we will give the condition for the existence of the diffeomorphism $\Phi_u^q(x)$ which cancels all quadratic terms in sub-dynamic \dot{x}_u^q . As $\Phi_i^q(x)$, $f(x)$, and $\beta^{qu}(y)$ are quadratic homogeneous polynomials terms in x , then we can rewritten in the following matrix from

$$\Phi_i^q(x) = x^T \mathbf{\Phi}_i^q x, f_u^q(x) = x^T \mathbf{f}_u^q x$$

and

$$\beta_u^q(y) = y^T \mathbf{\beta}_u^q y = C_o^q{}^T \mathbf{\beta}^{qu} C_o^q$$

where $\mathbf{\Phi}_i^q$, \mathbf{f}_u^q and $\mathbf{\beta}^{qu}$ are symmetric matrices. Then we have:

$$\begin{aligned}
 \frac{d\Phi_i^q(x)}{dt} &= \frac{d(x^T \mathbf{\Phi}_i^q x)}{dt} = \frac{dx^T}{dt} \mathbf{\Phi}_i^q x + x^T \mathbf{\Phi}_i^q \frac{dx}{dt} \\
 &= (Ax)^T \mathbf{\Phi}_i^q x + x^T \mathbf{\Phi}_i^q (Ax) \\
 &= x^T (A^T \mathbf{\Phi}_i^q + \mathbf{\Phi}_i^q A) x.
 \end{aligned}$$

Let $x_i^j = z_i^j - \Phi_i^j(x)$ and $x_u^q = z_u^q - \Phi_u^q(x)$, then the sub-dynamic \dot{x}_u^q becomes

$$\begin{aligned}
 \dot{x}_u^q &= \dot{z}_u^q - \frac{d\Phi_u^q(z)}{dt} \\
 &= \alpha^q z_u^q + \sum_{i=1}^p \sum_{j=1}^{r_i} \lambda_{ij}^q z_i^j + f_u^q(z) - \frac{d\Phi_u^q(z)}{dt} \\
 &= \alpha^q (x_u^q + \Phi_u^q(x)) + \sum_{i=1}^p \sum_{j=1}^{r_i} \lambda_{ij}^q (x_i^j + \Phi_i^j(x)) + f_u^q(x) - \frac{d\Phi_u^q(x)}{dt} \\
 &= \alpha^q x_u^q + \sum_{i=1}^p \sum_{j=1}^{r_i} \lambda_{ij}^q x_i^j + f_u^q(x) + \alpha^q \Phi_u^q(x) + \sum_{i=1}^p \sum_{j=1}^{r_i} \lambda_{ij}^q \Phi_i^j(x) - \frac{d\Phi_u^q(x)}{dt},
 \end{aligned}$$

or equivalently:

$$\dot{x}_u^q = \alpha^q x_u^q + \sum_{i=1}^p \sum_{j=1}^{r_i} \lambda_{ij}^q x_i^j + \bar{f}_u^q(x) + \beta^{qu}(y)$$

which implies that

$$f_u^q(x_u^q) + \alpha^q \Phi_u^q(x) + \sum_{i=1}^p \sum_{j=1}^{r_i} \lambda_{ij}^q \Phi_i^j(x) - \frac{d\Phi_u^q(x)}{dt} = \bar{f}_u^q(x) + \beta_u^q(y)$$

which is equivalent in a matrix form to

$$\begin{aligned}
 x^T \mathbf{f}_u^q x + \alpha^q x^T \Phi_u^q x + \sum_{i=1}^p \sum_{j=1}^{r_i} \lambda_{ij}^q x^T \Phi_i^j x - x^T (A^T \Phi_u^q + \Phi_u^q A) x &= x^T \bar{\mathbf{f}}_u^q x + x^T C^T \beta^{qu} C x \\
 x^T \left[-f_u^q + C_o^T \beta_u^q C_o + \sum_{i=1}^p \sum_{j=1}^{r_i} \lambda_{ij}^q \Phi_j^q \right] x &= x^T \alpha^q \Phi_u^q x - x^T (A^T \Phi_u^q + \Phi_u^q A) x.
 \end{aligned}$$

As $\bar{f}_u^q(x) = 0$

$$\begin{aligned}
 -x^T \mathbf{f}_u^q x + x^T C_o^T \beta^{qu} C_o x + \sum_{i=1}^p \sum_{j=1}^{r_i} \lambda_{ij}^q x^T \Phi_i^j x &= \alpha^q x^T \Phi_u^q x - x^T (A^T \Phi_u^q + \Phi_u^q A) x \\
 -\mathbf{f}_u^q + C_o^T \beta^{qu} C_o + \sum_{i=1}^p \sum_{j=1}^{r_i} \lambda_{ij}^q \Phi_i^j &= [\alpha^q I_n - A^T] \Phi_u^q - \Phi_u^q A.
 \end{aligned}$$

Now let

$$\begin{aligned}
 \hat{A} &= [\alpha^q I_n - A^T] \in \mathbb{R}^{n \times n}, \\
 \hat{B} &= -A \in \mathbb{R}^{n \times n}
 \end{aligned}$$

and

$$\hat{C} = -\mathbf{f}_u^q + C_o^T \beta^{qu} C_o + \sum_{i=1}^p \sum_{j=1}^{r_i} \lambda_{ij}^q \Phi_i^j \in \mathbb{R}^{p \times n}$$

So to eliminate the terms of $f_u^q(z)$, the problem reduces to find the $\Phi_u^q \in \mathbb{R}^{p \times n}$ symmetric matrix solution to the following Sylvester equation

$$\hat{A} \Phi_u^q - \Phi_u^q \hat{B} = \hat{C}. \tag{2.29}$$

Remark 2.3.6 The Sylvester equation (2.29) is a linear system with $p \times n$ unknowns and the same number of equations.

Theorem 2.3.3 In quadratic observability normal form (2.28) for system (2.24), we can eliminate the quadratic terms on the sub-dynamic unobservable mode, if and only if the Sylvester equation (2.29) has a unique solution $\Phi_u^q \in \mathbb{R}^{p \times n}$ for any $\hat{C} \in \mathbb{R}^{p \times n}$. This is equivalent to $\Delta f_u^q = 0$, if and only if \hat{A} and \hat{B} do not share any eigenvalue.

Proof 2.3.4 (Proof of Theorem 2.3.3) Assume that \hat{A} and \hat{B} do not share any eigenvalue. Let Φ_u^q be a solution to the equation $\hat{A}\Phi_u^{qT} - \Phi_u^q\hat{B} = 0$. Then $\hat{A}\Phi_u^{qT} = \Phi_u^q\hat{B}$, which can be lifted to $(\hat{A})^k \Phi_u^q = \Phi_u^q(\hat{B})^k$ for each $k \geq 0$ by mathematical induction. Consequently, $P(\hat{A})\Phi_u^q = \Phi_u^q P(\hat{B})$ for any polynomial P . In particular, let P the characteristic polynomial of \hat{A} , and according Cayley-Hamilton theorem, $P(\hat{A}) = 0$, from the spectral mapping theorem we have $\lambda(P(\hat{B})) = P(\lambda(\hat{B}))$, where $\lambda(\cdot)$ denotes the spectrum of a matrix. Since \hat{A} and \hat{B} do not share any eigenvalue, $P(\sigma(\hat{B}))$ does not contain 0, and hence $P(\hat{B})$ is nonsingular. Thus $\Phi_u = 0$.

Now assume that \hat{A} and \hat{B} share an eigenvalue λ . Let $V_{\hat{A}}$ be a corresponding right eigenvector for \hat{A} , $V_{\hat{B}}$ be a corresponding left eigenvector for \hat{B} and $\Phi_u^q = V_{\hat{A}}V_{\hat{B}}^*$. Then $\Phi_u \neq 0$, and

$$\hat{A}\Phi_u^{qT} - \Phi_u^q\hat{B} = \hat{A}V_{\hat{A}}V_{\hat{B}}^* - V_{\hat{A}}V_{\hat{B}}^*\hat{B} = \lambda V_{\hat{A}}V_{\hat{B}}^* - \lambda V_{\hat{A}}V_{\hat{B}}^* = 0.$$

Then Φ_u^q is a nontrivial solution to the equation $\hat{A}\Phi_u^{qT} - \Phi_u^q\hat{B} = 0$, thus justifying the "only if" part of the theorem. Consequently, the Sylvester equation (2.29) has a unique solution $\Phi_u^q \in \mathbb{R}^{p \times n}$ for any $\hat{C} \in \mathbb{R}^{p \times n}$ if and only if \hat{A} and \hat{B} do not share any eigenvalue. In other words, The Sylvester equation (2.29) has a unique solution $\Phi_u^q \in \mathbb{R}^{p \times n}$ for any $\hat{C} \in \mathbb{R}^{p \times n}$ if and only if \hat{A} and \hat{B} do not share any eigenvalue. Hence it is uniquely solvable for any given \hat{C} if and only if the homogeneous equation $\hat{A}\Phi_u^{qT} - \Phi_u^q\hat{B} = 0$ admits only the trivial solution 0.

Discussion 2.3.1 1) if $\Delta f_{r_q}^q$ is functions of x_u^q , we can recover quadratically the observability of x_u^q , otherwise we have to pass to the equivalence of order 3, otherwise of order 4 and so on until we can recover the observability from the higher resonant terms.

2) From the terms $x_i^j x_u^q$ ($i, j \in [1, n_o]$) of the normal form (2.28), it is also possible to recover locally the quadratic observability of x_u^q for $1 \leq q \leq p$ with $\sum_{i=q}^p r_q = n_o$.

3) In normal form (2.28), by isolating the terms in the unobservable direction x_u^q , the locally observability singularity surface is:

$$S_u^q = \left\{ x, \text{ such that } \frac{d}{dx_u^q} \left(\Delta f_{r_q}^q(x) \right) = \tilde{f}_{r_q}^q(x_o, x_u^q) = 0 \right\}.$$

4) If $\tilde{f}_{r_q}^q(x_o, x_u^q) = 0$ we can have the following cases:

- a) if $\alpha^q < 0$, x_u^q is detectable,
- b) if $\alpha^q > 0$, x_u^q is locally unstable.
- c) if $\alpha^q = 0$, we use the center manifold theory to analyze the stability and the detectability of x_u^q (see [16, 31]).

5) The resonant terms on the last sub-dynamic \dot{x}_u^q , brings nothing for the local quadratic observability.

Remark 2.3.7 For nonlinear single-output systems ($p = 1$), we have (see [10])

$$\begin{aligned}\Delta f_{r_q}^q &= \Delta f_{n-1}^1 = \sum_{j \geq i=2}^n h_{ij} x_i^1 x_j^1 + h_{1n} x_1^1 x_n^1 \quad \text{and} \\ \Delta f_u^q &= \Delta f_u^1 = f_n^1(x) + \alpha^1 \Phi_u^1(x) + \sum_{i=1}^{n-1} \lambda_i^1 \Phi_i^1(x) - \frac{\partial \Phi_u^1}{\partial x} A_o^1 x \\ \Delta g_i^q &= \Delta g_i^{q1} = \sum_{j=2}^n k_{ij} x_j^1 u \\ \Delta g_u^q &= \Delta g_u^1 = \sum_{i=2}^n k_i^{1n} x_i^1 u\end{aligned}$$

for $1 \leq i \leq n-1$.

2.4 Sliding mode observer design

In this section, from the results of chapter 2, we present a method for observer design that is based on the step-by-step sliding modes approach. First, we require the following assumption:

Assumption 2.4.1 Assume that the resonant terms $\bar{f}_{r_q}^q(x)$ on the sub-dynamic $\frac{dx_{r_q}^q}{dt}$ has the following form:

$$\bar{f}_{r_q}^q(x) = \bar{f}_{r_q}^q(x_u, x_o) = x_u^q \tilde{f}_{r_q}^q(x_o).$$

Now, we propose the following sliding mode observer ([101], [80], [22]) for $1 \leq q \leq p$ with $\sum_{i=q}^p r_i = n_o$

$$\left\{ \begin{array}{l} \frac{d\hat{x}_1^q}{dt} = a_1^q x_1^q + \hat{x}_2^q + \beta_1^q(y) + \delta_1^q \text{sign}(x_1^q - \hat{x}_1^q) \\ \frac{d\hat{x}_2^q}{dt} = a_2^q x_1^q + \hat{x}_3^q + \beta_2^q(y) + E_1^q \delta_2^q \text{sign}(\tilde{x}_2^q - \hat{x}_2^q) \\ \vdots = \vdots \\ \frac{d\hat{x}_{r_q-1}^q}{dt} = a_{r_q-1}^q x_1^q + \hat{x}_{r_q}^q + \beta_{r_q-1}^q(y) + E_{(r_q-2)}^q \delta_{(r_q-1)}^q \text{sign}(\tilde{x}_{r_q-1}^q - \hat{x}_{r_q-1}^q) \\ \frac{d\hat{x}_{r_q}^q}{dt} = a_{r_q}^q x_1^q + \hat{x}_u^q \tilde{f}_{r_q}^q(\tilde{x}_o) + \beta_{r_q}^q(y) + E_{(r_q-1)}^q \delta_{r_q}^q \text{sign}(\tilde{x}_{r_q}^q - \hat{x}_{r_q}^q) \\ \frac{d\hat{x}_u^q}{dt} = \alpha_u^q \tilde{x}_u^q + \sum_{i=1}^p \sum_{j=1}^{r_i} \lambda_{ij} \tilde{x}_i^j + \bar{f}_u^q(\tilde{x}_u, \tilde{x}_o) + \beta_u^q(y) + E_u^q \delta_u^q \text{sign}(\tilde{x}_u^q - \hat{x}_u^q) \end{array} \right. \quad (2.30)$$

with the following auxilliary states for $1 \leq q \leq p$.

$$\left\{ \begin{array}{l} \tilde{x}_2^q = \hat{x}_2^q + E_1^q \delta_1^q \text{sign}(x_1^q - \hat{x}_1^q) \\ \tilde{x}_3^q = \hat{x}_3^q + E_2^q \delta_2^q \text{sign}(\tilde{x}_2^q - \hat{x}_2^q) \\ \vdots = \vdots \\ \tilde{x}_{r_q}^q = \hat{x}_{r_q}^q + E_{(r_q-1)}^q \delta_{(r_q-1)}^q \text{sign}(\tilde{x}_{r_q-1}^q - \hat{x}_{r_q-1}^q) \\ \tilde{x}_u^q = \frac{E_s^q}{f_{r_q}^q(x_o) + E_s^q - 1} E_{r_q}^q \delta_{r_q}^q \text{sign}(\tilde{x}_{r_q}^q - \hat{x}_{r_q}^q) \end{array} \right. \quad (2.31)$$

which respected the following conditions:

- if $\hat{x}_1^q = x_1^q$ then $E_1^q = 1$, otherwise $E_1^q = 0$,
- if $\hat{x}_2^q = \tilde{x}_2^q$ and $E_1^q = 1$ then $E_2^q = 1$ otherwise $E_2^q = 0$,

- \vdots
- if $\hat{x}_{r_q}^q = \tilde{x}_{r_q}^q$ and $E_1^q = E_2^q = \dots = E_{r_q-1}^q = 1$ then $E_{r_q}^q = 1$ otherwise $E_{r_q}^q = 0$, and
- if $\tilde{f}_{r_q}^q(\tilde{x}_o) \neq 0$ then $E_s^q = 1$ otherwise $E_s^q = 0$.

Which leads to the following proposition.

Proposition 2.4.1 *Let us consider the observer given by equation (2.30) with the auxiliary equation (2.31), then for any initial condition $x = (x_o^T, x_u^T)^T$, there exists a scalar $\tau > 0$ such that $\forall t > \tau$*

$$\hat{x}_o(t) = \tilde{x}_o(t) = x(t), \text{ and}$$

$$\lim_{t \rightarrow +\infty} \|x_u(t) - \hat{x}_u(t)\| = 0 \text{ for } \tilde{f}_{r_q}(x_o) \neq 0.$$

Proof 2.4.1 *Let us consider the observer error $e^q = x^q - \hat{x}^q$, then the proof will be realized in the following steps:*

- **First step:** *assuming that $E_1^q = 0$ (if $E_1^q = 1$, we directly move to the next step), the observation error dynamic ($\dot{e}^q = \dot{x}^q - \dot{\hat{x}}^q$) is:*

$$\begin{aligned} \dot{e}_1^q &= e_2^q - \delta_1^q \text{sign}(x_1^q - \hat{x}_1^q) \\ \dot{e}_2^q &= e_3^q \\ &\vdots \\ \dot{e}_{r_q-1}^q &= e_{r_q}^q \\ \dot{e}_{r_q}^q &= x_u^q \tilde{f}_{r_q}^q(x_o) - \hat{x}_u^q \tilde{f}_{r_q}^q(\hat{x}_o) \\ \dot{e}_u^q &= \alpha_u^q e_u^q - \sum_{i=1}^p \sum_{j=1}^{r_i} \lambda_{ij}^q e_i^j + \bar{f}_u^q(x_u, x_o) - \bar{f}_u^q(\hat{x}_u, \hat{x}_o) \end{aligned}$$

Thanks to the finite time convergence of the sliding mode, if $\delta_1^q > \|e_2^q\|_{\max}$, there exists $t_1 \geq 0$ such that $\forall t \geq t_1$, $\hat{x}_1^q = x_1^q$, then $E_1^q = 1$ and $\dot{e}_1^q = 0$. Moreover, we have:

$$\begin{aligned} e_2^q &= \delta_1^q \text{sign}(x_1^q - \hat{x}_1^q) \text{ and} \\ \tilde{x}_2^q &= \hat{x}_2^q + E_1^q \delta_1^q \text{sign}(x_1^q - \hat{x}_1^q). \end{aligned}$$

- **At $(r_q - 1)$ step:** *as $\hat{x}_{r_q-2}^q = x_{r_q-2}^q$, then $E_{r_q-2}^q = 1$ and $\dot{e}_{r_q-2}^q = 0$ for all $t \geq t_{r_q-2}$ and we have:*

$$\begin{aligned} e_{r_q-1}^q &= E_{r_q-3}^q \delta_{r_q-2}^q \text{sign}(\tilde{x}_{r_q-2}^q - \hat{x}_{r_q-2}^q) \text{ and} \\ \tilde{x}_{r_q-1}^q &= \hat{x}_{r_q-1}^q + E_{r_q-2}^q \delta_{r_q-2}^q \text{sign}(\tilde{x}_{r_q-2}^q - \hat{x}_{r_q-2}^q). \end{aligned}$$

Till now we have recovered the state x_o^q states for $1 \leq q \leq p$ with $\sum_{i=q}^p r_i = n_o$. Now we can recover the state x_u^q through sub-dynamic $\dot{x}_{r_q}^q$ as follows:

If $\delta_{r_q}^q > \|e_u^q\|_{\max}$, there exists $t_{r_q} > t_{r_q-1} > \dots > t_1$ such that $\forall t \geq t_{r_q}$, $\hat{x}_{r_q}^q = \tilde{x}_{r_q}^q = x_{r_q}^q$, then $E_{r_q}^q = 1$ and $\dot{e}_{r_q}^q = 0$. We have also:

$$0 = e_u^q \tilde{f}_{r_q}^q(\tilde{x}_o) - E_{r_q-1}^q \delta_{r_q}^q \text{sign}(\tilde{x}_{r_q}^q - \hat{x}_{r_q}^q)$$

and

$$\tilde{x}_u^q = \hat{x}_u^q + \frac{E_{r_q}^q \delta_{r_q}^q}{\tilde{f}_{r_q}^q(\tilde{x}_o)} \text{sign} \left(\tilde{x}_{r_q}^q - \hat{x}_{r_q}^q \right). \quad (2.32)$$

In order to take the singularity ($\tilde{f}_{r_q}^q(\tilde{x}_o) = 0$) into account, we introduce $E_s^q = 1$ if $\tilde{f}_{r_q}^q(\tilde{x}_o) \neq 0$ otherwise $E_s^q = 0$, which modifies equation (2.32) into the following form:

$$\tilde{x}_u^q = \hat{x}_u^q + \frac{E_s^q E_{r_q}^q \delta_{r_q}^q}{\tilde{f}_{r_q}^q(\tilde{x}_o) + E_s^q - 1} \text{sign} \left(\tilde{x}_{r_q}^q - \hat{x}_{r_q}^q \right).$$

If $\delta_{r_q}^q > \|e_u^q\|_{\max}$, there exists $t_u > t_{r_q} > \dots > t_1$ such that $\forall t \geq t_u$, $\hat{x}_u^q = \tilde{x}_u^q = x_u^q$, then $E_s^q = 1$ and $\dot{e}_u^q = 0$.

• So we obtain:

$$\begin{aligned} \dot{e}_1^q &= e_2^q - \delta_1^q \text{sign}(x_1^q - \hat{x}_1^q) = 0 \\ \dot{e}_2^q &= e_3^q - E_1^q \delta_2^q \text{sign}(\tilde{x}_2^q - \hat{x}_2^q) = 0 \\ &\vdots \\ \dot{e}_{r_q-1}^q &= e_{r_q}^q - E_{r_q-2}^q \delta_{r_q-1}^q \text{sign}(\tilde{x}_{r_q-1}^q - \hat{x}_{r_q-1}^q) = 0 \\ \dot{e}_{r_q}^q &= \tilde{f}_{r_q}^q(x_o) - E_s^q E_{r_q-1}^q \delta_{r_q}^q \text{sign}(\tilde{x}_{r_q}^q - \hat{x}_{r_q}^q) = 0 \\ \dot{e}_u^q &= \alpha_u^q e_u^q - \sum_{i=1}^p \sum_{j=1}^{r_i} \lambda_{ij}^q e_i^j + \bar{f}_u^q(x_u, x_o) - \tilde{f}_u^q(\hat{x}_u, x_o) - E_u^q \delta_u^q \text{sign}(\tilde{x}_u^q - \hat{x}_u^q) = 0 \end{aligned}$$

and consequently $\lim_{t \rightarrow +\infty} \|x_u(t) - \hat{x}_u(t)\| = 0$ for $\tilde{f}_{r_q}^q(x_o) \neq 0$.

2.4.1 Application to Generalized Lorenz System

2.4.1.1 Generalized Lorenz System description

Consider the generalized Lorenz system [84] with five states, characterized by a set of coupled nonlinear differential equations. This system extends the classic Lorenz equations to include two additional states, allowing for more complex dynamics.

The system dynamics are described by [84]:

$$\begin{cases} \dot{\xi}_1 &= \sigma(\xi_2 - \xi_1) + \alpha \xi_3 \xi_5 \\ \dot{\xi}_2 &= \rho \xi_1 - \xi_2 - \xi_1 \xi_3 \\ \dot{\xi}_3 &= -\beta \xi_3 + \xi_1 \xi_2 + \gamma \xi_4 \xi_5 \\ \dot{\xi}_4 &= -\delta \xi_4 + \xi_2 \xi_3 \\ \dot{\xi}_5 &= -\tau \xi_5 + \eta \xi_1 \xi_4 \end{cases} \quad (2.33)$$

where:

- $\xi_1, \xi_2, \xi_3, \xi_4$ and ξ_5 are the state variables, representing different dimensions of the system's dynamics.
- σ, ρ , and β are the classic Lorenz parameters, typically chosen to be $\sigma = 10$, $\rho = 28$, and $\beta = \frac{8}{3}$, which are values known to produce chaotic behavior.
- $\alpha = 0.8$, $\gamma = 1.5$, $\delta = 3$, $\tau = 2$, and $\eta = 2$ are additional parameters introduced to create coupling between states and to add complexity to the system's dynamics.

This five-dimensional generalized Lorenz system introduces nonlinear coupling terms such as $\xi_3\xi_5$, $\xi_4\xi_5$, and $\xi_1\xi_4$, which increase the richness of the dynamics by allowing interactions across different states. The system's nonlinearity and dimensionality make it a strong candidate for studying chaotic synchronization, as well as for applications in fields that require complex, unpredictable behavior. The system is equipped with two outputs, which can be used to observe and synchronize the dynamics: $y^1 = \xi_1$ and $y^2 = \xi_4$. The choice of two outputs allows for effective monitoring and potential synchronization of the system in applications such as secure communication or chaos-based control.

2.4.1.2 Quadratic observability normal form calculation

Now, consider the following change of coordinates:

$$\begin{cases} z_1^1 &= \xi_1 \\ z_2^1 &= \xi_1 + 10\xi_2 \\ z_u^1 &= \xi_3 \\ z_1^2 &= \xi_4 \\ z_u^2 &= \xi_5 \end{cases} \implies \begin{cases} \xi_1 &= z_1^1 \\ \xi_2 &= -\frac{1}{10}z_1^1 + \frac{1}{10}z_2^1 \\ \xi_3 &= z_u^1 \\ \xi_4 &= z_1^2 \\ \xi_5 &= z_u^2 \end{cases}$$

which transforms the system into the Brunovsky normal form:

$$\begin{cases} \dot{z}_1^1 &= -11z_1^1 + z_2^1 + 0.8z_u^1z_u^2 \\ \dot{z}_2^1 &= 270z_1^1 - 10z_1^1z_u^1 + 0.8z_u^1z_u^2 \\ \dot{z}_u^1 &= -\frac{8}{3}z_u^1 - \frac{1}{10}(z_1^1)^2 + \frac{1}{10}z_1^1z_2^1 + 1.5z_1^2z_u^2 \\ \dot{z}_1^2 &= -3z_1^2 + -\frac{1}{10}z_1^1z_u^1 + \frac{1}{10}z_2^1z_u^1 \\ \dot{z}_u^2 &= -2z_u^2 + 2z_1^1z_1^2 \end{cases} \quad (2.34)$$

It's easy to show that the pair (A, C) is not observable in 2 directions, with:

$$A = \begin{bmatrix} -11 & 1 & 0 & 0 & 0 \\ 270 & 0 & 0 & 0 & 0 \\ 0 & 0 & -\frac{8}{3} & 0 & 0 \\ 0 & 0 & 0 & -3 & 0 \\ 0 & 0 & 0 & 0 & -2 \end{bmatrix}, C = \begin{bmatrix} 1 & 0 & 0 & 0 & 0 \\ 0 & 0 & 0 & 1 & 0 \end{bmatrix}$$

Now, consider the change of coordinates $x_o = z_o - \varphi_o(z)$ and $x_u = z_u - \varphi_u(z)$, such that:

$$\begin{aligned} x_o &= \begin{bmatrix} x_1^1 \\ x_2^1 \\ x_1^2 \end{bmatrix} = \begin{bmatrix} z_1^1 - \varphi_1^1(z) \\ z_2^1 - \varphi_2^1(z) \\ z_1^2 - \varphi_1^2(z) \end{bmatrix} \\ x_u &= \begin{bmatrix} x_u^1 \\ x_u^2 \end{bmatrix} = \begin{bmatrix} z_u^1 - \varphi_u^1(z) \\ z_u^2 - \varphi_u^2(z) \end{bmatrix} \end{aligned}$$

and by using the homological equations we have:

$$\begin{cases} \varphi_1^1(x) &= \varphi_1^2(x) = 0 \\ \varphi_2^1(x) &= -f_1^1(x) + \beta_{11}^{11}(x_1^1)^2 + \beta_{11}^{21}(x_1^2)^2 + \beta_{12}^{11}x_1^1x_1^2 \\ &= -0.8x_u^1x_u^2 + \beta_{11}^{11}(x_1^1)^2 + \beta_{11}^{21}(x_1^2)^2 + \beta_{12}^{11}x_1^1x_1^2 \\ \beta_{11}^{11} &= \beta_{11}^{21} = \beta_{12}^{11} = 0 \end{cases}$$

For x_u^1 and x_u^2 the Sylvester equation gives

$$\begin{cases} \varphi_u^1(x) = -\frac{3}{25}x_1^1x_2^1, \beta_{11}^{u1} = -\frac{323}{10} \text{ and } \beta_{22}^{u1} = \beta_{12}^{u1} = 0. \\ \varphi_u^2(x) = 0, \beta_{12}^{u2} = -2 \text{ and } \beta_{11}^{u2} = \beta_{22}^{u2} = 0. \end{cases}$$

as solution of:

$$\begin{cases} -\frac{8}{3}\varphi_u^1(x) - \frac{\partial\varphi_u^1(x)}{\partial x}Ax + f_u^1(x) + \beta_{11}^{u1}(x_1^1)^2 + \beta_{22}^{u1}(x_2^1)^2 + \beta_{12}^{u1}x_1^1x_2^1 = 0 \\ -2\varphi_u^2(x) - \frac{\partial\varphi_u^2(x)}{\partial x}Ax + f_u^2 + \beta_{11}^{u2}(x_1^1)^2 + \beta_{22}^{u2}(x_2^1)^2 + \beta_{12}^{u2}x_1^1x_2^1 = 0 \end{cases}$$

and we obtain the following observability quadratic normal form of the generalized Lorentz system:

$$\begin{cases} \dot{x}_1^1 = -11x_1^1 + x_2^1 \\ \dot{x}_2^1 = 270x_1^1 - 10x_1^1x_u^1 - 4.533x_u^1x_u^2 \\ \dot{x}_u^1 = -\frac{8}{3}x_u^1 \\ \dot{x}_1^2 = -3x_1^2 - \frac{1}{10}x_1^1x_u^1 + \frac{1}{10}x_2^1x_u^1 \\ \dot{x}_u^2 = -2x_u^2 \end{cases} \quad (2.35)$$

In normal form (2.35), thanks to the resonant terms $-10x_1^1x_u^1$ and $-4.533x_u^1x_u^2$ on the dynamics \dot{x}_2^1 and $-\frac{1}{10}x_1^1x_u^1$ and $\frac{1}{10}x_2^1x_u^1$ on the dynamics \dot{x}_1^2 we recover respectively the quadratic observability of x_u^2 and x_u^1 . And, by isolating the terms in the unobservable direction x_u^1 , the locally observability singularity surface is:

$$S_u^1 = \{x, \text{ such that } -10x_1^1 - 4.533x_u^2 = 0\}.$$

and

$$S_u^2 = \left\{ x, \text{ such that } , -\frac{1}{10}x_1^1 + \frac{1}{10}x_2^1 = 0 \right\}.$$

2.4.1.3 sliding mode observer of Generalized Lorentz

Now, we give the sliding mode observer of system (2.35) as follows:

$$\begin{cases} \dot{\hat{x}}_1^1 = -11x_1^1 + \hat{x}_2^1 + \delta_1^1 \text{sign}(x_1^1 - \hat{x}_1^1) \\ \dot{\hat{x}}_2^1 = 270x_1^1 - 10x_1^1\hat{x}_u^1 - 4.533\hat{x}_u^1\hat{x}_u^2 + E_1^1\delta_2^1 \text{sign}(\tilde{x}_2^1 - \hat{x}_2^1) \\ \dot{\hat{x}}_u^1 = -\frac{8}{3}\tilde{x}_u^1 + E_u^1\delta_u^1 \text{sign}(\tilde{x}_u^1 - \hat{x}_u^1) \\ \dot{\hat{x}}_1^2 = -\frac{8}{3}\tilde{x}_u^1 - \frac{1}{10}x_1^1\hat{x}_u^1 + \frac{1}{10}\tilde{x}_2^1\hat{x}_u^1 + \delta_1^2 \text{sign}(\tilde{x}_1^2 - \hat{x}_1^2) \\ \dot{\hat{x}}_u^2 = -2\tilde{x}_u^2 + E_u^2\delta_u^2 \text{sign}(\tilde{x}_u^2 - \hat{x}_u^2) \end{cases} \quad (2.36)$$

In system (2.36) the auxiliary components \tilde{z}_i^j are determined algebraically:

$$\tilde{x}_2^1 = \hat{x}_2^1 + E_1^1\delta_1^1 \text{sign}(x_1^1 - \hat{x}_1^1)$$

$$\tilde{x}_u^1 = \hat{x}_u^1 + \frac{10E_s^1\delta_1^2}{x_2^1 - x_1^1 + E_s^1 - 1} \text{sign}(\tilde{x}_1^2 - \hat{x}_1^2)$$

$$\tilde{x}_u^2 = \hat{x}_u^2 - \frac{E_1^1E_s^2\delta_1^2}{10x_1^1 + 4.533\hat{x}_u^1 + E_s^2 - 1} \text{sign}(\tilde{x}_2^1 - \hat{x}_2^1)$$

with the following conditions:

$$\text{if } x_1^1 = \hat{x}_1^1 \text{ and } x_1^2 = \hat{x}_1^2 \text{ then } E_1^1 = 1, \text{ otherwise } E_1^1 = 0,$$

$$\text{if } \tilde{x}_2^1 = \hat{x}_2^1 \text{ and } x_1^1 = \hat{x}_1^1 \text{ and } x_u^1 = \hat{x}_u^1 \text{ then } E_u^2 = 1 \text{ otherwise } E_u^2 = 0,$$

$$\text{if } \tilde{x}_2^1 = \hat{x}_2^1 \text{ and } x_1^1 = \hat{x}_1^1 \text{ and } x_u^1 = \hat{x}_u^1 \text{ and } x_u^2 = \hat{x}_u^2 \text{ then } E_u^1 = 1 \text{ otherwise } E_u^1 = 0.$$

We can see that when $x_2^1 - x_1^1 = 0$, \tilde{x}_u^1 tends to infinity and when $-10x_1^1 - 4.533x_u^2 = 0$, \tilde{x}_u^2 tends to infinity, meaning that observability singularity occurs. Thus, to avoid the explosion of x_u^1 and x_u^2 , we introduce a filter E_S^1 and E_S^2 as follows:

$$\text{if } -10x_1^1 - 4.533x_u^2 = 0 \text{ then } E_s^2 = 0 \text{ otherwise } E_s^2 = 1.$$

$$\text{if } x_2^1 - x_1^1 = 0 \text{ then } E_s^1 = 0 \text{ otherwise } E_s^1 = 1.$$

In this case \tilde{x}_u^1 and \tilde{x}_u^2 become:

$$\tilde{x}_u^1 = \hat{x}_u^1 + \frac{10E_s^1\delta_1^2}{x_2^1 - x_1^1 + E_s^1 - 1} \text{sign}(\tilde{x}_1^2 - \hat{x}_1^2)$$

$$\tilde{x}_u^2 = \hat{x}_u^2 - \frac{E_s^1 E_s^2 \delta_1^2}{10x_1^1 + 4.533\tilde{x}_u^1 + E_s^2 - 1} \text{sign}(\tilde{x}_2^1 - \hat{x}_2^1)$$

Remark 2.4.1 *In order to not lose the observability for a long time at singularity surface, we must set correctly E_S^i by taking $E_S^i = 0$ during a short period of time.*

2.4.1.4 Simulation results

For these simulations, we have considered the following initial conditions: $\xi_1 = 10$, $\xi_2 = 20$, $\xi_3 = 30$ and $\hat{x}_1^1 = \hat{\xi}_1 = 0$, $\hat{x}_2^1 = \hat{\xi}_1 + 10\hat{\xi}_2 = 0$, $\hat{x}_u^1 = \hat{\xi}_3 = 10$.

Figures 1.4a and 1.4b display the simulation results obtained for the Lorenz system. Figure 1.4 shows the dynamics of both the observer and the Lorenz system over 10 seconds. Figure 1.5 presents the estimation error. It can be observed that the state x_1^1 converges to \hat{x}_1^1 in a finite time, and for the other states, convergence is achieved within 1,6 *seconds*.

2.5 Conclusion

In conclusion, this chapter presents a pivotal contribution to the field through the development of the Quadratic Observability Normal Form (QNF) for multi-input multi-output (MIMO) systems. This form is essential for comprehensively understanding the observability properties of complex nonlinear systems, providing a systematic framework to evaluate whether all states can be accurately estimated from available inputs and outputs.

Starting from Section 2.3, we explored the concept of quadratic observability in nonlinear multi-output systems, differentiating between linearly observable and unobservable cases. This analysis highlighted the structural dependencies inherent to observability, offering critical insights that inform both control strategies and state estimation techniques.

In Section 2.4, we extended our investigation to nonlinear MIMO systems, further illustrating the versatility and importance of the QNF. By analyzing both observable and unobservable scenarios, we emphasized

the necessary conditions for effective state recovery, thus enhancing our understanding of system dynamics.

Section 2.5 introduced the design of sliding mode observers, underscoring the importance of the principles derived from the QNF. The methodologies presented for observer design are closely linked to the observability characteristics discussed earlier, ensuring that our state estimation techniques are robust and reliable.

Overall, the methodology for the QNF is a foundational element of this thesis, significantly enhancing our ability to analyze and design control systems for MIMO structures. By clarifying observability properties, we pave the way for more effective state estimation strategies, ultimately improving the performance and reliability of complex dynamic systems in real-world applications. This chapter not only lays a strong groundwork for future research in quadratic observability but also provides valuable tools for addressing the challenges associated with nonlinear system dynamics, fostering innovative approaches to managing the intricacies of MIMO systems.

Chapter 3

Aplicacion to cardiovascular system

Contents

3.1	Introduction	67
3.2	Presentation of cardiovascular system	68
3.2.1	State of the art of cardiovascular system models	68
3.2.2	Anatomy and physiology of the cardiac cycle	69
3.2.3	Valve pathologies	71
3.3	Description of the cardiovascular system model	71
3.3.1	Equivalent electric model	71
3.3.2	Elastance	72
3.3.3	Cardiovascular system modeling phases	74
3.3.4	Mathematical model of the cardiovascular system	80
3.4	Quadratic normal form of the cardiovascular system	80
3.4.1	Validation of the quadratic normal form of the CVS model	81
3.5	Observability analysis and observer design of the cardiovascular system	83
3.5.1	Observability analysis of the cardiovascular system	83
3.5.2	Sliding mode observers design for CVS	84
3.6	Conclusion	87

3.1 Introduction

In this chapter, we summarize the functioning of the heart in order to provide an adequate description of the dynamic behavior of the cardiovascular system.

The human cardiovascular system is a complicated and essential ensemble that controls blood circulation to ensure the transportation of nutrients, oxygen, and carbon dioxide as well as the removal of metabolic waste. Its operation depends on precise interactions between the anatomy and physiology of the cardiac cycle, but it can also malfunction and result in diseases such as valvular disorders.

This chapter offers a comprehensive approach to modeling the cardiovascular system by first describing the anatomy and physiology of the cardiac cycle and then introducing common diseases. In order to simplify the cardiovascular dynamic and enable a more accessible analysis of the system's characteristics, an electrical

equivalent model will thereafter be presented. The mathematical model will be developed using the concept of elasticity, a main variable in cardiac mechanics.

Next, we will examine the normal quadratical form of the cardiovascular model, a mathematical framework that makes it easier to analyze the system's stability and dynamic properties. Finally, an analysis of observability and the idea of observers, even in a sliding mode, will be covered in detail. These methods are crucial for reconstructing the system's internal data from external measurements.

In general terms, it is possible to describe the CVS as a distribution grid (blood vessels) that supplies oxygenated blood to the organs by means of a pump (heart). The heart generates the pressure necessary to pump the blood that travels through the body's cells from the aorta and through the arteries. First, through the arteries, the systemic circulation is generated, which is responsible for the transport and distribution of oxygenated blood from the heart to the capillaries of the body and then through the veins the pulmonary circulation is generated, which is responsible for returning the poorly oxygenated blood from the blood capillaries to the heart to be oxygenated again in the lung.

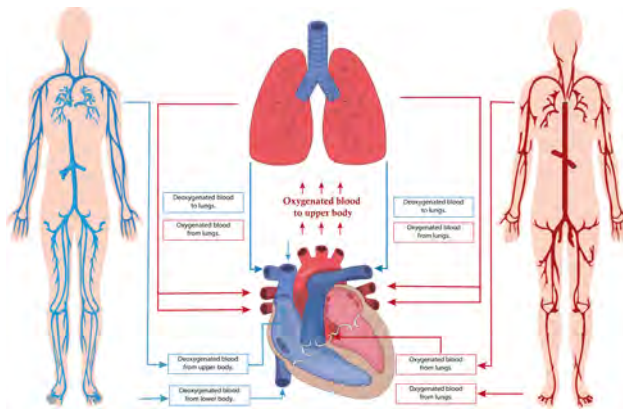


Figure 3.1: Blood flow of the human heart.

The heart is divided into two parts, the right and left parts, composed of an auricle and a ventricle, where the auricles act as preloading cameras and the ventricles perform the ejection function of a pump. The cameras are also divided by unidirectional valves that prevent backflow between the cameras (atrial valves) and outflow from the ventricles (semilunar or ventricular valves).

3.2 Presentation of cardiovascular system

3.2.1 State of the art of cardiovascular system models

The state of the art in the field of cardiovascular system encompasses a diverse range of research and advancements. Over the years, significant progress has been made in modeling the cardiovascular system, driven by advancements in computational technology, imaging techniques, and a better understanding of cardiovascular physiology. These mathematical models are becoming increasingly important in research and clinical applications. Researchers have explored various approaches to enhance better understanding of cardiovascular physiolog [46, 92, 23, 99]. By reviewing the existing literature and examining the latest developments, this section provides an overview of the current state of the art dedicated to mathematical models of the CVS from different perspectives. Below are the main methodologies that have been used:

Lumped parameter models: Describe in a simplified manner the predominant behavior of each of the components involved in the CVS. These models simplify the cardiovascular system by representing it as a series of discrete components (e.g., resistances, capacitances, and inductances) without considering spatial variations. Commonly used for simulating overall hemodynamics and evaluating system dynamics in a simplified manner [17, 61, 79, 94, 23, 63, 45, 26, 90, 62, 47, 68, 13].

Distributed parameter models: Describing the cardiovascular system including the one, two or three dimensional models based on finite element software. Unlike lumped models, distributed parameter models take into account the spatial distribution of properties and variables throughout the cardiovascular system. They often use partial differential equations to describe blood flow and pressure variations. Commonly used for detailed analysis of blood flow in specific vessels or regions, such as studying wave propagation and reflections in arterial systems [79, 89, 86, 74].

Modeling from a hydraulic approach: Describing the cardiovascular system is similarly to hydraulic systems, focusing on fluid dynamics principles. It examines the flow of blood as a viscous, incompressible fluid through elastic and rigid vessels. Often employed in studies of blood flow dynamics, pressure drops, and resistance in the vasculature [96, 82].

Computational Models: Describing the cardiovascular system is similarly to using computational algorithms and simulations to represent the behavior of the cardiovascular system. They can be either lumped or distributed and often rely on numerical methods to solve complex equations. Commonly used in research and clinical settings for predicting hemodynamic responses, optimizing treatment strategies, and simulating surgical procedures [19, 83, 81, 75].

Modeling from the Energy Approach: Describes the cardiovascular system emphasizing the conservation of energy principles within the cardiovascular system, analyzing how energy is transformed and dissipated as blood flows through various components. Commonly used for understanding energy losses due to friction and turbulence, as well as the work done by the heart [38, 35].

Multiscale Models: Describing the cardiovascular system in these representation integrate processes at multiple scales, from cellular and tissue levels to organ-level dynamics. They account for the interactions between different biological scales to provide a comprehensive understanding of cardiovascular function [33, 78].

This section is dedicated to describing the dynamic behavior of the CV system from both a medical and control theory perspective.

3.2.2 Anatomy and physiology of the cardiac cycle

The dynamic behavior of the cardiac cycle can be described as a distribution network of blood vessels to supply oxygenated and deoxygenated blood throughout the body, thanks to the heart behaving as a pump and its pressure–volume (PV) loops.

- **Blood circulation pathway**

The path followed by the blood is presented as a closed circuit, starting at the heart, which is responsible for pumping blood. This is illustrated in Figure 3.2 through a schematic cross-section of the heart, consisting of double atria-ventricular chambers on both sides. Where, the ventricles act as the primary pumps, while the atria serve as preload chambers that regulate the distinct paths of blood circulation. Specifically, the right side of the heart regulates blood flow in to the pulmonary artery, which carries to the lungs, where blood is oxygenated in the lungs and then it returns to the left side of the heart entering through the left

atrium. Subsequently, the oxygen-rich blood is pumped by the left ventricle through the aorta, regulating blood circulation to the rest of the body [93]. Additionally, it is important to note that blood flows in one direction only, due to one-way valves being situated between the chambers to prevent reflux, and at the output of the ventricles, called semilunar valves as shown in Figure 3.2.

- **Cardiac cycle phases**

From a functional point of view, the cardiac cycle is divided into two alternating phases: diastole (dilatation period) and systole (contraction period), which are simplified into four stages as shown in Figure 3.2:

- ① The first stage is atrial diastole and the beginning of ventricular systole, during which the atria relax while the ventricles contract and the atrioventricular valves close. This increases the pressure inside the ventricles but not enough to open the semilunar valves.
- ② The second stage is ventricular diastole, when the pressure inside the ventricles rapidly decreases, the atrioventricular valves open, and the chambers passively fill due to their relaxation combined with atrial systole, during which the atria contract to fill the ventricles.
- ③ The third stage is atrial systole, during which the pressure in the ventricles rises until it exceeds that of the arteries. This leads to the opening of the semilunar valves and the ejection of blood into the pulmonary artery, marking the beginning of systemic circulation.
- ④ The last stage marks the end of ventricular systole and the start of the ventricular and atrial diastole. During this phase, the pressure in the ventricles decreases rapidly, and all chambers passively fill due to their relaxation. This transition leads into a new cardiac cycle, beginning with atrial systole.

An alternative method to graphically describe and characterize the cardiac cycle is through the use of a left ventricle (PV) loop. This loop illustrates the relationship between left ventricular pressure (LVP) and left ventricular volume (LVV) across the four stages of the cardiac cycle. It enables the identification of changes in cardiac function, including the factors related to preload and afterload, as well as heart contractility (for more information see [99]).

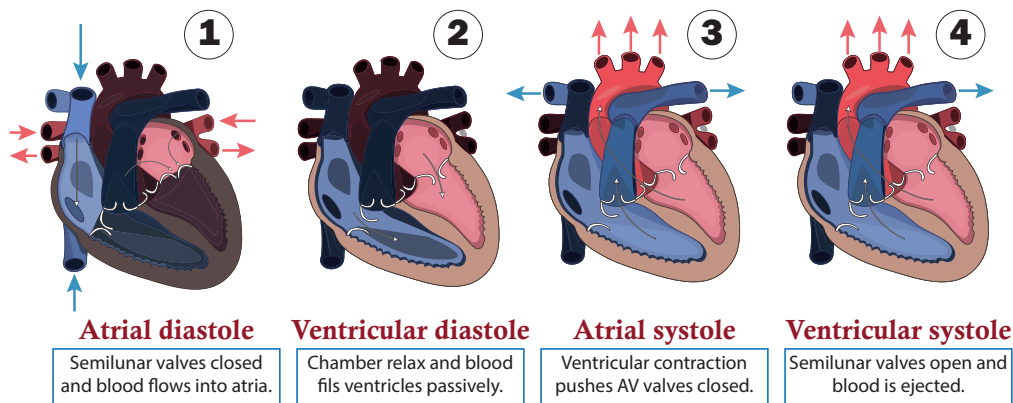


Figure 3.2: Cardiac cycle of circulatory system.

3.2.3 Valve pathologies

Valvular heart diseases are a leading cause of cardiovascular morbidity and mortality worldwide [77, 32]. Among the most frequent valve pathologies are those impacting the aortic and mitral valves. These pathologies often result in both stenosis (narrowing) and regurgitation (impaired closure).

Aortic valve stenosis refers to the insufficient opening of the valve during systole, often caused by congenital abnormalities or the progressive buildup of calcium on the valve leaflets with age [99, 1, 37]. Conversely, a malfunction in the aortic valve closure, known as aortic valve regurgitation, results in backward leakage into the left ventricle during diastole. This condition shares similar causes with aortic valve stenosis [1].

Both aortic stenosis and regurgitation lead to the hypertrophy of the left ventricle in response to increased stress, resulting in the thickening of the left ventricular muscle and the subsequent elevation of left ventricular pressure.

3.3 Description of the cardiovascular system model

This section outlines the equivalences between electrical and hydrodynamic indices. We can simulate the CVS electrically by utilizing the equivalencies between hydrodynamic and electrical indicators. This model addresses the simulation of the system and the contractile activity of the heart once the relationships and equivalencies between an electrical circuit and the behavior defined by a segment of the CVS are established.

3.3.1 Equivalent electric model

The heart is a highly complex system that presents significant challenges for mathematical modeling. In recent years, numerous dynamical state-space models with varying levels of complexity have been developed [79]. The main methodology employed is that of lumped parameter models, which provide simplified descriptions of the predominant behavior of each component involved in the CVS [17, 61, 79, 94, 63].

The model discussed in this work is based on an electrical representation of the CVS, as proposed in [94, 17, 63]. The choice of this model is motivated by the need for a comprehensive model that can be validated from a medical perspective and is capable of describing cardiovascular phenomena, such as valve pathologies, which are among the primary risk factors for cardiovascular diseases (CVDs). This model primarily targets the left chambers of the heart, assuming that voltages are analogous to pressure and currents are analogous to blood flow. The systemic resistance R_S is the resistance to flow from the descending aorta through the capillary vessels, venous, and pulmonary circulation to reach the left atrium. Left ventricular pressure (LVP) is represented by the voltage across the time-varying contractile capacity $C(t)$, where its capacitance is defined as the inverse of left ventricular elastance $E(t)$.

The term $E(t)$ represents the elastance of the heart at time t , which is a function of the pressure. The mitral and aortic valves are represented as ideal diodes, D_A and D_M , in series with resistance R_A and R_M , respectively. The capacitor C_A , represents the elasticity of the ascending aorta, simulating the pressure variations caused by the opening and closing of the aortic valve. Finally, the remaining components model the anatomical characteristics of the circulatory system, including the elasticity represented by C_S , inertia (L_S), and resistance R_C of the descending aorta [99].

The electrical model circuit in Figure 3.3 has been thoroughly analyzed in [93, 99].

The state variables and parameter values of the cardiovascular circuit model shown in Figure 3.3, as referenced from [99, 8, 93], are detailed in Tables 3.1 and 3.2 below:

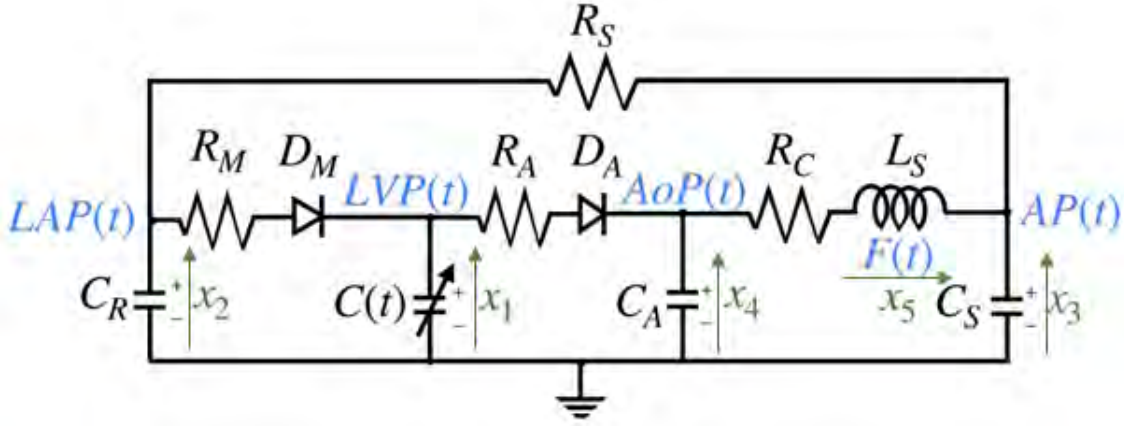


Figure 3.3: Cardiovascular circuit model.

Table 3.1: State variables of the cardiovascular system and their physiological significance of the circuit model shown in Figure 3.3.

Variables	Abbreviation	Physiological Meaning (Unit)
$x_1(t)$	LVP(t)	Left ventricular pressure (mmHg)
$x_2(t)$	LAP(t)	Left atrial pressure (mmHg)
$x_3(t)$	AP(t)	Descending arterial pressure (mmHg)
$x_4(t)$	$A_o(t)$	Ascending aortic pressure (mmHg)
$x_5(t)$	F(t)	Total aortic flow (mL/s)

3.3.2 Elastance

Elastance, denoted as $E(t)$, relates to the state of contraction of the left ventricle. It represents the relationship between the pressure and volumes of the LV , as defined by the following expression:

$$E(t) = \frac{LVP(t)}{LVV(t) - V_0} = \frac{x_1(t)}{LVV(t) - V_0} \quad (3.1)$$

where $LVP(t)$ is the left ventricular pressure, $LVV(t) = \frac{x_1(t)}{E(t)} + V_0$ is the left ventricular volume, and V_0 is a reference volume, which corresponds to the theoretical volume in the ventricle at zero pressure. The elastance function $E(t)$ has been addressed in various studies [93]. These studies concur that the definition can be mathematically approximated using an expression where the points at which the left ventricular function reaches its maximum and minimum are identified used the expression:

$$E(t) = (E_{max} - E_{min})E_n(t_n) + E_{min} \quad (3.2)$$

where E_{max} and E_{min} are constants related to the end-systolic volume (ESV) and end-diastolic volume (EDV), representing the left ventricular volumes at systole and diastole, respectively. The end-systolic

Table 3.2: Parameter values of the CVS circuit model shown in Figure 3.3.

Parameter	Value	Physiological Meaning (Unit)
C_S	1.33	Systemic compliance
C_R	4.40	Left atrial compliance
C_R	4.40	Aortic compliance
L_S	0.0005	Inertia of blood in aorta
R_C	0.0398	Characteristic resistance
R_M	0.005	Mitral valve resistance
R_A	0.001	Aortic valve resistance
Left Ventricle		
E_{max}	2	Maximum volume in diastole
E_{min}	0.06	Minimum volume in diastole
V_o	10	Reference volume at zero pressure (ml)
H_R	75	Heart rate (bpm)
Elastance		
	1.17	Shape parameter
	0.7	Shape parameter
	1.55	Amplitude
	1.9	Ascending slope of the LV relaxation time
	21.9	Descending slope of the LV relaxation time

pressure–volume relationship (ESPVR) denotes the maximal pressure of the left ventricle.

The elastance function is implemented using a number of mathematical approximations, including $E_n(t_n)$, the so-called “double hill” [73].

In this work, $E_n(t_n)$ represents the normalized elastance at time t_n . “normalized” means that it has been adjusted or expanded to fit a specific range, often between 0 and 1 or -1 and 1 . The normalized elastance $E_n(t_n)$ is scaled proportionally between E_{min} and E_{max} . Specifically, when $E_n(t_n) = 0$, $E(t)$ equal E_{min} , and when $E_n(t_n) = 1$, $E(t)$ equal E_{max} . In the context of the cardiovascular system, $E_n(t_n)$ describes how elastance dynamically varies over time adjusted to heart rate, and this relationship is expressed by:

$$E_n(t_n) = 1.55 \left(\frac{(\frac{tn}{0.7})^{1.9}}{1 + (\frac{tn}{0.7})^{1.9}} \right) \left(\frac{1}{1 + (\frac{tn}{1.17})^{21.9}} \right) \quad (3.3)$$

where $t_n = t / (0.2 + 0.15 \frac{60}{H_R})$, with H_R being the heart rate expressed in beats per minute (bpm). The first term within the brackets describes the ascending segment of the curve, while the subsequent term portrays its descending counterpart. The value 1.55 corresponds to the amplitude of elastance, which is associated with the maximum arterial pressure. Additionally, 1.9 and 21.9 indicate the ascending and descending slopes during the LV relaxation period, respectively, while 0.7 and 1.17 are constants that determine the proportional representation of each curve over the cardiac cycle. Figure 3.4 illustrates the graphical representations of these curves.

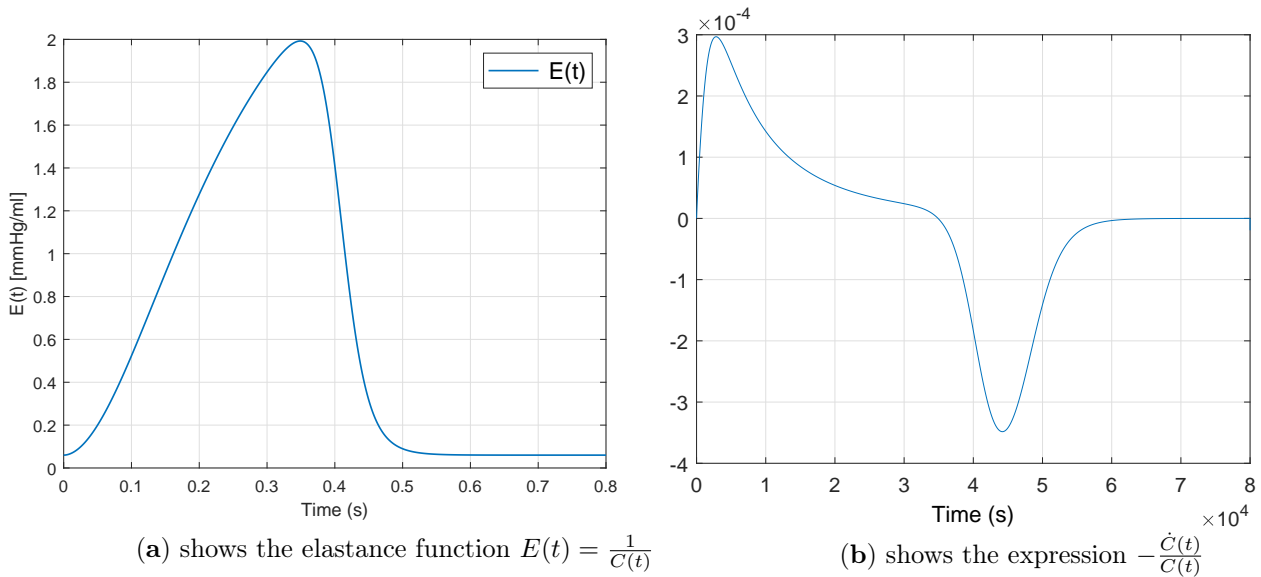


Figure 3.4: Plot the elastance function for a healthy heart during a single cardiac cycle.

3.3.3 Cardiovascular system modeling phases

The transitions between system modes are given by ideal (non-linear) valve operations (i.e., diodes). Remember that the opening and closing of the mitral and aortic valves is driven by the pressure difference between the LAP and the *LVP*, the *LVP* and *AoP* which are system states; that is, the mode change is state-driven. The figure3.5 shows the four modes of the system with their corresponding transition conditions.

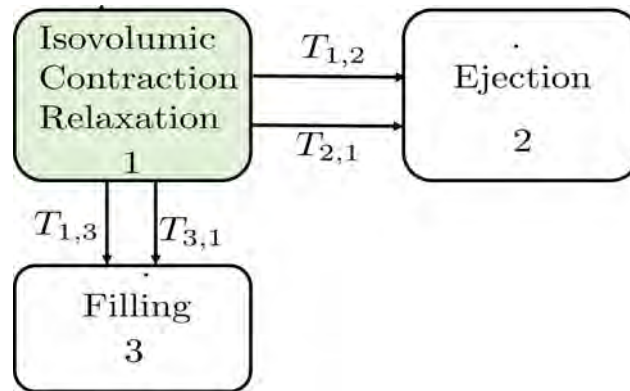


Figure 3.5: Interpretation of the cardiac cycle using a hybrid system

Let $\mathcal{Q} = \{q_i : i \in M\}$, with $M = \{1, 2, 3\}$ represent the set of possible discrete modes. Define $\mathcal{X} \subseteq \mathbb{R}^n$ as the continuous-time state space of dimension n . The state vector $x \in \mathbb{R}^n$ belongs to this space. The couple $(q_i(t); x_i(t)) \in \mathcal{Q}\mathcal{X}$ represents the state of the hybrid system in mode i . The subscript i stands for the active mode q_i of the system, i.e. Filling, ejection or isovolumic contraction/ relaxation.

Let the vector $u \in \mathbb{R}^2$ be the natural input vector representing the mitral valve u_1 and aortic valve u_2 .

The valves of u are give by:

$$u_1 \begin{cases} 0, & x_2 < x_1 \\ 1, & x_2 \geq x_1 \end{cases} \quad (3.4)$$

$$u_2 \begin{cases} 0, & x_1 < x_4 \\ 1, & x_1 \geq x_4 \end{cases} \quad (3.5)$$

where $u_1 = \{0, 0, 1, 0\}$ and $u_2 = \{1, 0, 0, 0\}$ are the sequence of natural control inputs of the system (the state of the diodes D_M and D_A). The values of these signals, as described in the previous equations, take values of 1 or 0.

Filling phase ($q_1 = F$)

During the filling phase the aortic valve is closed and the mitral valve is open. According to the phase of the diode D_A is not conducting while the diode D_M allows the flow of current. A representation of the electrical circuit is depicted in Figure 3.6 observe that, while the left ventricle (LV) is being filled with blood, systemic circulation is carried out by the elastic properties of the arterial system. In other words, after losing energy due to the opposing characteristic resistance of the aortic wall (R_C) and affected by the inertial of the blood mass (L_S), the blood flow reaches the peripheral arterial system; that is, capacitor C_S . At the same time, blood returns to the left atrium (C_R), losing energy on the way due to resistance of the walls of the arterial systems (R_C).

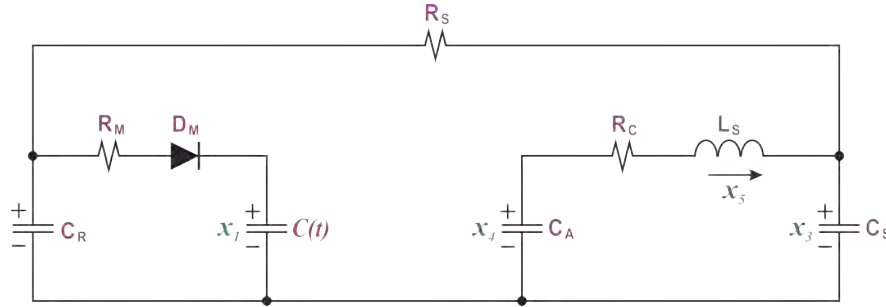


Figure 3.6: Electrical representation of the Filling phase ($q_1 = F$)

The dynamics of the circuit in the figure 3.6 are obtained by using Kirchhoff's laws. Considering that $i_C(t) = i_{RM}$ and $i_{RM} = \frac{1}{R_M}(x_2 - x_1)$, perform a mesh and node analysis.

In this case the capacitance of the left ventricle is variable in time so the current circulating in this capacitor is $i_C(t) = \dot{C}(t)x_1 + C(t)\dot{x}_1$, then the expression $i_C(t) = i_{RM}$ gives $\dot{C}(t)x_1 + C(t)\dot{x}_1 = \frac{1}{R_M}(-x_1 + x_2)$

Thus \dot{x}_1 we have the form:

$$\dot{x}_1 = \frac{1 + \dot{C}(t)}{C(t)R_M}x_1 + \frac{1}{R_M}x_2 \quad (3.6)$$

From a node analysis, the current circulating in node 1 is considered to be equal to

$$-x_2 + R_M i_{RM} + x_1 = 0 \quad (3.7)$$

solving i_{RM} we have

$$i_{RM} = -\frac{1}{R_S}(x_2 + x_3) - C_R \dot{x}_2 \quad (3.8)$$

then i_{RM} is the same as $i_{RM} = i_{R_s} - i_{C_R}$ and replacing in the equation (3.8), we have the form:

$$-\frac{1}{R_M}x_1 + -\frac{1}{R_M}x_2 = -\frac{1}{R_S}(x_2 + x_3) - C_R \dot{x}_2 \quad (3.9)$$

Clearing to \dot{x}_2 of the equation (3.9) which gives :

$$\dot{x}_2 = \frac{1}{C_R R_M}x_1 - \frac{R_M + R_S}{C_R R_M R_S}x_2 - \frac{1}{C_R R_S}x_3 \quad (3.10)$$

From the mesh analysis it is obtained that:

$$-V_{CR} + V_{RS} + V_{RS} = 0 \quad (3.11)$$

and substituting $-V_{CR}$, V_{RS} y V_{RS}

$$-x_2 + R_s i_{RS} + x_3 = 0 \quad (3.12)$$

if we carry out the mesh analysis for the first mesh and it is considered that $i_{RS} = x_5 - i_{CS} = x_5 \dot{x}_3$, then:

$$-x_2 + R_S(x_5 - C_S \dot{x}_3) + x_3 = 0 \quad (3.13)$$

$$-x_2 + R_s x_5 - R_S C_S \dot{x}_3 + x_3 = 0 \quad (3.14)$$

$$-R_s C_S \dot{x}_3 = x_2 - R_S x_5 - x_3 \quad (3.15)$$

$$\dot{x}_3 = \frac{1}{R_S C_S}x_2 - \frac{1}{R_S C_S}x_3 - \frac{1}{C_S}x_5 \quad (3.16)$$

$$\dot{x}_3 = \frac{1}{R_S C_S}(x_2 - x_3) - \frac{1}{C_S}x_5 \quad (3.17)$$

performing in node analysis at C_A where $i_{CA} = x_5 = C_A \dot{x}_4$ then:

$$x_5 = C_A \dot{x}_4 \quad (3.18)$$

clearing \dot{x}_4

$$\dot{x}_4 = -\frac{1}{C_A}x_5 \quad (3.19)$$

Performing the mesh analysis of the L_S is obtained;

$$-V_{CA} + V_{RC} + V_{LS} + V_{CS} = 0 \quad (3.20)$$

and substituting V_{CA} , V_{RC} , V_{LS} y V_{CS} then:

$$-x_4 + R_C i_{RC} + L_S \dot{x}_5 + x_3 = 0 \quad (3.21)$$

Clearing \dot{x}_5

$$\dot{x}_5 = -\frac{1}{L_S}x_3 + \frac{1}{L_S}x_4 - \frac{1}{L_S}(R_C i_{RC}) \quad (3.22)$$

We take into account that the current in $i_{RC} = x_5$ and replace it in the equation (3.22), \dot{x}_5 nos which gives:

$$\dot{x}_5 = -\frac{1}{L_S}x_3 + \frac{1}{L_S}x_4 - \frac{R_C}{L_S}x_5 \quad (3.23)$$

The matrix representation of such dynamics in the form of state space is this given by:

$$A_1(t) = \begin{bmatrix} -\frac{1+\dot{C}(t)R_M}{C(t)R_M} & \frac{1}{C(t)R_M} & 0 & 0 & 0 \\ \frac{1}{C_R R_M} & -\frac{R_M+R_S}{C_R R_M R_S} & \frac{1}{C_R R_S} & 0 & 0 \\ 0 & \frac{R_M+R_S}{C_R R_M R_S} & -\frac{1}{C_S R_S} & 0 & \frac{1}{C_S} \\ 0 & 0 & 0 & 0 & -\frac{1}{C_A} \\ 0 & 0 & -\frac{1}{L_S} & \frac{1}{L_S} & -\frac{R_C}{L_S} \end{bmatrix} \quad (3.24)$$

Ejection phase ($q_2 = E$)

In this phase, the mitral valve is closed (D_M is not conducting) and the left ventricle is pumping blood through the open aortic valve (D_A is active). In the figure 3.7 there is no physical connection between the left atrium (represented by capacitor C_R) and the left ventricle due to the none-conducting diode D_M . In this phase, as $C(t)$ discharges, i.e. the left ventricle pushes blood, capacitor C_A charges.

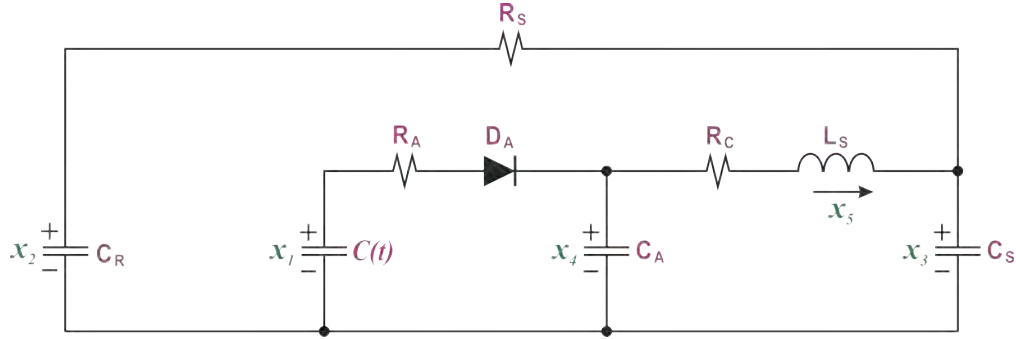


Figure 3.7: Electrical representation of the ejection phases ($q_2 = E$)

The dynamics of the circuit in the figure 3.7, are obtained by using Kirchhoff's laws. To solve it we made a mesh analysis in the mesh of the inductor L_S to be able to obtain \dot{x}_5 .

$$-V_{CA} + V_{RC} + V_{LS} + V_{CS} = 0 \quad (3.25)$$

and sustaining V_{CA}, V_{RC}, V_{LS} and V_{CS} which give:

$$-x_4 + R_C i_{RC} + L_S \dot{x}_5 + x_3 = 0 \quad (3.26)$$

clearing \dot{x}_5

$$\dot{x}_5 = -\frac{1}{L_S}x_3 + \frac{1}{L_S}x_4 - \frac{1}{L_S}(R_C i_{RC}) \quad (3.27)$$

If we take into account that the current in $i_{RC} = x_5$ and substitute in the equation (3.27), \dot{x}_5 which give:

$$\dot{x}_5 = -\frac{1}{L_S}x_3 + \frac{1}{L_S}x_4 - \frac{R_C}{L_S}x_5 \quad (3.28)$$

While to obtain \dot{x}_3 is considered that $i_{RS} = x_5 - i_{CS} = x_5 - C_S \dot{x}_3$ and mesh analysis is performed, then:

$$-x_2 + R_S(x_5 - C_S\dot{x}_3) + x_3 = 0 \quad (3.29)$$

clearing \dot{x}_3 which give

$$\dot{x}_3 = \frac{1}{R_S C_S}(-x_2 + x_3) + \frac{1}{C_S}x_5 \quad (3.30)$$

To obtain \dot{x}_4 we develop a mesh analysis and obtain

$$-x_1 + R_A i_{RA} + x_4 = 0 \quad (3.31)$$

we consider that $i_{RA} = \frac{1}{R_A}(x_1 - x_4)$ and that $i_{CA} = i_{RA} - i_{RC} = C_A \dot{x}_4 - x_5$ and we replace them in $-x_1 + R_A i_{RA} + x_4 = 0$ which give

$$C_A \dot{x}_4 - x_5 = \frac{1}{R_A}(x_1 - x_4) \quad (3.32)$$

clearing \dot{x}_4

$$\dot{x}_4 = \frac{1}{R_A C_A}x_1 - \frac{1}{R_A C_A}x_4 + \frac{1}{C_A}x_5 \quad (3.33)$$

We take into account that the capacitance in the left ventricle is variable in time, so the current circulating in this capacitor is $i_C(t) = \dot{C}(t)x_1 + C(t)\dot{x}_1$, therefore the expression $i_C(t) = -i_{RA}$ which give $\dot{C}(t)x_1 + C(t)\dot{x}_1 = C_A \dot{x}_4 - x_5$

A from a node analysis, the current circulating in node 1 is considered, and substituting $C_A \dot{x}_4 - x_5$ we obtain that

$$\dot{C}(t)x_1 + C(t)\dot{x}_1 = \frac{1}{R_A}(x_1 - x_4) \quad (3.34)$$

clearing \dot{x}_1 we get:

$$\dot{x}_1 = \frac{1 + \dot{C}(t)R_A}{C(t)R_A}x_1 + \frac{1}{R_A}x_4 \quad (3.35)$$

In order to get \dot{x}_2 it is noted that

$$C_R \dot{x}_2 = x_5 - C_S \dot{x}_3 \quad (3.36)$$

if we substitute \dot{x}_3 we obtain that

$$C_R \dot{x}_2 = x_5 - C_S \left[\frac{1}{R_S C_S}(-x_2 + x_3) + \frac{1}{C_S}x_5 \right] \quad (3.37)$$

clearing \dot{x}_2

$$\dot{x}_2 = \frac{1}{R_S C_R}(-x_2 + x_3) \quad (3.38)$$

The matrix representation of such dynamics in the form of state space is thus given by

$$A_1(t) = \begin{bmatrix} -\frac{1+\dot{C}(t)R_A}{C(t)R_A} & 0 & 0 & \frac{1}{C(t)R_A} & 0 \\ 0 & -\frac{1}{C_R R_S} & \frac{1}{C_R R_S} & 0 & 0 \\ 0 & \frac{1}{C_S R_S} & -\frac{1}{C_S R_S} & 0 & \frac{1}{C_S} \\ \frac{1}{C_A R_A} & 0 & 0 & -\frac{1}{L_S} & -\frac{C_A}{R_C} \\ 0 & 0 & -\frac{1}{L_S} & \frac{1}{L_S} & -\frac{1}{L_S} \end{bmatrix} \quad (3.39)$$

Isovolumic phase ($q_3 = I$)

The isovolumic phase occurs twice. First when the left ventricle contracts and the second when it relaxes. These two phases have a short duration compared to the ejection and filling phases. Both valves are closed, meaning that neither diode D_M nor D_A are conducting. Thanks to the discharge of capacitors C_A and C_S (contraction of aorta and arteries) blood is able to complete its journey back to the heart.

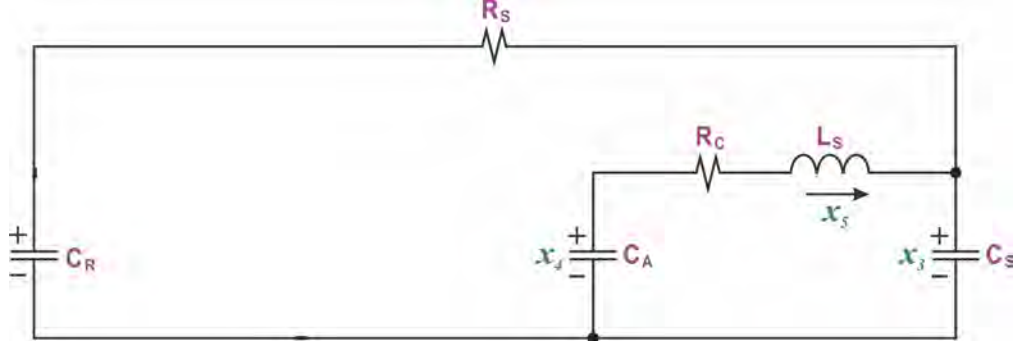


Figure 3.8: Electrical representation of the isovolumic phase ($q_3 = I$)

To solve this, we perform a mesh analysis on the L_S which give \dot{x}_5 .

$$-V_{CA} + V_{RC} + V_{LS} + V_{CS} = 0 \quad (3.40)$$

and substituting V_{CA}, V_{RC}, V_{LS} y V_{CS} which give

$$-x_4 + R_C i_{RC} + L_S \dot{x}_5 + x_3 = 0 \quad (3.41)$$

clearing \dot{x}_5

$$\dot{x}_5 = -\frac{1}{L_S} x_3 + \frac{1}{L_S} x_4 - \frac{1}{L_S} (R_C i_{RC}) \quad (3.42)$$

we take into account that the current in $i_{RC} = x_5$ to replace it in the equation (3.42), \dot{x}_5 which give:

$$\dot{x}_5 = -\frac{1}{L_S} x_3 + \frac{1}{L_S} x_4 - \frac{R_C}{L_S} x_5 \quad (3.43)$$

Although in order to obtain \dot{x}_3 is considered the analysis of nodes where $i_{RS} = x_5 - i_{CS} = x_5 - C_S \dot{x}_3$ then

$$-x_2 + R_S(x_5 - C_S \dot{x}_3) + x_3 = 0 \quad (3.44)$$

clearing \dot{x}_3 which give

$$\dot{x}_3 = \frac{1}{R_S C_S} (-x_2 + x_3) + \frac{1}{C_S} x_5 \quad (3.45)$$

To obtain \dot{x}_4 analysis of meshes is carried out and it is considered that $i_{CA} = -i_{RC} = C_A \dot{x}_4$ y $i_{RC} = -x_5$. Based on the above relationships, it is known that

$$C_A \dot{x}_4 = -x_5 \quad (3.46)$$

If we clear \dot{x}_4 obtains

$$\dot{x}_4 = -\frac{1}{CA}x_5 \quad (3.47)$$

To obtain \dot{x}_3 the following is considered to be $i_{RS} = x_5 - C_S\dot{x}_3$ a node analysis is performed, then by means of the mesh analysis it is obtained that

$$-C_R\dot{x}_2 = x_5 + \frac{1}{R_S}(x_2 - x_3) + x_5 \quad (3.48)$$

If we clear \dot{x}_2

$$\dot{x}_2 = -\frac{1}{C_R R_S}(x_2 + x_3) \quad (3.49)$$

To obtain \dot{x}_1 through the analysis of the capacitance it is established that

$$i_C(t) = \dot{C}(t)x_1 + C(t)\dot{x}_1 = 0 \quad (3.50)$$

then clearing \dot{x}_1

$$\dot{x}_1 = \frac{-\dot{C}(t)}{C(t)}x_1 \quad (3.51)$$

3.3.4 Mathematical model of the cardiovascular system

We consider the CVS model basically given by the following equations [94]:

$$\begin{pmatrix} \dot{x}_1 \\ \dot{x}_2 \\ \dot{x}_3 \\ \dot{x}_4 \\ \dot{x}_5 \end{pmatrix} = \begin{pmatrix} \frac{-\dot{C}(t)}{C(t)} & 0 & 0 & 0 & 0 \\ 0 & -\frac{1}{R_S C_R} & \frac{1}{R_S C_R} & 0 & 0 \\ 0 & \frac{1}{R_S C_S} & -\frac{1}{R_S C_S} & 0 & \frac{1}{C_S} \\ 0 & 0 & 0 & 0 & -\frac{1}{C_A} \\ 0 & 0 & -\frac{1}{L_S} & \frac{1}{L_S} & -\frac{R_C}{L_S} \end{pmatrix} \begin{pmatrix} x_1 \\ x_2 \\ x_3 \\ x_4 \\ x_5 \end{pmatrix} + \begin{pmatrix} \frac{1}{C(t)R_M} & \frac{1}{C(t)R_A} \\ \frac{-1}{C_R R_M} & 0 \\ 0 & 0 \\ 0 & \frac{-1}{C_A R_A} \\ 0 & 0 \end{pmatrix} \begin{pmatrix} D_M(x_2 - x_1) \\ D_A(x_4 - x_1) \end{pmatrix} \quad (3.52)$$

where $(x_1 \ x_2 \ x_3 \ x_4 \ x_5)^T$ represents the state vector of CVS circuit model (see Figure 3.3 and Tables 3.1 and 3.2) and $\begin{pmatrix} D_M \\ D_A \end{pmatrix}$ represents the natural control input sequences of cardiovascular system, with D_M is the state of the mitral valve and D_A is the state of the aortic valve given by:

$$D_M = \begin{cases} 0, & x_2 < x_1 \\ 1, & x_2 \geq x_1 \end{cases}, D_A = \begin{cases} 0, & x_1 < x_4 \\ 1, & x_1 \geq x_4 \end{cases} \quad (3.53)$$

3.4 Quadratic normal form of the cardiovascular system

For the remainder of our work of the cardiovascular system, we take the output vector as

$$y(t) = \begin{pmatrix} y_1 \\ y_2 \end{pmatrix} = \begin{pmatrix} x_5 \\ x_4 \end{pmatrix} \text{ and the input vector as } u(t) = \begin{pmatrix} u_1 \\ u_2 \\ u_3 \\ u_4 \end{pmatrix} = \begin{pmatrix} D_M \\ D_A \\ D_M \frac{1}{C(t)} \\ D_A \frac{1}{C(t)} \end{pmatrix}.$$

Given this output, it is easy to demonstrate that x_1 is linearly unobservable in system (3.52). To proceed with calculating the quadratic normal form, we introduce the following change of coordinates:

$$\begin{aligned}
 z_1^1 &= x_5 \\
 z_2^1 &= -\frac{1}{L_S}x_3 \\
 z_3^1 &= -\frac{1}{L_S R_S C_S}x_2 + \frac{1}{L_S R_S C_S}x_3 \\
 z_1^2 &= x_4 \\
 z_2^2 &= C(t)x_1(t)
 \end{aligned} \tag{3.54}$$

which is equivalent to

$$\begin{aligned}
 x_1 &= \frac{1}{C(t)}z_2^2 &= \xi_1 \\
 x_2 &= L_S R_S C_S z_3^1 + L_S z_2^1 &= \xi_2 \\
 x_3 &= -L_S z_2^1 &= \xi_3 \\
 x_4 &= z_1^2 &= \xi_4 \\
 x_5 &= z_1^1 &= \xi_5
 \end{aligned} \tag{3.55}$$

We directly obtain the quadratic normal form (QNF) [10, 12] of the CVS model:

$$\left\{ \begin{aligned}
 \dot{z}_1^1 &= -\frac{R_C}{L_S}z_1^1 + z_2^1 + \frac{1}{L_S}z_1^2 &= f_1 \\
 \dot{z}_2^1 &= -\frac{1}{L_S C_S}z_1^1 + z_3^1 &= f_2 \\
 \dot{z}_3^1 &= \frac{1}{L_S R_S C_S^2}z_1^1 - \beta z_3^1 - k_1 z_3^1 u_1 - k_2 z_2^1 u_1 - k_3 z_2^2 u_3 &= f_3 \\
 \dot{z}_1^2 &= -\frac{1}{C_A}z_1^1 - \frac{1}{C_A R_A}z_1^2 u_2 - \frac{1}{C_A R_A}z_2^2 u_4 &= f_4 \\
 \dot{z}_2^2 &= \frac{L_S R_S C_S}{R_M}z_3^1 u_1 - \frac{L_S}{R_M}z_2^1 u_1 + \frac{1}{R_A}z_1^2 u_2 - \frac{1}{R_M}z_2^2 u_3 - \frac{1}{R_A}z_2^2 u_4 &= f_5 \\
 y_1 &= z_1^1 \\
 y_2 &= z_1^2
 \end{aligned} \right. \tag{3.56}$$

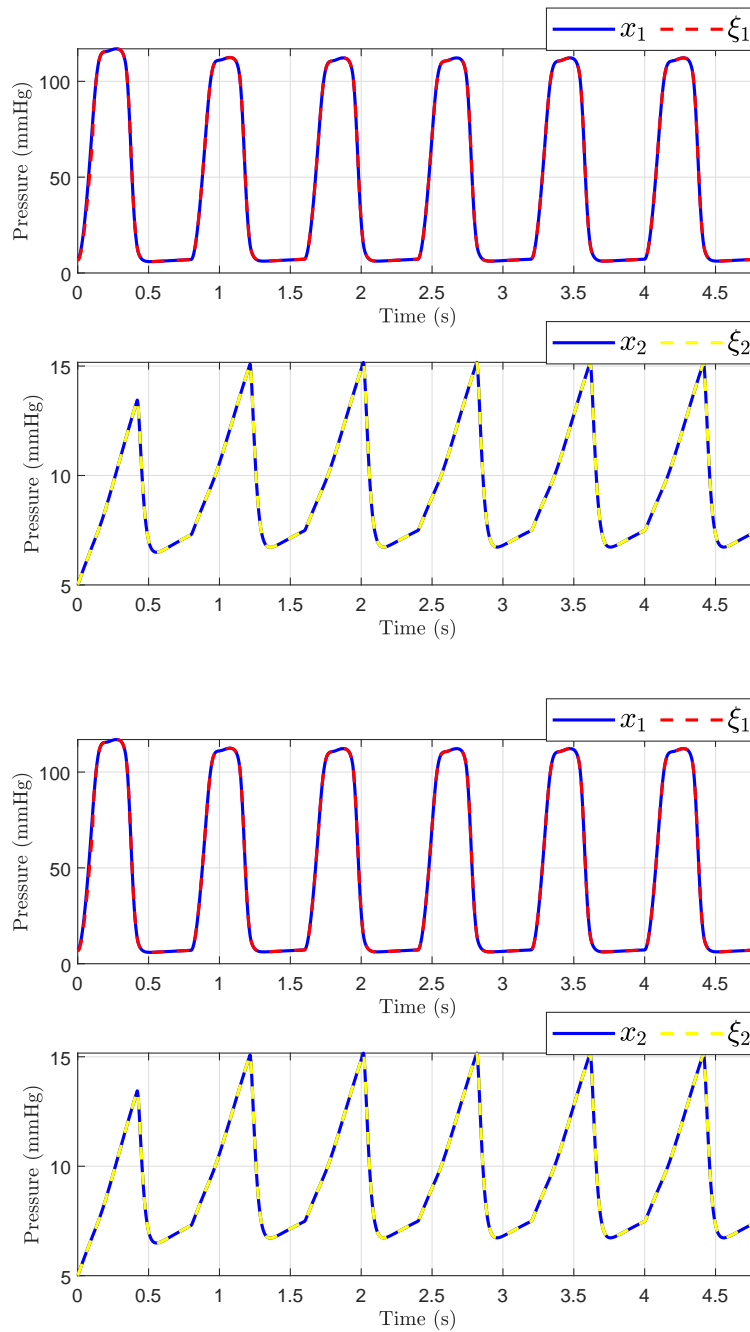
where $\beta = \frac{1}{R_S C_R} + \frac{1}{R_S C_S}$, $k_1 = \frac{1}{C_R R_M}$, $k_2 = \frac{1}{R_S C_S C_R R_M}$ and $k_3 = \frac{1}{L_S R_S C_S C_R R_M}$.
 And $u_1 = D_M$, $u_2 = D_A$, $u_3 = D_M \frac{1}{C(t)}$ and $u_4 = D_A \frac{1}{C(t)}$.

Remark 3.4.1 As a result, building on the work in [12], thanks to the quadratic terms $k_3 u_3 z_2^2$ and $\frac{1}{C_A R_A} z_2^2 u_4$, we can recover observability for z_2^2 .

3.4.1 Validation of the quadratic normal form of the CVS model

This section presents the validation process for the quadratic normal form of the CVS model obtained, drawing upon previously established validations and incorporating diverse analytical perspectives, as detailed in seminal works such as [8, 99]. Initially, the accuracy of the model is corroborated by putting the waveforms of the main variables, as shown in Figure 3.9, with empirical data from healthy subjects reported in [99]. In addition, the figure shows the original states $x_i(t)$ and QNF states $\xi_i(t)$ of CVS are shown in Figure 3.9, where we can observe the the hemodynamic waveforms of the CVS model (3.52) compared with the experimental data.

The validation of the model also involves a dynamic analysis concerning preload and after load factors. To evaluate this aspect, we analyze the preload and after load signals generated by both the original and the quadratic normal form of the CVS model. Figure 3.10 displays the left ventricular pressure data and the corresponding pressure–volume loop obtained from our model using a volume of $V_0 = 10 \text{ mL}$. It is observed that the dynamics obtained are consistent with those described in [99].



With these results, we can affirm that the quadratic normal form obtained offers a novel alternative for the representation of the classical model presented in the literature. Additionally, it is crucial to emphasize that a significant advantage of the quadratic normal form is its capacity to enable the design of observers. These observers can estimate the states of the system that are not directly measurable and apply other control theory concepts. An example of such an application, as discussed in this work, is fault detection and estimation.

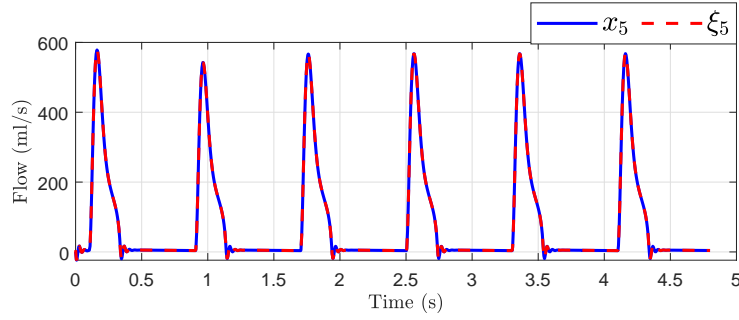
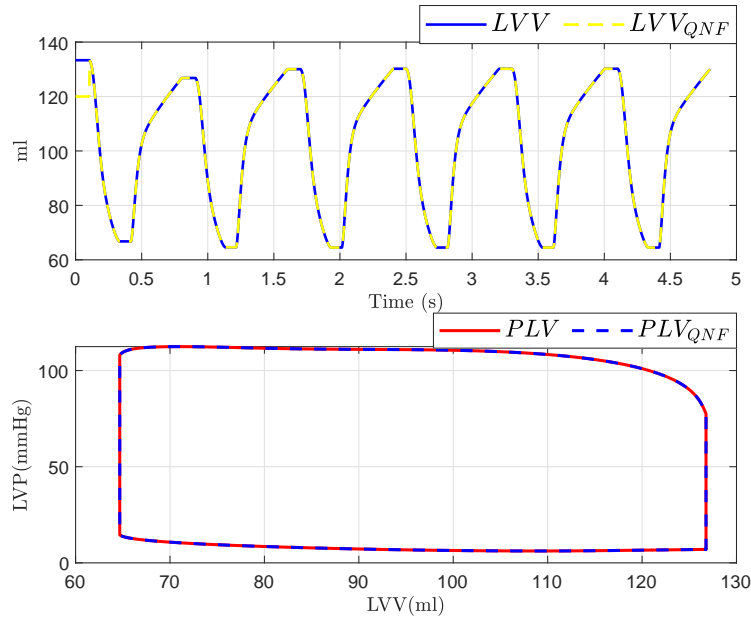

 Figure 3.9: Hemodynamic waveforms of the CVS mode: Original states $x_i(t)$ and QNF states $\xi_i(t)$ of CVS


Figure 3.10: Hemodynamic of left ventricular volume (LVV) and preload volume (PLV) in original and QNF system

3.5 Observability analysis and observer design of the cardiovascular system

3.5.1 Observability analysis of the cardiovascular system

Now, we will do a structural analysis of observability applied to the CVS model (3.56). For this, let O the observability matrix given by:

$$O = [dy_1, dy_2, dL_f y_1, dL_f y_2, dL_f^2 y_1]^T \quad (3.57)$$

where $f = [f_1 \ f_2 \ f_3 \ f_4 \ f_5]^T$ was defined in equation (3.56), which gives

$$O = \begin{bmatrix} 1 & 0 & 0 & 0 & 0 \\ 0 & 0 & 0 & 1 & 0 \\ -\frac{R_C}{L_S} & 1 & 0 & \frac{1}{L_S} & 0 \\ \frac{-1}{C_A} & 0 & 0 & \frac{-1}{C_A R_A} u_2 & \frac{-1}{C_A R_A} u_4 \\ M_{11}^1 & -\frac{R_C}{L_S} & 1 & M_{14}^1 & -\frac{R_S C_S}{R_M} u_4 \end{bmatrix} \quad (3.58)$$

with $M_{11}^1 = \frac{R_C^2}{L_S^2} - \frac{1}{L_S C_S} - \frac{1}{L_S} \frac{1}{C_A}$, $M_{14}^1 = \frac{R_C}{L_S^2} - \frac{1}{L_S C_A R_A} u_2$. Then,

$$\det(O) = \frac{-1}{C_A R_A} u_4.$$

In the literature [10], the term "observability singularity manifold" or "unobservability submanifold" refers to the subset S defined by

$$S = \{z \in \mathbb{R}^5 / \det[dh_1, dh_2, dL_f h_1, dL_f^2 h_1]^T = 0\}.$$

Then, for the cardiovascular systems considered we have:

$$S = \left\{ z \in \mathbb{R}^5 / \frac{-1}{C_A R_A} u_4 = 0 \right\}.$$

when CVS evolves on S we lose the linear and nonlinear observability. Then,

- (1) If $u_4 \neq 0$, then $\text{rank}(O) = 5$ and therefore we recover the quadratic observability of z_2^2 .
- (2) If $u_4 = 0$, then $\text{rank}(O) = 4$ and therefore we lose the observability of z_2^2 .

3.5.2 Sliding mode observers design for CVS

In this subsection, we will outline the structure of the observer. For a deeper exploration into the design and analysis of observability, readers are encouraged to consult the works cited in [87]. The observer structure presented here accounts for quadratic observability singularities that arise due to state separation or universal input. This methodology is derived from the step-by-step sliding mode approach as detailed in references [7, 24, 5]. We assume that the states z_1^1 and z_1^2 are directly measurable, but the others are not. The sliding mode observer is described as follows:

$$\begin{cases} \dot{\hat{z}}_1^1 &= -\frac{R_C}{L_S} z_1^1 + \hat{z}_2^1 + \frac{1}{L_S} z_1^2 + \delta_1^1 \text{sign}(z_1^1 - \hat{z}_1^1) \\ \dot{\hat{z}}_2^1 &= -\frac{1}{L_S C_S} z_1^1 + \hat{z}_3^1 + E_1^1 \delta_2^1 \text{sign}(\hat{z}_2^1 - z_2^1) \\ \dot{\hat{z}}_3^1 &= \frac{1}{L_S R_S C_S^2} z_1^1 - \beta \hat{z}_3^1 - k_1 \hat{z}_3^1 u_1 - k_2 \hat{z}_2^1 u_1 - k_3 \hat{z}_2^2 u_3 + E_2^1 \delta_3^1 \text{sign}(\hat{z}_3^1 - z_3^1) \\ \dot{\hat{z}}_1^2 &= -\frac{1}{C_A} z_1^1 - \frac{1}{C_A R_A} (z_1^2 u_2 + \hat{z}_2^2 u_4) + \delta_1^2 \text{sign}(z_1^2 - \hat{z}_1^2) \\ \dot{\hat{z}}_2^2 &= -\frac{L_S R_S C_S}{R_M} \hat{z}_3^1 u_1 - \frac{L_S}{R_M} \hat{z}_2^1 u_1 - \frac{1}{R_M} \hat{z}_2^2 u_3 + \frac{1}{R_A} z_1^2 u_2 - \frac{1}{R_A} \hat{z}_2^2 u_4 \\ &\quad + E_1^2 \delta_2^2 \text{sign}(\hat{z}_2^2 - z_2^2) \end{cases} \quad (3.59)$$

In system (3.60), the auxiliary components \tilde{z}_i^q are calculated algebraically as follows:

$$\begin{aligned} \tilde{z}_2^1 &= \hat{z}_2^1 + \delta_1^1 \text{sign}(z_1^1 - \hat{z}_1^1) \\ \tilde{z}_3^1 &= \hat{z}_3^1 + \delta_2^1 \text{sign}(\hat{z}_2^1 - z_2^1) \\ \tilde{z}_2^2 &= \hat{z}_2^2 + \frac{E_{SM}}{k_3 u_3 + E_{SM} - 1} E_2^1 \delta_3^1 \text{sign}(\hat{z}_3^1 - z_3^1) \end{aligned}$$

with the following conditions:

- if $\hat{z}_1^1 = z_1^1$ and $\hat{z}_1^2 = z_1^2$ then $E_1^1 = E_1^2 = 1$ otherwise $E_1^1 = E_1^2 = 0$,
- if $\hat{z}_2^1 = z_2^1$ and $E_1^1 = E_1^2 = 1$ then $E_2^1 = 1$ otherwise $E_2^1 = 0$.

And, to ensure observability is not lost near the observability singularity, you must accurately set E_{SA} and E_{SM} , such that:

- if $u_1 = 1$ then $E_{SM} = 1$ otherwise $E_{SM} = 0$,
- if $u_4 = 1$ then $E_{SA} = 1$ otherwise $E_{SA} = 0$.

Which gives:

$$\begin{aligned}\tilde{z}_3^1 &= \hat{z}_3^1 + \frac{E_{SM}}{-\frac{L_S R_S C_S}{R_M} u_1 + E_{SM} - 1} \delta_2^2 \text{sign}(\tilde{z}_2^2 - \hat{z}_2^2) \\ \tilde{z}_2^2 &= \hat{z}_2^2 + \frac{C_A R_A E_{SA}}{u_4 + E_{SA} - 1} E_1^2 \delta_1^2 \text{sign}(z_1^2 - \hat{z}_1^2)\end{aligned}$$

Remark 3.5.1 The quality of the estimation of z_2^2 depends on the choice of E_{SA} and E_{SM} . Therefore, it is essential to adjust E_{SA} and E_{SM} within a small neighborhood of the singularity to ensure that the structure without feedback is applied for the minimum amount of time necessary.

Remark 3.5.2 Since u_1 and u_2 cannot be equal to one at the same time, also $u_3 = u_1 \frac{1}{C(t)}$, and $u_4 = u_2 \frac{1}{C(t)}$ then when $u_3 = 1$ and $u_4 = 0$, we use the quadratic term $k_3 z_2^2 u_3$ to recover the information of z_2^2 in this case

$$\tilde{z}_2^2 = z_2^2 + \frac{E_{SM}}{k_3 u_3 + E_{SM} - 1} E_2^1 \delta_3^1 \text{sign}(\tilde{z}_3^1 - \hat{z}_3^1)$$

and when $u_3 = 0$ and $u_4 = 1$, we use the quadratic term $\frac{1}{C_A R_A} z_2^2 u_4$ to recover the information of z_2^2 in this case

$$\tilde{z}_2^2 = \hat{z}_2^2 + \frac{C_A R_A E_{SA}}{u_4 + E_{SA} - 1} E_1^2 \delta_1^2 \text{sign}(z_1^2 - \hat{z}_1^2)$$

Now, we present the proof of the convergence of the observer (3.60). The study of the observer's stability and convergence uses equivalent vector methods [21]. The observer convergence strategy is carried out step by step on different sliding surfaces and ensures convergence of the observation error in 3 steps and in finite time to zero in the Lyapunov sense ([7], [24], [5]).

Proof 3.5.1 The dynamics of the observer error ($e = z - \hat{z}$) is written:

$$\begin{cases} \dot{e}_1^1 &= -\frac{R_C}{L_S} e_1^1 + e_2^1 + \frac{1}{L_S} e_1^2 + \delta_1^1 \text{sign}(z_1^1 - \hat{z}_1^1) \\ \dot{e}_2^1 &= -\frac{1}{L_S C_S} e_1^1 + e_3^1 + E_1^1 \delta_2^1 \text{sign}(\tilde{z}_2^1 - \hat{z}_2^1) \\ \dot{e}_3^1 &= \frac{1}{L_S R_S C_S^2} e_1^1 - \beta e_3^1 - k_1 e_3^1 u_1 - k_2 e_2^1 u_1 - k_3 e_2^2 u_3 + E_2^1 \delta_3^1 \text{sign}(\tilde{z}_3^1 - \hat{z}_3^1) \\ \dot{e}_1^2 &= -\frac{1}{C_A} e_1^1 - \frac{1}{C_A R_A} (e_1^2 u_2 + e_2^2 u_4) + \delta_1^2 \text{sign}(z_1^2 - \hat{z}_1^2) \\ \dot{e}_2^2 &= -\frac{L_S R_S C_S}{R_M} e_3^1 u_1 - \frac{L_S}{R_M} e_2^1 u_1 - \frac{1}{R_M} e_2^2 u_3 + \frac{1}{R_A} e_1^2 u_2 - \frac{1}{R_A} e_2^2 u_4 + E_1^2 \delta_2^2 \text{sign}(\tilde{z}_2^2 - \hat{z}_2^2) \end{cases} \quad (3.60)$$

• **Step 1:** Assume $z_1^1(0) \neq \hat{z}_1^1(0)$ and $z_1^2(0) \neq \hat{z}_1^2(0)$ and as $E_1^1 = E_2^1 = E_1^2 = 0$ in the first step, we obtain the following observation error dynamics:

$$\begin{aligned}\dot{e}_1^1 &= -\frac{R_C}{L_S} e_1^1 + e_2^1 + \frac{1}{L_S} e_1^2 + \delta_1^1 \text{sign}(z_1^1 - \hat{z}_1^1) \\ \dot{e}_2^1 &= -\frac{1}{L_S C_S} e_1^1 + e_3^1 \\ \dot{e}_3^1 &= \frac{1}{L_S R_S C_S^2} e_1^1 - \beta e_3^1 - k_1 e_3^1 u_1 - k_2 e_2^1 u_1 - k_3 e_2^2 u_3 \\ \dot{e}_1^2 &= -\frac{1}{C_A} e_1^1 - \frac{1}{C_A R_A} (e_1^2 u_2 + e_2^2 u_4) + \delta_1^2 \text{sign}(z_1^2 - \hat{z}_1^2) \\ \dot{e}_2^2 &= -\frac{L_S R_S C_S}{R_M} e_3^1 u_1 - \frac{L_S}{R_M} e_2^1 u_1 - \frac{1}{R_M} e_2^2 u_3 + \frac{1}{R_A} e_1^2 u_2 - \frac{1}{R_A} e_2^2 u_4\end{aligned}$$

Let $S_1 = \{e_1^1 = e_2^1 = 0\}$ be the sliding surface and the Lyapunov function $V_1^1 = \frac{(e_1^1)^2}{2}$ and $V_1^1 = \frac{(e_2^1)^2}{2}$. The sliding surface is attractive if and only if $\dot{V}_1^1 = e_1^1 \dot{e}_1^1 < 0$ and $\dot{V}_1^2 = e_2^1 \dot{e}_1^2 < 0$, then

$$e_1^1 \left(-\frac{R_C}{L_S} e_1^1 + e_2^1 + \frac{1}{L_S} e_2^1 + \delta_1^1 \text{sign}(z_1^1 - \hat{z}_1^1) \right) < 0 \text{ and}$$

$$e_2^1 \left(-\frac{1}{C_A} e_1^1 - \frac{1}{C_A R_A} (e_1^2 u_2 + e_2^2 u_4) + \delta_1^2 \text{sign}(z_1^2 - \hat{z}_1^2) \right) < 0$$

By choosing, $\delta_1^1 > \|e_2^1\|_{\max}$ and $\delta_1^2 > \|e_2^2\|_{\max}$, there exists a finite time $\tau_1 \geq 0$ such that $\forall t \geq \tau_1$ we have $\hat{z}_1^1 = z_1^1$, $\hat{z}_1^2 = z_1^2$ and $E_1^1 = E_1^2 = 1$. Then $\dot{e}_1^1 = \dot{e}_1^2 = 0$. Therefore

$$\begin{aligned} \dot{z}_2^1 &= \dot{z}_2^1 + \delta_1^1 \text{sign}(z_1^1 - \hat{z}_1^1) \text{ and} \\ \dot{z}_2^2 &= \dot{z}_2^2 + \frac{C_A R_A}{u_4} E_1^2 \delta_1^2 \text{sign}(z_1^2 - \hat{z}_1^2) \end{aligned}$$

So we can see that when $u_4 = 0$, \dot{z}_2^2 tends to infinity, meaning that observability singularity occurs. Thus, to avoid the explosion of \dot{z}_2^2 we introduce a E_{SA} as follows: If $u_4 = 0$ then $E_{SA} = 0$ otherwise $E_{SA} = 1$. Then \dot{z}_2^2 becomes:

$$\dot{z}_2^2 = \dot{z}_2^2 + \frac{C_A R_A E_{SA}}{u_4 + E_{SA} - 1} E_1^2 \delta_1^2 \text{sign}(z_1^2 - \hat{z}_1^2)$$

and consequently, by choosing, $\delta_1^1 > \|e_2^1\|_{\max}$ and $\delta_1^2 > \|e_2^2\|_{\max}$, there exists a finite time $\tau_1 \geq 0$ such that $\forall t \geq \tau_1$ we have $\dot{e}_1^1 = \dot{e}_1^2 = 0$ and $\dot{z}_2^1 = \dot{z}_2^1$ and $\dot{z}_2^2 = \dot{z}_2^2$.

• **Second Step:** The aim of this step is to reach $e_1^1 = e_2^1 = 0$. So $\forall t \geq \tau_1$, we have $\dot{z}_2^1 = \dot{z}_2^1$ and $\dot{z}_2^2 = \dot{z}_2^2$. As $\hat{z}_1^1 = z_1^1$ and $\hat{z}_1^2 = z_1^2$ then $E_1^1 = 1$, $E_1^2 = 1$ then $e_1^1 = 0$ and $e_2^1 = 0$ for all $t \geq \tau_1$ then $e_2^1 = 0$ and $\dot{e}_2^1 = 0$ then consequently, invoking the equivalent vector, $\dot{z}_2^1 = \dot{z}_2^1$ and $\dot{z}_2^2 = \dot{z}_2^2$, we obtain:

$$\begin{aligned} \dot{e}_1^1 &= 0 \\ \dot{e}_2^1 &= e_3^1 + \delta_2^1 \text{sign}(\dot{z}_2^1 - \hat{z}_2^1) \\ \dot{e}_3^1 &= -(\beta + k_1 u_1) e_3^1 \\ \dot{e}_1^2 &= 0 \\ \dot{e}_2^2 &= -\frac{L_S R_S C_S}{R_M} e_3^2 u_1 + \delta_2^2 \text{sign}(\dot{z}_2^2 - \hat{z}_2^2) \end{aligned}$$

To do this, let's pose the Lyapunov function: $V_2^1 = \frac{(e_1^1)^2}{2} + \frac{(e_2^1)^2}{2}$ and $V_2^2 = \frac{(e_1^2)^2}{2} + \frac{(e_2^2)^2}{2}$. The sliding surface $S_2 = \{e_1^1 = e_2^1 = e_1^2 = e_2^2 = 0\}$ is attractive if and only if

$$\dot{V}_2^1 = e_2^1 \dot{e}_2^1 = e_2^1 (e_3^1 + \delta_2^1 \text{sign}(\dot{z}_2^1 - \hat{z}_2^1)) < 0$$

and

$$\dot{V}_2^2 = e_2^2 \dot{e}_2^2 = e_2^2 \left(-\frac{L_S R_S C_S}{R_M} e_3^2 u_1 + \delta_2^2 \text{sign}(\dot{z}_2^2 - \hat{z}_2^2) \right) < 0$$

By choosing, $\delta_2^1 > \|e_3^1\|_{\max}$ and $\delta_2^2 > \left\| \frac{L_S R_S C_S}{R_M} e_3^2 u_1 \right\|_{\max}$, there exists a finite time $\tau_2 \geq \tau_1 \geq 0$ such that $\forall t \geq \tau_2$, we have $\dot{z}_2^1 = \dot{z}_2^1$, $\dot{z}_2^2 = \dot{z}_2^2$ and $E_1^1 = E_1^2 = E_2^1 = E_2^2 = 1$. Then $\dot{e}_2^1 = \dot{e}_2^2 = 0$. Therefore

$$\begin{aligned} \dot{z}_3^1 &= \dot{z}_3^1 + \delta_2^1 \text{sign}(\dot{z}_2^1 - \hat{z}_2^1) \text{ or} \\ \dot{z}_3^1 &= \dot{z}_3^1 - \frac{1}{\frac{L_S R_S C_S}{R_M} u_1} \delta_2^2 \text{sign}(\dot{z}_2^2 - \hat{z}_2^2) \end{aligned}$$

Due to the finite time convergence of the sliding mode, there exists $\tau_2 > \tau_1 > 0$ such that $\forall t \geq \tau_2$, $\hat{z}_2^1 = \tilde{z}_2^1 = z_2^1$ and $\hat{z}_2^2 = \tilde{z}_2^2 = z_2^2$ then we pass to the:

- **Third Step:** The aim of this step is to reach $e_1^1 = e_2^1 = e_1^2 = e_2^2 = 0$. So $\forall t \geq \tau_2$, we have $\tilde{z}_3^1 = z_3^1$.

As $\hat{z}_1^1 = z_1^1$, $\hat{z}_2^1 = z_2^1$, $\hat{z}_1^2 = z_1^2$ and $\hat{z}_2^2 = z_2^2$ then $E_1^1 = E_1^2 = E_2^1 = 1$, then consequently, invoking the equivalent vector, $\tilde{z} = z$, we obtain:

$$\begin{aligned}\dot{e}_1^1 &= 0 \\ \dot{e}_2^1 &= 0 \\ \dot{e}_3^1 &= \delta_3^1 \text{sign}(z_3^1 - \hat{z}_3^1) \\ \dot{e}_1^2 &= 0 \\ \dot{e}_2^2 &= 0\end{aligned}$$

Let $S_3 = \{e_1^1 = e_2^1 = e_3^1 = e_1^2 = e_2^2 = 0\}$ be the sliding surface and the Lyapunov function $V_3^1 = \frac{(e_1^1)^2}{2} + \frac{(e_2^1)^2}{2} + \frac{(e_3^1)^2}{2}$. The sliding surface is attractive if and only if

$$\dot{V}_3^1 = e_3^1 \dot{e}_3^1 = e_3^1 (\delta_3^1 \text{sign}(z_3^1 - \hat{z}_3^1)) < 0$$

Then e_3^1 converges to 0 in a finite time $\tau_3 > \tau_2$ for any value of $\delta_3^1 > 0$ and if all conditions δ_1^1 , δ_2^1 , δ_1^2 and δ_2^2 are satisfied after τ_2 .

3.6 Conclusion

This chapter has provided a comprehensive overview of the cardiovascular system (CVS), detailing its dynamic behavior and the underlying principles governing its function. We have described the heart's role as a pump that generates the necessary pressure for blood circulation, both systemic and pulmonary.

We reviewed the state of the art in cardiovascular modeling, highlighting the use of electrical analogies to represent hydrodynamic indices of the CVS. This approach was justified and validated through comparisons with clinical and experimental data, confirming its effectiveness in capturing the complexities of cardiovascular dynamics.

Additionally, the chapter introduced the quadratic normal form of the cardiovascular system, demonstrating its potential to provide a refined representation of the system's behavior. This advanced form of analysis enables more accurate modeling and improves the ability to detect anomalies within the cardiovascular system. The adaptation of this model for anomaly detection was also discussed, showcasing its practical applications in monitoring cardiovascular health.

In summary, this chapter has advanced the understanding of cardiovascular dynamics by integrating theoretical insights with practical modeling techniques. The introduction of the quadratic normal form and its application to anomaly detection represents a significant step forward in cardiovascular system analysis, offering a robust framework for enhancing diagnostic and monitoring tools in the field.

Chapter 4

Diagnostic and detection anomaly of CVS

Contents

4.1	Introduction	88
4.2	Diagnostic and fault detection methodology	89
4.2.1	Classification of fault detection and diagnosis methods	90
4.3	Expansion of the cardiovascular model for detection of anomalies	92
4.3.1	Residual generator for cardiovascular anomalies detection	93
4.4	Simulation Results	95
4.4.1	Scenario 1: Mitral Regurgitation	98
4.4.2	Scenario 2: Aortic Regurgitation	102
4.4.3	Scenario 3: Simultaneous mitral and aortic regurgitation	105
4.5	Conclusions	107

4.1 Introduction

This chapter explores the design of sliding mode observers for multi-Input multi-Output (MIMO) nonlinear systems are, with a focus on addressing the challenges of observability in both linearly observable and linearly unobservable cases.

Building on prior research by [10], [12], and [15], which utilizes quadratic approximation and a specialized normal form involving a quadratic input-output injection, this work leverages these methods to reveal the inherent observability properties of nonlinear systems. The quadratic normal form is particularly advantageous, as it reduces the complexity of analyzing nonlinear systems while preserving the structural properties essential for observability studies. This form serves as a middle ground between exact linearization techniques and the complexities of strongly nonlinear systems.

Recent studies such as [12] and [52] introduce the concept of an observability singularity manifold in the vicinity of certain critical points, where the system experiences a loss of observability. In such cases, it is possible to recover some observability properties by employing universal inputs and resonant terms. To address these issues and fully utilize the structural properties of the system, we propose the use of sliding mode observers. As suggested by [101], [80], and [22], these observers, with their variable structure, provide

a robust approach to overcoming the challenges of observability singularities. The sliding mode approach thus offers a promising solution for the design of observers that maintain observability even in the presence of singularities, ensuring reliable performance for a broader class of nonlinear systems.

4.2 Diagnostic and fault detection methodology

For many centuries, detecting faults or malfunctions relied solely on human senses, a method still widely used today. This involved observing changes in appearance, listening for unusual sounds, feeling for vibrations or heat, and detecting odors from leaks or overheating. Eventually, measuring instruments were developed to provide more precise data on key physical parameters. However, these sensors also became susceptible to failure, leading to the issue of false alarms. This problem grew even more critical when sensors were integrated into automated control systems, where malfunctions could have immediate and severe consequences, and human intervention was often removed from the process.

In this context, fault detection and diagnosis (FDD) techniques are essential for ensuring the safety, reliability, and performance of complex systems. Specifically, in cardiovascular system, FDD plays a critical role in maintaining patient safety and ensuring the proper functioning of medical devices. This section will begin with an introduction to the field of fault detection and diagnosis, followed by an example related to cardiovascular system. The first example will focus on the detection and isolation of valve faults within the cardiovascular system. The second example will address fault detection challenges within a cardiovascular system model.

In general, faults can be described as deviations from the expected behavior of the system or its instrumentation. The faults of interest typically fall into the following categories:

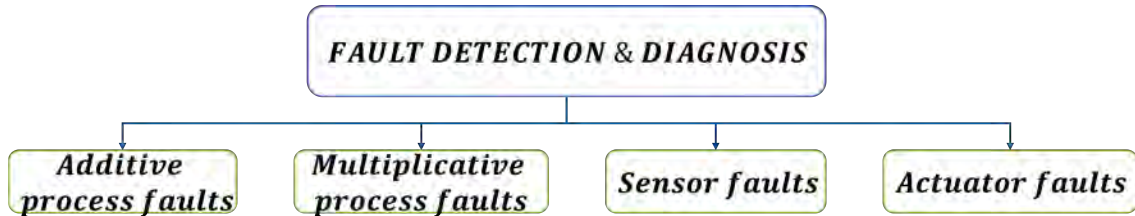


Figure 4.1: Stages of model-based fault detection and diagnosis

Table 4.1: Types of faults in systems.

Faults	Description	Examples	Effect
Additive process faults.	These are unknown inputs acting on the system, typically absent under normal conditions, when present, they affect the system outputs independent of the known inputs.	system leaks, external loads, and similar disturbances.	Changes in system outputs independent of known inputs.
Multiplicative process faults	These involve abrupt or gradual changes in some system parameters, which lead to output variations that depend on the magnitude of the known inputs.	Surface contamination, blockages, power loss.	Changes in system outputs that depend on the magnitude of known inputs.

Table 4.1: (continued)

Faults	Description	Examples	Effect
Sensor faults	These occur when there is a discrepancy between the measured and actual values of system variables. Generally, sensor faults are additive, as they are independent of the magnitude being measured. However, some sensor malfunctions, like sticking or total failure, may be better represented as multiplicative faults.	Measurement errors, sensors sticking or total failure.	Typically additive, but some may be better characterized as multiplicative.
Actuator Faults	These arise when there is a mismatch between the input command given to an actuator and its actual output. Actuator faults are commonly treated as additive, but certain types (e.g., sticking or total failure) might be more accurately modeled as multiplicative faults.	Actuators sticking or complete failure.	Usually additive, but can be multiplicative in certain cases.

On the other hand, fault detection and diagnosis (FDD) systems perform the following key tasks:

1. **Fault detection:** Identify whether a fault has occurred within the system by continuously monitoring sensor data, control signals, and outputs. This task aims to recognize deviations from normal system behavior.
2. **Fault isolation:** Pinpoint the specific location or component in the system where the fault has occurred. This requires distinguishing between different potential faults that may produce similar symptoms.
3. **Fault identification:** Determine the nature and severity of the fault. This includes categorizing the fault type (e.g., additive, multiplicative, sensor, actuator) and assessing its impact on system performance.

In practice, many fault detection and diagnosis systems are structured to focus primarily on the detection and isolation tasks, often referred to as FDI systems. This approach aligns with real-world operational needs, where quick fault detection and isolation are paramount for maintaining system reliability and safety. The FDI systems typically feature robust mechanisms for detecting faults and isolating them effectively, enabling rapid response to issues without the added complexity of full fault identification.

4.2.1 Classification of fault detection and diagnosis methods

Fault detection and diagnosis (FDD) methods can be broadly classified into two major categories based on their reliance on mathematical models of the system:

Model-Free Techniques

Model-free techniques do not depend on a mathematical representation of the system's dynamics. Instead, they utilize data-driven approaches to identify faults. Common model-free techniques include:

- **Statistical Methods:** These involve analyzing historical data to identify patterns indicative of faults. Techniques such as control charts, regression analysis, and hypothesis testing are often employed.

- **Machine Learning Approaches:** Algorithms like support vector machines, decision trees, and neural networks are trained on input-output data to detect anomalies and predict faults without explicit system models.
- **Signal Processing Techniques:** Methods such as time-frequency analysis and wavelet transforms analyze signals for deviations from expected behavior, helping to identify potential faults.
- **Rule-Based Systems:** These systems apply predefined rules to the data, allowing for fault detection based on known symptoms or patterns.

Model-Based Methods

Model-based fault detection and diagnosis method approaches leverage a specific mathematical model of the monitored system. Most model-based fault detection and diagnosis methods are grounded in the principle of analytical redundancy. Unlike physical redundancy, where measurements from parallel sensors are compared, this approach involves comparing sensory measurements with analytically computed values of the corresponding variable. This concept can also be expanded to the comparison of two analytically generated quantities derived from different sets of variables. In both cases, the resulting differences, referred to as residuals, indicate the presence of faults within the system.

The generation of residuals, they must be evaluated to make detection and isolation decisions as shown in figure 4.2. Due to the influence of noise and model inaccuracies, the residuals are never zero, even in the absence of faults. Consequently, making a detection decision involves assessing the residuals against established thresholds, which can be determined empirically or through theoretical analysis.

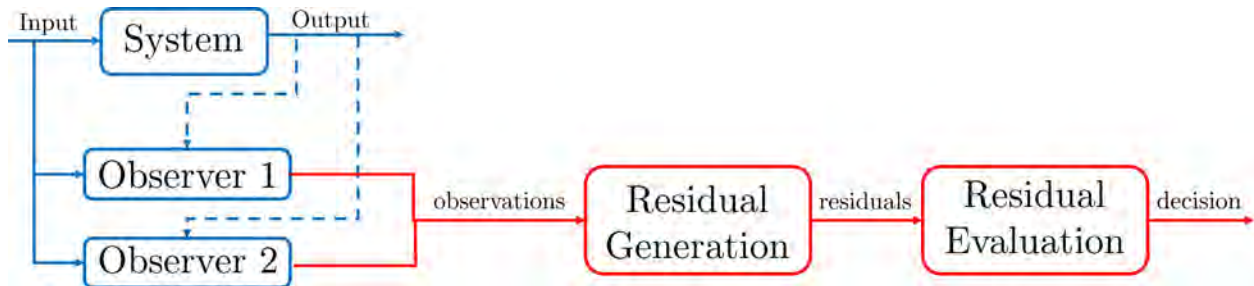


Figure 4.2: Stages of model-based fault detection and diagnosis

Residual generation is a critical step in model-based fault detection and isolation (FDI) systems. It involves creating a signal (residual) that indicates the presence of faults by comparing the expected behavior of the system (as predicted by the model) to the actual behavior. Here are four overlapping approaches to residual generation:

Kalman Filtering: They provide a way to estimate system states and can also be employed for fault detection by analyzing the residuals generated from the filter. The residual signal, defined as the difference between the actual output and the estimated output, will have a mean of zero if there is no fault (and disturbance) and becomes nonzero in the presence of faults.

Diagnostic observers: Observer-based methods involve the design of observers (like Luenberger observers or sliding mode observers) to estimate system states. The residuals are generated by comparing the observer's output with the actual output of the system. An observer is designed to estimate the states based

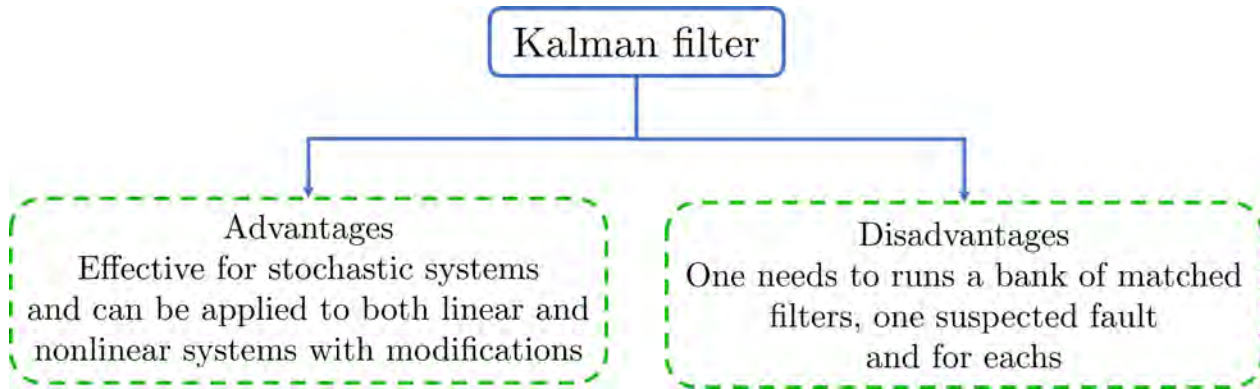


Figure 4.3: Kalman Filtering

on input and output measurements. The residual is computed as:

$$r = y - \hat{y}$$

Observers are constructed to estimate system states. The comparison between estimated and actual states provides insights into potential faults.

Parameter estimation: Parameter estimation serves as an effective method for detecting and isolating parametric (multiplicative) faults. The process begins by creating a reference model of the system during normal operation, free of faults. Parameters are then continuously re-estimated in real time. Any deviations from this reference model are utilized for fault detection and isolation. Although parameter estimation can offer greater reliability compared to analytical redundancy approaches, it demands more computational resources and specific input excitation conditions for effective implementation.

Parity relations: The parity space method involves transforming the system equations into a form that highlights discrepancies (residuals) between expected and actual outputs. This is achieved by using mathematical manipulations of the system's equations. The system is described in terms of state-space or output equations. A parity relation is derived, relating inputs and outputs under fault-free conditions. Residuals are then generated by examining deviations from this relation. This method can be advantageous for systems with a high level of redundancy, as it can detect multiple faults simultaneously.

In this work we are based on a method based on diagnostic observers under the methodology presented in the following sections.

4.3 Expansion of the cardiovascular model for detection of anomalies

In this section, we will present the adaptation of the model (3.52) by including the following fault vector F , which describes the variations affecting the mitral valve f_m and the aortic valve f_{ao} . In the context of the cardiovascular system, variations affecting the mitral valve D_m and the aortic valve D_a are significant contributors to valvular heart diseases, which are a leading cause of cardiovascular morbidity and mortality.

We conceptualize the fault in the mitral valve (f_m) as the nominal value modeled as a percentile addition or subtraction to the input value (1 or 0) defined in Equation (3.53). Similarly, the fault in the aortic valve (f_{ao}) is considered. As shown in Figure 4.4, the fault vector is added into the input signal of the system.

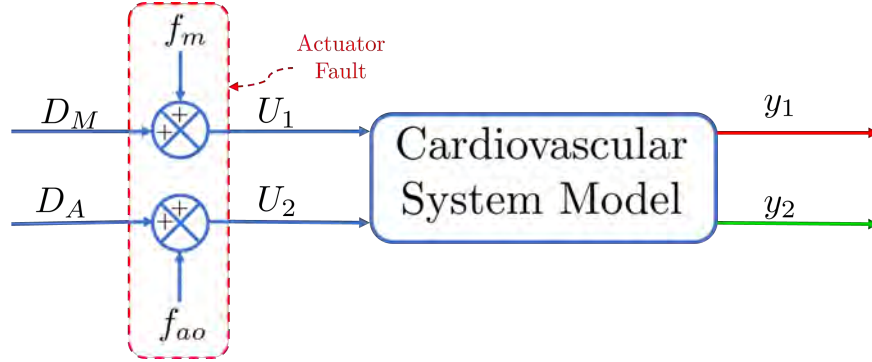


Figure 4.4: Cardiovascular system with fault in the mitral valve.

We consider faults in the inputs D_M and D_A for detecting anomalies in the mitral and aortic valves. As described before, the valves are an input vector that can only have 0 or 1, representing the ideal opening and closing of the mitral and aortic valves. However, there are cases when a valve either does not close completely or does not open fully. This medical terms to refer to these situations are valve regurgitation (fault closing) and valve stenosis (fault opening). Now, we propose to adapt the model (3.52) by including the following fault vector F , which describes variations acting on the mitral valve f_m and the aortic valve f_{ao} .

$$F(t) = \begin{bmatrix} f_m \\ f_{ao} \end{bmatrix}, \text{ such as: } \begin{cases} U_1 = D_M + f_m \\ U_2 = D_A + f_{ao} \end{cases} \quad (4.1)$$

where D_M and D_A are the nominal values of the real state of the mitral and aortic valves, respectively, f_m and f_{ao} are the faults corresponding to the mitral and aortic valves, respectively. The fault model of the CVS have the following form:

$$\begin{cases} \dot{x}_1 = \frac{-\dot{C}(t)}{C(t)}x_1 - \frac{1}{C(t)R_M}(x_1 - x_2)U_1 - \frac{1}{C(t)R_A}(x_1 - x_4)U_2 \\ \dot{x}_2 = \frac{1}{R_S C_R}(x_3 - x_2) + \frac{1}{C_R R_M}(x_1 - x_2)U_1 \\ \dot{x}_3 = \frac{1}{R_S C_S}(x_2 - x_3) + \frac{1}{C_S}x_5 \\ \dot{x}_4 = -\frac{1}{C_A}x_5 + \frac{1}{C_A R_A}(x_1 - x_4)U_2 \\ \dot{x}_5 = -\frac{1}{L_S}x_3 + \frac{1}{L_S}x_4 - \frac{R_C}{L_S}x_5 \end{cases} \quad (4.2)$$

Remark 4.3.1 In observer design, U_1 and U_2 are considered as bounded unknown inputs [24, 5].

4.3.1 Residual generator for cardiovascular anomalies detection

The most common valve pathologies are related to the aortic and mitral valves. In both cases, these involve a defect in the closure of the valve, known as valve regurgitation. Aortic valve regurgitation refers to a defect in the valve closure that leads to backward leakage into the left ventricle during diastole. Patients with aortic regurgitation exhibit PV loops with increased amplitude and displacement to the right, indicating that the stroke work is higher, and the pressure–volume area is also increased compared to a healthy case. Similarly, mitral valve pathologies involve leakage during systole from the LV to the left atria (LA).

Based on this information, this section presents the design of the fault detection and isolation (FDI) system, this design is based on the assumption that only one fault can occur at any given time. Therefore, two simulation scenarios were considered for fault detection based on the analysis of the generated waveforms

pressure.

As shown in Figure 4.5, the first scenario is mitral regurgitation (f_m), and in scenario 2, the fault is aortic regurgitation (f_{ao}). To meet this requirement effectively, the sliding mode observers presented in [88] are used, which enable precise estimation of sensor measurements.

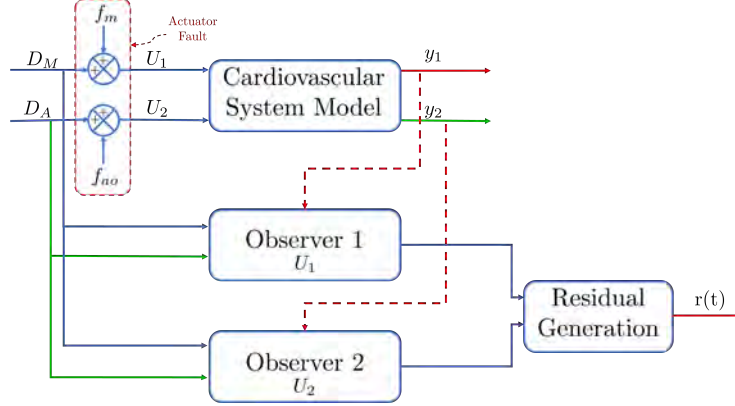


Figure 4.5: Bank of observers for all actuator faults estimation.

In Figure 4.5, the $y(t)$ denotes the output vector of CVS, where $y_1 = x_5$ and $y_2 = x_4$. These outputs serve as inputs to the observer, as they are the signals required for the observer to initiate the estimation process. In this thesis, the residuals are defined as the difference between the output variables represents that the most basic residual $r(t)$ can be expressed as:

$$r = y(t) - \hat{y}(t) = (\text{sing}(\bar{y}))_{eq} \quad (4.3)$$

Define $e = x - \hat{x}$ as the state estimation error, where

$$\begin{aligned} \hat{x}_1 &= \frac{1}{C(t)} \hat{z}_2^2 \\ \hat{x}_2 &= -L_S \hat{z}_2^1 - L_S R_S C_S \hat{z}_3^1 \\ \hat{x}_3 &= -L_S \hat{z}_2^1 \\ \hat{x}_4 &= \hat{z}_1^2 \\ \hat{x}_5 &= \hat{z}_1^1 \end{aligned} .$$

The bank of two observers and the residual generator proposed is associated with the SMO designed previously in ([88]).

In this work, the residual generation is achieved by the means of two single step-by-step sliding mode observer, where the faults have been estimated by the observers. When there is no fault, i.e., $f_m = 0$ and $f_{ao} = 0$, the error will asymptotically converge to the true state. We also observed that the residuals in the presence of an anomaly in the mitral valve (U_2) are almost the same as the residuals in the aortic valve (U_1). However, the changes in the pressure and flow signals of the system are different. This is why, due to the robustness of the observer, we could implement failure isolation and determine when a failure occurs in the mitral and aortic valves.

Below, Table 4.2 presents a comprehensive signature for residual generation. This table is instrumental in understanding the nuanced differences in residual patterns, which are key to our failure isolation strategy.

Each signature has been meticulously derived to ensure the precise detection and localization of anomalies within the mitral and aortic valves, highlighting the sophisticated nature of our observer's diagnostic capabilities.

Table 4.2: Signature for the residual generation.

Residuals/Faults	Anomalie on U_1	Anomalie on U_2
$r_1(t)$	0	0
$r_2(t)$	0	0
$r_3(t)$	1	1
$r_4(t)$	0	0
$r_5(t)$	1	1

4.4 Simulation Results

For the initial condition, we refer to those specified in [8], defined as follows:

$$x = [7.4, 5, 85, 82, 0]^T \text{ and } \hat{z} = [5, -11 \times 10^4, 5.7143 \times 10^4, 0, 150]^T.$$

Figure 4.6 illustrate the effectiveness of the choice of E_{SA} and E_{SM} for the good estimation z_1^1 , z_2^1 , z_3^1 , z_1^2 and z_2^2 . We can see that from the transformation presented in 3.55 we can obtain the estimated states \hat{x}_2 and \hat{x}_3 from the measurable outputs. In Figure 4.6, we assume that $E_{SA} = 0$ if $u_4 = 0$ and $E_{SM} = 0$ if $u_3 = 0$.

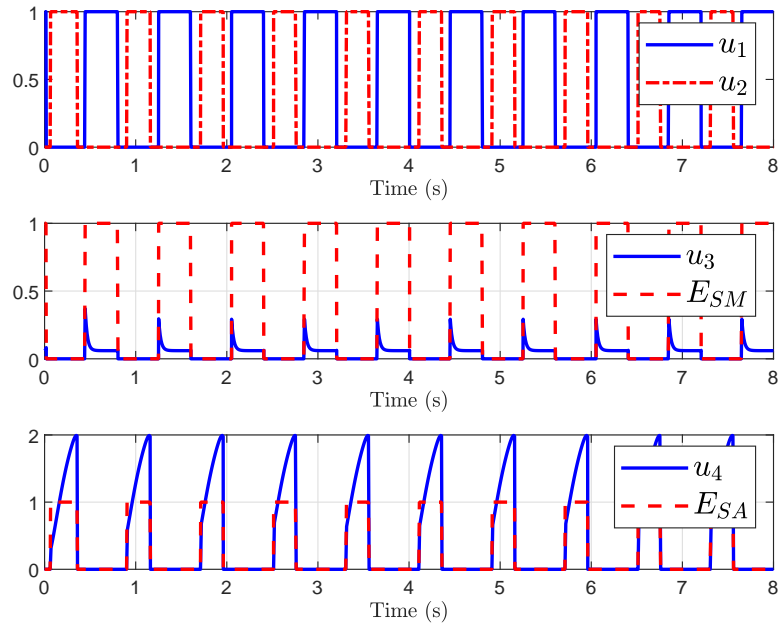
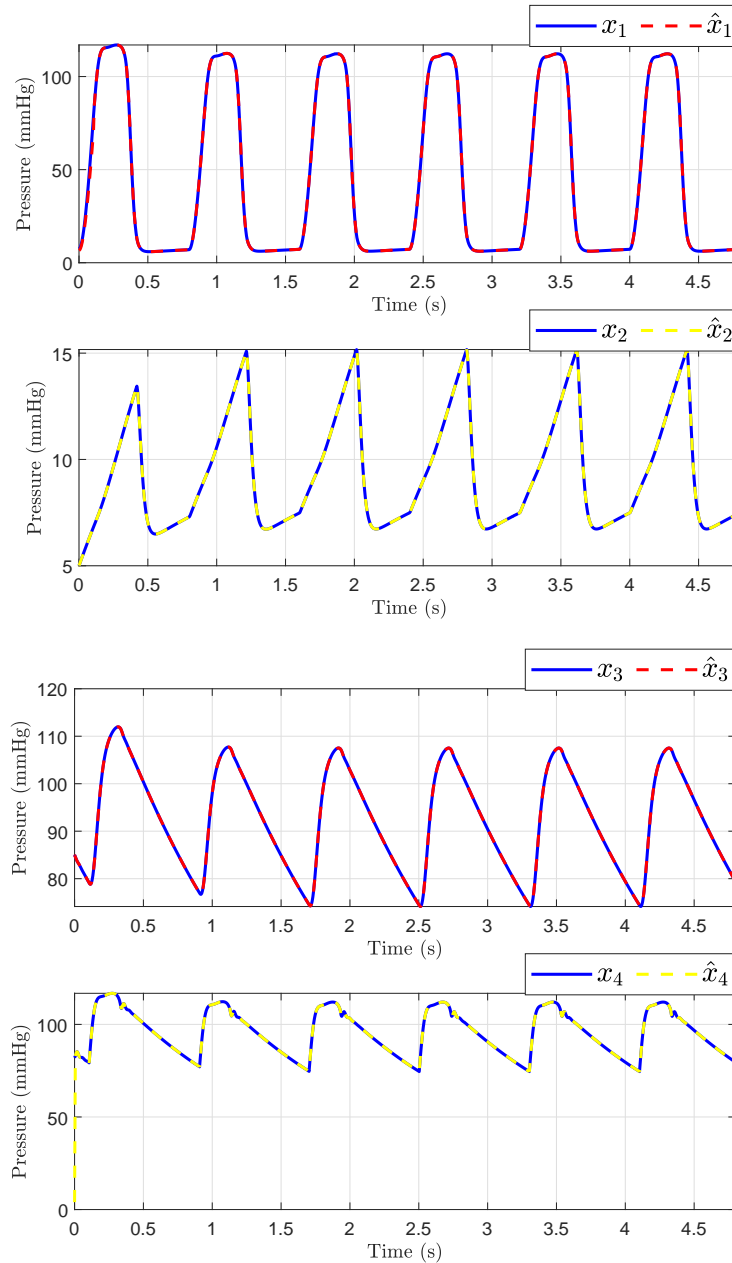
Figure 4.6: States of u_3 , E_{SM} , u_4 and E_{SA}

Figure 4.7 shows the hemodynamic waveforms for a healthy individual with a heart rate (HR) of 75 bpm. The waveforms are consistent, as will be explained. The systolic pressure (LAP) and diastolic pressure (LVP) were measured at 117 mmHg and 77 mmHg, respectively. The ascending aorta pressure (AoP), resulting from the opening and closing of the aortic valve and the pressure wave propagation along the aorta, presented a delayed waveform. From the transformation presented in Equation (3.1), we can derive the estimated states \hat{x}_1 , \hat{x}_2 , and \hat{x}_3 from the measurable outputs \hat{x}_4 and \hat{x}_5 . Figure 4.7 presents the states of systems (3.52) and the observer (3.60). It demonstrates how the state estimation converges completely for all states within a time frame of 0.2 s.



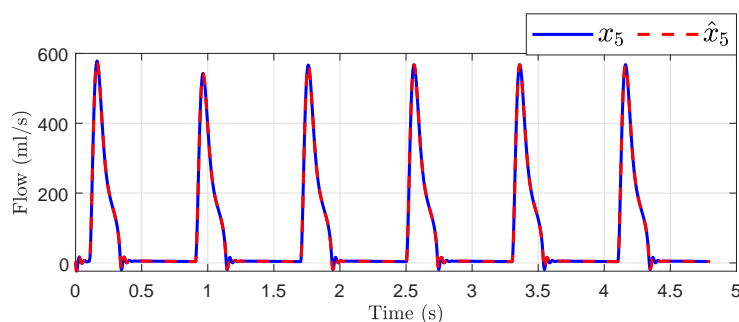


Figure 4.7: Hemodynamic waveforms of the original states $x_i(t)$ and observer states $\hat{x}_i(t)$ for a normal heart

Then, the left ventricle volume and preload volume (LVV) in Figure 4.8 represent the result of changing afterload conditions. Even with variations in preload and afterload, the relationship between end-systolic pressure and left ventricular volume should be roughly linear if the model functions as predicted. This relationship is known as the end-systolic pressure–volume relationship. By employing an especially built sliding mode observer to estimate the system’s state x_1 , we were able to determine the left ventricle’s volume and preload volume using expression (3.1). This is because the state x_1 is described by recalling Frank–Starling’s law, allowing us to gain more insight into the hemodynamic behavior of the heart in a healthy individual. The conditions were simulated with $E_{\max} = 2$ mmHg/mL, $E_{\min} = 0.05$ mmHg/mL, and $V_0 = 10$ mL.

Remark 4.4.1 *These data are compared and confirmed with the results described in [93, 99, 17], where the aortic pressure and flow waveforms are all consistent with hemodynamics data on healthy individuals.*

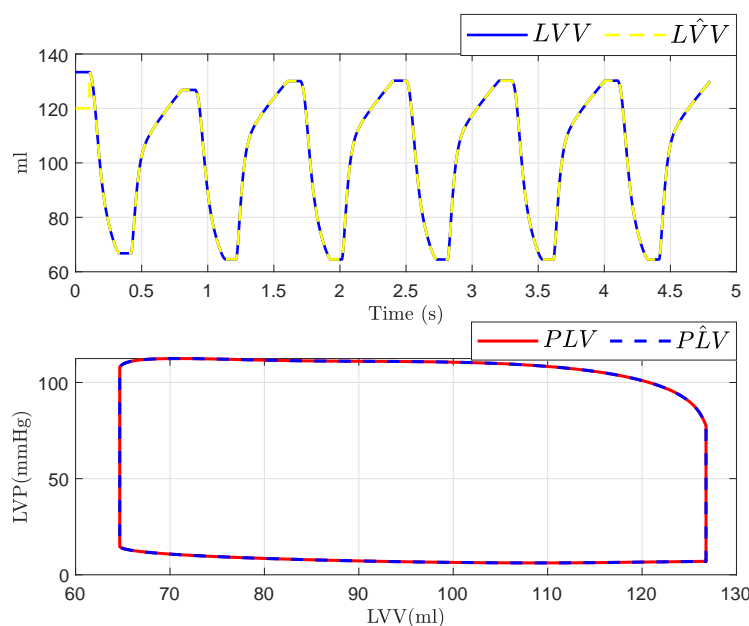


Figure 4.8: Hemodynamic of the left ventricular volume (LVV) and preload volume (PLV) in original and SMO of CVS.

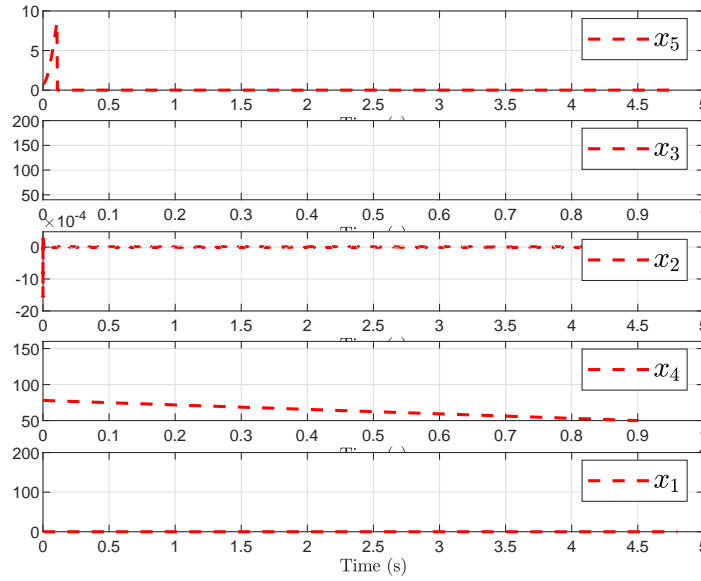


Figure 4.9: Error between the original states $x_i(t)$ and observer states $\hat{x}_i(t)$ error

In the following sections, three different fault scenarios are presented: Scenario 1 involves mitral regurgitation, while Scenario 2 involves aortic regurgitation and Simultaneous mitral and aortic regurgitation.

4.4.1 Scenario 1: Mitral Regurgitation

In this scenario, we consider a 50% regurgitation in the mitral valve (i.e., $f_m = 0.5$ when $u_1 = 0$ and $f_{ao} = 0$). The simulation of the mitral valve fault was modeled by adding a binary value (1 or 0) to the input u_1 . This modification was introduced at time $t = 2.5$ s. corresponding to the fourth cardiac cycle.

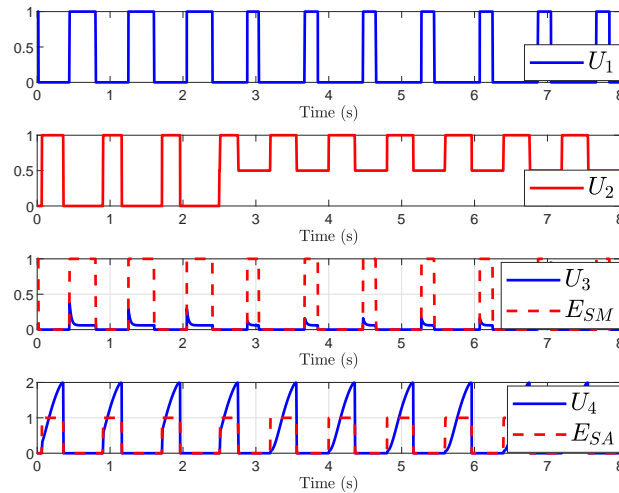


Figure 4.10: States of input with fault f_m

Figure 4.10 illustrates the outcomes following the fault occurrence in the mitral valve. It is observed that, post-fault, the dynamics of the aortic valve, u_3 and u_4 are altered due to their dependence on u_1 and u_2 . Figure 4.11 presents the simulated hemodynamic waveforms for an individual with heart failure. Here x_i is the original model and \hat{x}_i is the estimated signal provided by the observer (for $i = 1, 2$). We can verify that when the failure occurs, the SMO is not able to estimate the volume correctly due to the loss of x_1 , as illustrated in the figure showing the failure in the original model PLV_{f_m} and $P\hat{L}V_{f_m}$ (Figure 4.11). Also, the simulation indicates changes in the dynamic system upon fault occurrence, with a decrease in blood flow waveforms and alterations in pressure waveforms.

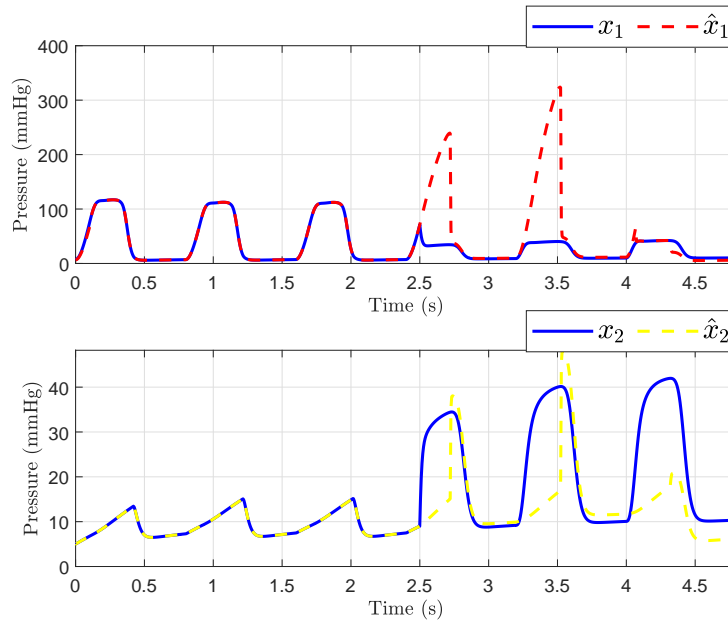
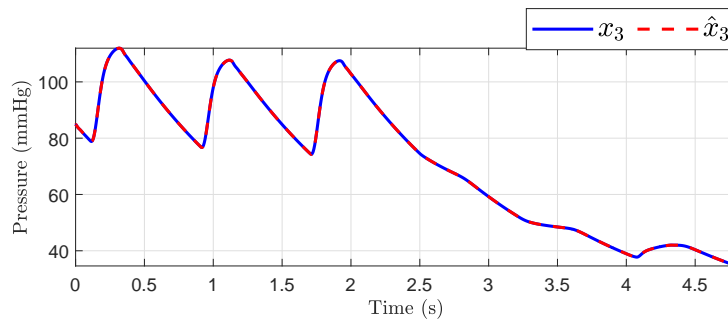


Figure 4.11: Original states $x_i(t)$ and observer states $\hat{x}_i(t)$ of CVS for an unhealthy heart ($i = 1, 2$)

On the other hand, as shown in Figure 4.12, we can show that the observer can reconstruct the unobservable state when the failure occurs, but only states x_3 , x_4 and x_5 are able to converge again to the true state. Here x_i is the original model and \hat{x}_i is the estimated signal provided by the observer (for $i = 3, 4, 5$). We show that the sliding mode observer can adapt to the change in the system dynamics.



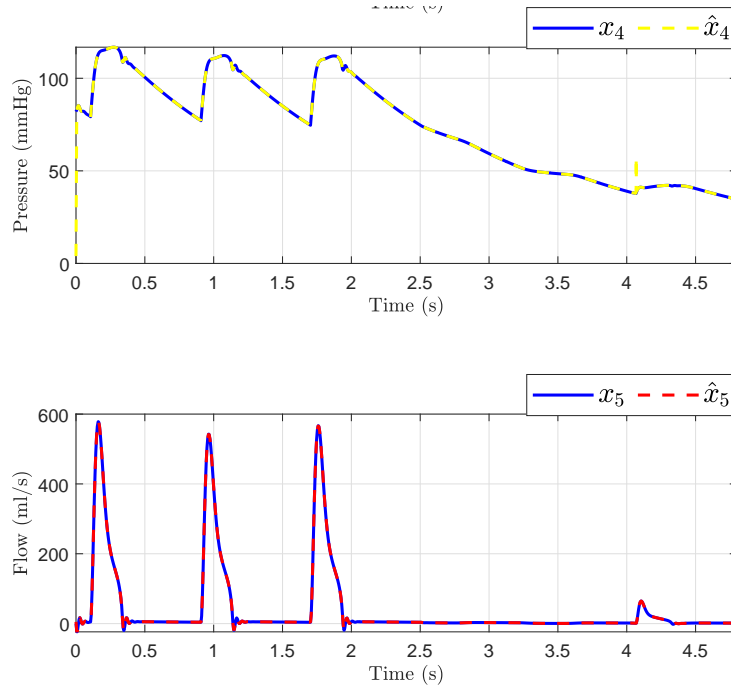


Figure 4.12: Hemodynamic waveforms of the original states $x_i(t)$ and observer states $\hat{x}_i(t)$ of CVS for an unhealthy heart ($i = 3, 4, 5$)

On the other hand, Figure 4.13 indicates that when mitral regurgitation is present, the SMO is unable to accurately estimate the volume due to the loss of x_1 , as shown in the comparison between the original model LVV and the observer-estimated model $L\hat{V}V$. However, we know that this information can be used to fault detection.

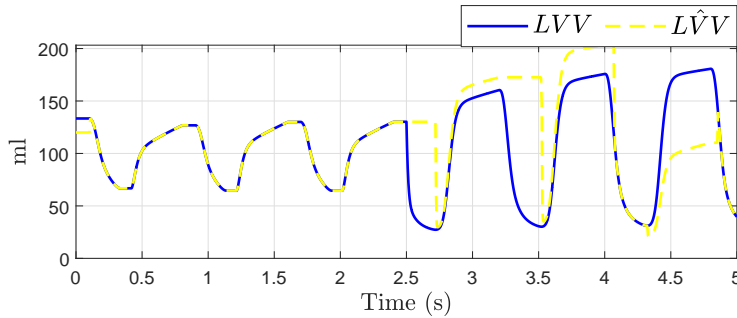


Figure 4.13: Left ventricular volume (LVV) in original and SMO of CVS

Similarly, we can also see that when a failure occurs, the dynamics of PLV_{f_m} and $\hat{P}LV_{f_m}$ are lost due to the loss of x_1 . This is seen in the comparison between the original model $PLV_{f_{ao}}$ and the model estimated by the observer $P\hat{L}V_{f_{ao}}$ as shown in Figure 4.14.

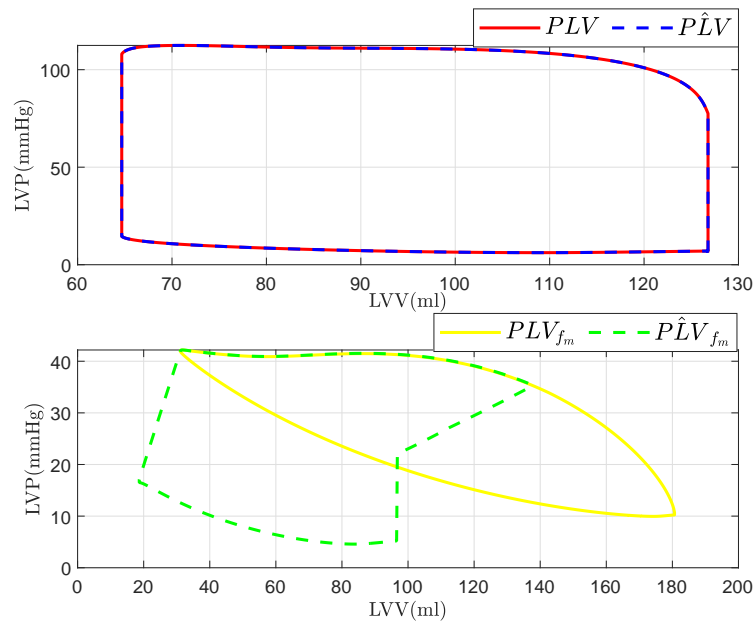
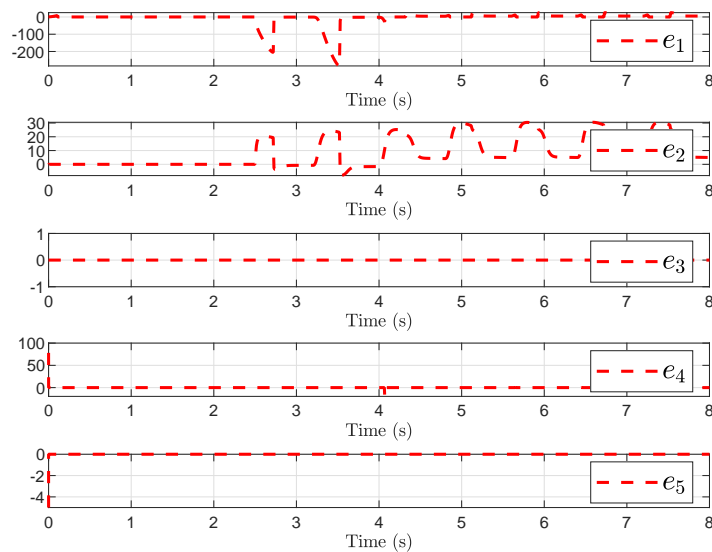


Figure 4.14: Preload volume (PLV) in original and SMO of CVS

Figure 4.15 shows the dynamic behavior of the error between the real system and the observer. As can be observed, states x_1 and x_2 present an error in the presence of the fault, contrary to the error in the remaining states converges to zero.

Figure 4.15: Estimation error of the original states $x_i(t)$ and observer states $\hat{x}_i(t)$ of CVS

4.4.2 Scenario 2: Aortic Regurgitation

In this scenario, we consider a 50% regurgitation in the aortic valve (i.e., $f_{ao} = 0.5$ when $u_2 = 0$ and $f_m = 0$). The simulation of fault in the aortic valve was modeled by adding a binary value (1 or 0) to the input u_2 . This change was introduced at the time $t = 2.5$ s.

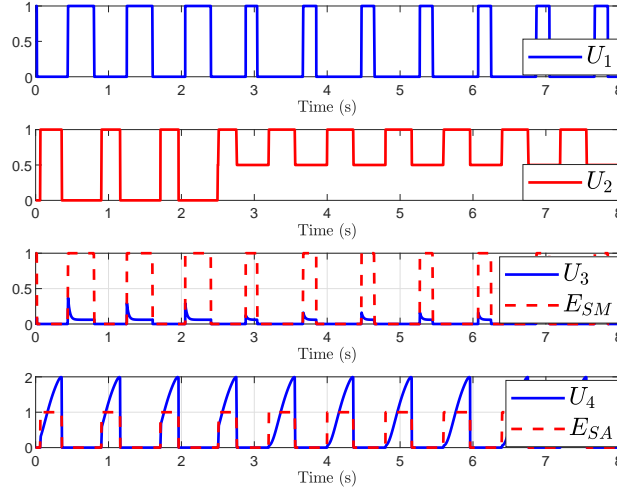


Figure 4.16: Input with fault f_{ao}

Figures 4.17 show the results after the fault occurs in the aortic valve. Figures 4.17 show simulation waveforms of hemodynamics for a patient with aortic regurgitation. Here x_i is the original model and \hat{x}_i is the estimated signal provided by the observer (for $i = 1, 2$).

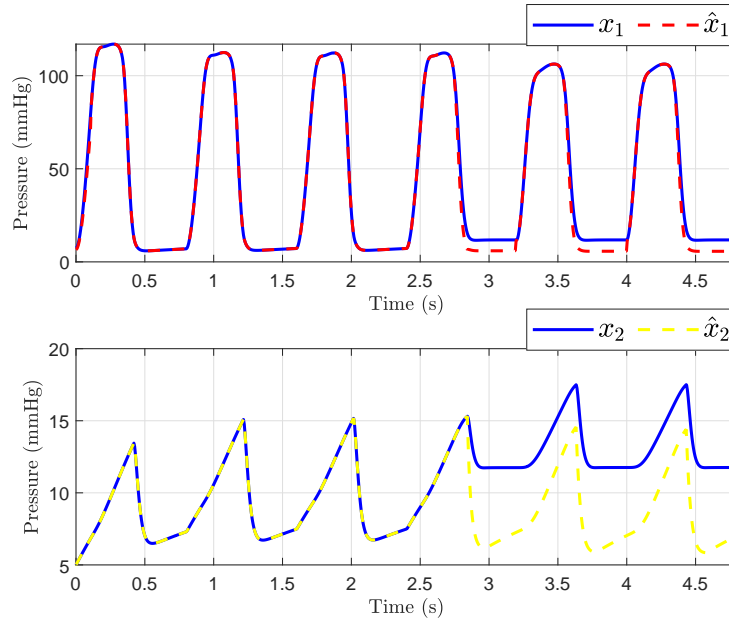


Figure 4.17: Original states $x_i(t)$ and observer states $\hat{x}_i(t)$ of CVS for an unhealthy heart ($i = 1, 2$)

SMO can adjust to changes in system dynamics. Additionally, when the failure occurs, the observer can rebuild the unobservable state; nevertheless, as shown in Figure 4.18, only the states x_3 , x_4 , and x_5 can converge to the original state. Here x_i is the original model and \hat{x}_i is the estimated signal provided by the observer (for $i = 3, 4, 5$). Additionally, we were able to determine the left ventricular volume using the response described by expression (3.1), assuming that the heart is healthy, as illustrated in Figure 4.19.

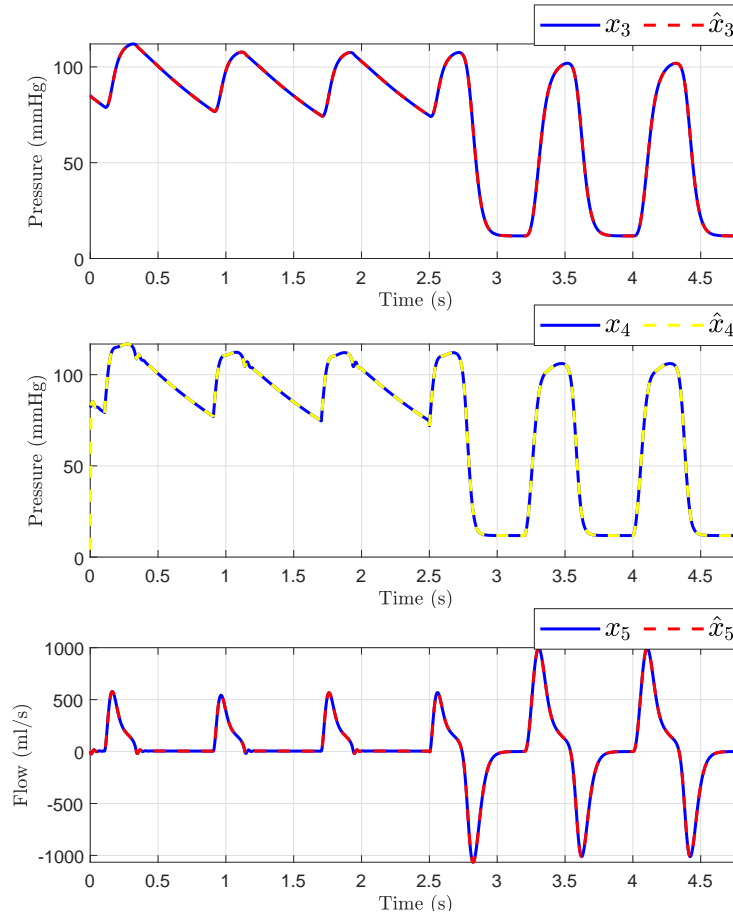


Figure 4.18: Original states $x_i(t)$ and observer states $\hat{x}_i(t)$ of CVS for an unhealthy heart ($i = 3, 4, 5$)

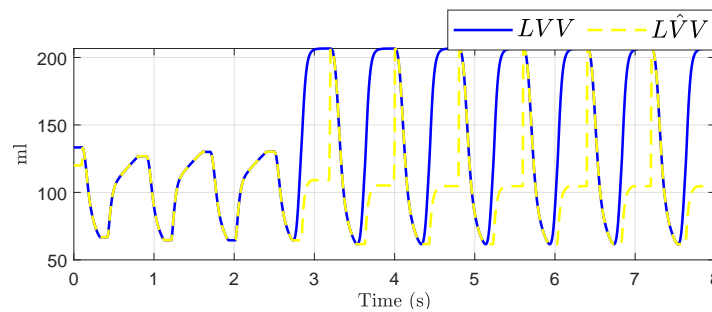


Figure 4.19: Hemodynamic for left ventricular volume (LVV) in original and SMO of CVS

Additionally, we were able to determine the preload volume using the response described by expression (3.1), assuming that the heart is healthy and that after some time the fault is presented, as illustrated in Figure 4.20.

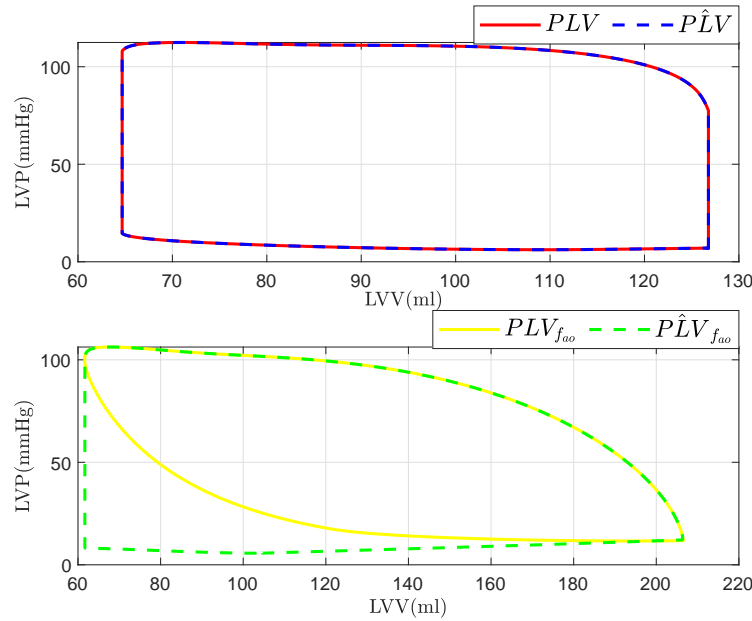


Figure 4.20: Simulated hemodynamic waveforms for preload volume (PLV) in original and SMO of CVS

Figure 4.21 shows the dynamic behavior of the error between the real system and the observer. As can be observed, states x_1 and x_2 present an error in the presence of the fault, contrary to the error in the remaining states converges to zero.

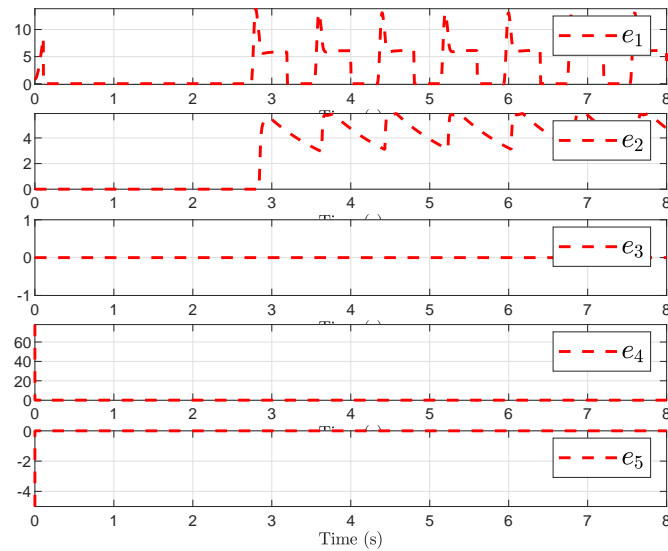


Figure 4.21: Estimation error of the original states $x_i(t)$ and observer states $\hat{x}_i(t)$ of CVS

In summary, the results align well with the hemodynamic parameters reported in the existing literature and experimental data, which support the validity of the proposed model and demonstrate its capability to produce results that are comparable to medical data. However, a larger-scale study with a greater number of tests would be necessary to obtain more precise results.

4.4.3 Scenario 3: Simultaneous mitral and aortic regurgitation

Simultaneous mitral and aortic regurgitation refers to the concurrent leakage of blood backward through both the mitral valve and the aortic valve. This dual valve dysfunction can lead to significant hemodynamic consequences, as it affects both the inflow and outflow of blood in the heart, often resulting in heart failure if untreated.

The complexity of managing valvular heart disease increases significantly when both the aortic and mitral valves are involved, as their simultaneous dysfunction impacts both the inflow and outflow of blood within the heart. As we have already seen, each valve plays a distinct role in maintaining proper blood circulation: the mitral valve regulates blood flow between the left atrium and left ventricle, while the aortic valve controls blood leaving the left ventricle into the systemic circulation. When both valves are affected, their combined dysfunction can lead to significant hemodynamic instability.

In this section, we consider the case of a patient with simultaneous aortic and mitral regurgitation. For this purpose, we consider the following conditions, 50% on both valves (i.e. $f_{ao} = 0.5$ and $f_m = 0.5$). The simulation of the valve faults was modeled by adding a binary value (1 or 0) to the input u_1 and u_2 . This change was introduced at time $t = 2.5$ s.

In the figure 4.22, we can see that after the fault occurs in the aortic valve and mitral valve, there is a change in the mitral and aortic valves (D_M and D_A). It is evident that, after the fault occurs in the valves, u_3 and u_4 exhibit altered dynamics due to their dependence on u_1 and u_2 .

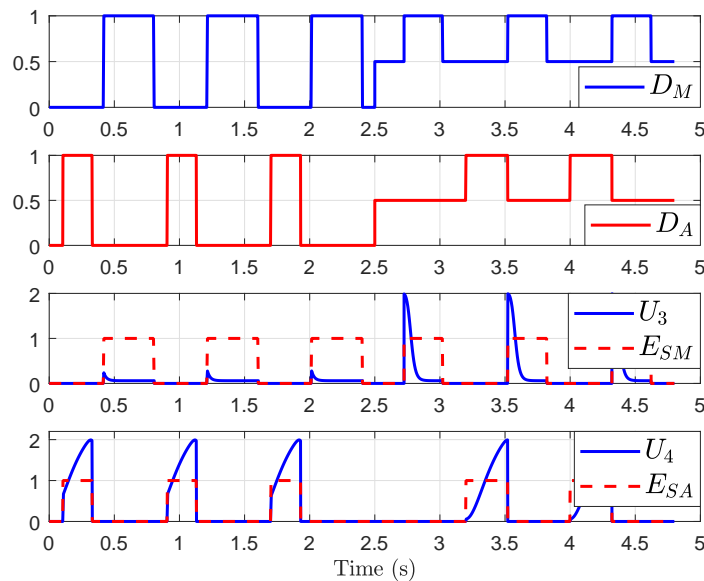


Figure 4.22: States of input with fault in f_m and f_{ao}

Figure 4.23 represents the results after the fault occurs in the valves, this figure presents the simulation waveforms of the hemodynamics for an individual with simultaneous of aortic and mitral regurgitation. When simultaneous mitral and aortic regurgitation occurs we observe changes in the system dynamics when the fault occurs, including variations in blood flow waveforms (decrease in blood flow) and an increase in pressure waveforms. In this case, x_1 and x_2 presents an increase in pressure, while x_3 and x_4 presents a decrease in the pressure. As shown in Figure 4.23, this phenomenon occurs due to concurrent backward leakage of blood through the mitral valve and aortic valve. Here x_i is the original model and \hat{x}_i is the estimated signal provided by the observer (for $i = 1, 2, 3, 4$).

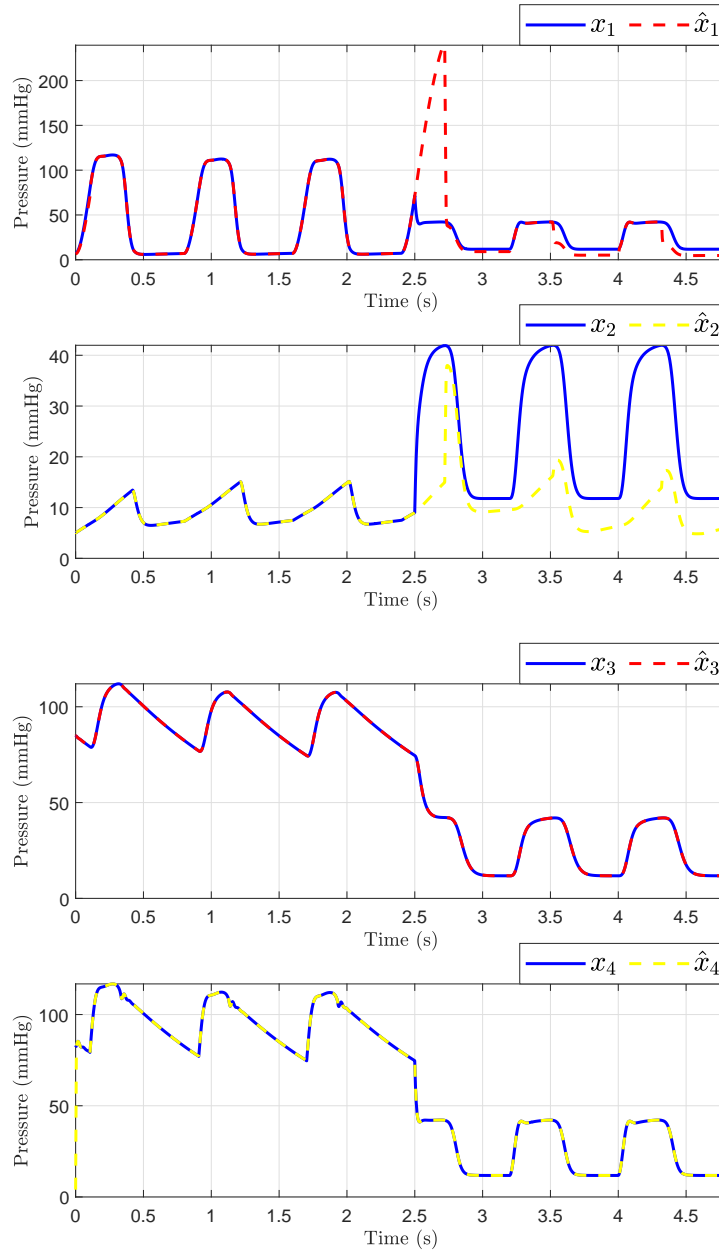


Figure 4.23: Original states $x_i(t)$ and observer states $\hat{x}_i(t)$ of CVS for an unhealthy heart ($i = 1, 2, 3, 4$)

On the other hand we can observe that the SMO has the capacity to adapt to the change in system dynamics. The observer is able to reconstruct the unobservable state when the fault occurs; however, only the states x_3 , x_4 and x_5 can be convergent again to the true state, while state x_1 , x_2 have a constant error, as depicted in Figure 4.24.

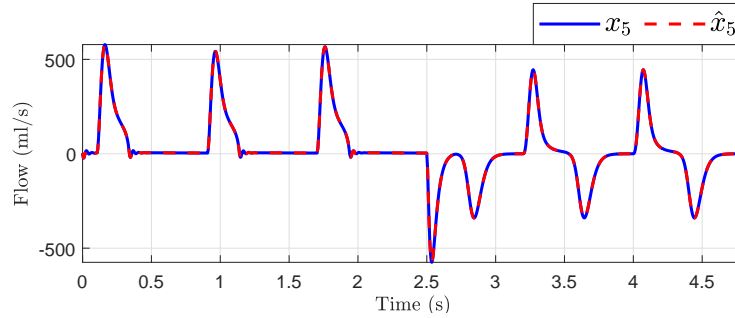


Figure 4.24: Original states $x_5(t)$ and observer states $\hat{x}_5(t)$ of CVS for an unhealthy heart

Additionally, we were able to determine the left ventricular volume and preload volume using the response described by expression (3.1), assuming that simultaneous failure occurs across the mitral and aortic valves (simultaneous mitral and aortic regurgitation), as illustrated in Figure 4.25.

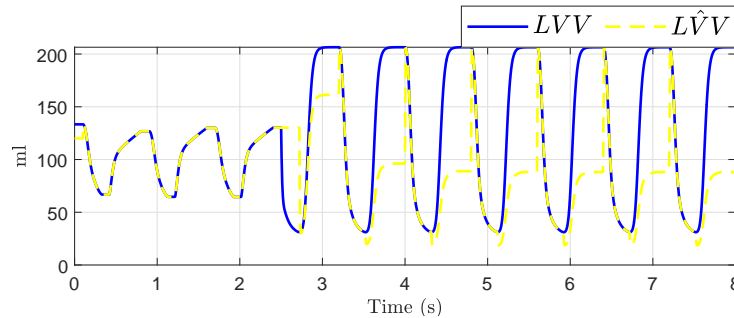


Figure 4.25: Hemodynamic for a Left ventricular volume (LVV) in original and SMO of CVS

On the other hand, when a failure occurs, the SMO is unable to accurately estimate the preload volume due to the loss of x_1 , as shown in the comparison between the original model $PLV_{f_{ao}}$ and the observer-estimated model $P\hat{L}V_{f_{ao}}$ (Figure 4.26). However, we believe that despite these results we can use the observer to detect faults in the system.

Figure 4.27 shows the dynamic behavior of the error between the real system and the observer. As can be observed, states x_1 and x_2 present an error in the presence of the fault, contrary to the error in the remaining states converges to zero. Finally, we can say that the simulated hemodynamic waveforms for a failing heart with simultaneous fm and fao valve failure were presented.

4.5 Conclusions

This chapter has provided a comprehensive mathematical model of the cardiovascular system capable of simulating both normal and pathological states, specifically focusing on fault detection and isolation. The proposed model, which incorporates electrical analogies, offers a novel representation by transforming the

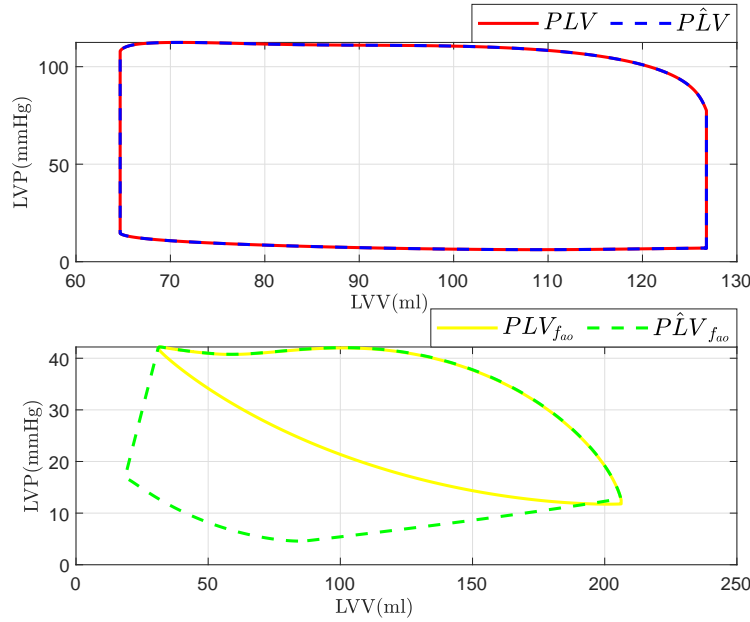


Figure 4.26: Hemodynamic for a reload volume (PLV) in original and SMO of CVS

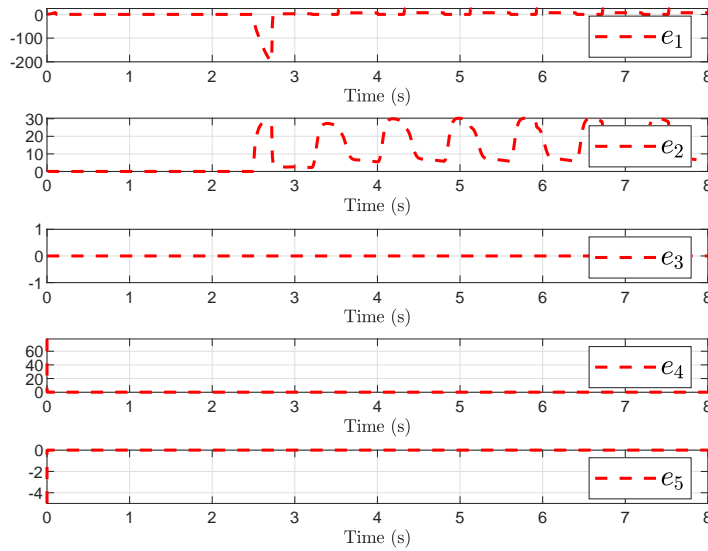


Figure 4.27: Estimation error of the original states $x_i(t)$ and observer states $\hat{x}_i(t)$ of CVS

cardiovascular system into a QONF. This form facilitates the design of a sliding mode observer, enhancing the model's ability to estimate system states and detect anomalies such as valvular heart diseases, which are significant risk factors for cardiovascular diseases.

Our results indicate that the SMO can adapt to changes in system dynamics and reconstruct unobservable states when faults occur. The observer successfully estimated the states x_3 , x_4 , and x_5 , while x_1 and x_2 showed persistent errors under fault conditions. The model's validity was affirmed through simulations that replicated hemodynamic parameters that are consistent with the existing literature and experimental data. Additionally, the SMO demonstrated its effectiveness in scenarios of aortic and mitral valve regurgitation by accurately reconstructing the system dynamics post-failure. The results obtained were validated by comparing the data and the simulations presented in [93, 99, 17].

The findings underscore the potential of the proposed model and observer in clinical decision support, offering a less invasive, economical, and efficient alternative for monitoring cardiovascular health and diagnosing pathologies. However, further studies with larger datasets and a higher number of tests are recommended to refine the model and enhance the precision of the results. This work contributes significantly to the field of cardiovascular modeling, providing a robust tool for understanding and managing cardiovascular diseases through advanced fault detection and isolation techniques.

General conclusions and perspectives

Conclusions

This thesis has presented a comprehensive exploration of the higher-order observability normal form for nonlinear multi-input multi-output (MIMO) systems, leveraging the second-order Poincaré normal form to develop a novel approach for solving homological equations. The quadratic observability normal form introduced in this work offers a more general and less restrictive framework compared to traditional methods, providing a deeper insight into the structural properties of both linearly observable and linearly unobservable systems, and improves the understanding of system observability in complex nonlinear settings.

The introduction of the quadratic observability normal form marks a significant advancement in the study of nonlinear systems. This form allows for a more detailed characterization of system dynamics by extending the classical observability theory to higher-order terms, which is particularly important when dealing with complex nonlinearities. The research demonstrates that the quadratic normal forms obtained in this study differ fundamentally from those presented in previous works. By outlining the conditions under which a diffeomorphism can transform a given nonlinear system into its quadratic observability normal form, this thesis provides a robust theoretical foundation for analyzing observability properties across a wider range of applications. The method effectively captures the intrinsic characteristics of the system, allowing for a clearer distinction between observable and unobservable modes.

Furthermore, the practical application of this method is demonstrated through its use in modeling a nonlinear cardiovascular system. Specifically, the transformation of the cardiovascular system into its normal observable form enables a more precise understanding of its dynamics, particularly under pathological conditions. By converting the model into a quadratic normal form, the study reveals how various physiological parameters and their variations impact the system's observability. This transformation is key to accurately identifying the state variables that are critical to monitoring cardiovascular health, such as ventricular pressure, atrial pressure, and systemic pressure, which are often not directly measurable. The use of this normal form also facilitates the design of more effective state observers, which are essential for fault detection and diagnosis in complex biomedical systems.

At the same time, in this work, starting from the basis of the normal form of quadratic observability, the thesis develops a sliding mode observer (SMO) for general nonlinear systems. The SMO is designed to estimate the state variables that are not directly accessible from system outputs, even when the system is not linearly observable. By taking into account the singularities of observability, the proposed observer can recover the full state of the system under various conditions, demonstrating its robustness and adaptability. The observer's design is guided by the quadratic normal form, which simplifies the structural analysis of the system and provides a clear framework for handling the nonlinearities and singularities inherent in complex MIMO systems. This approach allows for enhanced performance in state estimation, making it highly applicable in diverse fields, such as engineering, robotics, and biological systems.

For this reason, the specific application of the sliding mode observer to a nonlinear cardiovascular model illustrates the practical utility of the theoretical developments in this thesis. The observer is tailored to detect anomalies such as mitral and aortic valve dysfunctions, which are significant risk factors for cardiovascular diseases. By using measurements like aortic pressure and total flow, the observer can estimate unmeasured states, enabling the reconstruction of the system dynamics even when faults occur. Numerical simulations demonstrate that the proposed observer can adapt to changes in physiological parameters and maintain accurate state estimation, even in the presence of faults like valve regurgitation. The effectiveness of the SMO in reconstructing unobservable states post-failure highlights its potential as a powerful tool for real-time monitoring and diagnosis of cardiovascular conditions.

The ability to detect and isolate cardiovascular anomalies is a key contribution of this research. By designing a residual generator based on the sliding mode observer, this thesis presents an innovative approach to identifying deviations in the performance of the heart's mitral and aortic valves. The residual generator is sensitive to changes in both vascular resistances and valve functions, providing a robust means of detecting and differentiating between different types of cardiovascular anomalies. The simulations confirm that the proposed methodology can effectively detect faults, such as valvular regurgitation, and reconstruct the system dynamics under abnormal conditions. This capability makes the approach highly valuable for clinical decision support, offering a less invasive, economical, and efficient alternative to conventional monitoring methods.

Overall, this thesis makes a significant contribution to the field of nonlinear system observability by extending the quadratic observability normal form and applying it to a real-world biomedical problem. The integration of advanced mathematical tools, such as the second-order Poincaré normal form, with practical observer design techniques, demonstrates the potential for innovative solutions in complex systems modeling and analysis. The proposed sliding mode observer, supported by robust theoretical underpinnings and validated through comprehensive simulations, provides a versatile tool for monitoring cardiovascular health and diagnosing pathologies.

Perspectives

This thesis opens several research opportunities for future works. Some of these are presented below:

- Apply the quadratic observability normal form to nonlinear systems in order to deal with more complex systems such as the human body, neuroscience, and robotics, where high-dimensional and highly nonlinear systems are prevalent.
- Extension of the observability quadratic normal form of MIMO systems for Discrete Time Systems.
- Design and implement adaptive sliding mode observers (SMOs) that can learn and adjust to changing system dynamics in real time. The current SMO design is robust for detecting faults and estimating states in nonlinear systems, but it assumes certain fixed system parameters. However, biomedical monitoring, involve systems that exhibit time-varying or uncertain parameters. For this reason, it seems interesting to study this idea.
- Develop patient-specific cardiovascular models that use the quadratic observability normal form and sliding mode observer frameworks to provide personalized health monitoring and diagnosis. Personalized models could provide more accurate predictions and diagnostics.
- Apply the quadratic observability normal form to design fault-tolerant observer strategies that can handle unexpected failures or sensor faults in real-time applications.

Bibliography

- [1] ALURU, J., BARSOUK, A., SAGINALA, K., RAWLA, P., AND BARSOUK, A. Valvular heart disease epidemiology. *In Med. Sci.* 10 (2022), 32.
- [2] ARNOLD, V. Geometrical methods in the theory of ordinary differential equations. *In Springer, New York* (1983).
- [3] ARNOLD, V. Chapitres supplémentaires de la théorie des équations différentielles ordinaires, 3ème édition en français, Éditions mir, librairie du glob.
- [4] ARNOLD, V. Mathematical methods of classical mechanics, 2nd éd. *In Springer, New York* 60 (1997).
- [5] BARBOT, J., AND FLOQUET, T. Iterative higher order sliding mode observer for nonlinear systems with unknown inputs. *In Dyn. Contin. Discret. Impuls. Syst.* 17 (2010), 1019–1033.
- [6] BARBOT, J.-P., BOUKHOBZA, T., AND DJEMAI, M. Sliding mode observer for triangular input form. *In proceedings of 35th IEEE conference on decision and control* 2 (1996), 1489–1490.
- [7] BARBOT, J.; BOUKHOBZA, T. D. M. Sliding mode observer for triangular input form. *In Proceedings of the 35th IEEE Conference on Decision and Control, Kobe, Japan* 2 (13 December 1996), 1489–1490.
- [8] BELKHATIR, Z., LALEG-KIRATI, T., AND TADJINE, M. Residual generator for cardiovascular anomalies detection. *In Proceedings of the European Control Conference (ECC)* (Strasbourg, France), pp. 1862–1868.
- [9] BOUKHOBZA, T., DJEMAI, M., AND BARBOT, J. Nonlinear sliding observer for systems in output and output derivative injection form. *In IFAC Proceedings Volumes, Elsevier* 29, No. 1 (1996), 2179–2184.
- [10] BOUTAT-BADDAS, L. Analyse des singularités d’observabilité et de détectabilité: Application a la synchronisation des circuits électroniques chaotiques. *In Ph.D. Thesis, Université de Cergy-Pontoise, Cergy, France* (2002).
- [11] BOUTAT-BADDAS, L., BARBOT, J., BOUTAT, D., AND TAULEIGNE, R. Sliding mode observers and observability singularity in chaotic synchronization. *In Mathematical Problems in Engineering* 1 (2004), 11–31.
- [12] BOUTAT-BADDAS, L., BOUTAT, D., BARBOT, J., AND TAULEIGNE, R. Quadratic observability normal form. *In Proceedings of the 40th IEEE Conference on Decision and Control (Cat. No.01CH37228), Orlando, FL, USA* 3 (4–7 December 2001), 2942–2947.
- [13] BROOMÉ, M. Closed-loop real-time simulation model of hemodynamics and oxygen transport in the cardiovascular system. *In BioMedical Engineering OnLine* 12, No. 69 (2013), 1–20.

-
- [14] BRUNOVSKY, P. A classification of linear controllable systems. *In Kybernetika 6* (1970), 173–188.
- [15] CHABRAOUI, S., BOUTAT, D., BOUTAT-BADDAS, L., AND BARBOT, J. Observability quadratic characteristic numbers. *In 42nd IEEE International Conference on Decision and Control (IEEE Cat. No. 03CH37475) 4* (2003), 3653–3658.
- [16] DANG-VU, H., AND DELCARTE, C. Bifurcation et chaos: Une introduction à la dynamique contemporaine avec des programmes en pascal, fortran et mathematica. *In Ellipse Edition Marketing S.A.* (2000).
- [17] DIAZ LEDEZMA, F., AND LALEG-KIRATI, T. A first approach on fault detection and isolation for cardiovascular anomalies detection. In Proceedings of the 2015 American Control Conference (ACC), Chicago, IL, USA 1–3 (2015), 5788–5793.
- [18] DINCIC, N. Solving the sylvester equation $ax - xb = c$ when $\text{spec}(a) \cap \text{spec}(b) \neq \emptyset$. *In Electronic Journal of Linear Algebra 35* (2019), 1–23.
- [19] DINGCHANG, CHEN, F., WONG, L. K. S., SHI, L., AND LEUNG, T. W. H. State-of-the-art computational models of circle of willis with physiological applications: A review. *In IEEE Access 8* (2020), 156261–156273.
- [20] DRAKUNOV, S., AND UTKIN, V. Sliding mode observers. tutorial. *In JProceedings of 1995 34th IEEE Conference on Decision and Control 4* (1995), 3376–3378.
- [21] DRAŽENović, B. The invariance conditions in variable structure systems. *In Automatica 5* (1969), 287–295.
- [22] EDWARDS, C., AND SPURGEON, S. K. Sliding mode control: theory and applications. *In Crc Press* (1998).
- [23] FERREIRA, A. AND CHEN, S., SIMAAN, M., BOSTON, J., AND ANTAKI, J. A nonlinear state-space model of a combined cardiovascular system and a rotary pump. *In Proceedings of the 44th IEEE Conference on Decision and Control, Seville, Spain, 15 December 2005*, 897–902.
- [24] FLOQUET, T., AND BARBOT, J.-P. Super twisting algorithm-based step-by-step sliding mode observers for nonlinear systems with unknown inputs. *In Int. J. Syst. Sci. 38* (2007), 803–815.
- [25] FRIDMAN, L., LEVANT, A., AND DAVILA, J. High-order sliding modes observer for linear systems with unbounded unknown inputs. *In 3rd IFAC Conference on Analysis and Design of Hybrid Systems 42, no. 17* (2009), 216–221.
- [26] FROLOV, S., SINDEEV, S., LISCHOUK, V., GAZIZOVA, D. S., LIEPSCH, D., AND BALASSO, A. A lumped parameter model of cardiovascular system with pulsating heart for diagnostic studies. *In Journal of Mechanics in Medicine and Biology 17, No. 03* (2017), 1750056.
- [27] G. ZHENG, L. BOUTAT-BADDAS, D. B., AND BARBOT, J. Unknown input observers for a class of nonlinear siso systems. *In IEEE CDC-ECC, Seville, Spain* (12-15 December 2005).
- [28] GAUTHIER, J P, H. H. Y. S. O. A simple observer for nonlinear systems applications to bioreactor. *In IEEE Transactions on Automatic Control 1* (1992), 875–879.
- [29] GAUTHIER, J., AND BORNARD, G. Observability for any $u(t)$ of a class of nonlinear systems. *In IEEE Transactions on Automatic Control 26, no. 4* (1981), 922–926.
- [30] GHANES, M. Contributions à l’observation des systèmes dynamiques non linéaires: Application aux systèmes électriques et chaotiques. *In thesis, Université de Cergy-Pontoise* (2012).

- [31] GLENDINING, P. Stability, instability and chaos: an introduction to the theory of nonlinear differential equations. In *Cambridge University Press* (1994).
- [32] GLOBAL BURDEN OF CARDIOVASCULAR DISEASES, T., RISK FACTORS: 2020, AND BEYOND. Title of the article. In *J. Am. Coll. Cardiol* 74 (2019), 2529–2532.
- [33] H. LIU, F. LIANG, J. W. T. F. W. Y. K.-I. T. M. S. Sugawara, multiscale modeling of hemodynamics in the cardiovascular system. In *Nature Reviews Cardiology* 31, No. 4 (2015), 46–464.
- [34] H. SOULEY ALI, L. BOUTAT-BADDAS, Y. B.-A. M. D. H-infinity control of a scara robot using polytopic lpv approach. In *14th IEEE Mediterranean Conference on Control and Automation, MED06, Ancona, Italy* (2006).
- [35] HASEGAWA, H., . K. T. Energy loss in the cardiovascular system: A theoretical approach. In *Simul. Pract. Theory* 49, No. 10 (2016), 2097–2104.
- [36] HASHLAMOUN, W.A., H. M. A.-E. New results on modal participation factors: revealing a previously unknown dichotomy. In *IEEE Trans. Autom. Control* 54, No. 7 (2009), 1439–1449.
- [37] HOLLENBERG, S. Valvular heart disease in adults: Etiologies, classification, and diagnosis. In *FP Essent.* 457 (2017), 11–16.
- [38] J. LEFÈVRE, L. LEFÈVRE, B. C. Bond graph model of chemo-mechanical transduction in the mammalian left ventricle, simul. pract. In *Simul. Pract. Theory* 7 (1999), 531–552.
- [39] J. P. BARBOT, I. B., AND BOUTAT-BADDAS, L. Observability normal forms. In *Lecture Notes in Control and Information, Springer* (2003).
- [40] J. P. BARBOT, L. B.-B., AND BELMOUHOU, I. Observability bifurcations: Application to cryptography. In *Chaos in Automatic Control, Marcel Dekker* 31 (Dec 2005), ISBN 0–8247–2653–7.
- [41] JD. BOUTAT, G. ZHENG, L. B.-B. M. D. A new reduced-order observer normal form for nonlinear discrete time systems. In *Systems and Control Letters* 61, No. 10 (October 2012), 1003–1008.
- [42] KAILATH., T. Linear systems. In *Prentice-Hall, Englewood, New Jersey* (1980).
- [43] KALMAN, R. A new approach to linear filtering and prediction problems. In *Transaction of the ASME - Journal of Basic Engineering* 82 (1960), 35–45.
- [44] KALMAN, R. ET BUCY, R. New results in linear prediction and filtering theory. In *Transaction of the ASME- Journal of Basic Engineering* 83 (1961), 95–108.
- [45] KOKALARI, I., KARAJA, T., AND GUERRISI, M. Review on lumped parameter method for modeling the blood flow in systemic arteries. In *Scientific Research Publishing* 1 (2013).
- [46] KORAKIANITIS, T., AND SHI, Y. A concentrated parameter model for the human cardiovascular system including heart valve dynamics and atrioventricular interaction. In *Med. Eng. Phys.* 28 (2006), 613–628.
- [47] KORAKIANITIS, T., AND SHI., Y. A concentrated parameter model for the human cardiovascular system including heart valve dynamics and atrioventricular interaction. In *Medical Engineering and Physics* 28, No. 07 (2006), 613–628.
- [48] KOTEICH, M., DUC, G., MALOUM, A., AND SANDOU, G. Observability of sensorless electric drives. In *arXiv preprint arXiv:1602.04468* (2016).

-
- [49] KRENER, A., AND ISIDORI, A. Linearization by output injection and nonlinear observer systems. *In Control Letters* 3 (1983), 47–52.
- [50] KRENER, A., AND RESPONDEK, W. Nonlinear observer with linearizable error dynamics. *In SIAM J. Control* 23 (1985), 197–216.
- [51] KRENER, A. J., AND XIAO, M. Observers for linearly unobservable nonlinear systems. *In Systems and Control Letters* 46, no 4 (2002), 281–288.
- [52] L. BOUTAT-BADDAS, D. B., AND BARBOT, J. Observability analysis by poincare normal forms. *In Mathematics of Control, Signals, and Systems* 21, no. 2 (2009), 147–170.
- [53] L. BOUTAT-BADDAS, D. B., AND BARBOT, J. P. Observability analysis by poincaré normal form. *In Mathematics of Control Signals and Systems* 21, No. 2 (202), 147–170.
- [54] L. BOUTAT-BADDAS, J.P. BARBOT, D. B., AND TAULEIGNE, R. Generalized quadratic transformation and observer design. *In 6th IFAC symposium, NOLCOS, Stuttgart* (17 September 2004).
- [55] L. BOUTAT-BADDAS, J.P. BARBOT, D. B., AND TAULEIGNE, R. Observability bifurcation versus observing bifurcations. *In 15th IFAC, World Congress b'02, 2002, Barcelone* (2002).
- [56] L. BOUTAT-BADDAS, J.P. BARBOT, D. B., AND TAULEIGNEH, R. Sliding mode observers and observability singularity in chaotic synchronization. *In Mathematical Problems in Engineering* (2004).
- [57] L. BOUTAT-BADDAS, D. B. E. J. B. Forme normales d'observabilité généralisées. *In CIFA, Douz, Tunisie* (22-23 Novembre 2004).
- [58] L. BOUTAT-BADDAS, J.P. BARBOT, D. B. E. R. T. Transmission par synchronisation de systèmes chaotiques avec et sans singularité d'observation. *In CIFA 2002, Nantes, 2002* (2002).
- [59] L. BOUTAT-BADDAS, D. BOUTAT, J. B., AND TAULEIGNE, R. Quadratic observability normal form. *In IEEE-CDC, 2001, Orlando, Floride* (2001).
- [60] L. BOUTAT-BADDAS, G. ZHENG, J. B., AND BOUTAT, D. Some comments on observability normal form and step-by-step sliding mode observer. *In SIAM Conference on Control and its Applications, New Orleans* (July 11-15, 2005).
- [61] LAUBSCHER, R., VAN DER MERWE, J., LIEBENBERG, J., HERBST, AND P. Dynamic simulation of aortic valve stenosis using a lumped parameter cardiovascular system model with flow regime dependent valve pressure loss characteristics. *In Med. Eng. Phys.* 106 (2022), 103838.
- [62] LAUBSCHER, R., VAN DER MERWE, J., LIEBENBERG, J., AND HERBST, P. Dynamic simulation of aortic valve stenosis using a lumped parameter cardiovascular system model with flow regime dependent valve pressure loss characteristics. *In Medical Engineering & Physics* 106 (2022), 103838.
- [63] LEDEZMA, F., AND LALEG-KIRATI, T. Detection of cardiovascular anomalies: Hybrid systems approach. *In IFAC Proc* 45 (2012), 222–227.
- [64] LEVANT, A. Sliding order and sliding accuracy in sliding mode control. *In International Journal of Control* 58, No.6 (1993), 1247–1263.
- [65] LI, Z., AND H.ZHOU. Spectral decomposition based solutions to the matrix equation $ax-xb=c$. *In IET Control Theory and Applications* 12 (2018), 19–128.
- [66] LIU, F. Synthèses d'observateurs à entrées inconnues pour les systèmes non linéaires. *In Thèse de doctorat, Université de Caen Basse-Normandie-France* (2007).

- [67] LIU, J. Sliding mode control using matlab. *In book Academic Press* (2017).
- [68] LUCA FORMAGGIA, DANIELE LAMPONI, M. T., AND VENEZIANI, A. Numerical modeling of 1d arterial networks coupled with a lumped parameters description of the heart. *In Computer methods in biomechanics and biomedical engineering* 9, No. 05 (2006), 273–288.
- [69] LUENBERGER, D. Observing the state of a linear system. *In Military Electronics, IEEE Transactions on, Signals* 8, no. 2 (1964), 74–80.
- [70] LUENBERGER, D. An introduction to observers. *In IEEE Transactions on automatic control* 16, no. 6 (1971), 596–602.
- [71] M. DAROUACH, M. Z., AND BOUTAT-BADDAS, L. Discussion on a comparison of sliding mode and unknown input observer in european journal of control. 261–266.
- [72] M. L’HERNAULT, L. BOUTAT-BADDAS, A. O., AND BARBOT, J. P. Chaotic frequency modulation in cryptography. *In International Workshop on Electronics and System Analysis, IWESA, Bilbao, Spain* (21-23 October 2004).
- [73] MANOLIU, V. Modeling cardiovascular hemodynamics in a model with nonlinear parameters. *In Proceedings of the E-Health and Bioengineering Conference (EHB), Iasi, Romania, (19–21, November 2015)*, 1–4.
- [74] MITTAL, R., SEO, J. H., VEDULA, V., CHOIAND, Y. J., LIU, H., HUANG, H. H., AND GEORGE, R. T. Computational modeling of cardiac hemodynamics: Current status and future outlook. *In Journal of Computational Physics* 305 (2015), 1065–1082.
- [75] NIEDERER, S.A., L. J., AND TRAYANOVA, N. Computational models in cardiology. *In Nature Reviews Cardiology* 16 (2018), 100–111.
- [76] NIKRAZ, N. Observadores funcionales de modo deslizante para clases de sistemas lineales y no lineales. *In thesis Universidad de Australia Occidental* (2008).
- [77] ORGANIZATION, W. H. “cardiovascular diseases”. *In [https://www.who.int/news-room/fact-sheets/detail/cardiovascular-diseases-\(cvds\)](https://www.who.int/news-room/fact-sheets/detail/cardiovascular-diseases-(cvds))* (2024), accessed on 8 May 2024.
- [78] ORTIZ-RANGEL, E. Modelado dinámico del sistema cardiovascular con fines de estimación, monitoreo y diagnóstico de cardiopatías en infantes. *In Tecnológico Nacional de México, thesis* (2021).
- [79] ORTIZ-RANGEL, E., GUERRERO-RAMÍREZ, G., GARCÍA-BELTRÁN, C., GUERRERO-LARA, M., ADAM-MEDINA, M., ASTORGA-ZARAGOZA, C., REYES-REYES, J., AND POSADA-GÓMEZ, R. Dynamic modeling and simulation of the human cardiovascular system with pda. *In Biomed. Signal Process. Control* 71 (2022), 103151.
- [80] PERRUQUETTI, W., AND BARBOT, J.-P. Sliding mode control in engineering. *In New York: Marcel Dekker* 11 (2002).
- [81] PETER KOHL, DENIS NOBLE, R. L. W., AND HUNTER, P. J. Computational modelling of biological systems: tools and visions. *In Royal Society* 8 (2000), 579–610.
- [82] QUARTERONI, A., AND FORMAGGIA, L. Mathematical modelling and numerical simulation of the cardiovascular system. *In Computational Models for the Human Body, Handbook of Numerical Analysis Elsevier* 12 (2004), 3–127.
- [83] QUARTERONI A, MANZONI A, V. C. The cardiovascular system: Mathematical modelling, numerical algorithms and clinical applications. *In Acta Numerica* 26 (2017), 365–590.

-
- [84] ROY, D., AND MUSIELAK, Z. Generalized lorenz models and their routes to chaos. ii. energy-conserving horizontal mode truncations. *In Chaos, Solitons and Fractals 31, Issue 3* (February 2007), 747–756.
- [85] S. CHABRAOUI, L. BOUTAT-BADDAS, D. B., AND BARBOT, J.-P. Observability quadratic characteristic numbers. *In IEEE-CDC, 2003, Hayatt Regency Maui, Hawaii, USA, (2003)*.
- [86] SCARSOGLIO, S., AND RIDOLFI, L. A review of multiscale 0d-1d computational modeling of coronary circulation with applications to cardiac arrhythmias. *In Reviews in cardiovascular medicine 22, No. 03* (2021), 1461–1469.
- [87] SERRANO-CRUZ, D., BOUTAT-BADDAS, L., DAROUACH, M., AND ASTORGA-ZARAGOZA, C.-M. Observer design for a nonlinear cardiovascular system. *In Proceedings of the 9th International Conference on Systems and Control, Caen, France (24–26 November 2021)*, 294–299.
- [88] SERRANO-CRUZ, D., BOUTAT-BADDAS, L., DAROUACH, M., ZARAGOZA, C., AND RAMIREZ, G. Sliding mode observer design for fault estimation in cardiovascular system. *In Proceedings of the Congreso Nacional de Control Automático, 25–27 October 2023, Acapulco, Mexico*.
- [89] SHI, Y., LAWFORDE, P., AND HOSE, R. Review of zero-d and 1-d models of blood flow in the cardiovascular system. *In Biomedical engineering online 10* (2011), 38.
- [90] SHIMIZU, S., UNE, D., KAWADA, T., HAYAMA, Y., KAMIYA, A., SHISHIDO, T., AND SUGIMACHI, M. Lumped parameter model for hemodynamic simulation of congenital heart diseases. *In The journal of physiological sciences 68, No. 03* (2018), 103–111.
- [91] SHTESSEL, Y., EDWARDS, C., FRIDMAN, L., LEVANT, A., ET AL. Sliding mode control and observation. *In book of Springer 10* (2014), 1247–1263.
- [92] SIMAAN, M. Modeling and control of the heart left ventricle supported with a rotary assist device. *In Proceedings of the 47th IEEE Conference on Decision and Control, Cancun, Mexico, 9–11 December 2008*, 2656–2661.
- [93] SIMAAN, M. Rotary heart assist devices. *In Springer Handbook of Automation, Nof, S., Ed., Springer: Berlin/Heidelberg, Germany* (2009), 1409–1422.
- [94] SIMAAN, M., FERREIRA, A., CHEN, S., ANTAKI, J., AND GALATI, D. A dynamical state space representation and performance analysis of a feedback-controlled rotary left ventricular assist device. *In IEEE Trans. Control. Syst. Technol. 17* (2018), 15–28.
- [95] SLOTINE, J.-J. E., H. J. K. . M. E. A. On sliding observers for nonlinear systems. *In Journal of Dynamic Systems, Measurement, and Control 109, No. 3* (1987), 245.
- [96] SMITH, N. P., . A. P. N. A hydraulic approach to modeling blood flow in arteries. *In Simul. Pract. Theory 48, No. 7* (2015), 1192–1200.
- [97] SPURGEON, S. K. Sliding mode observers: a survey. *In International Journal of Systems Science, Taylor & Francis 39, No. 8* (2008), 751–764.
- [98] TARCHALA, G. Influence of the sign function approximation form on performance of the sliding-mode speed observer for induction motor drive. *In International Symposium on Industrial Electronics, IEEE* (2011), 1397–1402.
- [99] TRAVER, J., NUEVO-GALLARDO, C., TEJADO, I., FERNÁNDEZ-PORTALES, J., ORTEGA-MORÁN, J., PAGADOR, J., AND VINAGRE, B. Cardiovascular circulatory system and left carotid model: A fractional approach to disease modeling. *In Fractal Fract. 6* (2022), 64.

- [100] UTKIN, V. Variable structure systems with sliding modes. *In IEEE Transactions on Automatic Control* 22, No. 2 (1977), 212–222.
- [101] UTKIN, V. Sliding modes in control optimization. *In Engineering Series, Springer-Verlag, Springer* (1992).
- [102] UTKIN, V., POZNYAK, A., ORLOV, Y. V., AND POLYAKOV, A. Road map for sliding mode control design. *In Springer* (2020).
- [103] WIGGINS, S. Introduction to applied nonlinear dynamical systems and chaos. *In 2nd éd., Springer, New York 2* (2003).
- [104] WONHAM., W. M. Linear multivariable control - a geometric approach. *In Springer-Verlag* (1985).